The fractionation and concentration of whey protein and casein streams from skimmed milk

Escursell Jove, Oriol

Award date:
2021

Awarding institution:
University of Bath

The fractionation and concentration of whey protein and casein streams from skimmed milk

Oriol Escursell Jove

Supervisor: Dr. Mike Bird

Co-supervisor: Professor John Chew, Professor Barbara Kasprzyk-Hordern and Dr. Jannis Wenk

A thesis submitted for the degree of Doctor of Philosophy

University of Bath

Department of Chemical Engineering

March 2021

Acknowledgements

I would like to express my sincere gratitude to Dr. Michael Bird for his excellence guidance during this PhD, as well as for all the advice both personal and professional. I would also like to thank Mike for all the time that he took to talk to me whenever I needed. I would also like to thank him for giving me the chance to develop my PhD in his research group.

In addition, I would also like to thank Professor John Chew for his support, advice and open-door policy during this project. I also acknowledge Professor Barbara Kasprzyk-Hordern and Dr. Jannis Wenk for their help and advice on the HPLC analytical technique developed and used during the project.

I would also like to acknowledge and thank the valuable technical input and support provided by Dr Jeanette Lindau and Dr Anitha Rasmussen of Tetra Pak, Sweden. Their help always brought new light and perspective to the lab-based research, which has been essential.

My thanks also go to Dr. Philip Fletcher from the Microscopy and Analysis suite of the University of Bath for their help in the scanning electron microscope and energy-dispersive X-ray (EDX or EDS) analysis, to Dr. Shaun Reeksting of the Chemical Characterisation and Analysis Facility (CCAF) for helping me understand and manage the use of UPLC equipment.

Especialment vull agrair a la Míriam (wife) el temps viscut abans i durant el projecte i que espero que duri per molts anys! Els anys del doctorat han sigut els millors de la meva vida professionalment i sobretot personalment! Viatges, amics i temps per disfrutar-ho tot plegat, gràcies per tot.

També vull agrair tot el suport, energia i paciència que la meva família m'han dedicat durant tot el projecte.

I would also like to thank Tetra Pak for the kind donation of the membranes used in this study.

Last but not least, this project was jointly funded by (i) Tetra Pak, Sweden and (ii) the European Union's Horizon 2020 research and innovation programme under the Marie Skłodowska-Curie grant agreement No 665992, through the Centre for Sustainable Technology at the University of Bath.

Abstract

Food processing systems face the challenge to feed a human population of 7.7 billion (2019) people that is expected to increase to 9.7 billion by 2050 (UN, 2015). Food production carries lots of environmental impacts, from the water used to grow crops and feed animals to the impacts of fertilisers on the water itself. Dairy products are no exception to that since they are the second main source of environmental impacts for the food sector, due to their total amount of product rather than the intrinsic impacts per unit of product, when compared to meat.

Dairy products include a wide range of products from milk and cheese to proteins and immunoglobulins. In order to separate the milk into its constituents (proteins, water, immunoglobulins, etc) several methods have been developed over the years, ranging from chemical precipitation to membrane filtration. Membrane filtration has gained special attention among the key industrial players because of membranes long lifespan, their versatility and their low impact on the food product due to the physical method employed for the separation.

However, milk fractionation to separate the different components, specially to separate the different protein groups (casein and whey proteins) still has some challenges that need to be overcome, such as the full separation of casein and whey protein groups using polymeric membranes. In this regard, this project studied the main operational factors affecting such separation, in order to achieve the full separation of casein and whey protein groups using polymeric membranes. There is great interest in industry in having pure streams of whey and casein proteins because they find applications in routinely used products such as infant formula or for the production of imitation cheeses.

This PhD thesis starts with a general introduction (Chapter 1) covering the key aspects of dairy technologies, proteins production and main uses. Furthermore, it also overviews the current challenges that need to be overcome, leading to the establishment of the project aims and objectives.

An extensive literature review (Chapter 2) was included to cover the properties of milk and milk proteins, with an special focus on casein micelles due to their major role in milk protein fractionation associated to micelle composition variations with temperature. The literature review also analyses the key analytical methods for milk proteins detection and quantification to determine the best analytical tool for the project. It can be highlighted that the High-Performance Liquid Chromatography (HPLC) methods have made great advances in the last 10 years making them one of the best approaches for milk protein detection nowadays.

Chapter 3 explains the main experimental work performed in this thesis, particularly on the filtration protocol, including the cleaning steps and the filtration equipment used for milk protein separation.

Chapter 4, 5 and 6 cover the results of this thesis. In particular, Chapter 4 covers the development of the selected analytical method using HPLC, Chapter 5 the study of the interactions between skimmed milk and the Polyvinylidene difluoride (PVDF) membrane and Chapter 6 the study of protein fractionation under a selection of industrial conditions.

The development of the analytical method described in Chapter 4 was carried out to have a tool to identify the main protein groups within milk. Interestingly, this method can identify and quantify in a single HPLC injection the alpha, beta and kappa casein proteins and the alpha-Lactalbumin, beta-Lactoglobulin and Bovine Serum Albumin of the whey proteins. Furthermore, the advancements of the project allowed us to use this method even for measuring fouling layer samples which allowed us to determine protein fouling layer compositions, a key factor for understanding membrane filtration processes.

The study of the milk and PVDF membrane interactions described in Chapter 5, focused on understanding the operational conditions that defined the protein separation. It must be highlighted that when fixing the crossflow velocity and transmembrane pressure casein rejection was controlled by two factors, outlet pressure and temperature, having higher casein rejection at higher pressure and having higher protein rejection at low temperatures (10 °C). Under the same conditions the whey proteins rejection behaviour was less pronounced which indicated that their rejection was controlled by temperature but not by outlet pressure.

Finally, Chapter 6 highlights the final experiments focused on studying the behaviour of proteins and the fouling layer composition under industrial conditions followed by slight modifications to test how pressure, crossflow velocity and temperature could improve the current industrial conditions. The results showed that the current low-pressure conditions in industry favours the fractionation of proteins. Transmembrane pressure increases from 1 bar to 2.8 and 4.7 bar only favoured casein proteins transmission reducing the final fractionation of proteins. The membrane fouling composition study revealed that at any operational condition the main components of the fouling layer were the casein proteins (>94% of all proteins) with a residual share of whey proteins (<6%).

The final chapter of this PhD summarises the main conclusions and compiles an overview of future research pathways to be carried out both in industry and academia.

Table of Contents

ACKNOWLEDGEMENTS ..... **I**

ABSTRACT ..... **II**

TABLE OF CONTENTS ..... **IV**

LIST OF FIGURES ..... **VII**

LIST OF TABLES ..... **XV**

NOMENCLATURE ..... **XVIII**

CHAPTER 1. INTRODUCTION **1**

1.1 Aim of the project **7**

1.2 Scope of the project **8**

CHAPTER 2. LITERATURE REVIEW **10**

2.1 The properties of milk **10**

2.2 Casein proteins **12**

2.2.1 Micelle formation and structure 13

2.3 Analytical techniques for protein detection **19**

2.3.1 High-Performance Liquid Chromatography (HPLC) 20

2.3.2 Mass spectrometry 27

2.3.3 Chemical based analysis 29

2.3.4 Analytical techniques summary 31

2.4 Methods of separation **33**

2.4.1 Modes of filtration 34

2.5 Fouling and cleaning **35**

2.5.1 Fouling mechanisms 35

2.5.2 Remedial actions 37

2.6 Membrane filtration 40
2.6.1 Membrane properties and types 40
2.6.2 Membrane materials 41
2.6.3 Temperature effects 45

CHAPTER 3. METHODOLOGY 49

3.1 Filtration Protocol 49
3.1.1 Coating layer removal 49
3.1.2 Pure water flux 50
3.1.3 Filtration cycle 51
3.1.4 Membrane cleaning 52

3.2 Filtration equipment 53
3.2.1 Bench scale M10 rig 53
3.2.2 The Pilot Scale rig 56
3.2.3 Bench Top M10 vs Pilot Scale 59

3.3 Mathematical models 59
3.3.1 Error propagation analysis 60

3.4 Membrane analysis 61
3.4.1 Scanning Electron Microscope 61
3.4.2 FTIR 61
3.4.3 Confocal thickness sensor 62

CHAPTER 4. PROTEIN ANALYSIS: DEVELOPMENT OF THE HPLC METHOD 63

4.1 Reagents and samples 63

4.2 Sample preparation 63

4.3 Equipment and solvents 64

4.4 Column selection 64

4.5 Gradient selection 67

4.6 Temperature selection 75
4.6.1 Method validation 80

4.7 Membrane protein analysis 81

4.8 HPLC method summary 83

CHAPTER 5. INTERACTIONS BETWEEN SKIMMED MILK AND PVDF MEMBRANE 85

5.1 Volume reduction studies 85

5.2 Full recirculation studies 90

5.2.1 General tests 90

5.2.2 Membrane concentration study 98

5.2.3 Design of Experiments 101

5.3 Sequential filtration 119

5.3.1 Analysis by protein groups 123

5.3.2 Permeate flux 126

5.3.3 Summary of sequential filtration 128

5.4 Membrane analysis 129

CHAPTER 6. INDUSTRIAL CONDITIONS STUDY 133

6.1 Filtration results 134

6.1.1 Protein rejection 134

6.1.2 Permeate flux 141

6.1.3 Summary of permeate flux and protein ratio 144

6.2 Membrane fouling composition 146

6.2.1 Temperature effect on membrane fouling 152

6.2.2 Summary of membrane fouling composition 155

6.3 Rinsing study 156

6.3.1 Rinsing time vs CFV 156

6.3.2 Rinse study: effect on reversible and irreversible fouling 159

6.3.3 Summary of rinse study 161

6.4 Membrane compaction 162

CHAPTER 7. GENERAL CONCLUSIONS 166

BIBLIOGRAPHY 171

List of Figures

Figure 1-1: Membrane applications by sectors and percentage of use (2017).[1] 1
Figure 1-2: Membrane applications in the dairy industry by membrane size and product obtained.[5,6] 3
Figure 2-1: Average cow milk composition, it does change based on the lactation stage, the cow's diet and the cow's breed .[10] 10
Figure 2-2: Skimmed-milk viscosity changes due to temperature. Based on Bakshi and Smith.[23] 11
Figure 2-3: Schematic representation of the Sub-micelle model developed by Schmidt (1980)[30] adapted from Horne (2005).[40] 14
Figure 2-4: Schematic representation of nanocluster model developed by Holt (1992)[31] adapted from Horne (2005).[40] The alpha proteins bind different nanoclusters together promoting chain growth. 15
Figure 2-5: Schematic representation of Dual binding model adapted from Horne (1998).[28] Alpha, beta and kappa casein are depicted as indicated. The assumption is that bonding occurs between the hydrophobic regions of each protein (shown as rectangular bars). The hydrophilic regions are linked by the colloidal calcium phosphate clusters (CCP). The kappa-casein proteins limit the growth and they are highlighted with a 'k'. 16
Figure 2-6: Schematic picture of a 200 nm casein micelle's cross section according to the sponge model of Bouchoux *et al.* (2010)[45]. The soft regions are voids filled with solvent and the hard regions contain all the CaP and protein materials. Based on their model the hard regions can be divided into cells that contain either one CaP nanocluster (*dark cells*) or casein molecules and solvent (*lighter cells*). Source: Bouchoux *et al.* (2010)[45]. 18
Figure 2-7: Effective diameter of CN micelles found raw skim milk at 6, 20 and 50 °C, when diluted with UF permeate. Source: Beliciu and Moraru (2009).[48] 19
Figure 2-8: Reverse phase stationary phase properties. Source: CHROMacademy.[65] 23
Figure 2-9: Separation of bovine milk proteins and protein standards by RP-HPLC at 220nm. Adapted from Bobe *et al.* (1998)[64] 24
Figure 2-10: RP chromatographic profile of a mixture of protein standard. UV detection is 214nm. The x axis represents the retention time in minutes, and the y axis is the absorbance. Adapted from Bordin *et al.* (2001)[25] 25
Figure 2-11: Mass spectrometric techniques for different needs arranged by main fields of application and estimated relative hardness or softness. Source: Mass spectrometry.[63] 27
Figure 2-12: MALDI-TOF-MS spectra of two milk whey proteins fractions collected during the CE separation step of typical IACE experiment. Source: Gasilova *et al.* (2012)[68] 28
Figure 2-13: Dead end and Crossflow filtration, adapted from Mulder M. (1991)[3] 35

Figure 2-14: Pore blocking mechanism and cake layer adapted from Bowen *et al.* (1995)[90] 36
Figure 2-15: Flux profile over time of a fouling/cleaning cycle. 38
Figure 2-16: Percentage clean water flux recovery versus sodium hydroxide concentration at 40 °C (Re ~ 3160), Shorrock and Bird (1998).[105].....39
Figure 2-17: Regenerated Cellulose, SEM image and basic chemical unit. Source: Fisher Scientific. 43
Figure 2-18: Structure of PVDF.....43
Figure 2-19: Structure of polyethersulfone (PES). 44
Figure 3-1: Concentration/Filtration protocol based on Argyle *et al.*[130] 51
Figure 3-2: DSS LabStack Bench Top M10 module (Alfa Laval) with the position of temperature and pressure sensors. 53
Figure 3-3: Schematic figure of the Bench Top M10 polysulfone plates (Argyle 2015)[131] ...54
Figure 3-4: Schematic diagram of the Pilot Scale filtration apparatus. Legend: FT - feed tank, H - oil circulation pump and heater, M - membrane module, F - flow meter, HE - heat exchanger, CP - centrifugal pump, PDP - positive displacement pump, T - thermocouple, S - sampling point and P - pressure transducer. Diagram adapted with permission from Head & Bird (2013)[132].....56
Figure 4-1: Chromatogram of all standards analysed at 214 nm, using ZORBAX column (C8 column with 300 Å), Gradient 1 and at 25 °C. 65
Figure 4-2: Chromatogram of all standards analysed at 214 nm, using ACQUITY column (C8 column with 130 Å), Gradient 1 and at 25 °C. 65
Figure 4-3: Gradient profile for gradient 1, showing the fraction of solvent B over time. 67
Figure 4-4: Chromatogram of all standards analysed at 214 nm, using the C8 column with 300 Å, and Gradient 1. Showing the separation of alpha proteins and beta proteins, but not the separation of casein and whey proteins. 68
Figure 4-5: Gradient profile for gradient 2, showing the fraction of solvent B over time. 68
Figure 4-6: Chromatogram of all standards analysed at 214 nm, using the C8 column with 300 Å, and gradient 2. Showing that the beta casein and beta whey are not fully separated. 69
Figure 4-7: Gradient profile for gradient 3, showing the fraction of solvent B over time. 69
Figure 4-8: Chromatogram of all standards analysed at 214 nm, using the C8 column with 300 Å, and gradient 3. It shows the capability to detect all protein groups except kappa-CN.....70
Figure 4-9: Chromatogram of BSA and Alpha-La standards analysed at 214 nm, using the C8 column with 300 Å, and gradient 3. 70
Figure 4-10: Chromatogram of Beta-CN and Beta-Whey standards analysed at 214 nm, using the C8 column with 300 Å, and gradient 3.....71
Figure 4-11: Gradient profile for gradient 4, showing the fraction of solvent B over time. ..71

Figure 4-12: Chromatogram showing the BSA, Alpha-La, Alpha-CN, Beta-CN and Beta-Lg standards analysed at 214 nm, using the C8 column with 300 Å, and gradient 4. Showing the overlapping of BSA, Alpha-La and Alpha-CN and the overlapping of Beta-CN and Beta-Whey..... 72
Figure 4-13: Gradient profile for gradient 5, showing the fraction of solvent B over time... 73
Figure 4-14: Chromatogram showing the BSA, Alpha-La, Alpha-CN standards analysed at 214 nm, using the C8 column with 300 Å, and gradient 5. It shows the overlapping of BSA with both Alpha proteins and a slight overlap of Alpha-CN and Alpha-La..... 73
Figure 4-15: Chromatogram showing the Beta-CN and Beta-Lg standards analysed at 214 nm, using the C8 column with 300 Å, and gradient 5. It shows the overlap of Beta-Cn and Beta-Whey..... 74
Figure 4-16: Gradient profile for gradient 6, showing the fraction of solvent B over time... 74
Figure 4-17: Chromatogram showing the BSA, Alpha-La, Alpha-CN, Beta-CN and Beta-Lg standards analysed at 214 nm, using the C8 column with 300 Å, and gradient 6. 75
Figure 4-18: Chromatogram showing the Beta-CN and Beta-Lg standards analysed at 214 nm, using the C8 column with 300 Å, and gradient 6, at a Temperature of 25 °C. 76
Figure 4-19: Chromatogram showing the Beta-CN standards analysed at 214 nm, using the C8 column with 300 Å, and gradient 6, at a range of Temperature from 25 to 50 °C. 77
Figure 4-20: Chromatogram showing the Beta-Lg standards analysed at 214 nm, using the C8 column with 300 Å, and gradient 6, at a range of Temperature from 25 to 50 °C. 77
Figure 4-21: Chromatogram showing the Beta-CN and Beta-Lg standards analysed at 214 nm, using the C8 column with 300 Å, and gradient 6, at a Temperature of 45 °C. The graph shows the minimal overlap of the Beta-CN and Beta-Lg peaks. 78
Figure 4-22: Chromatogram showing the Beta-CN and Beta-Lg standards analysed at 214 nm, using the C8 column with 300 Å, and gradient 6, at a Temperature of 40 °C. Red circle highlight the region of overlap compared to the 45 °C spectra..... 78
Figure 4-23: Chromatogram showing the Beta-CN and Beta-Lg standards analysed at 214 nm, using the C8 column with 300 Å, and gradient 6, at a Temperature of 50 °C. Red circle highlights the main region of overlap compared to 45 °C. 79
Figure 4-24: Chromatogram showing all standards except the Kappa-CN analysed at 214 nm, using the C8 column with 300 Å, and gradient 6, at a Temperature of 45ºC. 79
Figure 4-25: Chromatogram of the sample obtained by membrane soaking in 0.25 mL of HPLC solution (a) and membrane sonicated in 0.25 mL of HPLC solution (b). RP-HPLC system with UV-Vis detection at 214 nm, centred into the beta casein and whey peaks. 82
Figure 4-26: Chromatogram of samples obtained at different HPLC solution amounts and soaking time. a) 1 hours in 0.25 mL, b) 6h, 0.25 mL, c) 6h, 0.5 mL, d) 24h, 0.25mL and e)

24h, 0.5mL. RP-HPLC system with UV-Vis detection at 214 nm, centred into the beta casein and whey peaks. 83
Figure 5-1: Inlet, outlet Pressure and TMP calculation for chapter 6.[3] 86
Figure 5-2: Flux decline curves of the permeate stream using the 0.1 µm membranes (Synder Filtration, V01). All samples were produced at 10 °C. Error bars correspond to the standard deviation of 2 repeats for each data point. Samples have been denoted as following: Outlet pressure-TMP-CFV. 87
Figure 5-3: Membrane resistance values for filtration processes seen in Figure 5-2. Total ressistance values broken down into membrane resistance (Rm), reversible fouling resistance (Rrev) and Irreversible fouling resistance (Rir). All samples have been normalised for ease of comparison (calculated by dividing each resistance by the total resistance, see Equation 3-2), membrane resistance value was constant for all samples analysed. Error bars correspond to the standard deviation of 2 repeats for each data point. Samples have been denoted as following: Outlet pressure-TMP-CFV. 89
Figure 5-4: Flux decline curve of filtration at TMP of 1 bar and temperature of 50°C. 50°C-1.1 m s^{-1} and 50°C-1.6 m s^{-1} had CFV of 1.07 and 1.6 m s^{-1} respectively. Samples have been denoted as following: Temperature-CFV. 91
Figure 5-5: Flux decline curve for sample 50°C-1.1 m s^{-1}, 50°C-1.6 m s^{-1} and 10°C-1.5 m s^{-1}. Sample 10°C-1.5 m s^{-1} was processed at TMP 1 bar, temperature of 10°C and CFV of 1.53 m s^{-1}. Samples have been denoted as following: Temperature-CFV. 92
Figure 5-6: Protein fractions distribution by protein groups for 50°C-1.1 m s^{-1}, 50°C-1.6 m s^{-1} and 10°C-1.5 m s^{-1} experiments. Error bars correspond to the standard deviation of 3 repeats for each data point. Samples have been denoted as following: Temperature-CFV. 93
Figure 5-7: Flux decline curve for sample processed at 10°C (10°C-1.5 m s^{-1}, 10°C-1.3 m s^{-1}, 10°C-0.6 m s^{-1} and 10°C-0.8 m s^{-1}). Samples 10°C-1.5 m s^{-1} and 10°C-1.3 m s^{-1} were processed at TMP 1 bar, sample 10°C-0.6 m s^{-1} was processed at TMP of 0.25 bar and sample 10°C-0.8 m s^{-1} at TMP of 0.5 bar. Error bars correspond to the standard deviation of 3 repeats for each data point. Samples have been denoted as following: Temperature-CFV. 95
Figure 5-8: Protein fractions distribution by protein groups for 10°C-1.5 m s^{-1}, 10°C-1.3 m s^{-1}, 10°C-0.6 m s^{-1} and 10°C-0.8 m s^{-1} experiments at the initial feed, retentate and final permeate. Error bars correspond to the standard deviation of 3 repeats for each data point. Samples have been denoted as following: Temperature-CFV. 96
Figure 5-9: Steady-stat flux (Jv) vs ln[(1 - rcoeff)/rcoeff] were the bulk concentration of proteins was varied based on Table 5-7, operated at TMP of 0.5 bar, CFV 0.85 m s^{-1}, and temperature of 10 °C. 99

Figure 5-10: Total membrane resistance values based on milk concentration, from 100% milk to RO water. See Table 5-6 for exact dilutions. Error bars correspond to the standard deviation of 2 repeats for each data point. 100
Figure 5-11: Flux decline curve for DoE repeats, all of them were processed at 30 °C and outlet pressure of 0.3 bar. TMP and CFV were kept constant at 0.5 bar ± 0.01 bar and 1.4 m s^{-1} ± 0.3 m s^{-1}, respectively. 103
Figure 5-12: DoE summary of casein rejection. A) Casein rejection (%) based on outlet pressure (bar) sorted by temperatures. Circle 10°C, square 30°C, cross 50°C and triangle repeats. B) Casein rejection (%) based on temperature (°C). The lines indicate the tendencies observed during the DoE study, see Figure 5-15 for more information. Circle 0.2 bar, square 0.3 bar, triangle 0.4 bar and cross repeats. 105
Figure 5-13: DoE summary of whey protein rejection. A) Whey proteins rejection (%) based on outlet pressure (bar) sorted by temperatures. Circle 10°C, square 30°C, cross 50°C and triangle repeats. B) Whey proteins rejection (%) based on temperature (°C). The lines indicate the tendencies observed during the DoE study, see Figure 5-15 for more information. Circle 0.2 bar, square 0.3 bar, triangle 0.4 bar and cross repeats. 106
Figure 5-14: Permeate line protein ratio at the end of the filtration and outlet pressure of the processing sorted by processing temperature. Circle 10 °C, square 30 °C and triangle 50 °C. 111
Figure 5-15: Parameters coefficients of the factors studied (Outlet pressure and temperature) and the statistical reliance on the responses obtained. Left graph is factor influence over casein rejection. Right graph is factor influence over whey proteins rejection. 112
Figure 5-16: Resistance values for samples processed at 30 °C, TMP 0.5 bar ± 0.01 bar and CFV 1.4 m s^{-1} ± 0.3 m s^{-1}. Membrane resistance values of 3.3, 5.0 and 3.1 $x10^{+11}$ m^{-1} for the 0.17, 0.3 and 0.44 bar respectively. Total resistance (green cross), reversible fouling resistance (yellow square) and irreversible fouling resistance (red triangle). 113
Figure 5-17: Protein breakdown of samples processed at an operating temperature of 10 °C. Processing outlet pressure of 0.2 bar for exp 1, 0.3 bar for exp 7, and 0.4 bar for exp 2. ... 115
Figure 5-18: Protein breakdown of samples processed at an operating temperature of 30 °C. Processing outlet pressure of 0.16 bar for exp 5, 0.3 bar for exp 9, 0.3 bar for exp 11, and 0.44 bar for exp 6. 116
Figure 5-19: Protein breakdown of samples processed at an operating temperature of 50 °C, with the exception of exp no 8 that was at 58.3 °C. Processing outlet pressure of 0.2 bar for exp 3, 0.3 bar for exp 8, and 0.4 bar for exp 4. 117
Figure 5-20: Protein breakdown of exp 2 and 4 processed at 0.4 bar and exp 6 operated at 0.44 bar of outlet pressure. Processing temperature 10 °C for exp 2, 30 °C for exp 6, and 50 °C for exp 4. 118

Figure 5-21: Sequential filtration for the SF1 and SF1P experiment (values correspond to Table 5-20). 122
Figure 5-22: Sequential filtration for the SF2, SF2P (permeate line) and SF2R (retentate line) experiment (values correspond to Table 5-21. 123
Figure 5-23: SF1 experiment protein breakdown distribution data. Error bars correspond to the standard deviation of 2 repeats for each data point.....124
Figure 5-24: SF2 experiment protein distribution data for the permeate route. Error bars correspond to the standard deviation of 2 repeats for each data point. 125
Figure 5-25: SF2 experiment protein distribution data for the retentate route. Error bars correspond to the standard deviation of 2 repeats for each data point. 126
Figure 5-26: Final permeate flux and CN/Wy permeate ratio for sequential filtration 1, SF1 and SF1P final permeate data. Error bars correspond to the standard deviation of 2 repeats for each data point. 127
Figure 5-27: Final permeate flux and CN/Wy permeate ratio for sequential filtration 2, SF2, SF2R and SF2P final permeate data and SF2 retentate CN/Wy ratio (blue triangle). Error bars correspond to the standard deviation of 2 repeats for each data point. 128
Figure 5-28: SEM pictures of virgin membrane vs fouled membranes at 0.5 or 1 bar of TMP and at 10 or 50 °C of temperature. CFV was maintained at 1.5 m s^{-1} for the 10 °C samples and 1.3 m s^{-1} for the 50 °C samples. 130
Figure 5-29: FTIR spectra of a conditioned membrane (grey) and a fouled membrane (yellow). Red arrows highlight casein and whey proteins reference peaks.....131
Figure 5-30: FTIR spectra of CFV changes on peak intensity. Fouled samples obtained at 10 °C and 0.5 bar of TMP. Red circles highlight casein and whey proteins reference peaks. ..132
Figure 6-1: Set of initial industrial based conditions to study. 134
Figure 6-2: Casein (blue-straight lines), whey proteins (orange-diamonds) and differential rejection (casein rejection - whey rejection, green squares) values of the industrial conditions 1 bar-1 TMP, 1 bar-0.5 TMP and 0.5 bar-0.5 TMP as shown in Figure 6-1. Temperature and CFV for all samples were maintained at 10 °C and 1.3 m s^{-1}, respectively. Casein and whey rejection values are obtained compared to final feed composition. Samples have been denoted as shown in Figure 6-1. The error of the measurements was of 5%, 9% and 7% for the 1 bar-1 TMP, 1 bar-0.5 TMP and 0.5 bar-0.5 TMP, respectively. 135
Figure 6-3: Comparison of Casein/whey proteins ratio at the permeate line of the industrial conditions shown in Figure 6-1. Temperature and CFV for all samples were maintained at 10 °C and 1.3 m s^{-1}, respectively. Error bar corresponds to the standard deviation of 3 repeats for each data point. 136
Figure 6-4: Casein (blue-straight lines), whey proteins (orange-diamonds) and differential rejection (casein rejection - whey rejection, green squares) values of the 1 bar-1 TMP-11°C (1

bar-1 TMP), the 1 bar-1 TMP-48°C, the 1 bar-0.5 TMP-11°C (1 bar-0.5 TMP) and 1 bar-0.5 TMP-44°C. Outlet pressure and CFV for all samples were maintained at 1 bar and 1.3 m s^{-1}, respectively. Casein and whey rejection values are obtained compared to final feed composition. Samples have been denoted as Outlet pressure-TMP-Temperature. The error of the measurements was of 5%, 5%, 9% and 6% for the 1 bar-1 TMP-11°C (1 bar-1 TMP), the 1 bar-1 TMP-48°C, the 1 bar-0.5 TMP-11°C (1 bar-0.5 TMP) and 1 bar-0.5 TMP-44°C, respectively. 137
Figure 6-5: Comparison of Casein/whey proteins ratio at the permeate line of 1 bar-1 TMP-11°C (1 bar-1 TMP), the 1 bar-1 TMP-48°C, the 1 bar-0.5 TMP-11°C (1 bar-0.5 TMP) and 1 bar-0.5 TMP-44°C. Outlet pressure and CFV for all samples were maintained at 1 bar and 1.3 m s^{-1}, respectively. Error bar corresponds to the standard deviation of 3 repeats for each data point, with the exception of the 1 bar-1 TMP-48°C and the 1 bar-0.5 TMP-44°C that had 2 repeats each. 138
Figure 6-6: Casein (blue-straight lines), whey proteins (orange-diamonds) and differential rejection (casein rejection - whey rejection, green squares) values of samples obtained with increasing TMP: 0.5, 1, 1.4, 2.8 and 4.7 bar. CFV for all samples was at 1.3 m s^{-1} and temperature ranged between 10 and 20 °C. Casein and whey rejection values are obtained compared to final feed composition. Error bars correspond to the standard deviation of 3 repeats for each data point. 139
Figure 6-7: Comparison of Casein/whey proteins ratio at the permeate line of samples obtained with increasing TMP: 0.5, 1, 1.4, 2.8 and 4.7 bar. Outlet pressure and CFV for all samples were maintained at 1 bar and 1.3 m s^{-1}, respectively and temperature ranged between 10 and 20 °C. Error bars correspond to the standard deviation of 3 repeats for each data point. ... 140
Figure 6-8: Comparison of Casein/whey proteins ratio at the permeate line of all samples analysed based on temperature changes. Outlet pressure of 0.5 bar (orange dash), 1 bar (grey triangles) and 5 bar (yellow squares). Error bars correspond to the standard deviation of 3 repeats for each data point. 140
Figure 6-9: Flux decline curves of the 1 bar-1 TMP (Inlet and TMP at 1 bar), 1 bar-0.5 TMP (Inlet at 1 bar and TMP at 0.5 bar) and 0.5 bar-0.5 TMP (Inlet and TMP at 0.5 bar) conditions, processed at 10 °C and CFV of 1.3 m s^{-1}. 1 bar-1 TMP (blue triangles), 1 bar-0.5 TMP (orange dots) and 0.5 bar-0.5 TMP (grey squares). Error bars correspond to the standard deviation of 3 repeats for each data point. 141
Figure 6-10: Flux decline curves of the temperature modified Initial and 1 bar-0.5 TMP conditions: 1 bar-1 TMP-11°C (1 bar-1 TMP, blue triangle), the 1 bar-1 TMP-48°C (dark blue square), the 1 bar-0.5 TMP-11°C (1 bar-0.5 TMP, orange dot) and 1 bar-0.5 TMP-44°C (brown dash). Outlet pressure and CFV for all samples were maintained at 1 bar and 1.3 m s^{-1}, respectively. Samples have been denoted as Outlet pressure-TMP-Temperature. Error bars

correspond to the standard deviation of 3 repeats for each data point, with the exception of the 1 bar-1 TMP-48°C and the 1 bar-0.5 TMP-44°C that had 2 repeats each. 143
Figure 6-11: Flux decline curves of the samples obtained with increasing TMP: 0.5 (grey squares), 1 (blue triangles), 2.8 (dark-grey diamond) and 4.7 bar (yellow dash). CFV for all samples was at 1.3 m s^{-1} and temperature ranged between 10 and 20 °C. Casein and whey rejection values are obtained compared to final feed composition. Error bars correspond to the standard deviation of 3 repeats for each data point. 144
Figure 6-12: Comparison of final permeate flux to the CN/Wy ratio, based on processing temperature: at 6 °C (orange dots), 10 °C (grey triangles), 16-20 °C (yellow dash), 44 °C (blue square) and 48 °C (green cross). Error bars correspond to the standard deviation of 3 repeats for each data point, with the exception of the 44 and 48 °C conditions that have 2 repeats each. 145
Figure 6-13: Casein rejection in the permeate line compared to final permeate flux. Labels based on processing temperature: 6 °C (orange dots), 10 °C (grey triangles), 16-20 °C (yellow dash), 44 °C (blue square) and 48 °C (green cross). Error bars correspond to the standard deviation of 3 repeats for each data point, with the exception of the 44 and 48 °C conditions that have 2 repeats each. 146
Figure 6-14: Protein concentration on measured membranes, comparing fouled and rinsed membranes under the same conditions. Error bars correspond to the standard deviation of 2 repeats for each data point. Sample names are as follow: Outlet Pressure-TMP.....147
Figure 6-15: Chromatogram comparing fouled (a) and rinsed (b) samples obtained at 0.5 bar outlet pressure and 0.5 bar of TMP. The chromatogram is a representative example of all conditions shown in Figure 6-14. RP-HPLC system with UV-Vis detection at 214 nm, centred into the beta casein and whey peaks.....148
Figure 6-16: Protein distribution of fouled and rinsed samples obtained under the same conditions (Figure 6-14). Error bars correspond to the standard deviation of 2 repeats for each data point. Sample names are as follow: Outlet Pressure-TMP.....149
Figure 6-17: Protein distribution of milk compared to fouled samples obtained at increasing temperature. Error bars correspond to the standard deviation of 2 repeats for each data point. Sample names are as follow: Outlet Pressure-TMP-Temperature.....149
Figure 6-18: Protein distribution of milk compared to fouled samples obtained at increasing TMP. Error bars correspond to the standard deviation of 2 repeats for each data point. 150
Figure 6-19: Comparison of Normalised Casein/whey proteins ratio of milk and fouled samples shown in Figure 6-17. Error bar corresponds to the standard deviation of 2 repeats for each data point. Sample names are as follow: Outlet Pressure-TMP-Temperature. 151

Figure 6-20: Estimated fouling layer thickness based on protein amount on membranes. Blue triangles (TMP of 1 bar), orange dots (TMP 1 bar) and grey squares (TMP >1 bar). Error bars correspond to the standard deviation of 2 repeats for each data point. 152
Figure 6-21: Protein concentration on samples produced at increasing temperature while maintaining TMP and inlet/outlet pressures constant at 1 bar. Error bars correspond to the standard deviation of 2 repeats for each data point..... 153
Figure 6-22: Protein concentration on samples produced normalised by the amount of milk processed through the membrane, obtained at increasing temperature while maintaining TMP and inlet/outlet pressures constant at 1 bar. Error bars correspond to the standard deviation of 2 repeats for each data point. Sample names are as follow: Temperature..... 154
Figure 6-23: Effect of rinse step time duration modification while CFV was kept constant at 0.53 m s^{-1}. Error bars correspond to the standard deviation of 2 repeats for each data point. 157
Figure 6-24: Effect of rinse step CFV modification while time was kept constant at 10 min. Error bars correspond to the standard deviation of 2 repeats for each data point. 158
Figure 6-25: Total (resistance due to all fouling phenomenon), reversible (resistance due to fouling removed after the rinse step), and irreversible (resistance due to fouling that is not removed after the rinse step) resistances for fouling conditions at TMP 0.28 bar and 1.47 bar. Error bars correspond to the standard deviation of 2 repeats for each data point. 160
Figure 6-26: Flux data over time for incremental pressure modifications of 0.5 bar/step, using RO water at 30 ± 1.5 °C. 163
Figure 6-27: Flux data over TMP comparing the flux reduction at each step of pressure change, complementary to Figure 6-26, using RO water at 30 ± 1.5 °C. 1st, 2nd, 3rd and 4th make reference to the measurements order, after the 1st measurement all the other measurements were taken after the TMP had been increased and decreased. 163

List of Tables

Table 1-1: Applications of milk proteins in food products (modified from Fox *et al.* 2015).[10,15–18] 5
Table 2-1: Typical protein concentration by protein groups.[10,21] 11
Table 2-2: Summary table of the main articles in the field of milk protein analysis..... 31
Table 2-3: Casein and Whey main protein groups Isoelectric point and Average Molecular Weight.[10,33] 34
Table 2-4: Summary of MF and UF key parameters for polymeric membranes.[3] 40
Table 3-1: Crossflow experimental conditions used for Bench Top M10 and Pilot Scale adapted from Argyle 2015.[86] 49

Table 3-2: Pilot Scale membrane module specifications.....58
Table 3-3: Differences among Bench Top M10 and Pilot Scale. 59
Table 4-1: Results of analysis of Accuracy and precision. The concentrations for all proteins are 0.3, 1.6 and 4.2 mg mL^{-1}. 80
Table 4-2: Summary table of regression parameters, range analysed, LOD and LOQ. 81
Table 5-1: Protein rejections and processing conditions of Figure 5-2. All experiments were carried out at using the 0.1 µm PVDF membrane (Synder Filtration, V01) at 10 °C. Samples have been denoted as following: Outlet pressure-TMP-CFV.....88
Table 5-2: Operational conditions of flux decline curves 50°C-1.1 m s^{-1}, 50°C-1.6 m s^{-1} and 10°C-1.5 m s^{-1}. Samples have been denoted as following: Temperature-CFV.....90
Table 5-3: Protein rejection values at the end of filtration time (3600s) for samples 50°C-1.1 m s^{-1}, 50°C-1.6 m s^{-1} and 10°C-1.5 m s^{-1}, with the casein to whey protein ratio at the final permeate. Samples have been denoted as following: Temperature-CFV. 94
Table 5-4: Operational conditions of flux decline curves 10°C-1.5 m s^{-1}, 10°C-1.3 m s^{-1}, 10°C-0.8 m s^{-1} and 10°C-0.6 m s^{-1}. Samples have been denoted as following: Outlet pressure-TMP-CFV-Temperature. 94
Table 5-5: Protein rejection values at the end of filtration time (3600s) for samples 10°C-1.5 m s^{-1}, 10°C-1.3 m s^{-1}, 10°C-0.8 m s^{-1} and 10°C-0.6 m s^{-1}, with the casein to whey protein ratio at the final permeate. Samples have been denoted as following: Temperature-CFV.....96
Table 5-6: Sample concentration used in the concentration tests feed, the volume was kept at 3.7 L.....99
Table 5-7: Membrane concentration study data of all milk proteins, where low and medium concentrations were obtained by water dilution, always maintaining the same feed volume. The method error for protein concentration analysis was of ±5%. 99
Table 5-8: Membrane concentration study data of casein proteins, where low and medium concentrations were obtained by water dilution, always maintaining the same feed volume. The method error for protein concentration was of ±5%.....100
Table 5-9: Membrane resistance values breakdown for the concentration test, all test had feed volume of 3.7 L (Table 5-6). All resistances are $x10^{+11}$ (m^{-1}). Total resistance (Rt), membrane resistance (Rm), reversible fouling resistance (Rrev, obtained when subtracting Rir from Rt) and Irreversible fouling resistance (Rir, resistance measured after rinse step). 101
Table 5-10: Experiments of DoE test with the experiment order and factors of each experiment. 102
Table 5-11: Casein and whey proteins rejections values for the three repeats operated at the same conditions. 103

Table 5-12: DoE main results table, including input factors and analysed responses (casein and whey protein rejection and whey proteins ratio enhancement), as well as feed and permeate protein ratio based on responses data. 107
Table 5-13: DoE results based on outlet pressure 0.3 bar, showing the casein and whey proteins rejections and feed and permeate protein ratios (casein/whey) and the whey proteins ratio enhancement at the permeate line. 107
Table 5-14: DoE results showing pairs of same temperature and different outlet pressures, showing the casein and whey proteins rejections and feed and permeate protein ratios (casein/whey) and the whey proteins ratio enhancement at the permeate line. 108
Table 5-15: DoE results showing the effect of temperature when outlet pressure is 0.2 bar, showing the casein and whey proteins rejections and feed and permeate protein ratios (casein/whey) and the whey proteins ratio enhancement at the permeate line. 110
Table 5-16: DoE results showing the effect of temperature when outlet pressure is 0.4 bar, showing the casein and whey proteins rejections and feed and permeate protein ratios (casein/whey) and the whey proteins ratio enhancement at the permeate line. 110
Table 5-17: Experimental conditions of the case study experiments that were used to define the initial conditions for the sequential filtration test. 119
Table 5-18: Protein ratios (Casein/Whey) for the case study experiments that were used to define the initial conditions for the sequential filtration test. 120
Table 5-19: Operational conditions of the sequential filtrations experiments. 121
Table 5-20: Sequential experiments data of experiment SF1 with the sequential permeate line (SF1P). The table shows the ratio of casein to whey proteins in each step of the respective filtration process with the final permeate whey protein ratio enhancement at each step. The permeate concentration corresponds to the initial feed for the permeate sequential filtration and the final whey protein enhancement corresponds to the process initial feed to final permeate. 121
Table 5-21: Sequential experiments data of experiment SF2 with respective permeate (SF2P) and retentate lines (SF2R). The table shows the ratio of casein to whey proteins in each step of the respective filtration process with the final permeate whey proteins enhancement at each step. The retentate and permeate concentrations correspond to the initial feed for the permeate and retentate sequential filtration and the final whey protein ratio enhancement corresponds to the process initial feed to final permeate. 122
Table 6-1: Ratio of fouling components on the membrane, comparing all temperatures to 11 °C. Corresponding to Figure 6-21 and Figure 6-22 the total proteins and corrected total proteins, respectively. 154
Table 6-2: Processing conditions of time (left) and CFV (right) tests. The order of the tests was randomised for either factor, first condition for both tables is the same. 156

Table 6-3: Total resistance values shown in Figure 6-23, along with, description of retentate features. Error values correspond to the standard deviation of 2 repeats for each data point. 157
Table 6-4: Total resistance values shown in Figure 6-24, along with, description of retentate features. Error values correspond to the standard deviation of 2 repeats for each data point. 158
Table 6-5: Summary of all conditions studied in descending order of total resistance. Error values correspond to the standard deviation of 2 repeats for each data point. 159
Table 6-6: Total, reversible and irreversible resistance of fouling conditions TMP 0.28 bar and 1.47 bar. Error values correspond to the standard deviation of 2 repeats for each data point. 161
Table 6-7: Flux decrease after incremental pressure reached the 4.0 bar max value and it was returned to the original pressures, as shown above. 164

Nomenclature

CM	Casein Micelles
PVDF	Polyvinylidene difluoride
CCP	colloidal calcium phosphate
MCP	micellar calcium phosphate
TMP	Transmembrane pressure
CFV	Cross-flow velocity
MF	Microfiltration
UF	Ultrafiltration
α-CN	Alpha-casein
β-CN	Beta-casein
κ-CN	Kappa-casein
α-La	Alpha Whey or alpha-Lactalbumin
β-Lg	Beta whey or beta-Lactoglobulin
BSA	Bovine Serum Albumin (whey protein)
Ig	Immunoglobulins
SEM	Scanning Electron Microscope
HPLC	High-Performance Liquid Chromatography
ACN	Acetonitrile
TFA	trifluoroacetic acid
IP	Isoelectric point

Chapter 1. Introduction

Membrane technologies have grown in application in several sectors because of their advantages over traditional technologies of separation (sand filtration, coagulation, evaporation). The advantages are case specific but in general they offer improved quality and sustainability of the process, lower chemical use and lower risk. Figure 1-1 shows the different applications of membranes by sectors and their weight of the overall market. The leading application of membranes is the water and wastewater industry that accounts for 52% of all membrane applications, followed by the food and beverages industry with 21% of the applications and the pharmaceutical with 9%.

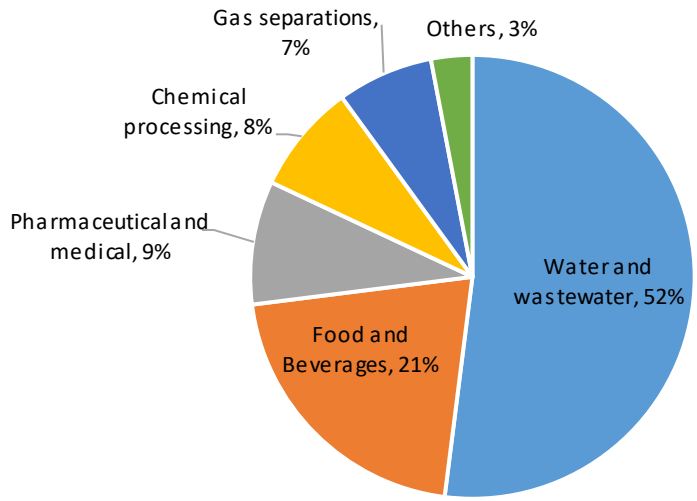

Figure 1-1: Membrane applications by sectors and percentage of use (2017).[1]

The membrane applications in dairy industry (within food and beverages) have evolved from the removal of fat and bacteria to the separation of proteins from lactose and water.

Historically, the membrane applications in the dairy industry started in the 1970s, however, the most important technological development was carried out in the 1960s by the development of a more (but not completely) reliable and reproduceable method of membrane production.[2]

The 1970s was the first-time membranes were used for dairy applications due to the development of materials with better chemical and mechanical resistance such as polysulfone and cellulose acetate and the development of the first sanitary modules.[3,4] The early applications of membrane processes in the 1970s dairy industry focused on the ultrafiltration (UF) of milk to pre-concentrate it before cheese making and for the recovery of protein from whey (by-product).

In the 1980s technological developments in membrane science led to new applications for dairy industry including the first attempts to concentrate milk on farms using UF and reverse-osmosis (RO) membranes, the creation of whey protein isolate using UF and the early separation of β-lactoglobulin and α-lactalbumin.

The 1990s saw further improvement of membrane applications taking advantage of ceramic membranes for microfiltration applications. Several membrane methods were developed to remove spores (improving shelf-life), removing fat from milk (reducing operational challenges) and some early casein removal methods to produce ideal whey (milk without caseins) or even the removal of bacteria using microfiltration (MF) ceramic membranes to produce extended shelf life (ESL) milk.[2]

A summary of the different applications of membranes (by pore size) can be found in Figure 1-2, where it shows the common industrial applications. Microfiltration membranes can be used to remove bacteria since this method avoids damaging the proteins and keeps them in their most active form preserving their chemical and organoleptic properties unaltered.[5] The removal of spores can be used for consumption milk to keep its properties, but it can also be used to reduce spores in milk used for cheese making allowing to reduce (eliminate) the amount of additives (e.g. nitrates) that are required.[3,4]

Milk protein standardization, usually done using UF membranes, and recently developed using microfiltration (MF), allows to either increase or reduce the amount of proteins present in milk, correcting for any variations in protein content of milk that occur naturally over the year, without the need to add milk powders. One of the industrial advantages of milk standardization is that when used for cheese making the rennet used can be adapted to the amount of proteins, allowing a better control of the process and also improving the post processing steps.[5] Another rising topic in the field, is the fractionation of casein from whey proteins using MF and UF, previously carried out using ceramic membranes. The move towards the implementation of polymeric membranes is due to the lower capital investment per unit and their flexibility to adapt to market trends (do to their lower capital cost) and shifts in product desire.[5]

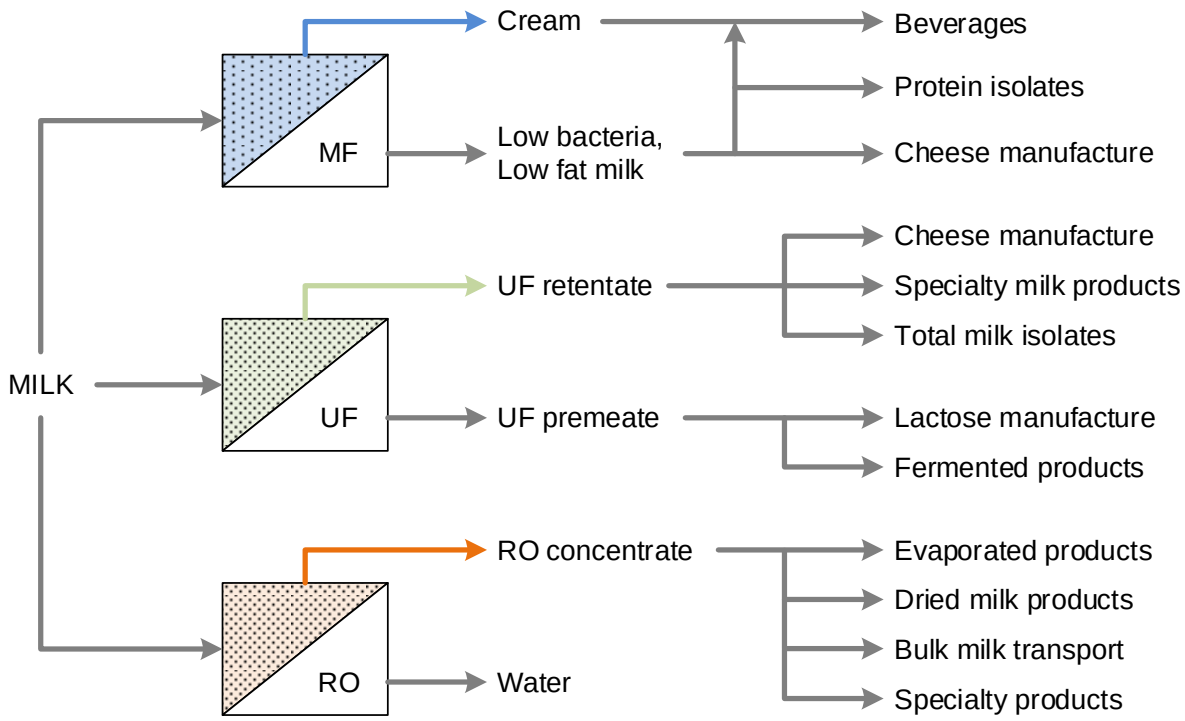

Figure 1-2: Membrane applications in the dairy industry by membrane size and product obtained.[5,6]

Nano-filtration membranes can be used for the demineralisation of the UF permeate (whey) to produce lactose and to concentrate the stream, reducing the amount of water (less energy cost) and the final volume to deal with.[5]

The advancements in membrane applications for the dairy industry were fuelled by the growing global dairy market. The dairy industry can be considered the major animal-sourced food industry by amount since in 2019 milk production reached the 888.1 million tonnes with an expected increase to 921.1 million tonnes for 2021.[7] Compared to meat production worldwide that was "just" of almost of 350 million tonnes by 2018 (almost 2.5 times lower).[8]

The industrial applications for milk proteins are varied and tied to their chemical and biochemical properties, ranging from health additives, to cheesemaking. Gaspard *et al.* (2017) worked on utilising the heat stability of casein proteins to enhance heat stability of the whole milk.[9] They expanded on previous studies that found that a protein ratio of casein/whey of 1/1 improved the heat stability of whey proteins for 30 minutes up to a temperature of 93 °C (above the denaturalisation temperature of whey proteins that starts at >60 °C).[10] Their work showed the chaperone activity that kappa-casein had over whey proteins improving their resistance to high temperatures, however, the temperature resistance enhancement was conditional to certain factors. If the milk had alpha and beta-casein protein group the chaperon activity was stronger, on the other hand, if the milk did undergo a pre-heat step the chaperone activity became less effective.

Infant formula products are of high social and industrial interest and one of the main applications of whey proteins. Interestingly, human milk composition is whey rich with a protein ratio casein/whey of 30/70 unlike bovine milk that is casein rich with a ratio of 80/20.[11] In addition, human milk also has different main protein groups composition. For instance, in human milk there is no β-Lg of the whey proteins or α-casein, which are dominant in bovine milk.

Further applications on dairy proteins are shown and summarised in detail in Table 1-1 .[10,12–14]

Table 1-1: Applications of milk proteins in food products (modified from Fox *et al.* 2015).[10,15–18]

Caseins/caseinates/co-precipitates		
	Used in	**Effect**
Dairy products	1. Imitation cheeses (vegetable oil, caseins/caseinates, salts and water) 2. Coffee creamers (vegetable fat, carbohydrate, sodium caseinate, stabilizers and emulsifiers) 3. Cultured milk products, e.g., yoghurt 4. Milk beverages, imitation milk, liquid milk fortification, milk shakes 5. High-fat powders, shortening, whipped toppings and butter-like spreads	1. Fat and water binding, texture enhancing, melting properties, stringiness and shredding properties 2. Emulsifier, whitener, gives body and texture, promotes resistance to feathering, sensory properties 3. Increased gel firmness, reduced syneresis 4. Nutritional, emulsifier, foaming properties 5. Emulsifier, texture enhancing, sensory properties
Bakery products	Bread, biscuits/cookies, breakfast cereals, cake mixes, pastries, frozen cakes and pastries, pastry glaze	Nutritional, sensory, emulsifier, dough consistency, texture, volume/yield
Beverages	1. Drinking chocolate, fizzy drinks and fruit beverages 2. Cream liqueurs, wine aperitifs 3. Wine and beer industry	1. Stabilizer, whipping and foaming properties 2. Emulsifier 3. Fines removal, clarification, reduce colour and astringency
Dessert products	1. Ice-cream, frozen desserts 2. Mousses, instant puddings, whipped toppings	1. Whipping properties, body and texture 2. Whipping properties, film former, emulsifier, imparts body and flavour
Confectionary	1. Toffee, caramel, fudges 2. Marshmallow and nougat	1. Confers firm, resilient, chewy texture; water binding, emulsifier 2. Foaming, high temperature stability, improve flavour and brown colour
Meat products	Comminute meat products	Emulsifier, water binding, improves consistency, releases meat proteins for gel formation and water binding

Whey proteins		
	Used in	**Effect**
Dairy products	1. Yoghurt, Quarg, Ricotta cheese 2. Cream cheeses, cream cheese spreads, sliceable/squeezable cheeses, cheese fillings and dips	1. Yield, nutritional, consistency, curd cohesiveness 2. Emulsifier, gelling, sensory properties
Bakery products	Bread, cakes, muffins, croissants	Nutritional, emulsifier, egg replacer
Beverages	1. Soft drinks, fruit juices, powdered or frozen orange beverages 2. Milk-based flavoured beverages	1. Nutritional 2. Viscosity, colloidal stability
Dessert products	Ice-cream, frozen juice bars, frozen dessert coatings	Skim-milk solids replacement, whipping properties, emulsifying, body/texture
Confectionary	Aerated candy mixes, meringues, sponge cakes	Whipping properties, emulsifier
Meat products	1. Frankfurters, luncheon meats 2. Injection brine for fortification of whole meat products	1. Pre-emulsion, gelatin 2. Gelation, yield

Combinations of proteins		
Pharmaceutical and medical products	Special dietary preparations for	1. Ill or convalescent patients 2. Dieting patients/people 3. Athletes (whey proteins are in high demand) 4. Astronauts
Pharmaceutical and medical products	Infant foods	1. Nutritional fortification 2. 'Humanized' infant formulae 3. Low-lactose infant formulae 4. Specific mineral balance infant foods 5. Casein hydrolysates: used for infants suffering from diarrhoea, gastroenteritis, galactosaemia, 6. malabsorption, phenylketonuria 7. Whey protein hydrolysates used in hypoallergenic formulae preparations 8. Nutritional fortification
Pharmaceutical and medical products	Specific drug preparations	1. β-Caseinomorphins used in sleep or hunger regulation or insulin secretion 2. Sulphonated glycopeptides used in treatment of gastric ulcers

In summary, fresh milk is still the most consumed dairy product with a growing interest for the proteins derives, such as whey proteins concentrates.[19,20] The focus of the market is to

export “safe” products like cheese and dry powders (milk or proteins). The FAO report highlighted that Europe, USA, New Zealand and Australia are the largest exporters of the previously mentioned products towards countries where the production has been exceeded by the consumption like China and the rest of the South of Asia. The exports of “safe” products refer to dairy products that overcome the challenge of dairy, long shelf-life while maintaining its nutritional values, hence the interest in spray-drying into powders the dairy products once the milk has been processed into the desired product. The growing demand for processed dairy products like protein isolates, requires better processing tools like membranes for enhanced protein separation.

As has been highlighted previously, milk is widely used as a food product with expanding applications in the food industry with a new focus on the health promoting benefits. In order to access the most valuable compounds in milk, proteins and immunoglobulins, separation methods are required. Filtration is one of the safest methods to initially process milk since it does not chemically alter the milk. However, the filtration methods do still not achieve the commercially desired rates of separation, especially when using polymeric membranes. There is a clear industrial interest into the improvement of the polymeric membrane separation methods and specially in understanding the mechanisms behind the separation and the effect that the fouling layer has over the whole process. This industrial interest is the main reason for the partnership with Tetra Pak that aimed at understanding the membrane-milk interaction when using MF membranes to process bovine milk.

1.1 Aim of the project

The aim of this project was to obtain permeate streams rich in whey proteins while keeping casein proteins in the retentate. The separation of these two broad groups of proteins (casein and whey) would act as the first step towards extracting the highest value out of milk components, for example, immunoglobulins which can be found within the whey proteins group. The project aims to contribute to a better separation of the protein groups to enhance their applications while keeping environmental costs at a minimum by improving the knowledge of the membrane separation and the key factors that influence it. In line with this, the overall objective of this thesis is to achieve a retention of casein proteins above 95% while minimising the whey proteins rejection when using 0.1 µm PVDF membranes and testing several processing conditions. In order to achieve it a set of objectives were defined:

- Develop an analytical methodology to detect and quantify the main proteins groups in bovine milk
- Understand the effect that Outlet pressure, transmembrane pressure and temperature have on protein separation
- Study a set of real industrial conditions to explain protein separation and fouling formation
- Study the changes in the fouling layer and its effect on the filtration process

1.2 Scope of the project

The project's scope is to achieve casein and whey proteins pure streams using microfiltration polymeric membranes to remove casein micelles from the milk while allowing whey proteins to go through the membrane.

The membranes were selected as the processing method to expand on current industrial operations that focus on membrane filtration when trying to fractionate casein and whey proteins. The industrial collaboration with Tetra Pak focused on testing current industrial practices to understand how the filtration happened, which factors had a major role in it and the effect in fouling composition. The membranes were of PVDF due to industrial requirements, since PVDF are widely used in industry in part due to their chemical stability that allow to apply a wide spectrum of cleaning regimes to the membranes without damaging them.

The project focused on the low temperature (10 °C) filtration because there are operational advantages at low temperature like the low rate of growth of bacteria, which allows for longer operational times. Another effect of the low temperatures is the unbinding of the beta-casein proteins from the casein micelle, favouring their monomer form which should slip through the membrane at a higher rate than the other casein proteins, which can be a challenge to produce whey-protein rich permeates and a boon to produce special products. This difference in casein proteins groups should be of interest for the production of whey-proteins rich permeate with a minor fraction of caseins, the greatest example are infant formula products. However, high temperatures (30 and 50 °C) were also studied for comparison of protein behaviour and filtration performance overall.

The used feed for the project was skimmed-milk. The main reason for using it was to replicate as closely as possible an industrial setting where the fat is also removed from the milk before the filtration step.

The protein analysis was done using HPLC and the membranes were characterised using the HPLC itself, SEM and FTIR to understand the interactions of the membrane and the milk components.

Chapter 2. Literature review

The following chapter provides an overview of membrane technology applied to food science, common analytical techniques and general protein behaviour. The review focuses on the main applications of membrane technology on milk processing.

2.1 The properties of milk

Bovine milk (milk refers to bovine milk if not specified, other types of non-human milk are not relevant to this study since it does focus on bovine milk) is a complex matrix formed by the combination of water, salt, lactose, fat and proteins (Figure 2-1). Proteins amount to just 3.4% of milk composition, casein being 2.8% and whey proteins 0.6% of the total composition, that is mainly composed of water (>80%).[10]

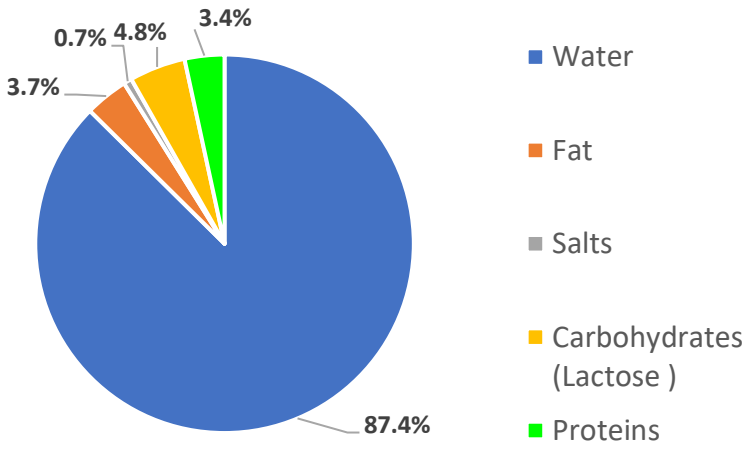

Figure 2-1: Average cow milk composition, it does change based on the lactation stage, the cow's diet and the cow's breed .[10]

Casein proteins are the dominant protein group in bovine milk representing 82% of all milk proteins whereas whey proteins only amount to 18% of the total proteins. Casein proteins can be defined as the proteins that precipitate when milk's pH is reduced to 4.6 at 20 °C, on the other hand whey proteins are the proteins that will remain in suspension in a pH of 4.6 at 20 °C.

The main proteins groups in milk are alpha-casein (α-CN), beta-casein (β-CN), kappa-casein (κ-CN) for the casein proteins, and alpha-Lactalbumin (α-la), beta-Lactoglobulin (β-lg) and Bovine Serum Albumin (BSA) for the whey proteins group.

Table 2-1: Typical protein concentration by protein groups.[10,21]

Protein group	α-CN	β-CN	κ-CN	α-La	β-Lg	BSA
Concentration (g l^{-1})	11.2	11.6	3.15	1.2	4.2	0.6

Immunoglobulins (Ig) represents the minor fraction of the whey proteins group that attracts the most of interest for their health promoting benefits, which makes them the target of recent studies.[17,18,22]

Milk viscosity has a strong dependency with temperature decreasing at high temperatures and increasing at low temperatures (see Figure 2-2).[23] The changes due to temperature are crucial for the processing of the milk since they affect the permeation trough the membrane. The low viscosity values should favour high permeate fluxes, whereas high viscosity values should favour lower permeation and higher demand from the system (energy-wise).

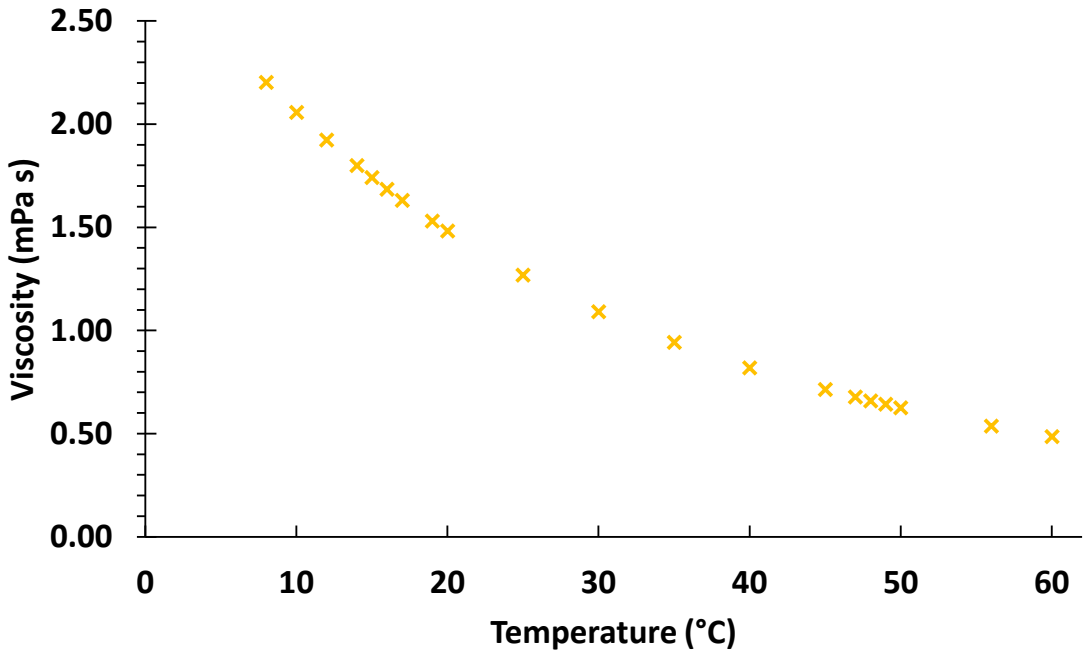

Figure 2-2: Skimmed-milk viscosity changes due to temperature. Based on Bakshi and Smith.[23]

The boiling point of milk is of no particular interest to this project since proteins denature before reaching it. Above 60 °C whey proteins start to denature, losing their nutritional properties and changing shape making the filtration process even more complicated to predict. On the other hand, the milk freezing point is relevant for the project, since casein proteins precipitate out of the milk when thrawn, which will be of interest for the preservation of sample (expanded on Chapter 4) and as an alternative method of separation to membrane filtration known as cryoprecipitation.[24]

The optical properties of milk proteins are relevant since they will influence the detection methods used to detect and quantify them. The protein detection can be carried out at the range 210-220 nm to detect the peptide bond or at 280 nm to detect the aromatic amino acids. When detecting at the lower range (210-220 nm) it is important to take into account that at 220 nm some alpha casein (α_{s2}-CN) are not detectable.[25,26]

Milk proteins display complex structures and depend on the type of protein. Casein proteins do not tend to have secondary or tertiary structure, it is assumed that one of the reasons is the high content of proline residues, which is more significant in β-CN that disrupt the α-helices and β-sheets, however, they form complex aggregations of proteins in the form of casein micelles.[10] On the other hand, the whey proteins do have examples of more complex structures like the β-Lg quaternary structure, even tough they do not display any form of aggregation like the casein micelles.[10]

2.2 Casein proteins

Milk has several biological functions from delivering proteins that enhance the immunological system to calcium carrying and absorption. One of the key functions of milk is to be a calcium carrier, that function is carried out by the casein micelles.

The simple definition of casein micelles is that they are structures of several casein proteins kept together by a combination of hydrophobic interactions and electrostatic interactions involving calcium binding.[27] However, this definition assumes that the dual-binding model presented by Horne (1998)[28] is the best approximation to the micelles.

The discrepancies over the interactions that hold together the micelles have lead several research groups to discuss and try to prove and disprove the different theories.[28–32] The main disagreement seems to rise from the main linking forces of the micelles, on one side the Horne model describe the linking as a mixture of forces between the hydrophobic interactions and electrostatic interactions involving calcium binding,[27] on the other hand we have Holt's (1992) approach that defines the holding force of the micelles as the main action of the calcium phosphate nanoclusters, which cross-link the proteins and keep the micelle together.[31] The Holt theory differs from the Horne theory in the fact that it disregards hydrophobic interaction as main forces in defining the casein structure, both of them agreeing in the importance of the calcium phosphate as a binding force.[27,31]

The above interactions refer to the internal structure of the casein micelles, a piece of micelle structure that holds some agreement is the "hairy micelle" that prevents micelle aggregation.[33]

The hairy micelle is composed of the C-terminal of the κ-casein extending from the surface, which implies electrostatic and steric repulsion keeping the micelles apart from each other.[33,34]

An example of this functionality is that an increase of ionic strength reduces the range of the electrostatic repulsion, which promotes larger polymer formation for both αs1-casein and β-casein whereas an increase in pH will increase the protein charge and it also decreases the final size of any polymer formed by both casein groups. The reduction of electrostatic repulsion can also explain the protein destabilisation and precipitation by acid addition, which will neutralise the surface protein charge when the isoelectric point is reached, or by the opposite method of adding calcium to highly phosphorylated members (that will also remove repulsion between protein clusters and induce aggregation).[35] The κ-casein is the only group that does not bind calcium and therefore it cannot be induced to aggregate by adding ionic calcium.[28]

There is interest in understanding the differences in κ-casein glycosylation in order to explain the "hair" charge and size of the hydrophilic C-terminal.[33] The theory points toward having more stable micelles when the degree of glycosylation increases, and therefore the micelles should be able to be bigger in size. The research regarding the degree of glycosylation points towards an inverse relation between overall presence (relative to the total casein) of κ-casein and final size of micelles,[33,36] and no definitive relation has been found between the glycosylation and the micelle size. It is important to highlight that some of the discrepancies between studies relating glycosylation are in part due to the experimental approach, at the best of the Holland's (2009, chapter 4) knowledge there is not sufficient scientific evidence to draw a conclusion.[33]

2.2.1 Micelle formation and structure

The formation and the stability of casein micelles is a key element in understanding the changes that the micelle, and therefore, the casein micelles will undergo in different processing conditions. For example, at the freezing point calcium phosphate precipitates which reduces the pH to 5.8, this reduction destabilizes the casein micelle that will precipitate when thrawn.[24]

Several models have been developed to describe the micelles over-time. One of the great models to describe the physical and technological properties of the micelles (understanding light scattering, diffusion and viscosity) is the one developed by Alexander *et al.* (2002) that defines the casein micelles as colloidal hard spheres.[37] However, beyond any critical point like having high amounts of whey, lactose or fat, the model loses validity since the internal structure of the micelle suffer radical modifications and alterations, as demonstrated by Horne (2003).[32,33] Other models focused on describing the casein micelles structure went into much detail and tried to develop casein micelle specific models.

One of the first models is the **Sub-micelle** model (see Figure 2-3**)** by Slattery and Evard (1973) and Slattery (1977) with chief elaboration by Schmidt (1980).[30,38,39] The main weakness of the sub-micelle model was that it first explained the casein formation based only on protein interactions, the colloidal calcium phosphate (CCP) did not have any role in the model. It is already known that the calcium and phosphate are involved in the process of phosphorylases the protein chain that occurs post-translation and it is assumed that happens before the creation of sub-micelles.[31,40,41] The revised model ended up being like a several steps process, first the hydrophobic interactions aggregate the caseins into subunits of 15-20 molecules each, each subunit then was "classified" based on the differences in κ-casein molecules. It marked the difference between inner and outer position in the final micelle, the interior of the micelle is composed of poor or depleted in κ-casein units and the exterior is formed by rich in κ-casein sub-micelles (see Figure 2-3). Later on Schmidt (1980) upgraded the model by adding the calcium phosphate as a linker of the sub-micelles.[30]

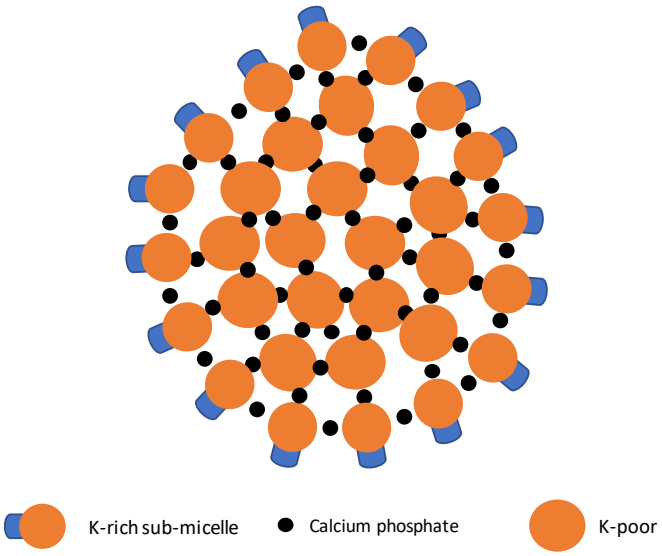

Figure 2-3: Schematic representation of the Sub-micelle model developed by Schmidt (1980)[30] adapted from Horne (2005).[40]

Horne (2006) claims that the sub-micelle model was disproved by SEM studies done by McMahon and McManus (1998),[29] their work even disproved previous work that supported the sub-micelle model by showing that previous results supporting sub-micelle model were an artefact of sample preparation and not real samples.[40] The evolution of this model perception and experimental continuous supports and disproval shows the difficulty to explain casein

micelles (and proteins in general), as well as, how the evolving analytical and optical techniques are helping researches to get closer to the "right" model.

The nanocluster model developed by Holt (1992) is based only on the interactions between calcium and the casein proteins, which hold the whole casein micelle together (Figure 2-4).[31,35] In contrast to the sub-micelle model where there was a combination of hydrophobic forces and calcium (added later on as explain above). The model has evolved, like all the others, with the research and the analytical equipment ending with the definition of calcium phosphate in the form of nanoclusters and with the phosphoseryl cluster of the proteins acting as interaction sites, since they are calcium sensitive. This approach focuses on αs1- and αs2-, making it possible to cross-link the nanoclusters and form 3D structures.[40,42] Compared to the sub-micelle model the nanocluster model is reinforced by the work done by McMahon and McManus (1998).[29]

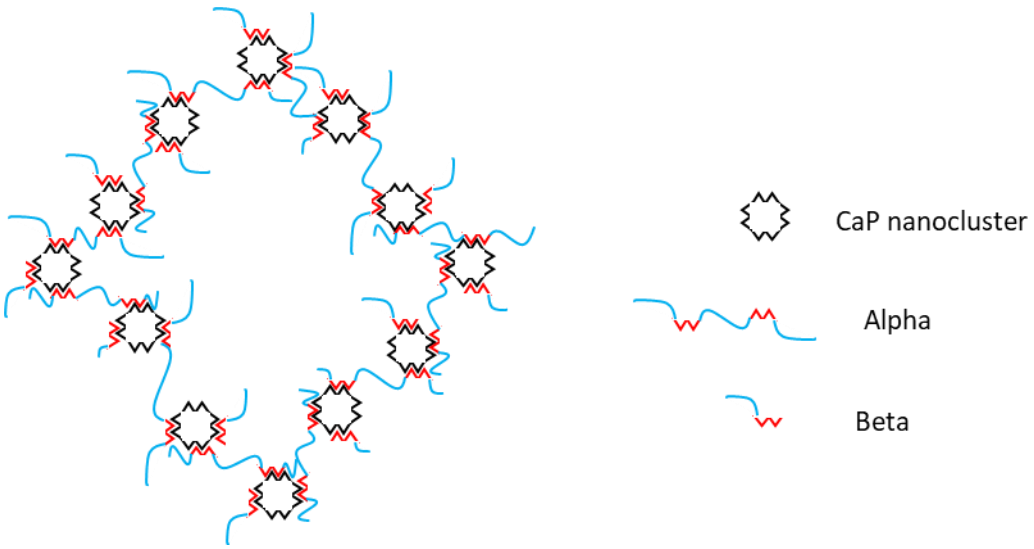

Figure 2-4: Schematic representation of nanocluster model developed by Holt (1992)[31] adapted from Horne (2005).[40] The alpha proteins bind different nanoclusters together promoting chain growth.

The main limitation to the Holt model is the lack of explanation for the role of the κ-casein in the micelle formation and how the micelles aggregation is prevented.

Horne (1998) developed a different version of casein micellar formation that linked the protein interactions with the calcium phosphate, the dual-binding model (see Figure 2-5).[28] Horne saw the calcium phosphate as both a cross-linker agent and a neutralizer. Since calcium phosphate is positively charged it binds to negative phosphoserine clusters (proteins) to reduce their charge, the reduction of the charge promotes other attractive interactions dominance. Horne postulates that in this situation the hydrophobic regions of the caseins can dominate as attractive interactions. The model is also postulated on the observed fact that casein proteins

self-assemble in a micellar type of structure even without calcium and the idea that the CCP will help to form the final bigger micelle.

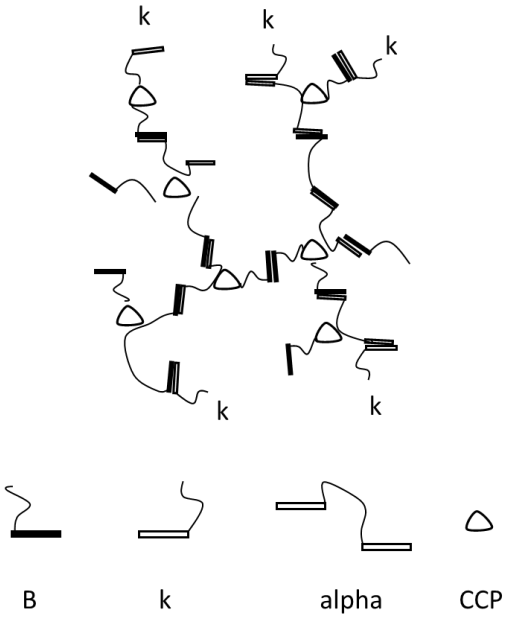

Figure 2-5: Schematic representation of Dual binding model adapted from Horne (1998).[28] Alpha, beta and kappa casein are depicted as indicated. The assumption is that bonding occurs between the hydrophobic regions of each protein (shown as rectangular bars). The hydrophilic regions are linked by the colloidal calcium phosphate clusters (CCP). The kappa-casein proteins limit the growth and they are highlighted with a 'k'.

The main difference between the nanocluster model of Holt and the dual-binding model of Horne is even though both consider calcium a key component of the micelle structure only Horne considers the hydrophobic interactions of the proteins as a key building block for the casein micelle structure.

In order to confirm any of the models several studies have been carried out, a small selection of them showing support for dual-binding or nanoclusters model are shown below:

The work done by Kruif *et al.* (2012) analyses the micelles internal structure using new techniques in order to validate or point towards the best casein micelles models.[42] All their calculations were based as a function of the composition and scattering contrast, then they calculated the static light scattering spectrum, the X-ray and small-angle neutron scattering (SLS, SAXS, SANS).

Kruif *et al.* (2012) summarised that in light of their results the nanocluster model predicted the analysed spectra "quite satisfactorily".[42] However, due to them relying on previously published data for the overall analysis their conclusions are hindered and they can only confirm that nanocluster model "captures the main features of the casein micelles". If their prediction is correct future experiments should validate the nanocluster model.

From the results shown they claim that the sub-micellar model is not consistent and that the scattering of the clusters defined by the model would be undetectable, and since the data shows detectable scatter they discard the model. This would be the second independent study that proves that the sub-micellar model does not agree with experimental data, as shown before by McMahon and McManus (1998).[29]

Referring to the dual-binding model Kruif *et al.* (2012) only claimed that the interaction of only a pair of molecules is not thermodynamically favourable, but they did not make any further comment to highlight why it does not "capture the main features of the casein micelles" like the nanocluster model.[42]

On the other hand, in order to validate the importance of hydrophobicity in casein micelle formation Horne *et al.* have carried several studies.[28,32,33,40,43] In Horne (2017) they found that 1 in 3 caseins residues are hydrophobic when examining their amino acid compositions, being distributed on 32% of αS1-casein, 30% of αS2-casein and 34% β-casein and 28% of κ-casein.[43] The abundant presence of prolyl residues was considered to be a disruptive factor by Slattery, that prevents and inhibits the formation of extended α-helical or β-sheet formations in the caseins, leading to open structures.[44]

Another study by Lucey and Horne (2018) reaffirms that the main drivers for casein association are hydrophobic interactions and electrostatic interactions involving calcium binding.[27] Some key parameters that explain the formation of casein micelles, as they are preventing globular protein structure, are the presence of proline and modifications to the caseins such as phosphorylation and glycosylation, that promote even further the hydrophilic nature of caseins. The phosphoserine residues tend to cluster and this dictates the type of aggregation that casein endures, some caseins may even have multiple clusters. These properties fit well in the dual-binding model since it is built around the idea that phosphoserine clusters are the core of the assembly processes, acting as templates for growth. Phosphate and Calcium binding effectively decrease the charge, helping to facilitate hydrophobic association. It is relevant to highlight that casein micelles are used to deliver calcium and it makes sense that the structure of the micelle requires binding calcium as building block. The removal of calcium by pH modification alters the casein micelles preventing them from remaining stable, if then the calcium and pH are restored a kind of artificial micelles are formed, but with different properties since the template nanoclusters would be lost.

The formation and structure work were later expanded to include the effect of protein concentration and temperature on the micelle and to try to explain their behaviour.

The work carried out by Bouchoux *et al.* (2010)[45] studied the effect that increasing the concentration of casein micelle had on their own structure and the response due to the increase

of concentration. The micelles behave like polydisperse repelling spheres if the aqueous phase that separates them is removed, however, their internal structure does not display any signs of being affected by the aqueous phase removal. The compression of the micelles did lead to a removal of the water that also linked to a volume shrinking.

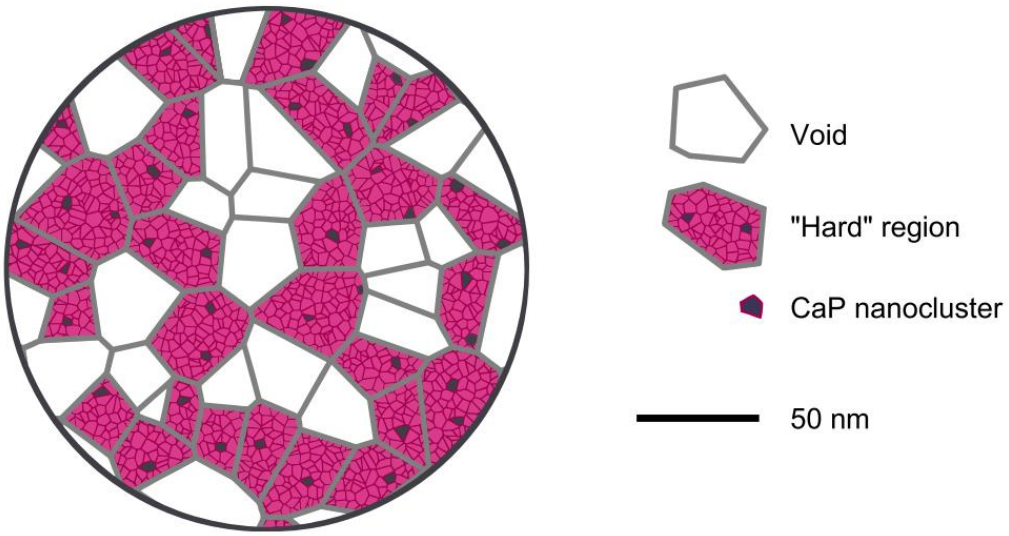

Figure 2-6: Schematic picture of a 200 nm casein micelle's cross section according to the sponge model of Bouchoux *et al.* (2010)[45]. The soft regions are voids filled with solvent and the hard regions contain all the CaP and protein materials. Based on their model the hard regions can be divided into cells that contain either one CaP nanocluster (*dark cells*) or casein molecules and solvent (*lighter cells*). Source: Bouchoux *et al.* (2010)[45].

Bouchoux *et al.* (2010)[45] found that the compression of the casein micelles is "non-affine", which means that not the whole micelle does collapse, certain regions do resist the deformation.[46] They formulated a spongelike casein micelle model that is made of random cells, some sections are empty and can collapse, whereas other are full and cannot be compressed. The model that would explain the behaviour has three-level structure:

The lowest level in the structure is made of CaP nanoclusters that bind the casein molecules. The intermediate level is made of hard regions that can sustain the compression and are made of nanoclusters, these regions range between 10-40 nm. The hard regions occupy around half of the total micelle volume. The superior structural level refers to the casein micelles with an average of ~120 nm).[47]

The work of Beliciu and Moraru (2009)[48] studied the effect of temperature on casein particle size analysing the temperatures 6, 20 and 50 °C, and the effect of the solvent type when using dynamic light scattering (DLS). They found that the best solvent for casein micelle detection was ultrafiltered milk permeate, since it prevented casein dissociation unlike water that favoured casein micelles dissociated leading to irregular results.

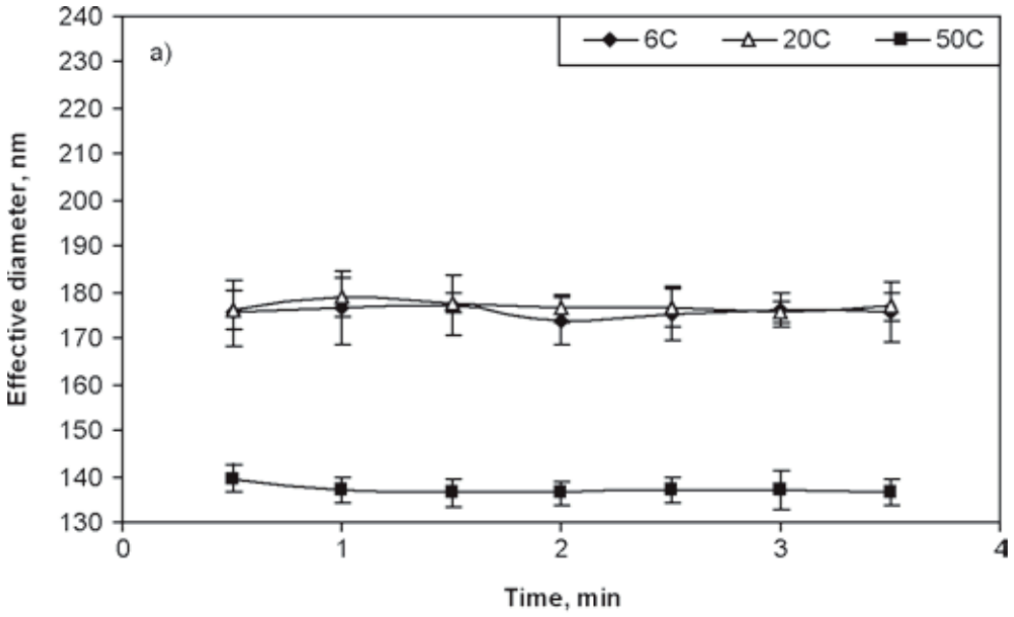

Figure 2-7: Effective diameter of CN micelles found raw skim milk at 6, 20 and 50 °C, when diluted with UF permeate. Source: Beliciu and Moraru (2009).[48]

The casein diameters at 6, 20 and 50 °C were of 180, 180 and 200 nm when using water and of 176, 177 and 137 nm when using ultrafiltered permeate as solvent. This study proved that solvent is a key issue in this type of analysis and that temperature does favour a reduction in casein micelles diameter. The reduced casein micelle diameter combined with a reduced viscosity at high temperature could influence the behaviour of milk filtration at high temperatures, in particular easing the transmission of casein proteins to the permeate, making it harder to fractionate casein and whey proteins.

On balance, lots of work has been carried out over the last 30 years to prove one of the different casein micelles models, as shown above. However, the only fact found so far in the literature is that big rivalries have arisen between Holt *et. al* and Horne *et. al* The agreement point in all of them is that calcium plays a key role in the micelle structure, and that is the main reason it exists.

2.3 Analytical techniques for protein detection

The analytical techniques for milk analysis range from qualitative analysis that determine the protein groups but do not quantify the amount of proteins present in the milk and quantitative methods that both detect the proteins and quantify them.

The analytical techniques used for milk analysis range from chromatography methods like RP-HPLC to methods based in sample digestion like Kjeldahl.[21,25,26,49–58]

The wide range of methods is due to the complexity of detecting all the compounds found in milk and the requirements for an ever-increasing level of separation and accuracy for each compound. The challenge complexity rises due to the natural variation of milk among the different breeds of bovine and the changes that the type of diet have on the milk compositions.[10,25] The complexity of the milk matrix and the improvement on the analytical techniques is the reason that the earlier methods focus on the general casein and whey detection and the most recent methods focus on detecting specific casein or whey protein fractions.[25,52,59,60] The methods range from the early chromatography methods using HPLC for wide spectrum analysis to more accurate analytical techniques that target groups of proteins like several variations of ion exchange used for the differentiation of beta-Lactoglobulin (β-Lg).[56]

2.3.1 High-Performance Liquid Chromatography (HPLC)

HPLC is a chromatographic technique that can be used for the separation and analysis of proteins.[4] Over the last 25 years the improvements to the HPLC speed, sensitivity and resolution have allowed more precise and accurate measurements revolutionising biological science.[52] These features combined with the increasing range of columns, materials and equipment increase the adaptability of HPLC.

The selection of mobile and stationary phase is crucial in HPLC applications to optimise the separation of the target compounds from the original matrix. The column parameters (particle size, stationary phase, length, charge, etc.) need to be selected to provide the right combination of conditions that allow each compound of interest to elute at different times with enough separation from the rest to be both detected and quantified. The challenge of using HPLC is to combine the right column, mobile phase and system to achieve the desired separation profile. The change in mobile phase or stationary phase can be used to modify the affinity of certain compounds which can be used to achieve greater separations. The modification of the temperature can also impact the separation because some particle may change shape based on temperature which will then alter the interaction with the column and phases, this temperature changes are of special interest when studying proteins.

The great adaptability of the HPLC systems has risen them to be one of the most widely used analytical methods. [25,52,61,62] The HPLC capabilities to study compounds range from small to large particles, from nonpolar to strongly polar compounds and ionic compounds, etc. Considering all the properties or modes of operation HPLC types can be catalogued as follow:

1. Reverse-phase chromatography (RPC) has a nonpolar column and uses a mobile phase that is a polar mixture of organic solvent (methanol, acetonitrile, etc.) and water. This is the most used HPLC application mode, extensively used for slightly polar samples that are soluble in water or any polar organic solvent.
2. Ion-exchange chromatography (IEX) can be used for the separation of any ionic or ionisable particle like acids or bases that RPC weakly retains. In this application the stationary phase contains charged groups of the opposite charge of the sample, the ion exchangers contain negative (cation exchangers) or positive (anion exchangers) charges. The aqueous or aqueous-organic mobile phase must contain a buffer or a salt to compete against the sample for the ion-exchange groups of the stationary phase.
3. Normal-phase chromatography (NPC) is used to separate less polar water insoluble samples and isomers. The column has a polar stationary phase (alumina, bare silica) and is paired with a mixture of less polar organic solvents as mobile phase.
4. Size-exclusion chromatography (SEC) is based on inert columns with a controlled distribution of pore sizes that are used to separate high molecular samples taking advantage of the difference in size. Each molecule will advance at a different speed through the column depending on the size, if the molecule cannot get into the pores it will move faster through the column, on the other hand, smaller particles can get into the inner pores increasing the total time to elute. The mobile phase is chosen based on the solubility of the sample and inert and the polarity of the phases depend on the sample polarity and lipophilicity.
5. Chiral chromatography is used on enantiomers separation, it can be used with either RPC or NPC systems with chiral selector additives added to the mobile phase or using a chiral enantio-selective stationary phase.

Each of the previous groups has modifications tailored to the type of molecules targeted and the required level of separation.

In an analytical method there are two parameters that need to be determined for every compound of a mixture in order to identify and quantify them: the limit of detection and the limit of quantification.

The limit of detection (LOD) is defined as the smallest flow or amount of target compound required to obtain a distinguishable signal from the background noise.[63] The signal to noise ratio (S/N) for LOD must be ≥3. Parameters like the sensitivity of the used equipment or the measurement technique Mass spectrometry or UV will allow or not to reach smaller values of detection. When trying to quantify a sample the key value is the limit of quantification (LOQ) which requires a S/N ≥10.

A summary of an HPLC analysis is that the mixture of compounds is injected alongside with the mobile phase into the column, then depending on the equilibrium with the mobile and stationary phase the compounds will create areas of the same particle that will elute at different speeds. In an ideal example all the compounds will be clearly separated by zones of pure mobile phase which makes the identification much easier and reliable.

2.3.1.1 Reverse phase (RP-HPLC)

Reverse phase HPLC uses the differences in hydrophobicity among the compounds to separate them. The separation is based on the hydrophobic binding of the solute compound from the mobile phase to the stationary phase that has hydrophobic ligands.[52]

Usually the sample is added in aqueous buffer followed by the organic phase aiming to elute the different components based on different hydrophobicity. There are two modes of operation, the first one is working with a constant ratio of aqueous and organic phase known as isocratic conditions. The second mode uses a variable ratio of aqueous and organic phase which aims to separate the compounds in increasing molecular hydrophobicity and is known as gradient mode. The combination of mobile phase, stationary phase, column and mode of operation grant a great adaptability to the HPLC systems for the separation of compounds. Milk proteins can be analysed using RP-HPLC as shown by the studies of Bobe *et al.* (1998)[64] and Bonfatti *et al.* (2008).[26] It is important to highlight that if the recovery of biologically active compounds is important there are reported cases of denaturation of proteins using RP-HPLC.[52]

The protein analysis usually employs n-alkylsilica-based as stationary phase with a gradient mode of operation with increasing organic phase, a common organic phase is acetonitrile with a minor addition of TFA as ionic modifier.[25,26] When aiming to differentiate protein groups the slope of the gradient can be modified to alter the speed of the interactions of the compounds with the stationary phase. Other options are the use of a different ionic modifier of the solvent or the organic phase completely, and above all when working with temperature sensible proteins are the changes due to temperature (for example protein configuration changes) since the elution time can suffer significative changes. The modifications of the solvent just need to take into account that they do not interfere with the detection methods, for example 2-propanool and methanol have high optical transparency at the right wave lengths for the analysis of proteins. As a summary acetonitrile is the less viscos solvent and 2-propanol the strongest eluent.[52] The detection wavelength for proteins in the range of UV are between 210 and 220 nm aiming at the peptide bond or 280 nm when targeting the tryptophan and tyrosine aromatic amino acids.

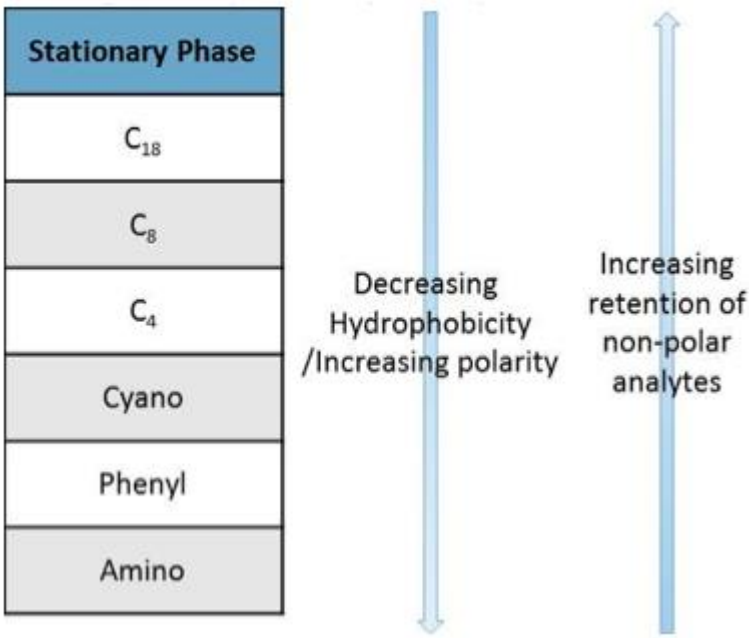

Figure 2-8: Reverse phase stationary phase properties. Source: CHROMacademy.[65]

The silica-based stationary phase also has a hydrophobic ligand attached to it which provides different types of selectivity, the ligands range from the n-octadecyl (C18) to n-octyl (C8) and n-butyl (C4) (Figure 2-8). The ligand selected will affect the separation properties based on the ligand relative hydrophobicity and chain length. The general rule for protein recovery is to use less hydrophobic ligands (n-butyl) with shorter chains. However, the protein recovery can also be obtained using the silica with n-octadecyl.

The pore diameter of the inner particles of the column is a key parameter to determine resolution and peak broadening. The general assumption for protein analysis is that the pore sizes should be ≥300 Å because the proteins will be able to fully interact with the stationary phase, avoiding a restricted diffusion effect that would lead to peak broadening and probably overlapping of protein peaks, negating the capability of detecting and quantifying the proteins.[52]

The method to separate the main protein groups in milk using RP-HPLC has been in development since the work of Bobe *et al.* (1998) and has been under constant improvement.[64] They developed a method to separate and quantify some of the most common genetic variations of the αs1-CN, αs2-CN, κ-CN , β-CN, β-LG and α-LA (Figure 2-9). The only undetected protein group was the BSA which represents up to 10 % of the whey proteins. They chose to detect the protein peaks at 220 nm because it did offer a baseline with less noise, however, at that wavelength the as2-CN was not visible and they had to reanalyse at 210 nm to detect it. The modern HPLC systems are equipped with multiple detectors that nullify this

challenge. They observed a variation of the results below 5.1 % within the same day of analysis and below 7.1 % between days of analysis.

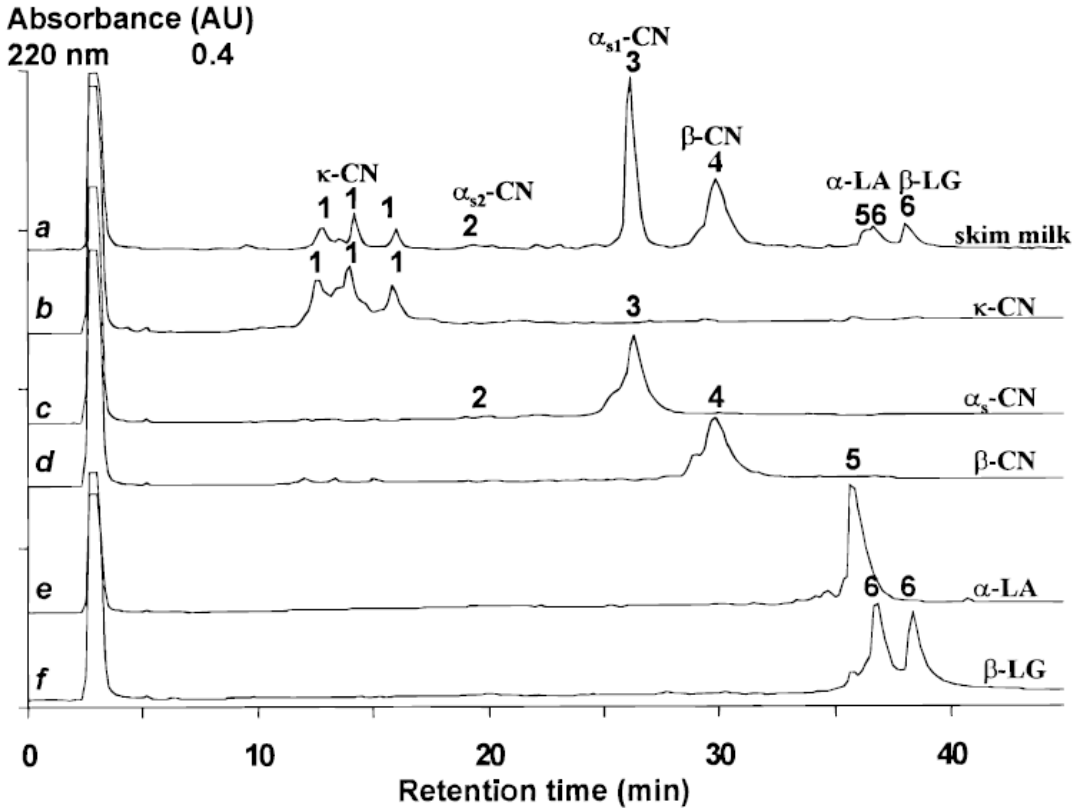

Figure 2-9: Separation of bovine milk proteins and protein standards by RP-HPLC at 220nm. Adapted from Bobe *et al.* (1998)[64]

Bordin *et al.* (2001)[25] used a C4 column to analyse milk proteins and detected them at 214 nm, they claimed that they could separate and quantify the proteins in a single run, and not requiring the previous isolation of whey and casein. The proteins analysed were κ-CN, αs1-CN, αs2-CN, β-CN, β-LG and α-LA with the A and B variants of the β-LG, however, the BSA and Ig whey proteins groups have not been detected yet (Figure 2-10). Bordin *et al.* (2001)[25] did not detect any carry-over of as2-CN when using the C4 column, unlike other studies were the carry-over was detected when using C8 and C18 columns.

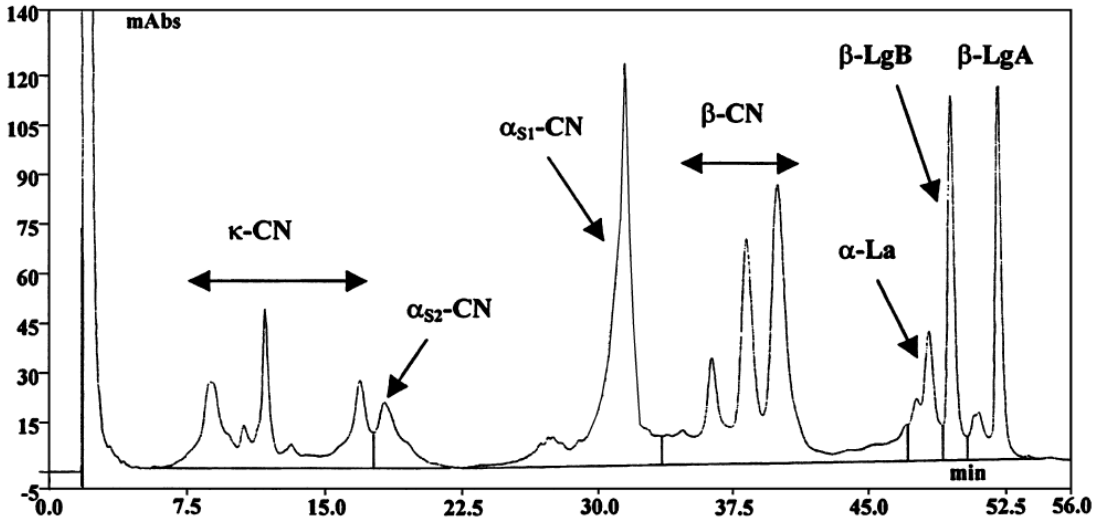

Figure 2-10: RP chromatographic profile of a mixture of protein standard. UV detection is 214nm. The x axis represents the retention time in minutes, and the y axis is the absorbance. Adapted from Bordin *et al.* (2001)[25]

Bonfatti *et al.* (2008)[26] worked on a RP-HPLC method to analyse the main bovine milk protein groups spanning αs1-CN, αs2-CN, κ-CN, β-CN, β-LG and α-LA and the most common variants by breed type. Their work expanded on the previous work done by Bordin *et al.* (2001).[25] However, like the work done by Bobe *et al.* (1998)[64] they did not focus on the combined separation and quantification of BSA. Overall this research developed a working method using RP-HPLC to detect and quantify the main protein groups and was able to even detect some common genetic variations because of breeds. They decided to detect the proteins at 214 nm that enhances protein signal compared to 280 nm were the signal and the intensity are better correlated.

In a later work by Wang *et al.* (2009)[54] they also used a C8 column and 214 nm detection wave length to separate and quantify κ-CN, αs1-CN, αs2-CN, β-CN, immunoglobulins and whey proteins. Their work was based on Bordin et al (2001)[25] which they claim to improve by adding Bis-Tris to the milk before processing to improve the separation and sharpen the peaks of the chromatogram.

The work of Gilar *et al.* (2005)[66] combined two different columns to have a two dimensional HPLC system both RP-HPLC that had different internal conditions. The aim of the study was to properly separate proteins and peptides, to do so they used two C18 columns, the first column was at pH 10 and the second column had an acid pH of 2.6. They managed to get minimal fraction overlap of both peptides and proteins without diluting the signal.

2.3.1.2 Ion exchange chromatography

Ion exchange chromatography (IEX) is based on the net surface charge of particles as separation principle. Each molecule has a different charge with different properties and therefore the degree of interaction with the chromatography media will vary depending on the charge density, the surface charge distribution, and the overall charge.[67] The process is pH dependant because the surface charge is a key parameter, due to this the IEX technique can be useful to take advantage of the link between net surface charge of proteins and pH. The elution in IEX allows to target molecules because it is carried out by the reversible interaction of the oppositely charge media and the charged molecules. In the case of proteins one of the parameters of control is the isoelectric point (IP), the pH in which the protein surface charge is neutralised. Proteins with a pH below the IP bind to cation exchangers (negative charged media), and if the pH is above the IP they bind to anion exchangers (positive charged media).[67]

The matrix of an IEX column is formed of spherical particles with ionic groups charged negatively or positively, which are porous with high surface area. The typical analysis process consists of a certain steps, starting with the addition of a buffer solution that will set the optimal ionic strength and pH, aiming to ensure that only the target proteins bind to it and the impurities do not. Once the sample has been added a buffer, with the same pH and ionic strength as the starting buffer, is used to wash up particles with the same charge as the ionic group and non-charged particles, isolating the target proteins. The remaining step consists on eluting the target proteins that are bound to the column, it can be achieve increasing the ionic strength by adding salt with Cl^- or Na^+ or modifying the pH.[67] The final step is the column regeneration using a buffer with high ionic strength to remove any compound still attached to the column. The bound proteins will elude in ascending order of their charge, the first proteins to elute are the ones with the lowest charged at the selected pH.

The IEX is a flexible analytical technique due to the pH and buffer selection, since both of them can modify the net charge of the column and selectively target proteins. The elution phase also allows to target for the separation of certain particles.

Ye *et al.* (2000)[59] studied the separation and recovery of whey proteins from rennet whey. They found that β-Lactoglobulin can be separated by the absorption and un-absorption to diethylminoethyl-Toy-opearl, a weak anion exchanger. However, they did report that α-Lactalbumin did not bind to the resin and was lost during the analysis. They also used quaternary aminoethyl-Toyopearl, a strong anion exchanger, to ensure that both whey proteins were retained by the resin and separated.

The work of Santos *et al.* (2012)[60] developed a method to separate whey proteins and to target β-Lg using a combined system with an anion exchanger column and a fast protein liquid

chromatography system. They managed to separate the whey proteins in α-Lactalbumin, immunoglobulins and BSA and two fractions of β-Lg. They used a gradient of salts with increasing ionic strength using NaCl, cheap compared to other buffers, which allowed to separate the beta fraction from the rest of whey fractions.

Holland *et al.* (2010) aimed to separate the main casein groups (αs1-CN, αs2-CN, β-CN, κ-CN) using a cation exchange column.[56] They achieved the separation using as elution buffer urea acetate with a NaCl gradient, without any organic component, compared to RP-HPLC.

2.3.2 Mass spectrometry

Mass spectrometry is an analytical technique used to analyse sample from separation techniques like the IEX, RP-HPLC or others, it improves the analysis of the different fractions obtained compared to the UV-Vis detection systems.

Mass spectrometry separates ions of the analysed compounds (inorganic or organic) based on their mass-to-charge ratio (m/Z).[63] The mass spectrometry systems can be organised depending on the targeted molecules or the ionization process used. Figure 2-11 shows the classification of the mass spectrometry applications based on the molecular mass of the target compounds and the hardness or softness of the ionisation phase.

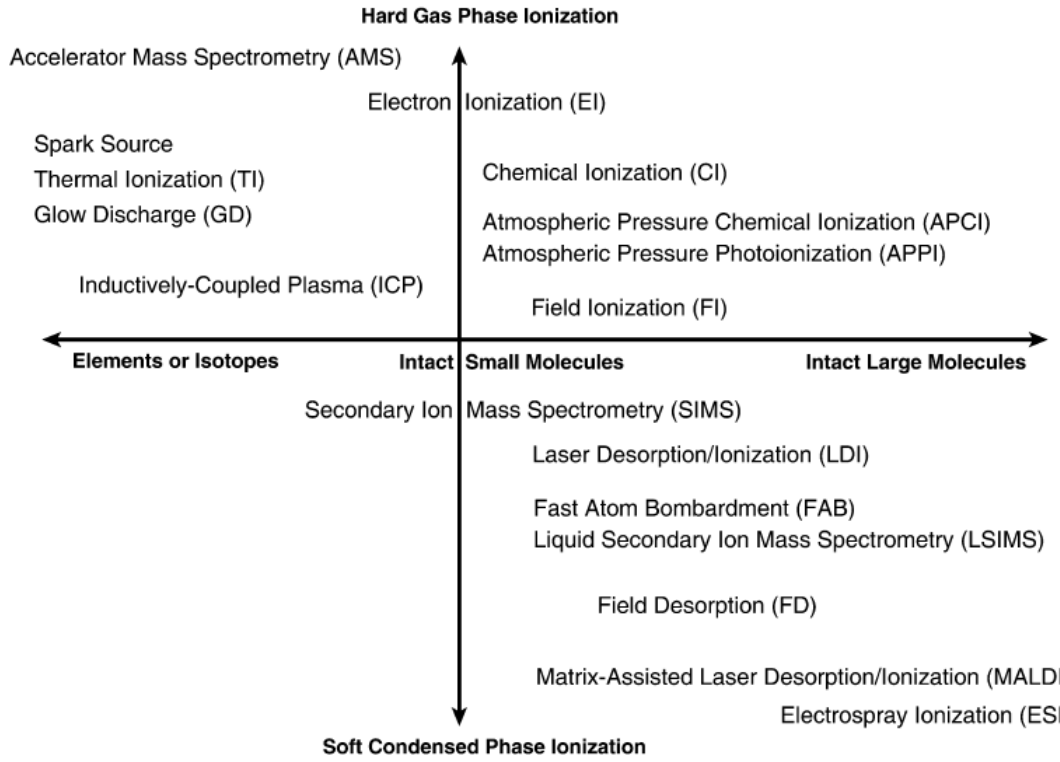

Figure 2-11: Mass spectrometric techniques for different needs arranged by main fields of application and estimated relative hardness or softness. Source: Mass spectrometry.[63]

Even though there is a large selection of mass spectrometry systems (Figure 2-11) they all share a working principle. The analyte can be ionized thermally, by impacting energetic electrons, ions, photons, by an electric field but also by energetic neutral atoms, electronic excited atoms, massive cluster ions and microdroplets that are electrostatically charged. It is important to take into account that ions can range from the clusters and molecules down to single ionized atoms and any of their associates and fragments. The separation of the ions could be effected by electric fields or static or dynamic magnetic fields or by field-free regions.[63]

Compared to detecting with UV-Vis mass spectrometry is a destructive technique which does not allow the recovery of the sample, the advantage is that it uses an extremely low amount of sample, which make it excellent for analysing sample that are hard to obtain or produce up to the nanograms scale.

Protein analysis using mass spectrometry can be carried out using Matrix-Assisted Laser Desorption/Ionization (MALDI). Protein fingerprinting can be done by MALDI up to the detail to determine for example if a cheese is made of goat or cow milk and if there is any contamination to the sample.[63]

Mass spectrometry can be used for a wide range of bovine protein detection, for example, Gasilova *et al.* (2012) worked on a α-lactalbumin and β-lactoglobulin detection method with MALDI-MS to develop a control technique for these two proteins since they are known allergens (Figure 2-12).[68] Their method captured the two proteins using functionalized magnetic beads with antibodies, followed by the application of a transient isotachophoresis and finally MALDI-MS was applied. The LOD was in the nanomolar range ((≤2.1 nM) for each protein.[68]

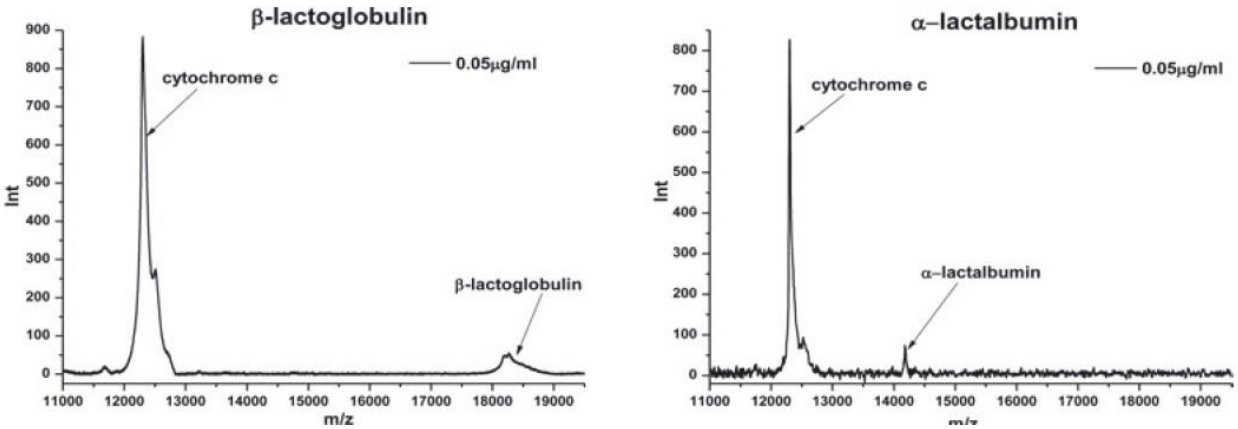

Figure 2-12: MALDI-TOF-MS spectra of two milk whey proteins fractions collected during the CE separation step of typical IACE experiment. Source: Gasilova *et al.* (2012)[68]

Lecoeur *et al.* (2010) worked on a method to differentiate proteins that have similar IP values.[57] Their method was able to quantify BSA, β-LG A, β-LG B and α-LA using extracted ion current (EIC) and single ion monitoring (SIM), the detection had a range of 57-136 nM and 11-67 nM respectively.

The food sector requires high quality standards for safety, for example food allergens must be advertised, in the dairy products product adulteration is one of the main focus.[69,70] The early study of Leonil *et al.* (1995)[69] worked on a method to detect bovine milk adulteration by other milk types or compounds based on mass spectrometry. The initial separation of proteins was carried out using a RP-HPLC column and then they used electrospray ionization mass spectrometry (ESI-MS) to detect all the molecular masses of the proteins to later compare them to the already known masses of bovine milk proteins and common adulteration compounds.

Pierre *et al.* (2013)[58] integrated in a system a capillary organic monolithic column with a high-resolution mass spectrometer (HRMS) to detect two casein protein groups αS-CN and β-CN. The aim was to detect the creation of low-molecular-weight protease-peptones that would indicate the degradation of the milk. In order to carry out the degradation study they extracted the monoisotopic and average molecular masses of the proteins using the excellent permeability, resolution and biocompatibility of organic monoliths for intact protein analysis.

2.3.3 Chemical based analysis

There is a range of chemical based analytical methods to determine the protein concentration. The techniques range from the overall fast protein concentration measurement like Bradford assay to the detailed protein analysis that determine the total amount of whey proteins and casein proteins, but not the individual groups of casein and whey, like the Kjeldahl method.[71–73]

2.3.3.1 Kjeldahl method

The Kjeldahl method is a digestion-based analysis that uses the fact that proteins have a unique nitrogen content to determine the protein groups present. The method it is an acid-based digestion using sulphuric acid to oxidize the organic matter of the sample.

The method protocol can be found in the ISO 8968-1:2014, and it will be described below:

The sample digestion is carried out using a mixture of concentrated sulphuric acid and potassium sulphate. Followed by the addition of sodium hydroxide to the cooled digest, in excess, to release the ammonium ion in the gas form of ammonia. The liberated ammonia gas is then distilled with steam into a boric acid solution in excess. In order to know the ammonia produced a titration with a standard volumetric solution of hydrochloric acid is used.[72] This process determines the amount of nitrogen found in the sample (the total nitrogen), however the quantification of whey and casein protein still requires some steps.

To calculate the total protein nitrogen there are two methods the indirect and the direct method.

The indirect method requires a fresh sample of the milk sample, first the precipitation of the proteins is induced with a solution of trichloroacetic acid, with a final concentration in the mix of around 12%. Proteins will precipitate and they will be removed by a filtration step, the filtrate nitrogen content is then measured following the Kjeldahl method and the non-protein nitrogen is obtained. The true protein nitrogen content can be calculated by making the difference between total nitrogen content and non-protein nitrogen content.

The direct method precipitates the proteins from a fresh sample by also adding a trichloroacetic acid aiming at a concentration of 12%, as well. This method also filters the protein precipitate, however, in the direct method the nitrogen measurement is carried out on the precipitate, calculating the total protein nitrogen.

The Kjeldahl method does not quantify the casein and whey proteins by its forming groups (*i.e* α-cn,β-cn and κ-cn), it can be used to determine the bulk casein and whey proteins present, however, the method can be combined with other techniques like electrophoresis to determine which protein groups are present and to quantify them. Jørgensen *et al.* (2016)[74] used the Kjeldahl method coupled with electrophoresis as analytical technique to analyse and quantify the permeate and retentate of milk after a filtration process.

One of the challenges of the Kjeldahl method is the requirement of specific equipment and trained personal due to the strong acids used and the safety requirements. All these requirements make this method unsuitable to compile with the fast, cheap and safe methodology required for this project. Another challenge it is that it cannot differentiate nitrogen-rich milk adulterations of low molecular mass from the native milk nitrogen, which as seen in the mass spectrometry section is a source of concern.

The study of Gao *et al.* (2015)[51] studied the effect of adulterations by urea, melanine, whey powder, ammonium chloride and ammonium sulphate comparing the ration between non-protein nitrogen (NPN) and crude protein nitrogen (CPN). They found that the non-adulterated milk had values ranging from 0.8084 to 1.4987, and when the adulterated milks were tested

the values were from outside these range, with the only exception of the melamine at low concentrations.

The study of DeVries *et al.* (2017)[75] analysed several method of using the Kjeldahl method to detect food adulterations. They found that when using molecular weight cut-off filtration or tannic acid precipitation in combination with Kjeldahl method could be used to detect adulterations by focusing into the non-protein nitrogen as control, allowing the detection of nitrogen-rich compounds. They defined the limit to detect an adulteration in powders after the filtration or tannic acid of a non-protein nitrogen concentration of ≥0.34 %.

2.3.4 Analytical techniques summary

Table 2-2 is a summary table of some of the relevant methods for protein detection and quantification and examples of research. Currently, the analytical methods developed allow to detect and quantify almost all major protein groups in bovine milk. The aims of the current project require the capability of detecting and quantifying the main protein groups for casein proteins (α-CN, β-CN and κ-CN) and for whey proteins (α-La, β-Lg and BSA) if possible in a single analytical run.

Table 2-2: Summary table of the main articles in the field of milk protein analysis.

Method	Advantages	Disadvantages	Relevant facts	Ref.
RP-HPLC + UV C8 column	Fractionation in a single run: αs1-CN, αs2-CN, κ-CN, β-CN, Ig and Whey proteins	No fractionation: BSA, α-LA and β-LG are not separated of each other	UV-Vis analysis at 214nm	21
RP-HPLC + UV C8 column	Fractionation in a single run: αs1-CN, αs2-CN, κ-CN, β-CN, β-LG and α-LA + most common genetic variants	No fractionation: Ig and BSA	Focus on the separation, detection and quantification of common genetic variants	22
RP-HPLC + UV C4 column	Fractionation of: αs1-CN, αs2-CN, κ-CN, β-CN, α-LA, β-LG B and β-LG A	No fractionation: Ig and BSA	Combination of HPLC+ second derivative UV spectra + peak area ratios	23

RP-HPLC + UV C-18 column	Fractionation of: αs1-CN, αs2-CN, κ-CN, β-CN, β-LG and α-LA	No fractionation: Ig and BSA	All proteins analysed were quantified	64
Anion exchange	Fractionation of: α-LA, β-LG B and β-LG A	No fractionation: κ-CN, α-CN and β-CN from casein group and BSA and Ig from whey proteins	Rennet recuperation of proteins using: Strong anion exchanger, quaternary aminoethyl-Toyopearl	59
Anion exchange	Fractionation of: Ig, BSA and α-LA together and β-LG B and β-LG A	No fractionation: α-CN, β-CN and κ-CN	Fractionation of Whey, separation of β-LG in one step	60
Cation exchange	Fractionation of: αs1-CN, αs2-CN, κ-CN, and β-CN	No fractionation: Ig, BSA, α-LA and β-LG	No need of organic phase. Use of NaCl as gradient and urea acetate.	56
Mass spectrometry MALDI-MS	Fractionation of: α-LA and β-LG	No fractionation: αs1-CN, αs2-CN, β-CN, κ-CN, BSA and Ig	LOD at ≤2.1nM for both proteins	68
Mass spectrometry EIC and SIM	Fractionation of: α-LA, BSA, β-LG B and β-LG A	No fractionation: αs1-CN, αs2-CN, κ-CN, β-CN and Ig	Separation of proteins with similar IP, LOD of 57-136nM (EIC) and 11-67nM (SIM)	57
High-resolution mass spectrometry	Fractionation of: αs-CN, β-CN	No fractionation: BSA, α-LA, β-LG B, β-LG A, κ-CN, and Ig	Separation by capillary organic monolithic column	76
Mass spectrometry ESI-MS	Fractionation of: αs1-CN, αs2-CN, κ-CN, β-CN, α-LA and β-LG	No fractionation: Ig and BSA	Use of RP-HPLC column for the separation and ESI-MS for the analysis	69

Kjeldahl method	Fractionation of: Casein and whey protein groups	No fractionation: Specific protein groups	Analysis of total nitrogen, true protein, non-protein nitrogen	74
Kjeldahl method	Analysis using non-protein nitrogen and crude protein nitrogen	All / None is fractionated	Food adulteration detection ratio NPN/CPN	51
Kjeldahl method	Analysis using non-protein nitrogen	None is fractionated	Food adulteration detection using tannic acid or filtration	75

Based on the literature researched the RP-HPLC methods are the most promising within the boundaries of the available equipment and the available knowledge, which should make the development of a method quite simple.

RP-HPLC is a well-known analytical method, as shown in the literature it has the potential to separate and quantify all interest protein groups, and it also has proven able to carry out the separation in a single analytical run. HPLC in general are flexible enough to be used with UV measurements and mass spectrometry which could be a way to refine the analytical method.

The ion exchange system has shown excellent performance for the separation of small fraction s or the purification of whey or casein proteins, the main drawback is that they require a cation exchanger for the casein proteins and anion exchanger for the whey proteins making it a less versatile option for bulk milk analysis.

2.4 Methods of separation

Membrane based separation methods have become a key step in industry particularly for the food industry since the food applications represent 21% of all membrane used in the whole industry. Membrane processes are easily scalable, they have low energy consumption and usually reduce the need of added water.[77]

Membrane processing of milk has a high commercial interest due to the several advantages of using membranes over other separation methods. First, there is no need of using chemicals in the food compared to the acid precipitation process, avoiding hygiene and safety regulation, however, chemicals are needed for the cleaning phase. Second, membranes can operate in continuous mode which results in a reduced energy consumption and higher volume of protein

produced per unit of surface area in comparison to cryoprecipitation system that requires bigger equipment.

Table 2-3: Casein and Whey main protein groups Isoelectric point and Average Molecular Weight.[10,33]

Properties		pH-isoelectric point			Size
		Average	min	max	Da
Casein Micelles		4.6	-	-	1.0×10^8
Casein	α-CN	4.45	4.2	4.7	2.4×10^4
	β-CN	4.85	4.6	5.1	2.4×10^4
	κ-CN	4.95	4.1	5.8	1.9×10^4
Whey	α-La	-	-	-	1.4×10^4
	β-Lg	5.2	-	-	1.8×10^4
	BSA	-	-	-	6.6×10^4

Amongst the different types of filtration, microfiltration and ultrafiltration are the most widely used for milk fractionation and concentration. Microfiltration is the filtration process where casein micelles can be recovered from skim milk by size exclusion, since the size of the micelles is at least 100 times bigger than the size of the whey proteins, as shown in Table 2-3.[4,78–80] Using this approach native casein micelles are retained at the retentate stream while whey, some casein, lactose and salts stay in the permeate stream. All this filtration processes are normally carried out in skim milk rather than milk (containing fat) due to the presence of fat in milk that would block the membrane.

Industrially the use of concentration steps has proven to increase the efficacy of the membrane separation step, increasing the yields of the process due to the higher content of proteins (reduced water content overall).[81–83] The process starts by concentrating the proteins to factors of 2-5 extracting the water, usually with membranes. The challenges of this approach are the high degree of fouling associated to processing highly concentrated feeds, which then can influence the overall filtration process, and the prevention of proteins loss during the concentration if membranes are used.[84,85] The concentration step can also be used as a first filtration step to start removing small proteins from the initial milk.

2.4.1 Modes of filtration

There are two main modes of filtration Dead end and Crossflow filtration, as shown in Figure 2-13. In Dead end filtration (Figure 2-13a) the feed can either go through the membrane or be trapped on the membrane. In this mode pressure is applied on the feed side forcing all material

liquid and solid to go through the membrane easily forming a cake layer, that will reduce the permeate flux, increasing the energy consumption. The flow is perpendicular to the membrane. This mode is used in batch or semi-batch applications, because the membrane must be removed after it is blocked.[3,86]

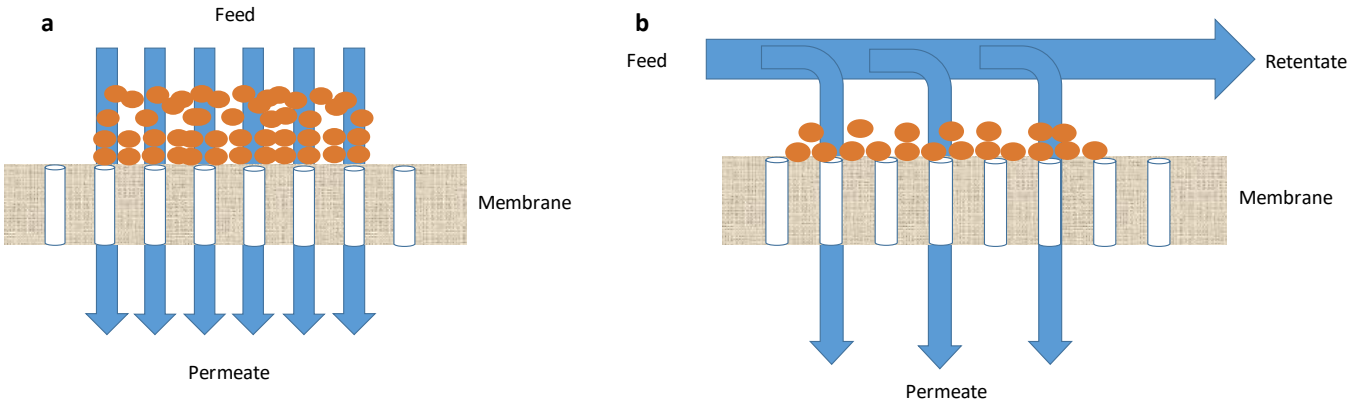

Figure 2-13: Dead end and Crossflow filtration, adapted from Mulder M. (1991)[3]

In crossflow filtration (Figure 2-13b) the pressure is also applied to the feed side, but in this mode the flow is tangential to the membrane, and thus only a fraction of it goes through the membrane, giving rise to two different flows; the retentate, which is the fraction of liquid that does not go through the membrane and the permeate, which is the liquid that goes through the membrane. A significant advantage of this mode is that the cake formation on the membrane is reduced due to the tangential flow that applies a shear force on the membrane, allowing longer runs of the system, with higher flow rates and higher feed concentrations due to reduced pore blocking, which in turns allows to clean the membranes to increase their life-time.[86]

2.5 Fouling and cleaning

2.5.1 Fouling mechanisms

One way to divide the fouling is based on where the fouling occurs and which forces induce it (Figure 2-14). Fouling phenomena has been modelled on several occasions and they are summarised in the work done by R. van Reis and A. Zydney (2007).[87]

Concentration polarisation (CP) is a phenomenon of boundary layer triggered by the partial retention of solute by the membrane. It happens when the solvent goes through the membrane but some of the solute does not, building-up at the retention side of the membrane. The flux decline due to concentration polarisation is very fast when starting a process, but is reduced when the steady-state concentration is reached at the membrane surface.[3,88,89] In plain words,

this phenomenon means that some solutes accumulate before the membrane creating a semipermeable wall that will reduce the flux over time. The main difference between CP and fouling is that CP is reversible, it can be dispersed just by stopping the flux, while fouling requires an active action like flushing with water or chemical cleaning to remove it.

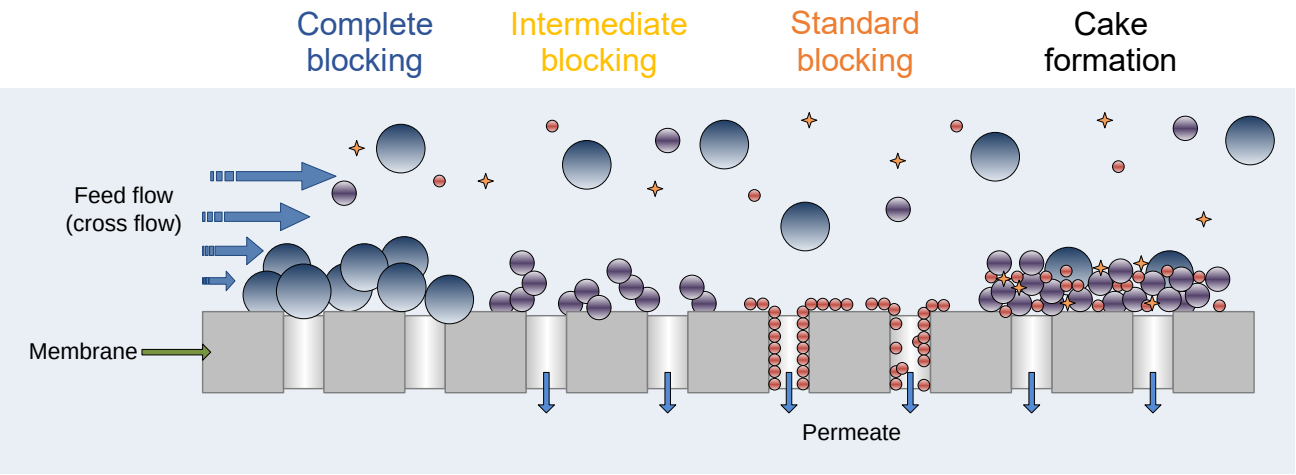

Figure 2-14: Pore blocking mechanism and cake layer adapted from Bowen *et al.* (1995)[90]

Figure 2-14 shows the fouling types of pore blocking and cake layer, being some of the most relevant in membrane applications. In general terms, when the flux exceeds the limiting flux the deposition of aggregated solute molecules on the membranes starts inducing particle deposition giving rise pore blocking and maybe later cake formation.[91]

The main difference between these two is that pore blocking occurs when the particles size is of the same range as the pore size increasing the membrane resistance because some particles manage to get into the pores blocking it. The pore blocking can be partially produced by particles that attach to the pores without blocking completely the flux or total when the addition of extra particles closes the pore opening.[92]

On the other hand, cake formation is the creation of an extra layer of resistance to the permeate flow by the addition of several layers of particles that attach to the previous particles being a feedback process (when it starts the effect is increased by each extra particle attached), and as soon as the cake has a diameter bigger than the pores it will act as a new layer of filtration heavily reducing the flux and stopping smaller particles than the membrane itself.[3,88,89,92,93]

The second effect of the cake is the "creation" of an extra layer of filtration that will retain smaller particles than the original membrane pores. This situation implies a change in selectivity, and can be considered negative because it is no longer known which is the effective filtration size of the membrane and particles that are expected to be in the permeate will be

found at the retentate instead. This effect had been detected in some of the work done by Beckman *et al.* (2010) where they noticed that the increase in fouling layer increase the whey proteins rejection.[94] Another relevant effect of this extra layer of filtration is the modification of the physicochemical conditions of the membrane, since the fouling components usually do not have exactly the same properties as the membrane.

In the food industry protein fouling seems to be a mixture of both pore blocking and cake layer, since the pore blocking facilitates the later cake layer formation. In line with this, the different types of fouling can be tackled by different systems, as reported in previous publications.[92,95–101]

Fouling types:

Fouling phenomena can also be classified based on the easiness of removing it.[99] Reversible fouling is the type of fouling that can be easily removed just by stopping the driving force (concentration polarisation) or by applying a water rinsing to the system to remove loose materials on the membrane (removing gel or loose cake components, Figure 2-15). On the other hand, irreversible fouling is any type of fouling that requires chemical cleaning or back flushing of the system to remove it (includes cake layer not removed by rinsing and in pore fouling).

2.5.2 Remedial actions

During past years several different fouling remedial actions were developed and they can be divided between pre-treatment of the feed, changes in membrane properties, changes in the module design and cleaning protocol. Pre-treatment methods include heat treatments, pre-filtration steps to remove certain particles like fat or pH adjustments. One example for milk applications is the pre-heat of the milk to make sure that all beta casein is found in the casein, since at low temperatures (below 10 °C at refrigeration temperature) beta casein partially gets out of the micelles into monomer form.[10,102] Changes in the membranes properties include the modification of the membrane charge, roughness or hydrophobicity. Changes in the module design focus on operational conditions like increasing crossflow velocity or adding turbulence sources to reduce fouling but increasing energy consumption.

In this project we will focus our attention to the effect of operational conditions and the cleaning methods, since the module cannot be modified, and the membranes are commercially available and are provided by my industrial partner Tetra Pak.

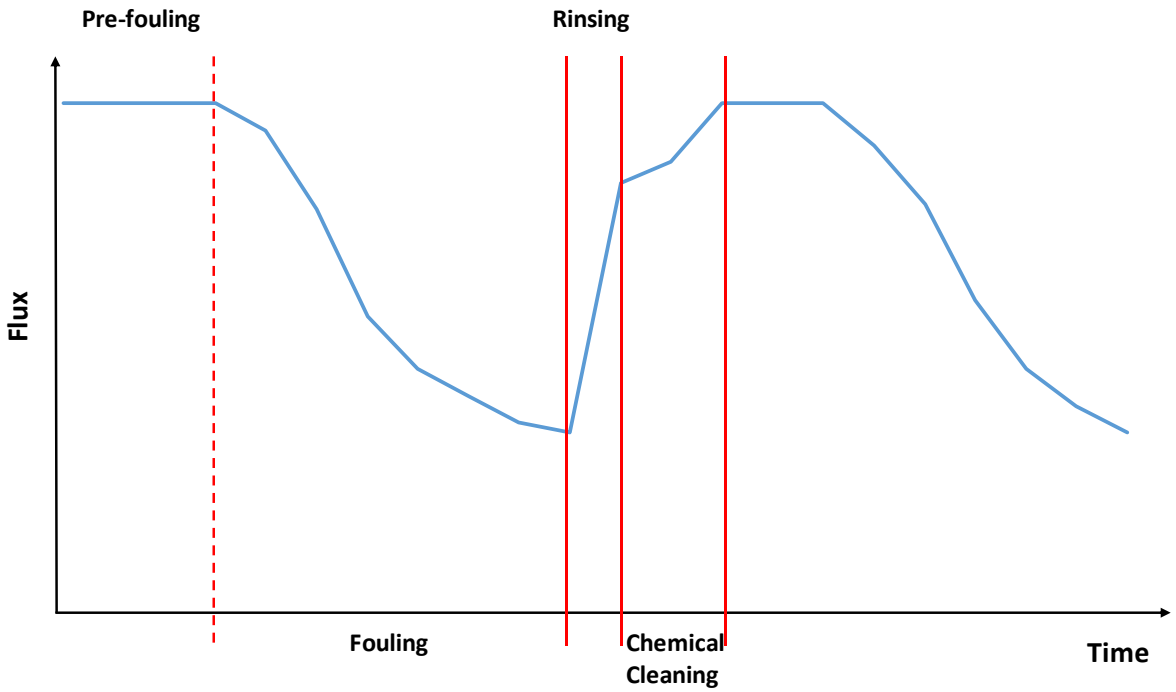

Figure 2-15: Flux profile over time of a fouling/cleaning cycle.

The remediation of fouling by a combination of chemical and physical cleaning is done to ensure that the membranes operate within a range of flux and rejection. Figure 2-15 shows a flux profile over time of filtration/cleaning cycle. It beings at maximum flux, then the flux is reduced due to the fouling phenomena effect and finally it is recovered to the original value. The flux recovery is done, first the CP can be reduced by stopping the flux of the system at a given moment, allowing the dispersion of the solutes and therefore recovering some of the flux.[99] Then, using a water rinsing to remove reversible fouling, recovering most of the lost flux and finally using chemical cleaning (or back flush) to remove the irreversible fouling and getting to the original flux value.[103]

The chemical removal of irreversible fouling can follow several approaches using acid, caustic agents or both like EDTA, Ultrasil 11 and NaOH.[94,104] The chemicals used will mainly depend on the fouling layer type, for example, in order to remove calcium deposits an acid base agent will get better results.[100] But it is also crucial to determine the right amount of chemical and the optimal combination of rinsing steps with the chemical cleaning.[101] A large number of research groups have used a base as chemical agent, NaOH being one of the most commonly used. Bartlett *et al.* (1994) found that for a ceramic membrane using 0.4 wt.% of NaOH lead to the best flux recovery after the membrane was fouled by whey protein.[101] This study also showed that the application of an excessive amount of NaOH reduced the flux recovery,

highlighting that the precise selection of cleaning agent is a key point and will help to reduce the need of chemicals in the system, making the process more sustainable.

Another example of the importance of choosing the right amount of cleaning agent is the study done by Shorrock and Bird (1998) where they studied the chemical cleaning of yeast cells by using NaOH (Figure 2-16). They found out that using NaOH at 0.01 wt.% was enough to produce a flux recovery of 93% independent of temperature and Reynolds number.[105] The chemical cleaning was complemented with two water rinsing steps, one before and one after the chemicals. The first rinsing step aims to remove loose cake and traces of fouling components, and the second is used to remove debris and chemicals. The analysis of the fouling layer showed the presence of salts as the factor that was not removed during the cleaning, so they decided to apply an acid cleaning after the NaOH in order to remove the salts. In this regard, they used 0.064 M of Nitric acid achieving a total recovery of the initial flux. This research shows the importance of combining different cleaning strategies to reach the maximum flux recovery at the minimum environmental cost.

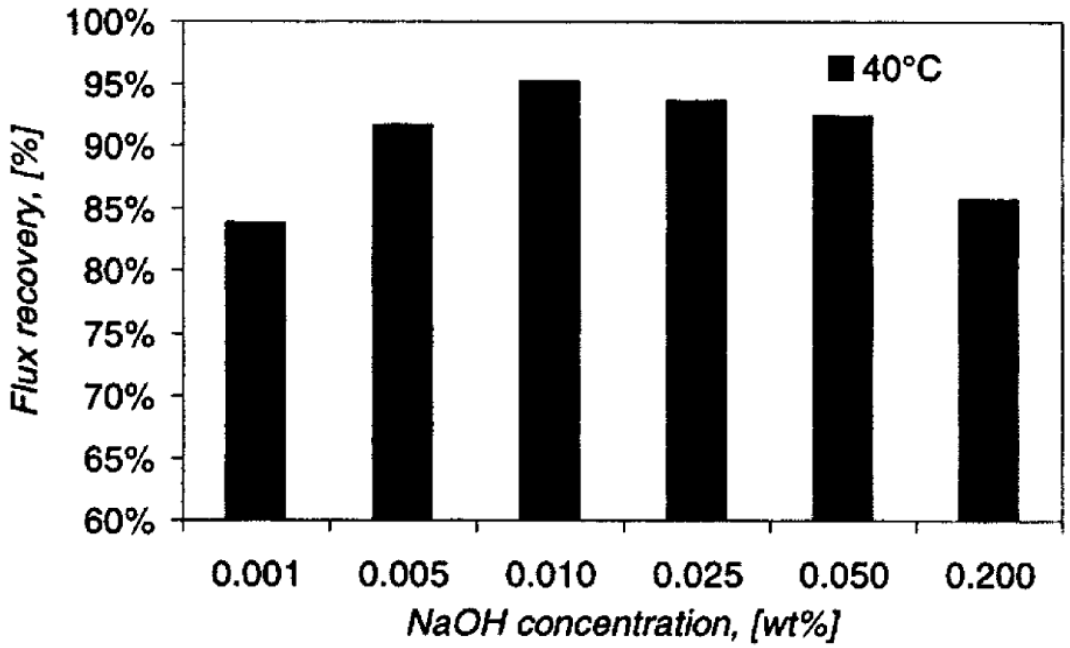

Figure 2-16: Percentage clean water flux recovery versus sodium hydroxide concentration at 40 °C (Re ~ 3160), Shorrock and Bird (1998).[105]

A key factor to decide which the best method for fouling removal is by checking the membrane properties such as the membrane material. For instance, in the case of polymeric membranes back flushing is not an option because they cannot sustain it without breaking.[77,106] In line with this, both the type of membrane and cleaning processes are key factors to take into account

especially in the food industry, as it can be seen in the wide spectrum of different membrane applications that prove it.[92,95–101]

2.6 Membrane filtration

In the following section membranes will be described in more detail from their history to their functionality and applications.

2.6.1 Membrane properties and types

Membranes are differentiated by the size of the pore (µm, nm) or the molecular weight cut off (kDa) and the driving separation mechanism (also known as driving force). In line with this, four main types of membranes exist according to the pore size; microfiltration (MF) having the highest pore size, ultrafiltration (UF), nanofiltration (NF) and reverse osmosis (RO) having the lowest pore size. Milk applications are varied, from fractionation of protein groups using MF membranes to proteins concentration or removal of lactose (UF). The separation process is often driven by an applied driving force in the form of pressure for MF and UF. NF and RO membranes are out of the scope of this review.[77] Table 2-4 shows a summary of key properties from MF and UF membranes.

Membranes can also be divided based on the material they are made of into ceramic membranes and polymeric membranes (more information in section 2.6.2).

Table 2-4: Summary of MF and UF key parameters for polymeric membranes.[3]

	Microfiltration	**Ultrafiltration**
Membranes	Symmetric or asymmetric	Asymmetric porous
Thickness of separating layer	~10 – 150 µm (sym) ~1 µm (asym)	~0.1 – 1.0 µm
Pore sizes	0.1 µm - 10 µm	~ 0.5 nm - 100 nm
Driving force	Pressure (<2 bar)	Pressure (1 – 10 bar)
Separation principle	Sieving mechanism	Sieving mechanism
Membrane materials	Poly - (PE, PP, PVDF)	Polymers (PSf, PEEK, PA PE, PP)
Main applications	Protein fractionation	Whey and casein proteins concentration

However, when membranes are used for any product processing two main challenges arise: flux reduction and lose of selectivity. The flux reduction is caused by the pore blocking and cake formation, and concentration polarisation. All of them are explained in more detail in section 2.5.1. The second problem is reduction of selectivity of the membrane caused by the membrane blocking, meaning that the membrane is no longer filtering the size it is supposed to and it is not fulfilling its purpose.

2.6.2 Membrane materials

The membrane applications can be determined by the material of the membrane due to its properties that define the operational capabilities like the chemical resistance for the cleaning steps, the temperature resistance for the processing that will determine the applicability of each membrane to the desired process. Membrane properties like hydrophobicity will also influence the processing of products like milk, for example favouring the membrane fouling, requiring frequent cleaning cycles or enhancing particle transmission. The membranes can be divided into two broad groups of currently used membranes, polymeric and ceramic membranes.

2.6.2.1 Polymeric membranes

Polymeric membranes have attracted a lot of interest in the recent years because they have a much lower capital cost for each unit and they are much easier to handle than ceramic membranes. However, due to the limitations of operational conditions (UTM) and a lower thermal, chemical and physical (to pressure) resistance ceramic membranes can still outperform the polymeric membranes in certain applications, as long as, other factor are not accounted for (like capital cost). These limitations are the main reason that polymeric membranes are under constant research to overcome or catch up with the levels of separation of ceramic membranes.

The fouling layer is a known factor that affects the filtration process reducing the permeate flow and modifying the effective separation process, controlling the formation of the fouling layer and the composition can be a key parameter to achieve the desired performance. Beckman and Barbano (2013)[85] found that the fouling layer modified the whey proteins separation and that the increase of the fouling layer led to an increase in β-Lg rejection. Conversely, Mercier-Bouchard *et al.* (2017)[107] work claimed that the fouling layer had no impact on the whey protein separation. The disagreements over the effects of the fouling layer

require further studies using polymeric PVDF membranes to deepen the understanding of the relationship between fouling layer and protein rejection.

So far it has been reviewed that two of the main properties of proteins, isoelectric point and size, are currently being used to separate the protein fraction of milk from the rest and to separate both protein fractions. Later on, the recent discoveries and work on membranes have shown the importance that they are gaining and their current expansion in the food industry and the dairy industry in particular.

The advantages of membranes over chemical precipitation are that membranes do not require external additive, they modify the milk composition not the milk chemistry and that membranes can be used for long operational times and if properly maintained they have long life-times. However, membranes are not still fully precise on targeting the right compositions of proteins in the permeate and retentate and they require chemicals, water and energy for the operation and maintenance of the system.

Some examples of membrane materials can be found below:

Regenerated cellulose is one of the most hydrophilic polymers, however, it also has a hydrophobic behaviour (strongly interacting with non-polar organic solvents). The most relevant properties of regenerated cellulose are the high moisture absorbency, their dyeability, flexibility, however, their challenge is the lack of favourable mechanical properties.[108] When using regenerated cellulose to for membrane applications the membranes are hydrophilic and tend to have higher fluxes, they also are chemical resistant (they can handle chemical cleaning) and have good wet strength. The membranes can be produced by first dissolving the desired amount of cellulose in LiOH/urea solution, Liu *et al.* (2010) used a ratio of cellulose and solvent of 5.0 wt%/12.0 wt% respectively.[109] The dissolution into the urea solution requires air bubbles removal to ensure reproducibility of membrane properties and the same ratio of cellulose to solution. The membrane preparation step is carried out by immersing the cellulose urea solution into a coagulant, for example 5 wt% H_2SO_4.[109] The main drawback of regenerated cellulose is the low lifetime, which is the main reason they are no longer used, even though they were among the first membranes to be used.

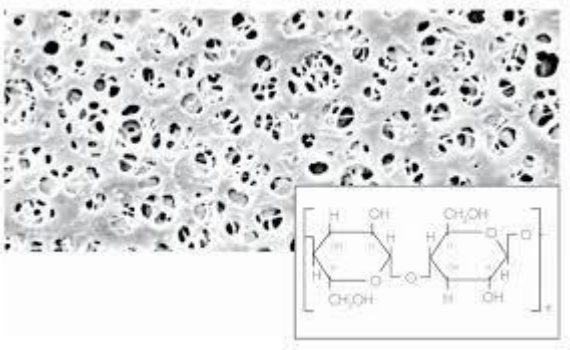

Figure 2-17: Regenerated Cellulose, SEM image and basic chemical unit. Source: Fisher Scientific.

Polyvinylidene difluoride (PVDF) membranes can withstand high temperatures and are chemically resistant (both ideal properties to ensure proper chemical cleaning step and long life of the membrane reducing the operational cost), however, they are hydrophobic and therefore the fluxes are typically lower than for the more hydrophilic membranes. PVDF membranes are produced by phase inversion, because of simplicity and capability of scaling the production to the needs of membrane. This material is the starting material for the project since they will last longer operational times and cleaning steps, being a key parameter when studying industrial viable membranes.

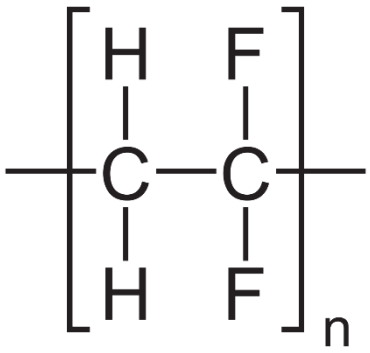

Figure 2-18: Structure of PVDF.

Crowley *et al.* (2015) compared PES and PVDF membrane of similar pore size, 1000 kDa and 0.1 µm and to test the effect of membrane material.[110] Even though the ideal comparison should be carried out in the exact same conditions, the work they carried out showed that membrane material can have an impact on the properties of the separation. They found that both membrane obtained the same separation of β-casein from skim milk, but the PES membrane displayed a higher permeate flux and lower fouling.[110]

Polyethersulphone (PES) membranes are hydrophobic (meaning that they have lower fluxes compared to RC membranes), they have low protein binding properties and are recommended for tissue culture media sterilisation and microbiology. Arkhangelsky *et al.* (2007) analysed the chemical stability of PES membranes based on typical cleaning protocols to test their

performance over time.[111] They found that the complete removal of the foulants lead to the modification of the membrane properties with an increased electronegativity of the membrane and an increase tendency to foul that ultimately lead to a more severe fouling. They also detected that the pore size increased due to a collapse of the PVP component of the matrix. The combination of all the factors lead to flux reduction over time with less selectivity of the membranes.[111]

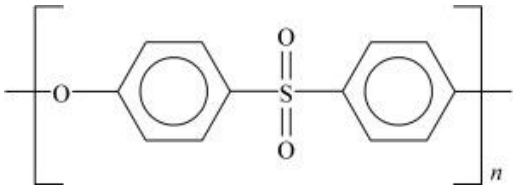

Figure 2-19: Structure of polyethersulfone (PES).

The work of Crowley *et al.* (2015)[110] studied the behaviour of a polyethersulfone (PES) membrane of 1000 kDa compared to two PVDF membranes of 0.1 and 0.45 µm for low temperature (4 °C) production of Serum protein concentrates (SPCs). They found that the 1000 kDa PES and the 0.1 µm PVDF membranes achieved the production of permeates with a ratio of casein and whey proteins of 50:50, where the casein fraction had a high purity of beta-casein. The main differences came from the fact that the PES membrane displayed an improved permeate flux accompanied of a lower degree of fouling compared to the PVDF 0.1 µm membrane. The only drawback of this reach was the use of reconstituted proteins that limit the applications of the results to a type of feed.

2.6.2.2 Ceramic membranes

Ceramic membranes have been used for protein fractionation since 1980s because they can achieve high crossflow velocities, which minimise the overall fouling, allowing to obtain high permeate flux.[112] Ceramic membranes are also chemically resistant allowing any kind of cleaning method to be employed and increasing the lifetime of the membranes. They can also resist high temperatures of operation and can also withstand backflow, which opens the cleaning options to back flush methods.[113,114] However, ceramic membranes are also the most expensive type of membranes, it is estimated that they require fluxes of 10% higher output compared to polymeric in order to be economically competitive.[115,116] Ceramic membranes in the milk industry have moved towards specialised applications where having more precisely defined pore sizes allow to produce pure retentate and permeate streams.[74] Ceramic membranes have been displaced despite their advantages in temperature, hydraulic and chemical properties, mainly because their high cost favours polymeric membranes for

"simple" applications, like casein standardisation for cheese production.[79,115,117,118] Ceramic membranes are not the scope of this study and they have not been investigated in any more detail.

2.6.3 Temperature effects

The study of milk filtration at low temperatures is of high industrial interest since it does provide an operational advantage over 50 °C in terms of microbiological safety. Any filtration system operated at 50 °C will be able to operate up to 8-9 hours, on the other hand, a system operating at 10 °C can increase the operating time until the 20 hours. The increased operation time carries a better product in microbiological quality and does require less water, steam and cleaning agents. The operation at low temperature (10 °C or below) does carry an added benefit, the beta-casein protein groups does dissociate from the casein micelle opening the possibility to produce permeate stream of whey proteins and beta-casein, which are closer to human milk than standard bovine milk.[11,110,119]

Lawrence *et al.* (2008) investigated the production of casein concentrates using SW-polymeric membrane of 0.3 and 0.5 µm PVDF.[120] They observed that both at 10 and 50 °C the permeate was essentially the same, claiming no notable changes due to temperature. The results for both pore sizes were similar under the same processing conditions leading to the conclusion that pore size was rapidly modified by the protein fouling layer. They expected to be able to control the fouling layer at lower TMP conditions (their lowest TMP was 0.5 bar) with high CFV. They claimed that the increase of temperature had no effect on the separation, unlike the increase of pressure that led to higher casein and whey proteins rejection. From their data the ideal operating pressure to achieve fractionation of casein and whey proteins would be to operate at 0.5 bar.

Hurt *et al* (2015)[121] studied the filtration temperature effect both on serum proteins removal and fouling layer above 50 °C since it is the temperatures which promote calcium phosphate precipitation. They used a 0.1 µm ceramic membrane. They also compared the skim milk to previously UF filtered milk to compare the effect of lactose and soluble components removal. The increase of temperature did not imply an increase of fouling due to calcium deposition, it did show a reduction in calcium concentration in the permeate. They also observed a reduction in serum proteins removal due to the increase in temperature which also correlated with a decrease in casein proteins, which meant a lower casein "contamination" of the permeate.

The work of Crowley *et al.* (2015)[110] focused on the enrichment of the beta-casein fraction at low temperatures using reconstituted skim milk (3.2 % protein). The work was at low

temperature to generate whey protein concentrates suitable for infant formula with a higher proportion of whey over casein proteins and higher beta-casein over alpha-casein.[11,110] The work was carried out at 4 °C in order to have monomeric β-casein (not in the micelle) that can go thought the membrane. They managed to achieve a ratio of casein and whey proteins of 50:50 and a high purity of beta-casein (between 97-100 % of casein detected). However, they still detected high levels of β-Lg which is not present on human milk. The only drawback of this research was the use of reconstituted proteins that limit the applications of the results to a type of feed.

The work carried out by McCarthy *et al.* (2017)[119] researched the production of infant milk formula which has a completely different composition to bovine milk, the casein to whey ratio is of 40/60 for infant milk formula and 80/20 for bovine milk. Their work combined the use of a 0.1 µm ceramic membrane to achieve the casein and whey proteins separation on a first step, then they followed with a concentration of the permeate using a 10 kDa UF polyethersulfone. In this study they targeted to produce and emulate the infant milk real composition and to do so the casein fraction had to be composed of beta-casein. In order to promote the beta-casein transmission to the permeate they filtered the milk at low temperature (8.9 °C) because beta-casein is mainly found in the monomer form easily getting though the membrane and separating form the rest of casein proteins. They managed to obtain a casein:whey ratio of 35:65 at 8.9 °C and a ratio of 10:90 at 50 °C. At low temperature the casein composition was only formed by beta-casein.

Beckman *et al.* (2010)[94] aimed to emulate some of the rejection values of the work done by Hurt *et al.* (2010)[117] using a 0.3 µm PVDF spiral-wound membrane instead of the 0.1 µm ceramic membrane. Beckman *et al.* (2010) worked at a concentration factor of 3 at a processing temperature of 50 °C, the mode of operation was a concentration step followed by two diafiltration steps with RO water. Their aim was to achieve a removal of whey proteins close to the 98.3 % obtained by Hurt *et al.* (2010) however, their final whey protein removal was much lower reaching a 70.3 %.

Beckman and Barbano (2013) continued studying the removal of whey proteins based on the effect of the concentration factor when using a 0.3 µm PVDF spiral-wound membrane operated at 50 °C.[85] The work was divided in the concentration phase that was operated in full recycle-mode and the second phase of filtration after reaching the desired concentration factors. The tested concentration factors were 1.5x, 2.25x and 3.0x and the associated whey protein removal were 10.6 %, 24.3 % and 35.3 %, respectively. The results showed a positive link between the concentration factor and the whey protein rejection indicating that the increase in rejection is only due to the fouling phenomenon since the membrane was the same.

They also concluded that the fouling characteristics have a higher impact on whey protein rejection than hydraulic resistance and that the first minutes of filtration are the key conditioning factors since they condition the type of fouling structures on the membrane. For example at lower concentration factors the pore blocking may be enhanced since more particles are loose due to a lower gel layer formation rate.

The temperature of filtration has been proven to also have an effect on the fouling layer properties. The study of Doudies *et al.* (2021)[122] claims that the filtration at high temperature (42 °C) lead to the formation of a more concentrated and with a thicker fouling layer that low temperature filtration at 12 °C for ultrafiltration of casein micelle dispersions. They also observed that once the pressure of the system was removed the fouling layer started to swell, easing the removal by the effect of the crossflow velocity. The swelling was more important for the highly fouled sample at 42 °C leading to a higher degree of removal. Casein micelles volume (and voluminosity, ratio of wet relative to dry casein micelles) is temperature dependent, for example, the voluminosity at 12 °C is of 4.52 ml g^{-1} and at 42 °C it is of 3.8 ml g^{-1}.[123,124]

The work by K.S.Y. Ng *et al.* (2018)[125] analysed the effect of filtration temperature (10, 30 and 50 °C) on fouling composition for ultrafiltration of skimmed milk using SDS-PAGE. First of all, they confirmed that the main fouling components are proteins, calcium being less than 1% of the foulants analysed. Among the whey protein groups they found that β-Lg only was detectable as a foulant component at 50 °C, unlike the results presented on this study that clearly detected β-Lg at all temperature ranges. They claimed that an increase in temperature favoured the monomer fraction of the β-Lg and between 45-55 °C the protein the monomer protein undergoes a transition that increases it hydrophobicity and the tendency to absorb onto the membrane of the study (polyethersulfone-PES). They confirmed that the first fouling layer of around 50 mg m^{-2} contributed to a similar amount of fouling resistance as the subsequent 1000 mg m^{-2}, both of them being roughly 7 $x10^{+12}$ m^{-1}.

Schopf *et al.* (2020)[126] studied the changes in fouling layer properties using an In-Situ MRI. They found that protein content on the fouled membrane increased with the temperature at their studied range 12-45 °C, obtaining the highest thickness at 45 °C. They also observed that at higher temperatures the fouling layer were more compressible, and that at high pressures the thickness could be lower than at lower pressures.

France *et al.* (2021)[127] studied the effect of low temperature (4-12 °C) on the filtration performance and the fouling layer. They found that at 4 °C they had the lowest initial permeate flux combined with the lowest flux decline. The low temperatures yielded high casein rejections, with the exception of the β-casein that saw higher permeate at lower temperatures.

Jimenez-Lopez *et al.* (2008)[128] studied the role of milk components on microfiltration fouling when operated at critical hydrodynamic conditions (CHC). They found that the presence of soluble proteins increased the irreversible fouling by 20%, which as it is known, the filtration at low temperatures carries a higher proportion of soluble proteins (beta-casein in particular). Calcium ions helped to create bonds between the membrane and the casein micelles as well as it kept binding micelles among themselves.

Chapter 3. Methodology

The methodology chapter will define the milk filtration protocol, the filtration system and equipment and the analytical methods used with the exception of the HPLC (described in Chapter 4).

3.1 Filtration Protocol

Filtration studies were carried out using 0.1 µm polymeric PVDF membranes (Synder Filtration, code: V01). The filtration protocol summarised in Table 3-1 was adapted from previous work reported in Argyle *et al.* (2015).[129] This protocol is the template for any filtration cycle from the initial membrane conditioning to the final pure water flux measurement. However, the protocol was modified and adapted in specific situations to either test conditions beyond the specified range of operations or for example to test the properties of membrane before the cleaning cycles (stopping the protocol before the cleaning steps).

Table 3-1: Crossflow experimental conditions used for Bench Top M10 and Pilot Scale adapted from Argyle 2015.[86]

Operation	Duration [min]	TMP [bar]	CFV [m s^{-1}]	Temp [°C]	Resistance measured
Membrane conditioning	90	1.0	1.5	60	-
PWF 1	10	0.1-7.0	1.0	20	R_m
Filtration	60	0.25-7	0.5-1.5	10-30-50	R_T
Rinse 1	10	1.0	1.5	20	-
PWF 2	10	0.1-7.0	1.0	20	R_{ir}
Cleaning	10	1.0	1.5	60	-
Rinse 2	5	1.0	1.5	20	-
PWF 3	10	0.1-7.0	1.0	20	$R_{m,3}$

3.1.1 Coating layer removal

Membrane manufacturers treat flat sheet polymeric membrane with an anti-humectant glycerol coating to extend its shelf life. This protective coating was removed by applying a modified protocol developed by Weis *et al.* (2005).[98] On the first use of each membrane set,

the first step was to condition the membranes in the same system where the membranes were going to be used. The conditioning was carried out with RO water at 60 °C for 90 minutes. The crossflow velocity (CFV) was kept at 1.5 m s^{-1} and the transmembrane pressure (TMP) was kept constant at the selected value for the experiments to perform usually between 0.5-1 bar.[98] The protocol developed by Weis *et al.* (2005) was carried out at 1 bar of transmembrane pressure, however, to minimise membranes' compaction the protocol was modified for the experiments carried out at a pressure lower to 1 bar (usually 0.5 bar).

3.1.2 Pure water flux

The pure water flux was used to determine both the intrinsic membrane resistance when the membrane was clean, and the total resistance when the membrane was fouled. The measurement was carried out in a range of pressure with step increase of the applied transmembrane pressure, always keeping the permeate valve open. Equation 3-1 (a modified Darcy's Law) was used to model and analyse the membrane resistance (if the flux was obtained on a clean membrane using RO water) or the total resistance including any fouling phenomena.[3]

$$J = \frac{TMP}{\mu R_t} = \frac{TMP}{\mu(R_m + R_{rev} + R_{ir})} \qquad 3\text{-}1$$

Where J (m s^{-1}) is the permeate flux, TMP (Pa) is the transmembrane pressure and the μ (Pa s) is the viscosity of the permeate. Using these parameters, the total resistance (R_t) (all resistances are in units of m^{-1}) can be determined, and the other resistance values can be obtained (Equation 3-2)

$$R_t = R_m + R_{rev} + R_{ir} \qquad 3\text{-}2$$

The membrane resistance, R_m, is the intrinsic resistance of the pristine membrane calculated using the flux of RO water, to avoid any fouling effect. The two main resistance values due to fouling are cake resistance (R_c) and in-pore resistance (R_i), however due to limitations of the filtration apparatus design this study has calculated reversible fouling resistance (R_{rev}) and irreversible fouling resistance (R_{ir}) instead. Irreversible fouling can be defined as the in pore and cake layer fouling that is not removed after a RO water rinsing step (see section 6.3 for a developed example). Reversible fouling then is defined as the fouling removed after a RO water rinsing step and it is calculated by subtraction of irreversible fouling from the total resistance at the end of the filtration cycle.

$$R_{rev} = R_t - R_m - R_{ir} \qquad 3\text{-}3$$

3.1.3 Filtration cycle

Filtration/Fouling experiments were carried out using skimmed milk (Co-operative Wholesale Society). The general flow of a filtration cycle is shown at Figure 3-1, the concentration step was only used in the concentration experiments and was avoided for all the other experiments. In this report, the term 'cycle' is defined as the complete process of filtration, including rinsing and cleaning steps (Figure 3-1).

In any filtration test samples of both feed and permeate were taken at different times of the experiments to understand protein separation and fouling layer composition. There were no retentate samples taken because it was recirculated to the feed tank.

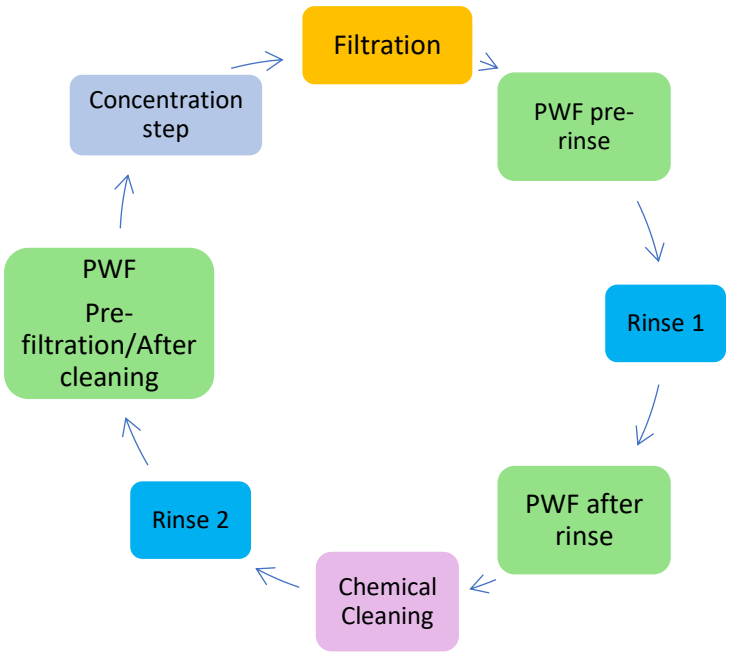

Figure 3-1: Concentration/Filtration protocol based on Argyle *et al.*[130]

Full recycling mode

In this mode of operation both the retentate and permeate were sent back to the feed tank to maintain the feed volume and concentration of components. This mode of operation assumed that the loses of components towards the fouling layer were minimal when compared to the overall concentration at the feed. This was the mode of operation used for all the experiments during the filtration step.

Concentration experiment

The concentration experiments were carried out in two steps, the first consisted in the volume reduction by a factor of 2, increasing the protein concentration of the feed by filtering components into the permeate and not returning the permeate to the feed tank. When the volume was reduced by a factor of 2 the filtration entered a full recirculation mode where both permeate and retentate were fully recirculated.

The volume reduction step (Figure 3-1) used 3.4 L of milk which were reduced to approximately 1.7 L. The volume reduction was carried out with the membranes itself and therefore the concentration step contributed to the fouling layer. Samples of the permeate were taken for analysis and the rest of the permeate was discarded. After achieving the volume reduction factor of 2 the filtration was carried out for an hour in full recirculation. The aim of the concentration step was to increase the protein content in the retentate side. The concentration experiments were carried out to test the effect of the increased feed concentration on the protein rejection, they amount to less than 10% of all the experiments carried out.

3.1.4 Membrane cleaning

The cleaning method was a multistage process that combined the chemical cleaning of 0.5 wt.% NaOH with the mechanical cleaning of the rinsing steps with RO water (see Figure 3-1). The method was based on previous studies that proved it worked on milk protein soil removal.[101]

RO water rinsing

The rinsing step was carried out before the chemical cleaning to eliminate rinseable fouling in order to maximise the chemicals cleaning efficacy. It aimed to flush any remnant feed in the system while removing loosely attached particles to the membrane (rinseable fouling), this reduced the need for chemical cleaning.[103] The second rinse step, after the chemical cleaning was designed to flush out of the system any leftover NaOH to prevent it affecting future filtrations or damaging the membrane. The rinsing steps were carried out at a pressure of 0.5 bar and 1.5 m s^{-1} CFV for 5 minutes, with the permeate lines closed, unless stated otherwise.

Chemical cleaning

The chemical cleaning step was carried out using 0.5 wt.% NaOH for 10 minutes, where the permeate lines were closed for the first half of the process. The aim of the chemical cleaning was to remove the remaining fouling particles that did not get removed by the rinsing step and to remove any fouling components inside the membrane pores. The TMP used was 0.5 bar, the CFV was 1.5 m s^{-1} and the temperature was 60 °C.[129]

3.2 Filtration equipment

The main work of the PhD has been carried out using two different filtration rigs. Both systems were designed to operate in crossflow filtration.

3.2.1 Bench scale M10 rig

A DSS LabStack M-10 module (designed by Alfa Laval) filtration rig was used for the filtration studies (Figure 3-2). The M10 was a system were the heat exchanger, pump and membrane module were integrated in a single pre-build unit. The feed went from the feed tank, through the heat exchanger to the positive displacement pump and to the membrane module and from there the retentate went back to the feed tank or was disposed.

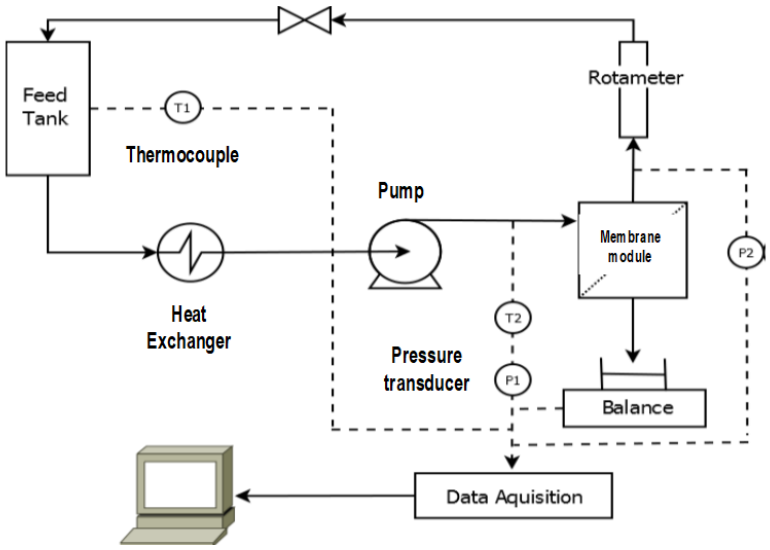

Figure 3-2: DSS LabStack Bench Top M10 module (Alfa Laval) with the position of temperature and pressure sensors.

Membrane module

The filtration module consisted of a stainless-steel frame that held 4 stacked polysulfone plates with pre-cut polymeric PVDF membranes (Figure 3-3). The total filtration area inside the module was 336 cm^2.[104]

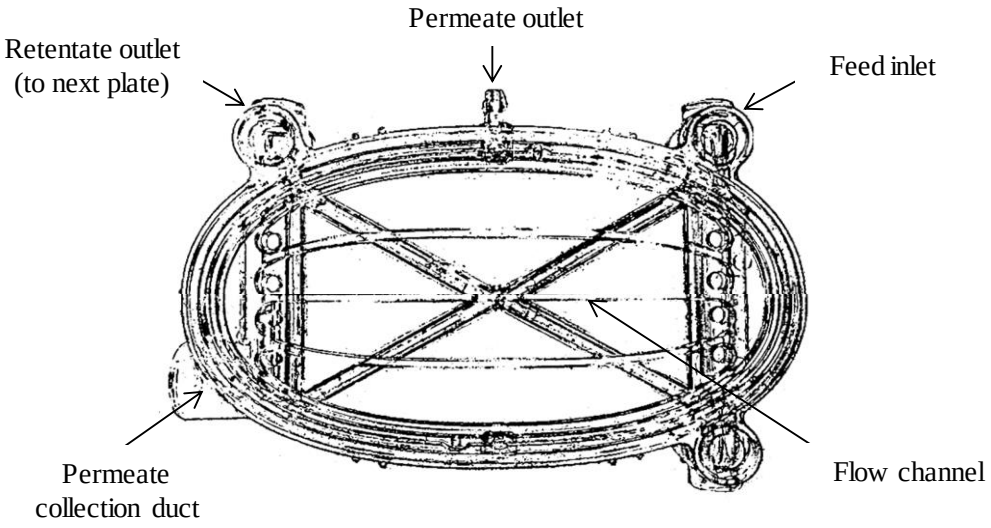

Figure 3-3: Schematic figure of the Bench Top M10 polysulfone plates (Argyle 2015)[131]

Pump

The pump of the Bench Top M10 was an ECO Gearchem with variable speed positive displacement pump (Pulsafeeder, NY, USA) that was capable of delivering up to 7 bar to the module (based on specifications). For this project the pressure never overcame 2 bar.

Rotameter

The system's rotameter was mounted on the retentate side of the membrane module. The flow rate range was of 0.2 - 4.5 L min^{-1} (±0.015). The CFV was calculated using this parameter and the specifications can be found on the work of Argyle (2015).[86]

Heat exchanger

The heat exchanger was designed and produced by Alfa Laval (Nakskov, Denmark) and it was a shell and tube model. The water for cooling or warming was supplied from the water bath by using an immersion circulator.

Permeate flow rate

The permeate flow was recorded using a balance (College B3001-S, Mettler Toledo AG, Greifensee, Switzerland) that had a systematic error of ± 0.05 g. The balance was connected to a data-logger (using LabVIEW software, National Instruments).

Temperature measurement

The temperature of the feed was measured before entering the membrane module using a thermocouple calibrated by a mercury thermometer, the reliability range was from 5 to 80 °C. Data was also logged using LabVIEW.

Pressure measurement

The TMP was measured using two pressure transducers, one at the feed side inlet (P_1) and the other at the outlet (P_2). TMP was calculated using equation 3-4, where P_3 is the pressure in the permeate line, maintained at atmospheric pressure. Data was also logged using LabVIEW.

Data acquisition and monitoring

Data was collected from the pressure transducers, thermocouple and balance via a 4-channel remote data acquisition module (model ADAM-4012, Advantech, Milpitas, USA), then it was processed using LabVIEW v10.0 (National Instruments, USA).

Feed tank

The Bench Top M10 10 L feed tank was custom made by Soham Scientific (Soham, UK) designed to hold boiling water, cleaning agents and feed solutions.

3.2.2 The Pilot Scale rig

The Pilot Scale filtration system was adapted to work using either ceramic or polymeric membranes (Figure 3-4). In this project the polymeric membranes were the only ones tested using this rig. The membrane module holds one membrane with an effective filtration area of 161 cm^2. The skimmed milk was fed into the module from a 30 L tank. In order to maintain the temperature the rig had two systems, an oil heater to warm the content of the feed tank directly and a cooling loop used to maintain the low temperatures. The temperature can be kept consistent in the range between 10 to 60 °C. The permeate flow was also recorded using a balance connected to a data-logger (using LabVIEW software, National Instruments). The TMP was measured using three pressure transducers, one at the feed side inlet (P_1), another at the outlet (P_2) and the permeate side (P_3). The overall TMP was calculated using equation (3-4), where P_3 is the pressure in the permeate line, the permeate line pressure ranged from atmospheric to high pressures up to 4 bar.

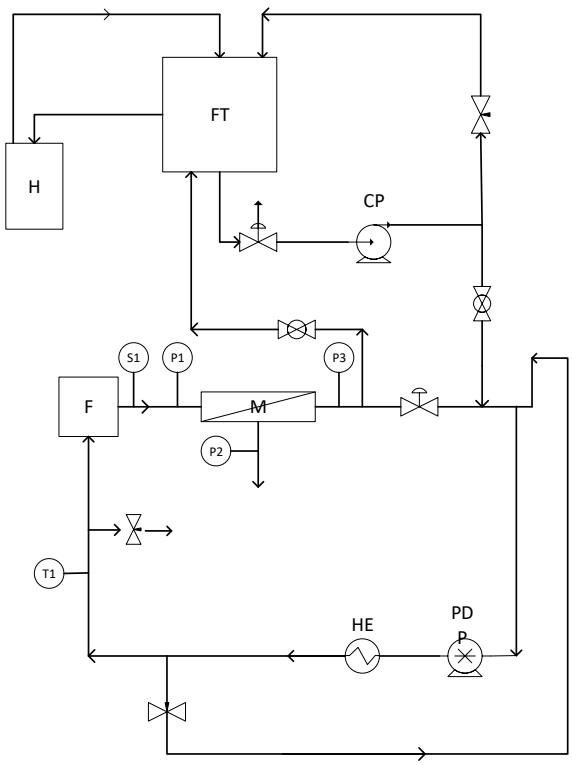

Figure 3-4: Schematic diagram of the Pilot Scale filtration apparatus. Legend: FT - feed tank, H - oil circulation pump and heater, M - membrane module, F - flow meter, HE - heat exchanger, CP - centrifugal pump, PDP - positive displacement pump, T - thermocouple, S - sampling point and P - pressure transducer. Diagram adapted with permission from Head & Bird (2013)[132].

Membrane module

The filtration module consisted of a stainless-steel frame that held 1 pre-cut polymeric PVDF membrane held by a double support system. The total filtration area inside the module was 161 cm^2.[104]

Pump

The Pilot Scale filtration apparatus contains two pressure loops (Figure 3-4). The first loop had the feed pump (Lowara centrifugal pump SKM70/30 SP) that circulated the feed from the tank to the membrane module. The second circulation loop had a triplex plunger positive displacement pump (CAT 1051, capable of reaching up to 15 bar while maintaining high CFV) to circulate the feed at higher pressures and speeds.

Rotameter

The feed speed was measured using an electromagnetic flow meter (Magflo MAG 2560) that was mounted on the feed side of the membrane module. The flow rate range measured range between 30 L h^{-1} to 600 L h^{-1}.

Temperature control and heat exchanger

The system contained two separate heat exchangers for temperature control. The feed tank had a heating loop straight to it with a Conair unit (Conair Churchill 18 200). The cooling loop had a second heat exchanger connected to a water bath that could be refrigerated.

Permeate flow rate

The permeate flow was recorded using a balance (Ohaus, Scout Pro, SPR4001) that had a systematic error of ± 0.04 g. The balance was connected to a data-logger (using LabVIEW software, National Instruments).

Temperature measurement

The temperature of the feed was measured after exiting the membrane module using a thermocouple calibrated by a mercury thermometer, the reliability range was from 5 to 90 °C. Data was also logged using LabVIEW.

Pressure measurement

The TMP was measured using three pressure transducers, one at the feed side inlet (P_1), another at the outlet (P_2) and the final one at the permeate line (P_3). The pressure transducers were calibrated to work in the range 0 - 7 bar. TMP was calculated using equation 3-4. Data was also logged using LabVIEW.

Data acquisition and monitoring

Data was collected from the pressure transducers, thermocouple and balance via a 4-channel remote data acquisition module (model ADAM-4012, Advantech, Milpitas, USA), then it was processed using LabVIEW v10.0 (National Instruments, USA).

Feed tank

The Pilot Scale 30 L feed tank was designed to hold boiling water, cleaning agents and feed solutions.

Membrane module

The Pilot Scale membrane module was a modification to adapt the system to be used with flat sheet polymeric membranes. The system was designed by Prof John Howell later modified by Dr. Mike Bird at the University of Bath.

Table 3-2: Pilot Scale membrane module specifications

Channel properties	Width	Depth	Length
7 channels	6.9 mm	1.2 mm	192 mm

3.2.3 Bench Top M10 vs Pilot Scale

The differences of both rigs can be divided along the operational conditions and have been summarised in Table 3-3. The effective differences are in the pressure ranges that the systems can operate, with an important overlap of pressure ranges, however, the Bench Top M10 rig cannot operate at constant conditions in the whole 0-2 bar pressure range.

The Bench Top M10 rig can operate at the range 0-2 bar but it is not able to keep the CFV constant in the whole range. On the other hand, the Pilot Scale double pump system can maintain the CFV constant in the whole 0-7 bar range of operation, allowing a full decouple of pressure and CFV and the study of the different operational conditions.

Another difference is the effective membrane area and module configuration, which will also have an impact on the pressure drop along the membrane unit. The Pilot Scale has a minimal pressure drop along the membrane module when filtering skimmed milk.

Table 3-3: Differences among Bench Top M10 and Pilot Scale.

Rig	Bench Top M10	Pilot Scale
Pressure range	0-2 bar	0-7 bar
Permeate line pressure	Atmospheric	Up to 4 bar
CFV	Up to 1.5 m s^{-1}	Up to 3 m s^{-1}
Pressure drop along the membrane	Up to 0.5 bar	Minimal
Effective filtration area	336 cm^2	92.3 cm^2

The main advantage of the Pilot Scale over the Bench Top M10 is the capability of decoupling the CFV and TMP, the second advantage of the Pilot Scale is the capability of pressurising the permeate line, expanding the combinations of pressures to study. The last difference among the two rigs is that the Pilot Scale has a small (negligible) pressure drop along the membrane module, giving us less uncertainty of the operational parameters that condition the filtration process, fouling layer formation and protein compositions both at the fouling layer and the permeate.

3.3 Mathematical models

The control of the filtration could be carried out by the measurement of the pressure, the permeate flux and temperature. These parameters were transformed into the key control

parameters like: Transmembrane pressure, permeate flux, Reynolds number and protein rejection.[3]

Transmembrane pressure was measured using equation 3-4, where P_1 and P_2 are the inlet and outlet pressures to the membrane module respectively and P_3 is the pressure in the permeate line.

$$TMP = \frac{P_1 + P_2}{2} - P_3 \qquad 3\text{-}4$$

Equation 3-5 is used to determine the rejection of each protein group comparing the concentration at the feed and the permeate:

$$Rejection = 1 - \frac{C_p}{C_f} \qquad 3\text{-}5$$

where c_p and c_f are the protein concentration at the permeate and the feed respectively.

3.3.1 Error propagation analysis

The errors and standard deviations shown in the results chapters were all obtained first of all after at least two repeats for each experiment, however, most of the data shown in results section is also the result of an analytical method and some calculations. The combination of repeats, analytical equipment and methods required to perform error propagation in order to ensure that the results were relevant. The employed method can be seen summarised below:[133]

1) For addition or subtraction calculations:

Assuming that:

$$D = a + b + \cdots + z \qquad 3\text{-}6$$

The final uncertainty for D is:

$$\delta D = \sqrt{(\delta a)^2 + (\delta b)^2 + \cdots + (\delta z)^2} \qquad 3\text{-}7$$

2) For multiplication or divisions:

If

$$D = a * b * c \quad \text{3-8}$$

The final uncertainty for D is:

$$\frac{\delta D}{|Q|} = \sqrt{(\frac{\delta a}{a})^2 + (\frac{\delta b}{b})^2 + (\frac{\delta c}{c})^2} \quad \text{3-9}$$

3.4 Membrane analysis

The analytical methods employed can be divided in the ones used for the analysis of the proteins and the ones used for the membrane characterisation. This section focuses on the membrane analysis using SEM, FTIR, AFM and contact angle.

3.4.1 Scanning Electron Microscope

Scanning Electron Microscope (SEM) was used to take visual representation of the membrane at different stages of the filtration process. The system used was a JEOL SEM6480LV microscope operated and owned by the Material and Chemical Characterisation Facility (MC2) of the University of Bath.

The membranes samples to analyse with the SEM need to be prepared in two steps. The first step is to dry any sample at the vacuum system overnight. The second step is to coat the samples with a thin gold layer that increases the resolution of the measurement.

3.4.2 FTIR

Fourier-transform infrared spectroscopy (FTIR) was used as a secondary measurement to validate the presence of casein and whey proteins on the membrane surface. There are two ranges where peaks could be attributed to casein and whey proteins, the presence of these peaks needed to be compared to the clean membrane. The range of casein and whey proteins are the one between 3000 and 3200 cm^{-1} and the one between 1500 and 1600 cm^{-1}.[134] The Perkin Elmer Frontier FTIR instrument was operated and owned by the Material and Chemical Characterisation Facility (MC2) of the University of Bath.

The membrane samples need to be fully dried to make sure that water is not present, because water peak overlap with the protein peaks.

3.4.3 Confocal thickness sensor

The confocal thickness sensor (CTS) was used to try to map out the membrane surface on a surface of 60 x 60 mm with a resolution of <100 microns. The system has an IFS2405-3 sensor connected to the IFC2461 controller from Micro-Epsilon. The samples require no preparation beforehand. The system was operated and owned by Prof. Ian Wilson from Cambridge University.

Chapter 4. Protein analysis: development of the HPLC method

In this chapter it is described in detail the development of the proteins analytical method employed to identify and quantify the six main protein groups found in milk including α-CN, β-CN and κ-CN of the casein proteins and α-La, β-Lg and BSA of the whey proteins.

It discusses the column, gradient and operational conditions chosen for the Reversed-Phase High-Performance Liquid Chromatography (RP-HPLC) method employed, which was adapted from previous work done by Bobe *et al.*(1998) and V.Bonfatti *et al.*(2008).[26,64]

4.1 Reagents and samples

Standards of the 6 main protein groups to analyse were obtained from Sigma-Aldrich (now Merck): the casein protein standards were α-casein (>70%), β-casein (>98%), κ-casein (>70%), and the whey protein standards were α-Lactalbumin (>85%), β-Lactoglobulin (>90%) and Bovine Serum Albumin (BSA) (>98%).

The reagents required to prepare the milk sample were Bis-Tris, Guanidine hydrochloride (GdnHCl), sodium citrate and DL-Dithiothreitol, and were purchased from Sigma-Aldrich.

Ultra-pure water (Milli-Q was obtained from the department) for the dilutions and HPLC water (Fisher Scientific UK Ltd., Bishop Meadow Road, Loughborough, LE115RG) was used for the HPLC analysis and the preparation of all the standards.

4.2 Sample preparation

The current method was adapted from the original which was designed to be used in raw milk, for the original method see Bobe *et al.*(1998) and V.Bonfatti *et al.*(2008).[26,64]

The milk samples were frozen in aliquots of 0.5 mL at -20 °C for preservation until measurement. A direct addition at 1:1 ratio (v:v) to the frozen sample was made of the solution (HPLC solution) containing 6 M GdnHCl, 5.37 mM sodium citrate, 0.1 M Bis-Tris buffer (pH 6.8) and 19.5 mM DTT (pH 7). The sample were left to thaw at room temperature, then they were shaken for 10s and left to rest for 1h at room temperature. The final step was to remove any fat by centrifugation at 16000 g for 5 min in a microcentrifuge. Finally the sample was further diluted by solvent C at a ratio of 1:3 (v:v). Solvent C was a made of water, acetonitrile and trifluoracetic acid (TFA) with the ratio 900:100:1 (v:v:v;).

4.3 Equipment and solvents

The HPLC system used was the Ultimate 3000 Thermo Fisher (Fisher Scientific UK Ltd., Bishop Meadow Road, Loughborough, LE115RG) equipped with a UV-Vis detector. The whole system was controlled using the software of Bruker Daltonics (Massachusetts, USA).

The HPLC flow rate was finally set at 0.4 mL min^{-1}, the injection volume was of 20 µL and the UV lamps was set at 214 nm for protein detection (to detect peptide bond).[26] The mobile phase used was a mixture of solvent A and solvent B, which were composed of water and acetonitrile both with 0.1% of TFA, respectively. The ratio of both solvents was optimised to achieve the separation of the 6 protein groups and is shown below in the following sections.

4.4 Column selection

The column selection processes compared the column used in the previous reference studies (Bobe *et al.* (1998) and V.Bonfatti *et al.* (2008)[26,64] with an available column that shifted some of the key parameters. The Zorbax column was the reference column used in the work carried out by V.Bonfatti *et al.* (2008),[26] and the Acquity column was another C8 column with a smaller particle size and pore diameter in order to test the effect of these parameters on peak broadening. The specs of the Agilent ZORBAX StableBond were C8 column, 300Å, 3.5 µm, 4.6 x 150 mm and the specs of the ACQUITY UPLC BEH were C8 column, 130Å, 1.7 µm, 2.1 mm x 50 mm.

In order to only compare the columns effect on protein separation, both the gradient and temperature were kept constant at Gradient 1 (Figure 4-3) and 25 °C.

Figure 4-1 and Figure 4-2 shows the spectra of injecting the main protein groups of milk using Zorbax and Acquity column, respectively. The results indicate that neither column achieved a full separation from the start. Zorbax column (Figure 4-1) achieved sharper peaks and an apparent better separation, even though it had multiple overlapped peaks. On the other hand, the Acquity column (Figure 4-2) suffered a significant peak broadening and it also did not manage a full separation.

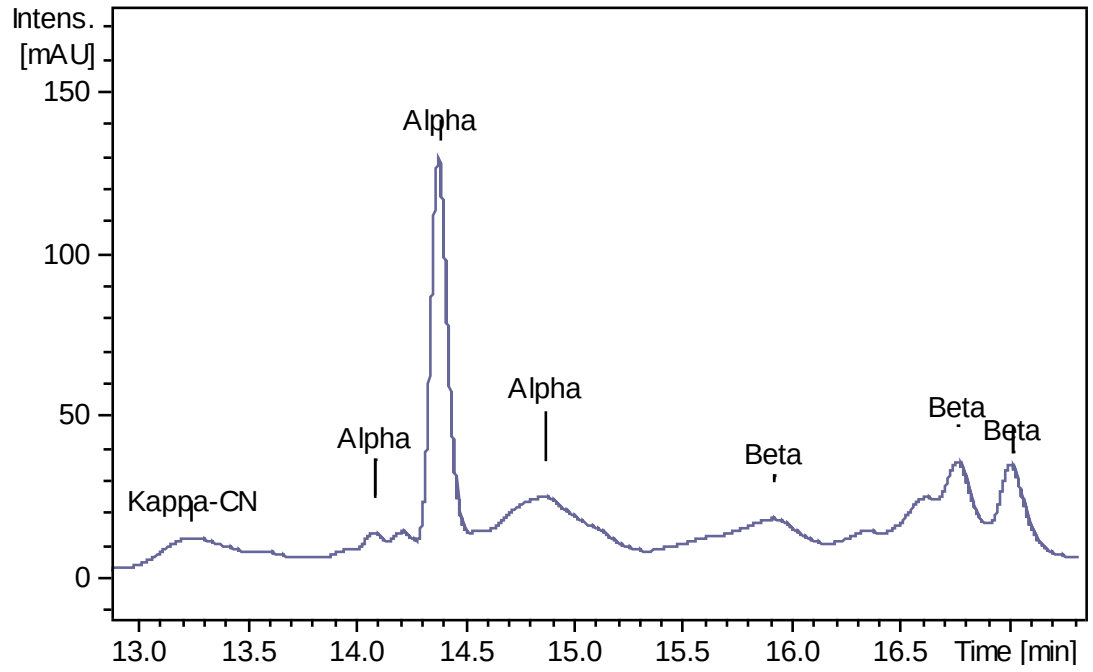

Figure 4-1: Chromatogram of all standards analysed at 214 nm, using ZORBAX column (C8 column with 300 Å), Gradient 1 and at 25 °C.

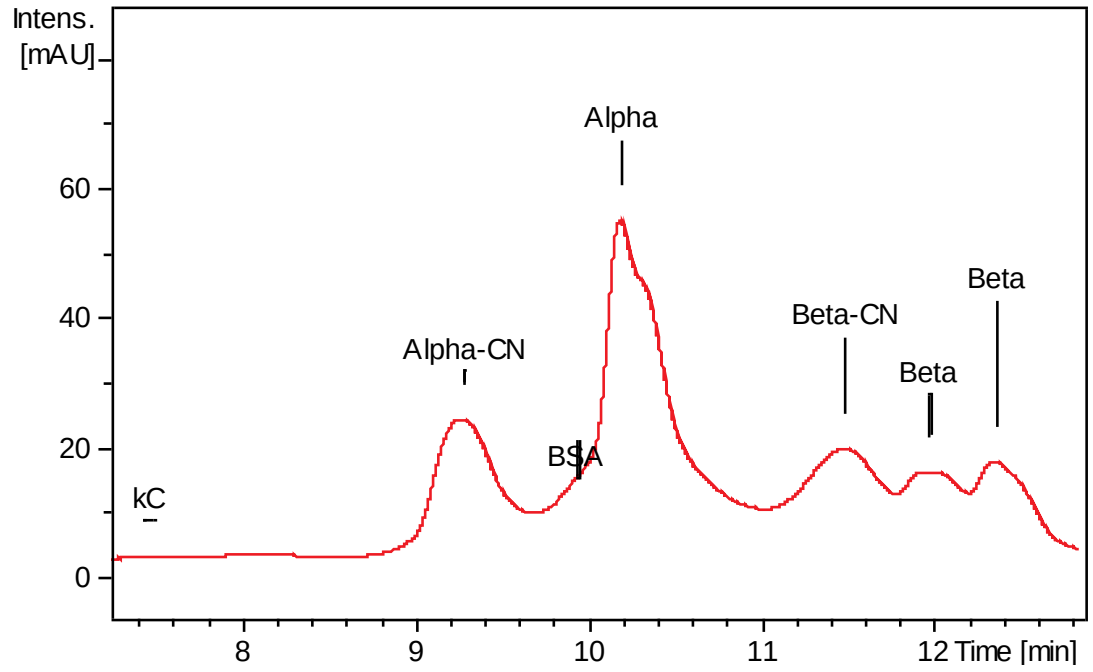

Figure 4-2: Chromatogram of all standards analysed at 214 nm, using ACQUITY column (C8 column with 130 Å), Gradient 1 and at 25 °C.

It was expected that the Zorbax column would perform better than the Acquity column due to the bigger internal diameter and the particle size in the column, since it was found in the literature that below the 300Å the peak broadening was promoted for protein analysis.[25,26,52,54,64]

In order to explain the peak broadening the Van Deemter equation (4-1) was used:[135]

$$HETP = A + \frac{B}{u} + C * u\ 1 \qquad 4\text{-}1$$

HETP measures the resolving power of a column, A is the Eddy-diffusion parameter, B is the longitudinal diffusion coefficient of eluting particles, u is the interstitial liner velocity and C is the reduced overall mass transfer coefficient.[135,136] Therefore, equation 4-1 defines three factors to explain peak broadening: Eddy Diffusion (factor A), Longitudinal Diffusion (factor B/u) and Mass Transfer (factor C*u).[135,136]

Using the Vam Deemter equation (4-1) the behaviour observed using Acquity column was linked to Eddy Diffusion. Eddy's effect relates to the internal path that solute particles can take when inside the column and links them to the peak broadening. Inside a column two particles of the same compounds may take different routes, which could lead to one of them requiring a longer elution time and resulting in the broadening of the measured peak. The pore sizes inside the column will affect the path that particles take, since big particles are not able to access small pore sizes eluting faster. In the case of protein with big natural variation within each protein group the broadening effect maybe promoted by having a smaller pore size (Acquity column) since some of the proteins will enter more pores than the bigger variants eluting much slower than the big proteins that can barely enter pores and elute faster. The above explained effects could explain why using the Zorbax column (which had bigger pores) the effect of broad peaks was less prominent. The assumption was that most of the proteins would be able to enter the pores reducing the difference in elution time among the bigger and smaller versions of the same protein group.

Based on the literature and the results of this section, the column used to carry gradient and temperature optimisation was the Agilent ZORBAX StableBond C8 300Å, 3.5 µm, 4.6 x 150 mm.

4.5 Gradient selection

The process was carried out in a gradient mode were the ratio of solvent A and B changed over time, in comparison to isocratic mode which keeps the ratio of solvents constant throughout. The aim behind the modification of the gradient was to take advantage of the differences in hydrophobicity between the different proteins to elute them at different times and with enough peak sharpness to differentiate each of them.

In order to test the effect of the gradient all the tests were carried out on the same column at 25 °C. The protein concentration to test the different gradients was 1 mg/mL for all proteins groups, nullifying the real differences in real milk, therefore the final gradient must have clear peaks with minimal or no overlapping since real samples peaks could be mistaken and miss assigned otherwise.

Gradient 1 was tested to achieve a fast separation of all the proteins (Figure 4-3), in order to minimise the overall injection time, however, the only separation obtained with this method was the one of alpha proteins from beta proteins, but not of casein from whey (Figure 4-4).

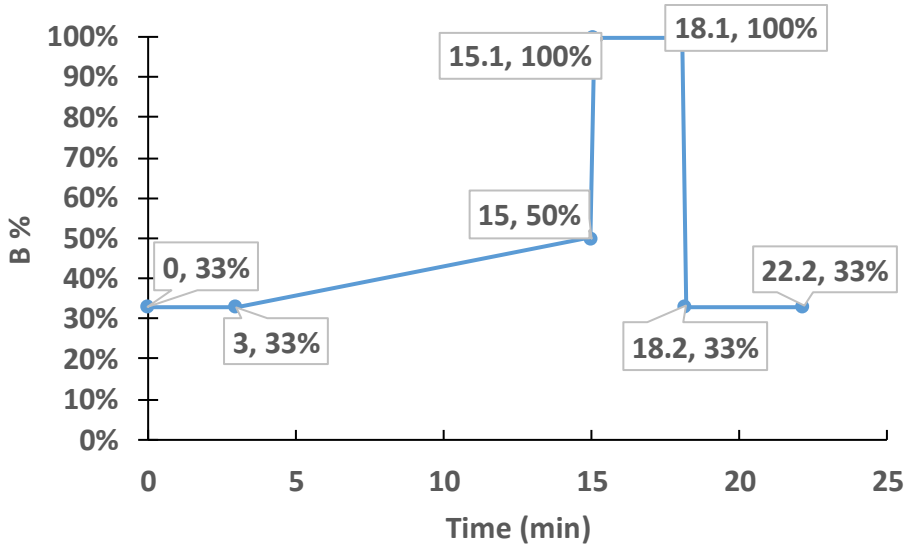

Figure 4-3: Gradient profile for gradient 1, showing the fraction of solvent B over time.

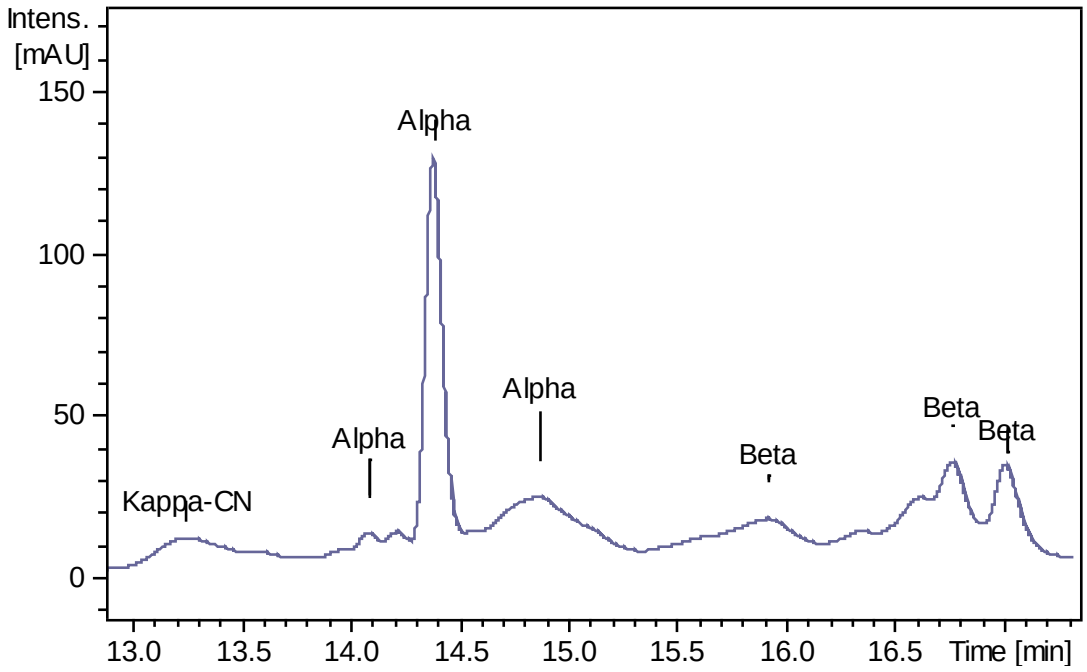

Figure 4-4: Chromatogram of all standards analysed at 214 nm, using the C8 column with 300 Å, and Gradient 1. Showing the separation of alpha proteins and beta proteins, but not the separation of casein and whey proteins.

To increase the differentiation of the target proteins the overall time was increased to accommodate a reduction of the gradient's slope which led to Gradient 2 (Figure 4-5). The lower slope managed to separate the alpha proteins into casein and whey, but it did not fully separate the beta casein from the beta whey (Figure 4-6), and it still did not have enough sharpness of peaks to fully quantify each different group. It seems that the separation time was still too short to obtain a proper full separation.

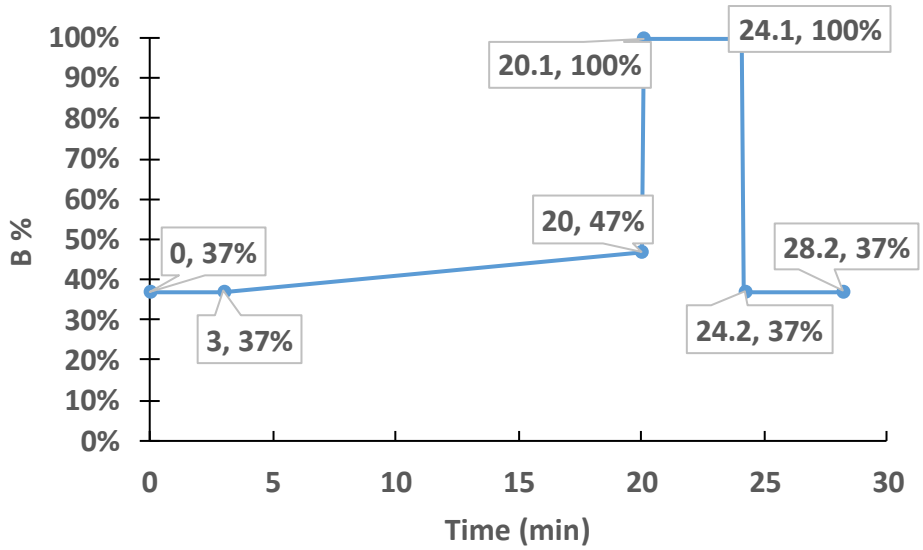

Figure 4-5: Gradient profile for gradient 2, showing the fraction of solvent B over time.

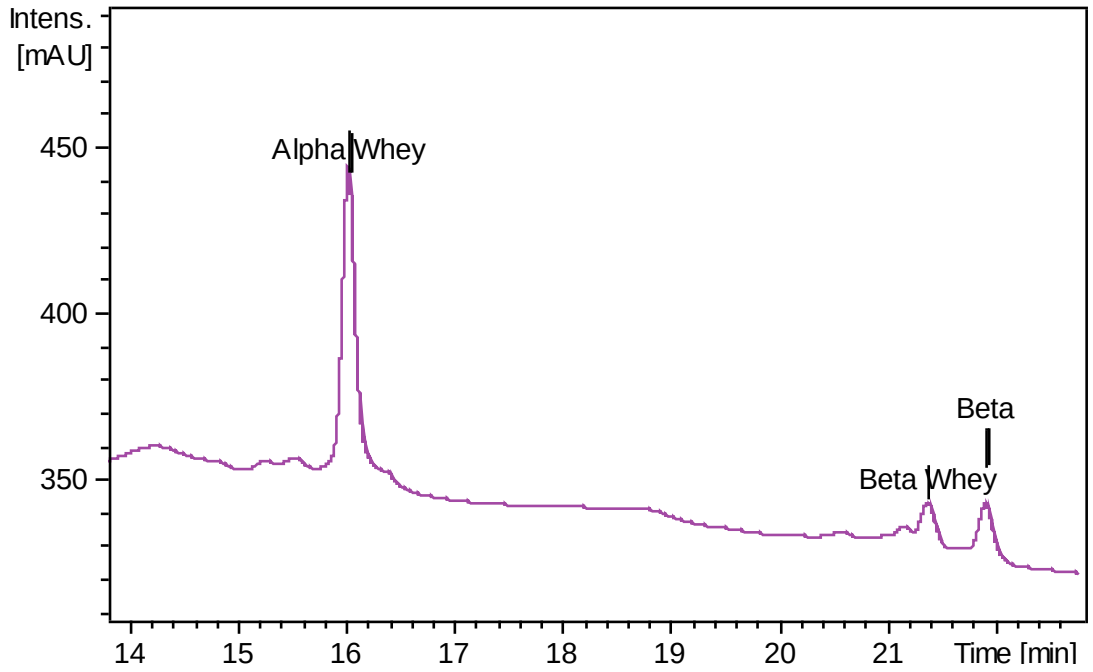

Figure 4-6: Chromatogram of all standards analysed at 214 nm, using the C8 column with 300 Å, and gradient 2. Showing that the beta casein and beta whey are not fully separated.

The next step was to increase the overall running time and higher organic content at the end of the separation, with a steady increase of the organic phase over a longer period of time (Figure 4-7). Gradient 3 kept a similar slope to Gradient 2 but it had a longer running time. The first highlight of this gradient was that all the proteins, except kappa-CN, had reference peaks (Figure 4-8). Looking into more detail the breakdown of the peaks seen at Figure 4-9 and Figure 4-10 shows that the proteins were still overlapping. At this point the method allowed to detect 5 of the protein groups just missing the Kappa-CN but it did not allow to quantify them due to the overlapping of peaks.

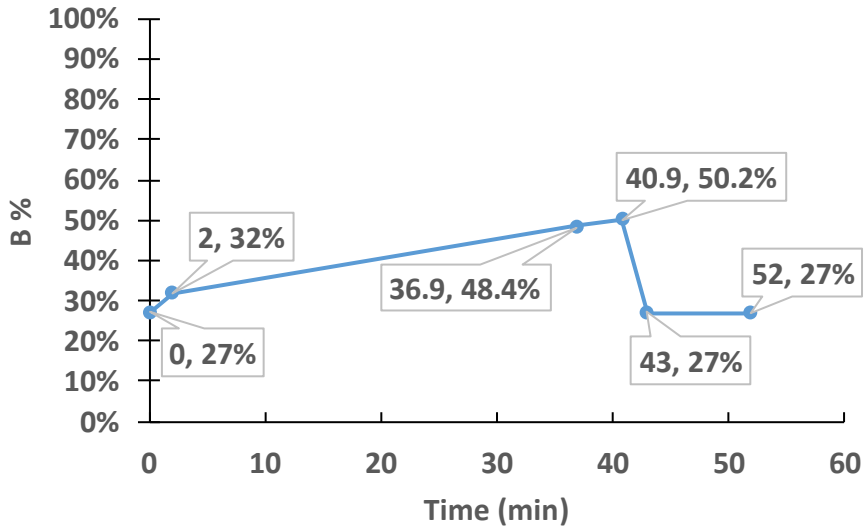

Figure 4-7: Gradient profile for gradient 3, showing the fraction of solvent B over time.

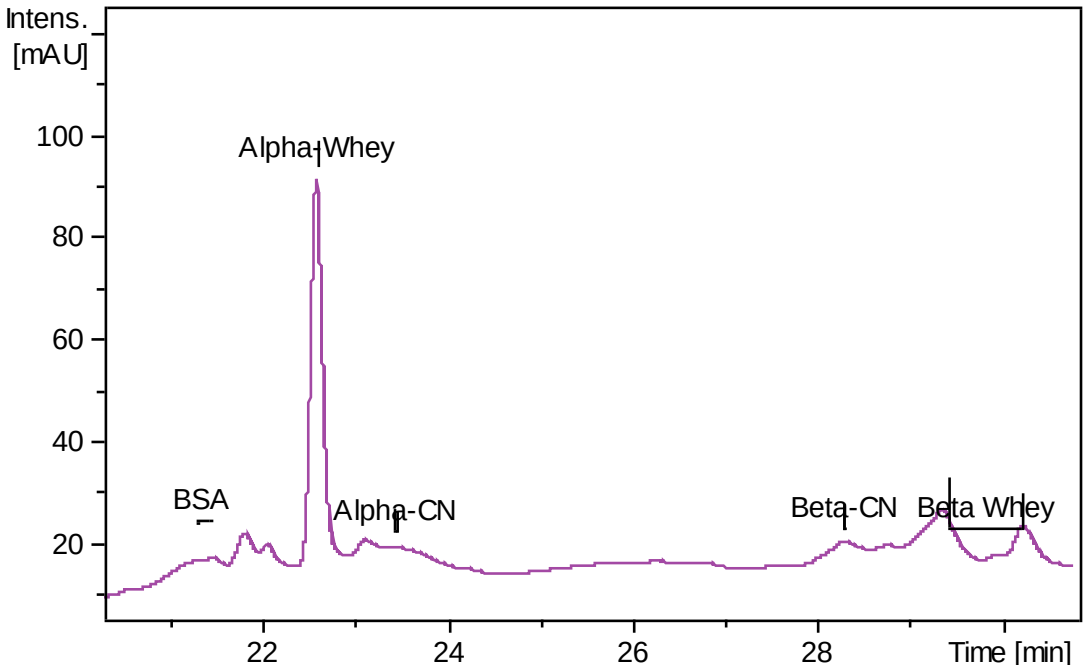

Figure 4-8: Chromatogram of all standards analysed at 214 nm, using the C8 column with 300 Å, and gradient 3. It shows the capability to detect all protein groups except kappa-CN.

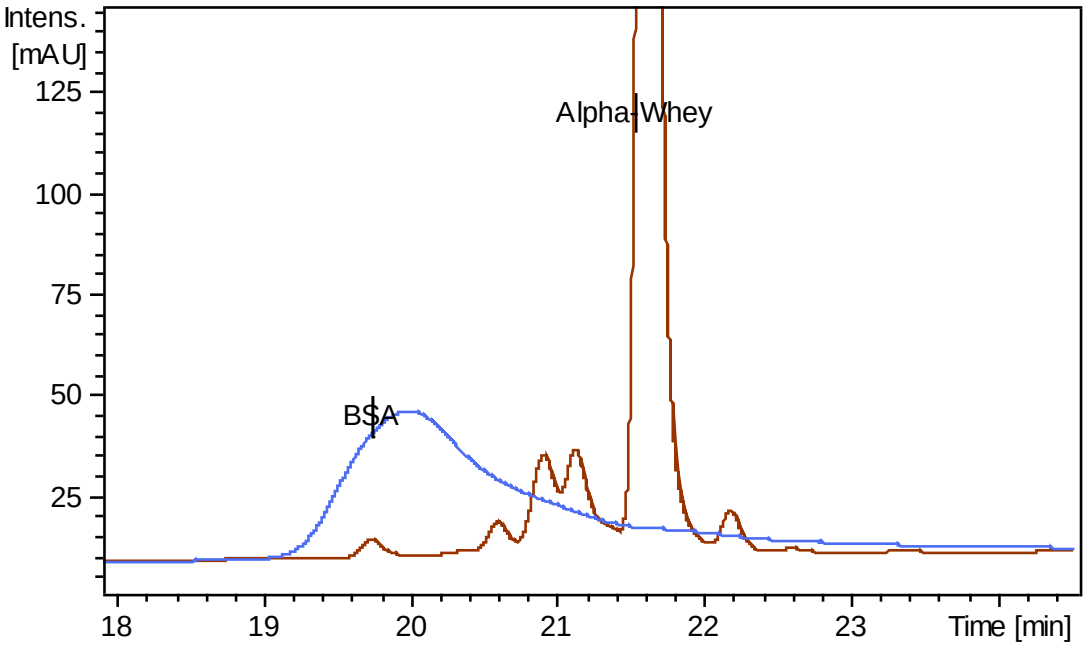

Figure 4-9: Chromatogram of BSA and Alpha-La standards analysed at 214 nm, using the C8 column with 300 Å, and gradient 3.

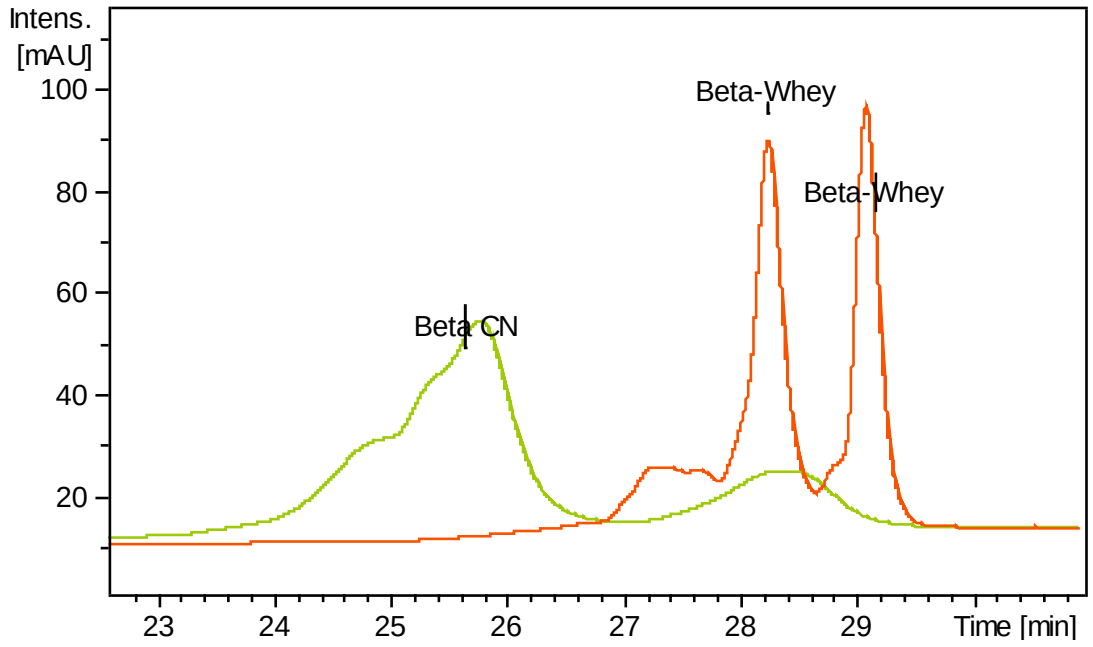

Figure 4-10: Chromatogram of Beta-CN and Beta-Whey standards analysed at 214 nm, using the C8 column with 300 Å, and gradient 3.

Gradient 4 increased the running time of gradient 3 and reduced the slope of the gradient ending in a lower final organic phases content (Figure 4-11). This approach was pursued after the fact that longer run times with small increases of organic phase led to better separation of the target proteins.

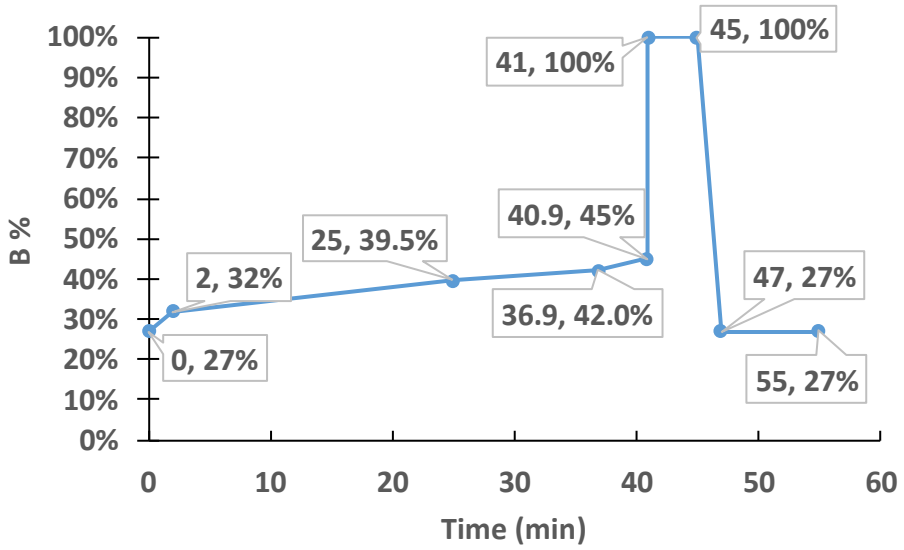

Figure 4-11: Gradient profile for gradient 4, showing the fraction of solvent B over time.

Figure 4-12 shows that the use of gradient 4 lead to the apparent separation of the alpha whey and casein, where there was just a tail of overlapping. However, the proper quantification could not be carried out with the level of overlapping among the BSA and both alpha proteins. Another challenge was the beta proteins did not fully separate and the fact that this gradient brought together the wide peaks of beta-CN and the peaks of alpha-CN. The remaining protein Kappa-CN (not shown) was fully separated without peak overlapping and it eluted in the first 14-20 minutes in a wide and quantifiable peak.

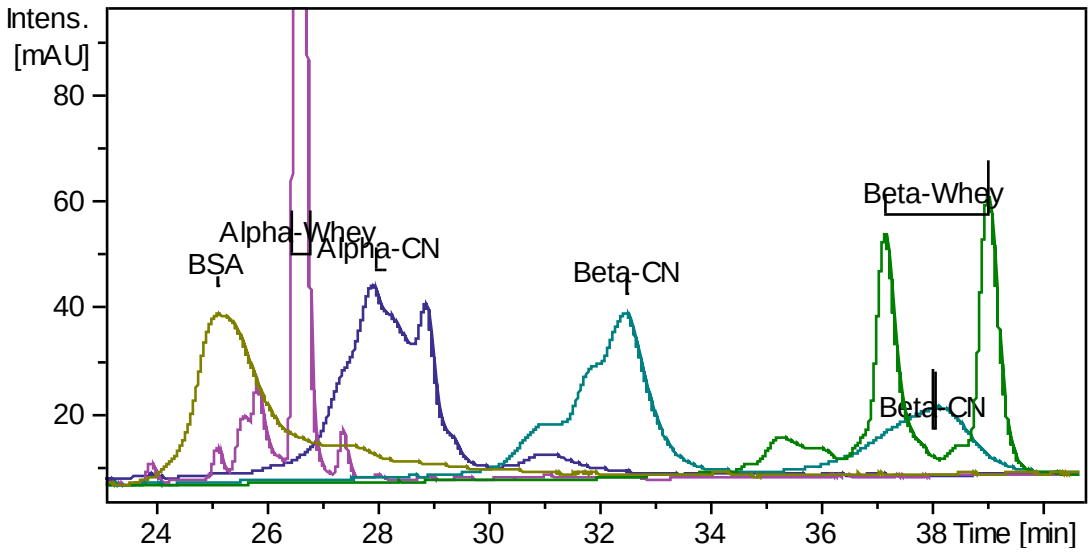

Figure 4-12: Chromatogram showing the BSA, Alpha-La, Alpha-CN, Beta-CN and Beta-Lg standards analysed at 214 nm, using the C8 column with 300 Å, and gradient 4. Showing the overlapping of BSA, Alpha-La and Alpha-CN and the overlapping of Beta-CN and Beta-Whey.

In order to elute the BSA faster to separate its overlapping from the alpha protein gradient 5 (Figure 4-13) had a “sharper” increase of organic content the first 22 minutes. Then the slope of the gradient was reduced to separate Alpha-La from Alpha-CN and to separate Beta-CN and Beta-Whey. Figure 4-14 shows that gradient 5 had reduced the overlap of BSA with both Alpha proteins but there was minor overlapping. Figure 4-15 shows that both Beta-CN and Beta-Lg were still overlapping.

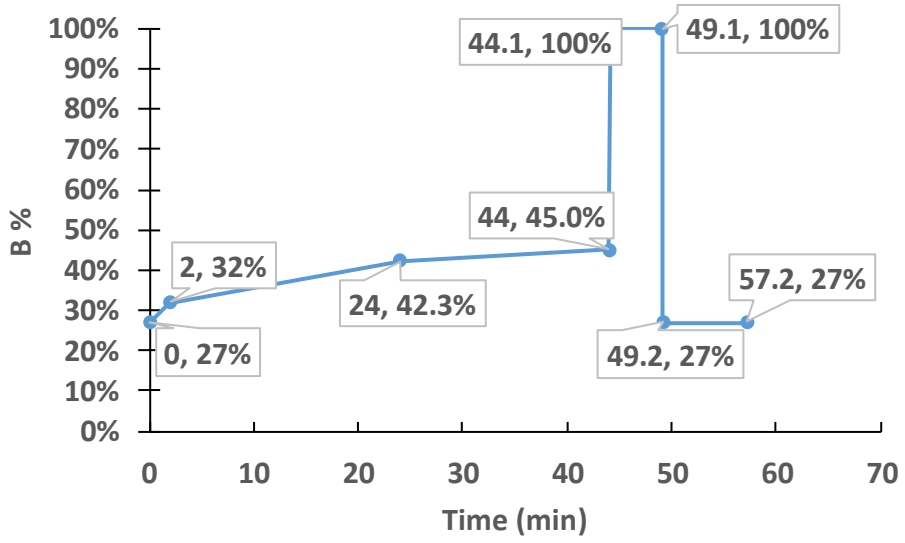

Figure 4-13: Gradient profile for gradient 5, showing the fraction of solvent B over time.

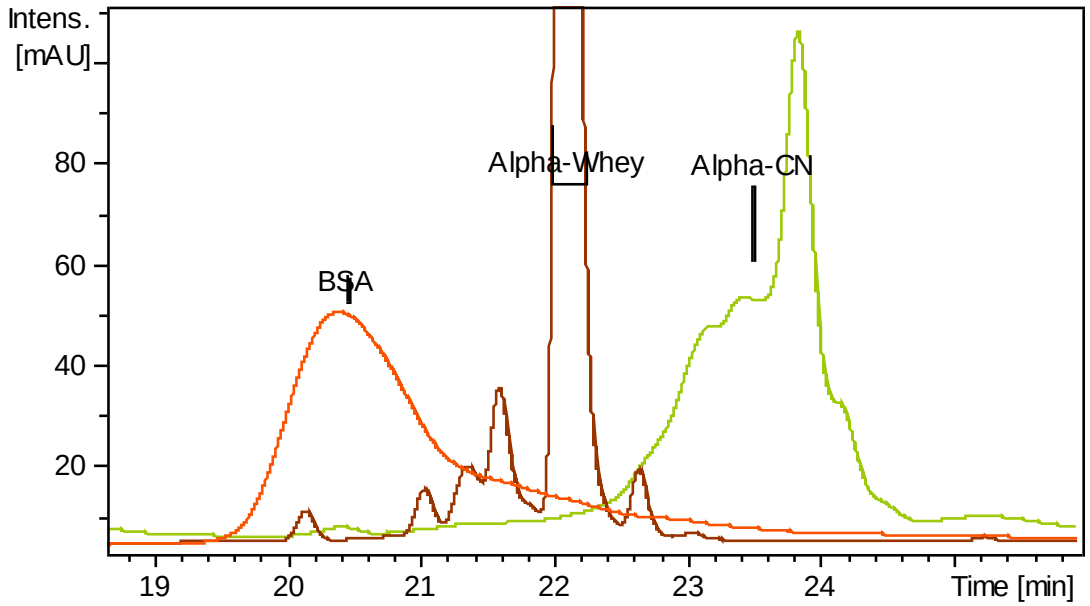

Figure 4-14: Chromatogram showing the BSA, Alpha-La, Alpha-CN standards analysed at 214 nm, using the C8 column with 300 Å, and gradient 5. It shows the overlapping of BSA with both Alpha proteins and a slight overlap of Alpha-CN and Alpha-La.

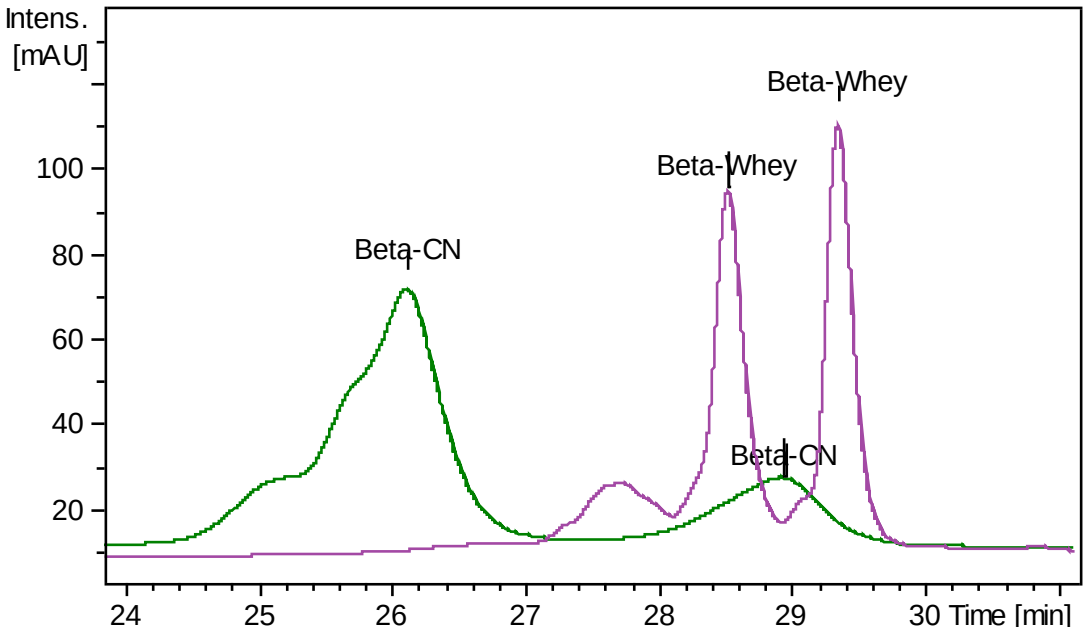

Figure 4-15: Chromatogram showing the Beta-CN and Beta-Lg standards analysed at 214 nm, using the C8 column with 300 Å, and gradient 5. It shows the overlap of Beta-Cn and Beta-Whey.

The next step was to focus on the separation of the Betas and to reduce the running time if possible. Gradient 6 has a running time of 42.2 min compared to the 57.2 minutes of gradient 5 (Figure 4-16). Gradient 6 could properly quantify the Kappa-CN and had minor peaks overlapping of BSA, Alpha-La and Alpha-CN. However, both Betas protein groups were still overlapping (the second peak of Beta-CN is in the middle of Beta-Lg peaks like in Figure 4-15). After this results Gradient 6 was chosen to be brought to the next step of optimisation being the best candidate for the whole separation and quantification (see Figure 4-17).

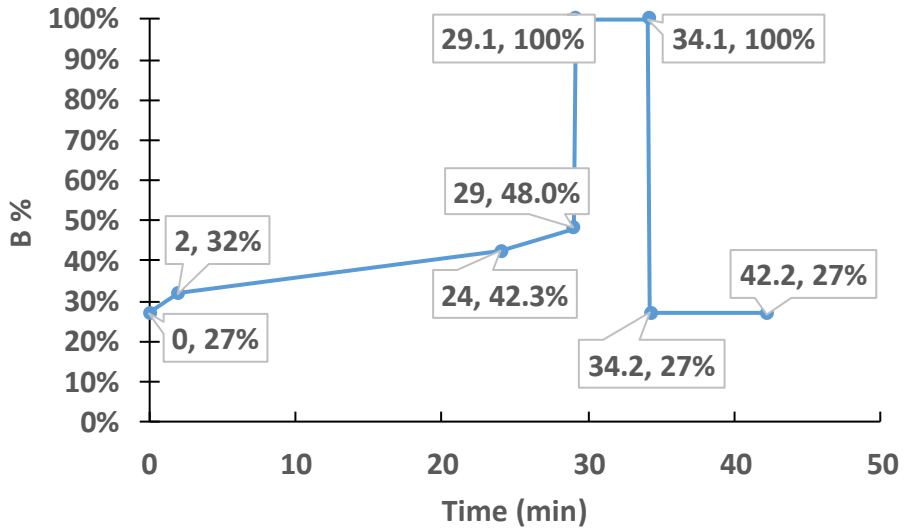

Figure 4-16: Gradient profile for gradient 6, showing the fraction of solvent B over time.

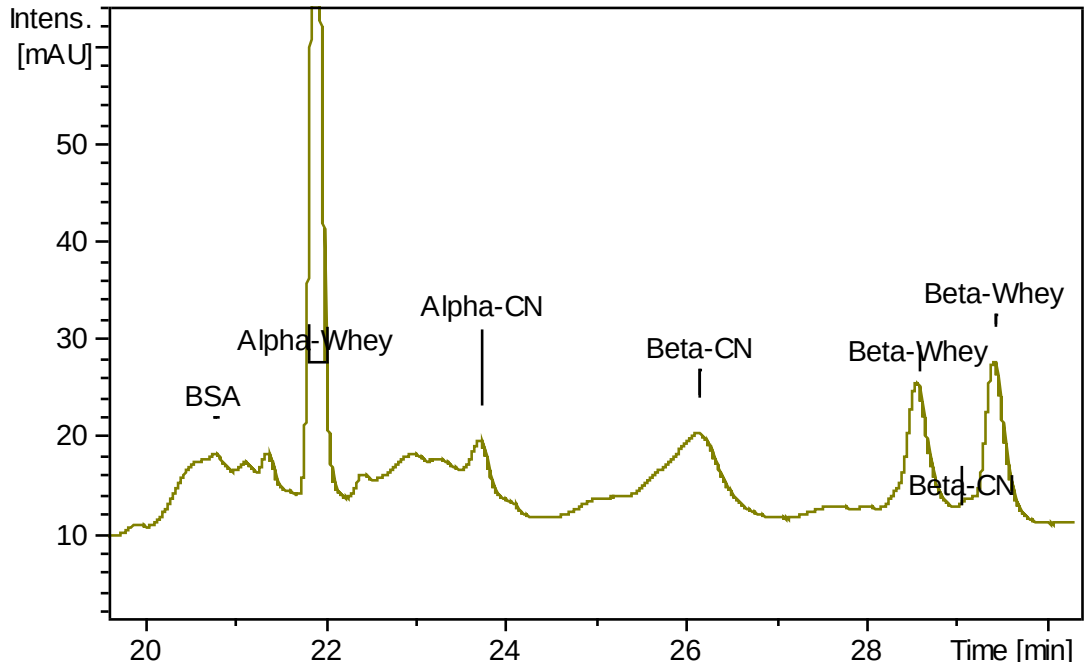

Figure 4-17: Chromatogram showing the BSA, Alpha-La, Alpha-CN, Beta-CN and Beta-Lg standards analysed at 214 nm, using the C8 column with 300 Å, and gradient 6.

4.6 Temperature selection

Proteins in general, and milk proteins in particular tend to be sensitive to temperature changes, that is the main reason that gradient selection was carried out at a constant temperature of 25 °C. In order to achieve a full separation of the protein groups the column temperature was the final parameter to test. The column temperature is a fix parameter once the injection has started, unlike the solvent gradient.

Temperature is one of the factors that has the biggest impact on the retention time of proteins. In general, proteins can change configuration with temperature, in particular some of the target casein and whey proteins will change configuration at the range 20-60 °C (whey proteins can denature at 60-65 °C, at 70 °C the denaturalisation is irreversible).[10] Higher temperatures also increases the rate of exchange of proteins between stationary phase and mobile phase, meaning faster elution time and maybe sharper peaks. The elution time can also increase if the solute (i.e proteins) suffer a confirmation shift and modifies its properties having a different interaction with the chosen column.[61]

The temperature optimisation was carried out using gradient 6 (Figure 4-16) with the aim to consolidate the separation of BSA, Alpha-CN and Alpha-La and to achieve the separation of Beta-Lg and Beta-CN. The base temperature of 25 °C was compared to 40, 45 and 50 °C. The analysis of the results has been based on the retention time of the first eluted peak of Beta-CN and Beta-Whey.

Figure 4-18 was the baseline of the temperature comparison, it showed both Beta proteins tested with gradient 6 at 25 °C. As said before, from these results both Beta-CN and Beta-Whey were clearly detectable since both had unique peaks, however due to the overlap of the second Beta-CN peak they were not quantifiable. Beta-CN retention times in function of temperature can be seen at Figure 4-19 and Beta-Lg at Figure 4-20. It can clearly be seen that the increase of temperature from 25 °C led to a longer elution time for the first peak for both betas. It can also be seen that increasing the temperature did not affect both protein groups the same way. Beta-CN elution time constantly increased with temperature having the longest elution time at 50 °C. On the other hand, Beta-Lg had a mixed order of elution based on temperature being 25, 50, 45 and 40 °C from fastest to slowest. These results do not follow the expected behaviour in RP-HPLC where an increase in temperature implies a reduction in elution times. It was found in the literature that a change in the protein structures may affect the kinetic behaviour between mobile and stationary phases and the analyte rising to higher retention times with the increase in temperature.[137–139] Following this a way to explain the higher retention times could be that proteins were changing their folding, the change in folding may allow higher interaction with the pores in the column. The increase in interaction with the column could explain the increase retention time as well as the improve in peak shape.

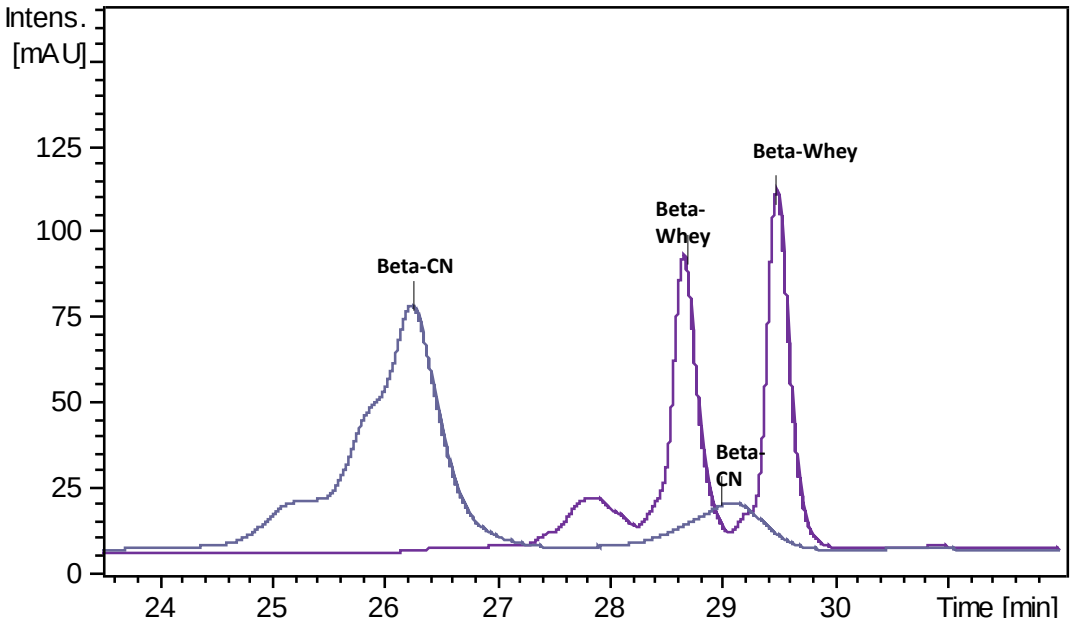

Figure 4-18: Chromatogram showing the Beta-CN and Beta-Lg standards analysed at 214 nm, using the C8 column with 300 Å, and gradient 6, at a Temperature of 25 °C.

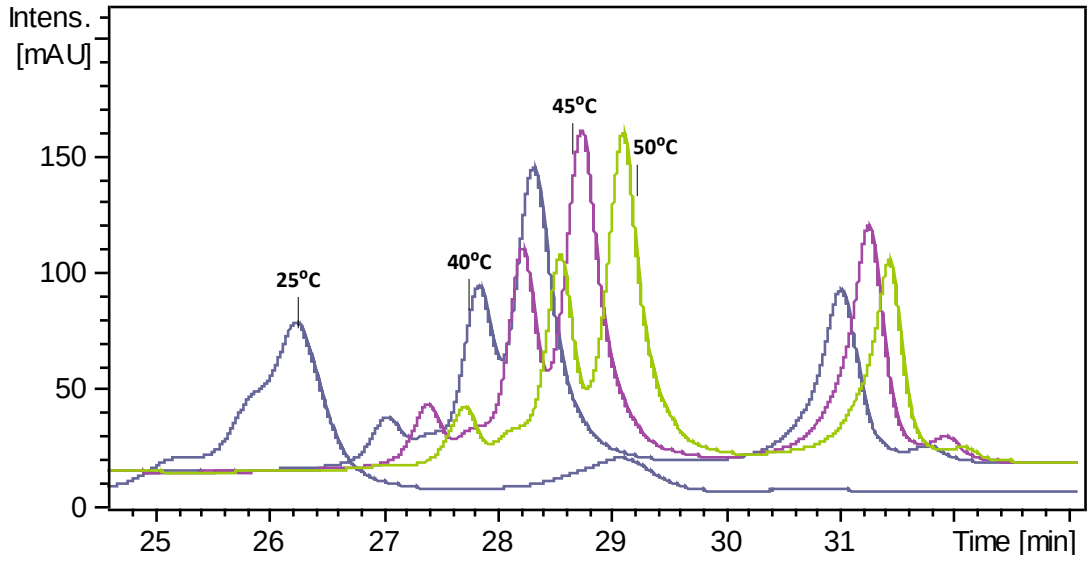

Figure 4-19: Chromatogram showing the Beta-CN standards analysed at 214 nm, using the C8 column with 300 Å, and gradient 6, at a range of Temperature from 25 to 50 °C.

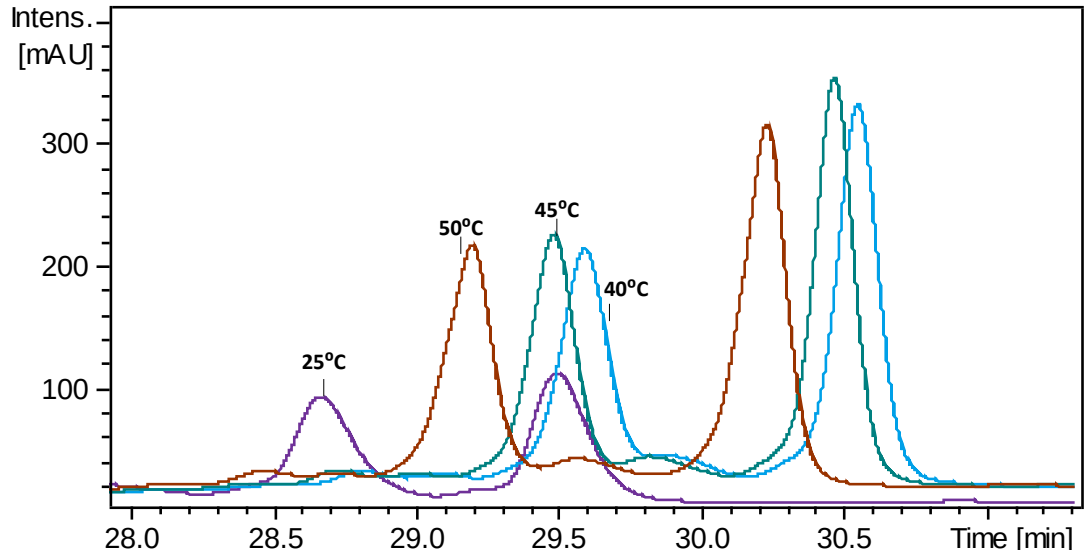

Figure 4-20: Chromatogram showing the Beta-Lg standards analysed at 214 nm, using the C8 column with 300 Å, and gradient 6, at a range of Temperature from 25 to 50 °C.

The final chosen temperature to obtain the best separation of Beta-CN and Beta-Lg is 45 °C. Figure 4-21 shows that the retention times of both proteins are different enough to quantify them reliably. At 40 °C (Figure 4-22) we can see a slight overlap of the final peak of Beta-Lg and the final peak of Beta-CN. This small overlap could have an effect on the measurement of milk samples and make the quantification a harder task.

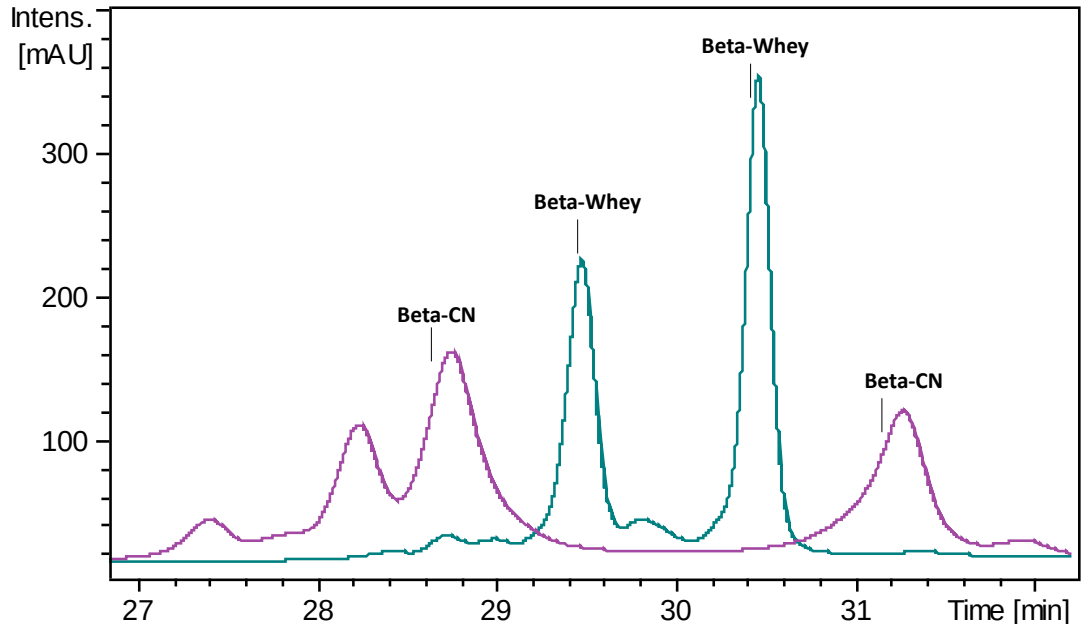

Figure 4-21: Chromatogram showing the Beta-CN and Beta-Lg standards analysed at 214 nm, using the C8 column with 300 Å, and gradient 6, at a Temperature of 45 °C. The graph shows the minimal overlap of the Beta-CN and Beta-Lg peaks.

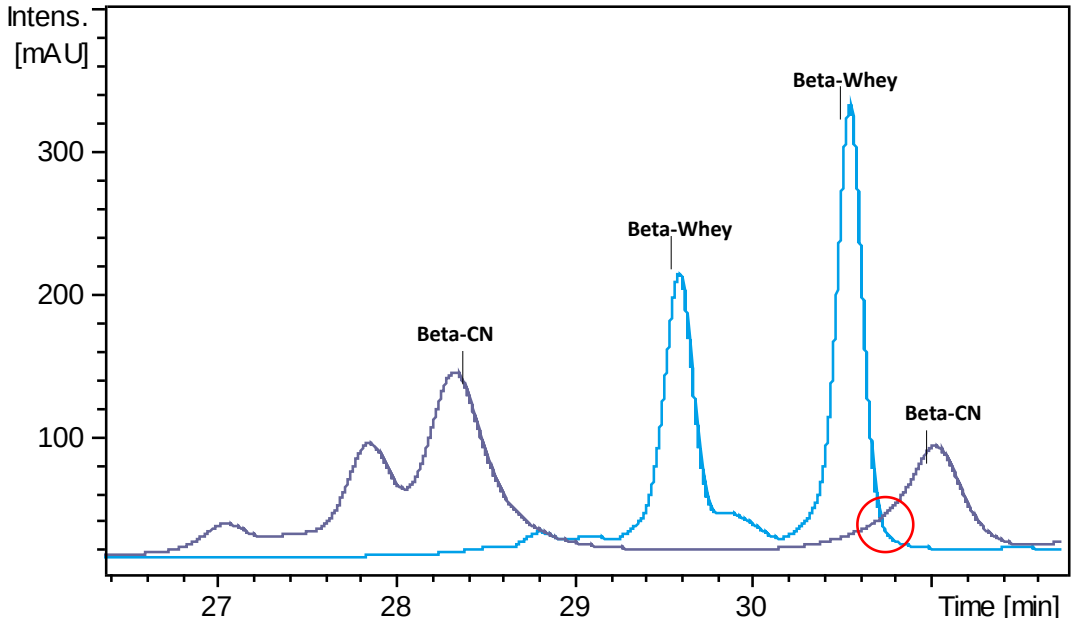

Figure 4-22: Chromatogram showing the Beta-CN and Beta-Lg standards analysed at 214 nm, using the C8 column with 300 Å, and gradient 6, at a Temperature of 40 °C. Red circle highlight the region of overlap compared to the 45 °C spectra.

Figure 4-23 shows the overlap of Beta-CN and Beta-Lg at its maximum expression (50 °C). This was due the combination of a delay of the Beta-CN and the minimum Beta-Lg elution time, making quantification impossible under this condition.

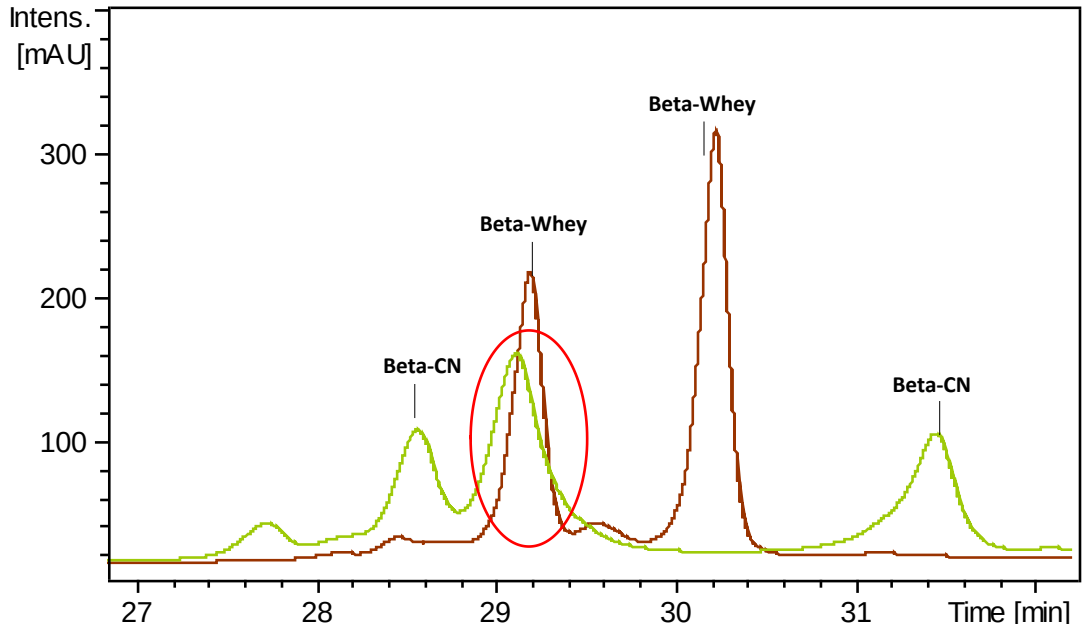

Figure 4-23: Chromatogram showing the Beta-CN and Beta-Lg standards analysed at 214 nm, using the C8 column with 300 Å, and gradient 6, at a Temperature of 50 °C. Red circle highlights the main region of overlap compared to 45 °C.

The final full spectra of proteins using the Agilent ZORBAX StableBond C8 300Å, 3.5 µm, 4.6 x 150 mm column, at 45 °C and gradient 6 can be seen at Figure 4-24.

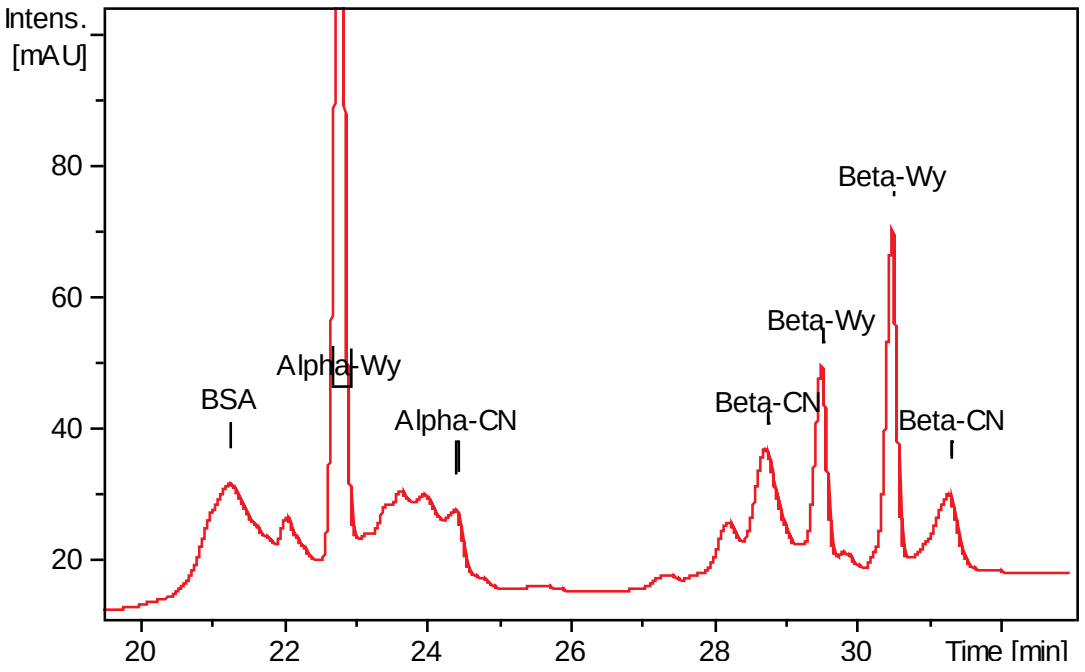

Figure 4-24: Chromatogram showing all standards except the Kappa-CN analysed at 214 nm, using the C8 column with 300 Å, and gradient 6, at a Temperature of 45ºC.

4.6.1 Method validation

The method was validated to ensure its robustness for the quantification of the target proteins using the Agilent ZORBAX StableBond C8 300Å, 3.5 µm, 4.6 x 150 mm column, at 45 °C and gradient 6.

The analysis of accuracy and precision can be found in Table 4-1. The accuracy results show that the method is able to obtain the right values for protein concentration at almost all protein concentrations, being beta-CN at low concentration the least accurate. The precision results display a partial shift and they show that at low concentrations the dispersion of the results increase, being the BSA the hardest to consistently measure.

Table 4-1: Results of analysis of Accuracy and precision. The concentrations for all proteins are 0.3, 1.6 and 4.2 mg mL^{-1}.

Protein concentration [mg mL^{-1}]	Accuracy table			Precision table		
	0.3	**1.6**	**4.2**	**0.3**	**1.6**	**4.2**
α-CN	0.6%	0.7%	0.9%	5.9%	2.9%	2.9%
β-CN	10.6%	3.7%	0.1%	7.6%	4.0%	6.0%
κ-CN	3.7%	2.0%	0.7%	3.3%	6.7%	1.1%
α-La	3.4%	0.4%	0.5%	4.8%	2.8%	1.4%
β-Lg	4.4%	7.5%	0.2%	2.3%	1.8%	1.0%
BSA	1.5%	1.6%	0.3%	5.8%	2.6%	4.4%

The chosen concentrations in Table 4-1 were based on the data shown in Table 2-1 and the dilution factor applied due to the preparation protocol (x6) explained in section 4.2. The diluted proteins fall within two ranges, 0.4 ±0.2 mg ml^{-1} and 1.9±0.05 mg ml^{-1}. The dilutions prepared that matched the selected regions where the 0.3 mg mL^{-1} for the lower range and the 1.6 mg mL^{-1} for the upper range.

Table 4-2 show the regression parameters, the limit of detection and limit of quantification for each protein group. The analysis of all proteins groups was quite robust since all of them had high R^2 values within almost the full range of analysed concentrations. However, it is important to highlight that the lowest concentrations carry a higher error than the higher ones for BSA. It is important to highlight that for all protein groups the limit of detection and limit of quantification were the same because the signal to noise ratio was always above 10.

Table 4-2: Summary table of regression parameters, range analysed, LOD and LOQ.

Protein	Range [mg mL^{-1}]		LOD [mg mL^{-1}]	LOQ [mg mL^{-1}]	R^2
	min	max			
α-CN	0.1	4.5	0.06	0.06	0.9978
β-CN	0.2	4.3	0.17	0.17	0.9988
κ-CN	0.0	4.1	0.03	0.03	0.9982
α-La	0.1	4.2	0.03	0.03	0.9981
β-Lg	0.0	4.2	0.05	0.05	0.9989
BSA	0.0	4.2	0.03	0.03	0.9982

4.7 Membrane protein analysis

The progress of the project required the capability to understand the protein composition on the membrane surface, in order to analyse it the HPLC method was adapted to work with fragments of membrane. The method adaptation was carried out to take advantage of available tools and knowledge. In this section the short description of how the method was adapted is shown with the main requirements and limitations of this membrane method. The critical factors for the method adaptation were, the soaking time, the reagent amount and protein detection.

The HPLC reagents used were the same ones used for liquid samples since their main purpose was to breakdown protein micelles and solubilise the proteins, which is even more important when analysing fouling layers on membranes. The protein peaks were detected using the same conditions as the liquid samples, since peaks did appear in the same order and locations. The peaks were also compared to the protein standards to ensure reliability of the detection.

The first stage focused on the foulant extraction either by scraping, sonication or using the HPLC solution to resuspend the proteins on the membrane. The membrane samples were cut on small pieces of 3mm x 3mm and dissolved into 0.25 mL of reagent.

The obtention of the fouling layer by physically scraping it off the membrane did not yield any reproducible signal and was discarded. Among the more reproducible signals sonication and protein extraction by soaking the membrane on the HPLC solution the method that yielded the higher and more consistent signal was the membrane soaking. As can be seen in Figure 4-25 the signal was significantly higher for the soaking method. The sonication did also have a lower rate of reproducibility, having 50% of the analysed samples with no signal.

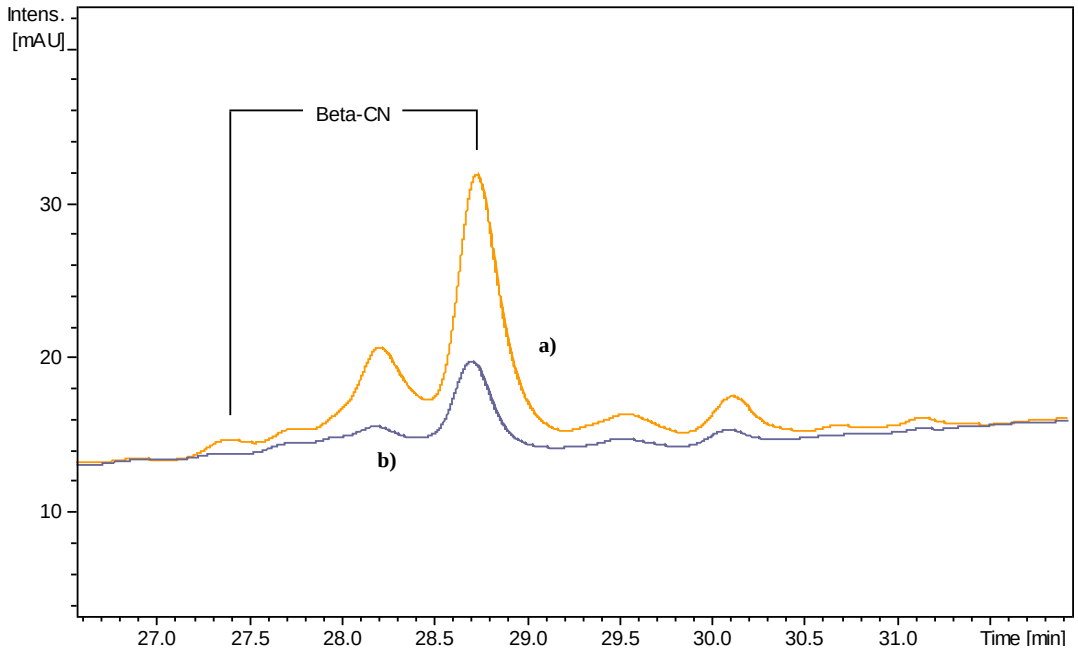

Figure 4-25: Chromatogram of the sample obtained by membrane soaking in 0.25 mL of HPLC solution (a) and membrane sonicated in 0.25 mL of HPLC solution (b). RP-HPLC system with UV-Vis detection at 214 nm, centred into the beta casein and whey peaks.

After selecting the membrane soaking method the soaking time effect was studied since it would be directly linked to protein extraction from the membrane. In order to test the effect of soaking time the same membrane was placed in the selected reagent for different amounts of time, increasing from 1, 6 and 24 hours.

The resuspension of the protein using the HPLC preparation (section 4.2) showed reliable constant peaks of comparable intensity for the same membrane when left in suspension for 1 hour (Figure 4-26). However, if the suspension was left for more than 6 hours the proteins signals were no longer detectable, as can clearly be seen in Figure 4-26. Since the method aims to resuspend proteins the lack of signal could be due to the proteins having precipitated again or being damaged by the reagents itself.

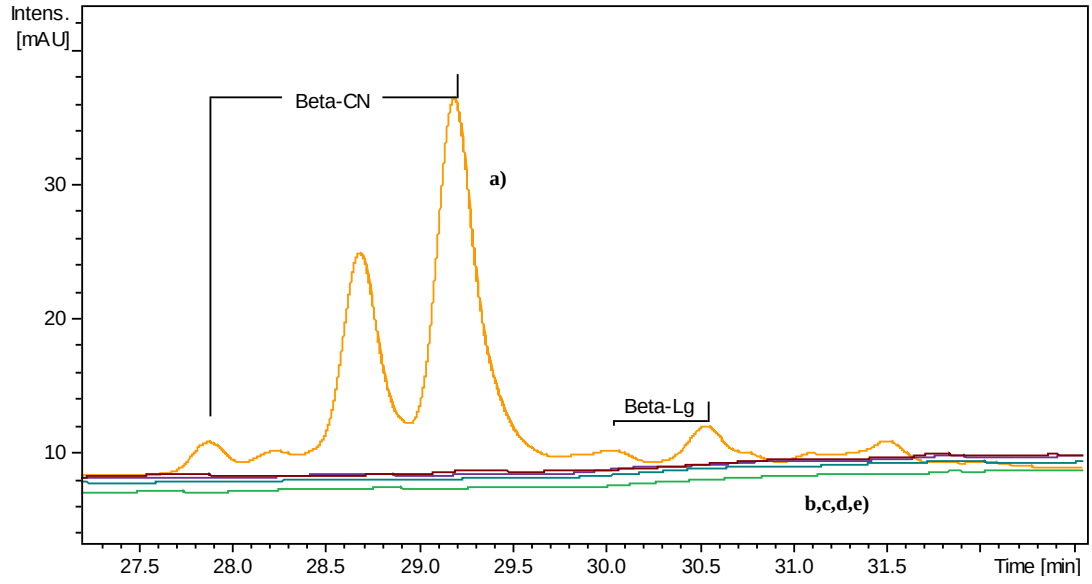

Figure 4-26: Chromatogram of samples obtained at different HPLC solution amounts and soaking time. a) 1 hours in 0.25 mL, b) 6h, 0.25 mL, c) 6h, 0.5 mL, d) 24h, 0.25mL and e) 24h, 0.5mL. RP-HPLC system with UV-Vis detection at 214 nm, centred into the beta casein and whey peaks.

The current known limitations of the method can be summarised into the lack of precision, it does extract the proteins on the membrane, but it is not clear if it includes all the proteins on the membrane sample and the pores or just the superior fouling layer. More work needs to be carried out on expanding this aspect, focusing on studying if there is a thickness of fouling layer that behaves as a tipping point beyond where the layers below the top cake do not get resuspended with the used method. The second limitation is that the method is perfectly valid to qualitatively assess the protein groups present but it does require further work to determine if the fouling proteins are fully extracted in order to fully use it as a quantitative method. Even though differences in protein concentration on the membrane did show in the chromatograms.

4.8 HPLC method summary

This chapter presents the method development of an RP-HPLC approach to detect and quantify the six main protein groups in milk (α-CN, β-CN and κ-CN from the casein proteins and, α-La, β-Lg and BSA from the whey proteins). The study has analysed the effect of the column, gradient and temperature had on the protein separation profile and finished by optimising the three parameters to allow the separation and quantification of each protein group. The final conditions chosen to analyse the protein groups were the Agilent ZORBAX StableBond C8 300Å, 3.5 µm, 4.6 x 150 mm column, using gradient 6 and at a temperature of 45 °C (Figure 4-24).

The separation process was designed to be able to both detect and quantify ($S/N \geq 10$) the six protein groups in a single injection. To the best of our knowledge this is the first time that in

a single injection the BSA protein group has been detected alongside with the α-CN, β-CN, κ-CN, α-La and β-Lg using a RP-HPLC system. The method was developed based on HPLC with UV detection aiming to be a widely applicable tool to any milk processing application like membrane filtration.

Future work should focus on the reduction of processing time aiming to free equipment time and reduce organic phase use and cost, another focus should be the study of common genetic variants to ensure detection and quantification.

Future research should focus on the use of mass spectrometry techniques to improve the detection of smaller fractions, aiming to follow the work on impurities and adulteration carried out by Leonil *et al.* (1995)[69] and to further detect genetic variants of the different proteins, since as demonstrated by the studies of Heidebrecht *et al.*[15–18] the use of certain "enhanced" immunoglobulins proteins can have great health benefits.

The work carried out in this study differ from previous studies using HPLC and C8 columns, mainly in the focus on BSA and the elution order of the proteins. The current study shows both casein proteins and whey proteins groups eluting alternatively unlike some of the previous studies where they reported a differentiated order of elution with the casein proteins eluting first followed by the whey proteins. The use of the adapted HPLC for membrane proteins detection is also a novelty carried out in this study.

Even though bovine animals have been around humans for 10.000 years the milk is still a matrix to be fully understood and therefore further improvements in the separation of proteins and other important components will be done in the coming years, as well as into the separation of them with less environmental impacts attached to the production processes, facilitating a healthier society that requires less of its environment.

Chapter 5. Interactions between skimmed milk and PVDF membrane

This chapter focuses on the results obtained using the Bench Top M10 rig (see Figure 3-2). The use of the Bench Top M10 focused on the study of the operational conditions (temperature, pressure, crossflow velocity, etc) and the effect they had on protein separation, specifically on the casein and whey rejections, with the aim to understand the factors that control the separation of each protein group in skimmed milk. All the studies have been performed with the final goal to achieve a full casein protein rejection while allowing through the membrane the highest amount possible of whey proteins.

The Bench Top M10 studies

The Bench Top M10 studies focused on understanding the interactions between the skimmed milk and the selected PVDF membranes, mainly the 0.1 µm PVDF membrane (Synder Filtration, V01). The studies were carried out at different operational conditions of inlet and outlet (which determined different TMP) pressure, temperature and crossflow velocities to evaluate the effects of these parameters on the protein separation, with the aim to explain the factors that controlled the casein and whey proteins fractionation.

The studies can be divided in two main groups: the first group consisting of all the tests carried out in concentration mode where the feed volume was reduced to half the initial value by filtration, and the mode of full recirculation where the feed volume was kept constant due to total recirculation of permeate and retentate (see Chapter 3 - Methodology). The volume reduction experiments were carried out to emulate more closely industrial conditions where the concentration step increases the protein content in the feed which also had the added effect of adding an extra filtration layer (due to the fouling layer). On the other hand, the full recirculation studies were aimed at describing a set of experimental conditions (temperature, TMP, CFV,…) and its behaviour over time to understand how the protein fractionation was affected.

5.1 Volume reduction studies

The volume reduction experiments were carried out using the 0.1 µm PVDF membrane (Synder Filtration, V01), as previously described in Chapter 3.

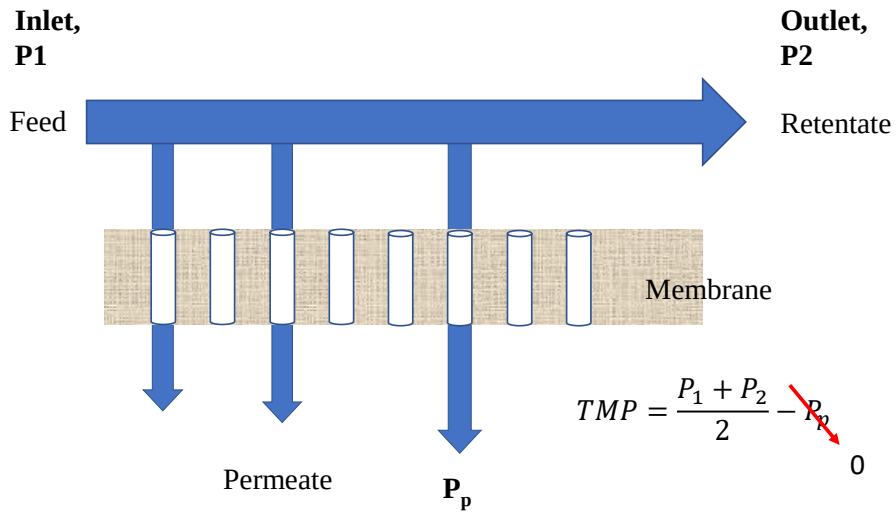

Figure 5-1: Inlet, outlet Pressure and TMP calculation for chapter 6.[3]

The volume reduction experiments can be summarised in Figure 5-2 where the most relevant results are shown. A wide range of conditions were tested to study both the effect of volume concentration factor on the filtration process and the effect that different operational conditions had. The main operational conditions that control the filtration process are cross flow velocity (CFV), inlet/outlet pressure (see Figure 5-1), transmembrane pressure (TMP) and temperature. In the current study the controlling factor was mainly the CFV. Transmembrane pressure and temperature were kept constant at 0.5 bar ±0.05 bar and 10 °C ±1 °C, respectively, during the concentration step, whereas outlet pressure was reported accordingly to the other factors. The aim of studying changes in CFV came from the intention to detect the effects of the fouling layer on the protein separation and permeate flux,[120] since they are two of the key parameters to define a membrane operation system.

Figure 5-2 shows the flux decline curves of the permeate flux during the concentration phase in order to reach a volume concentration factor of 2. The flux decline curves were obtained by concentrating the milk at different pressures and crossflow velocities (see Table 5-1), and keeping a constant temperature of 10 °C ±1 °C. The temperature of 10 °C was chosen because it is known that prevents microbiological growth allowing longer and safer filtration runs. The processing at low temperatures (10 °C and below) has a side effect on the beta-casein, which does undergo a transition from the micellar form to the monomer form facilitating its permeation through the membrane and enhancing its separation from the rest of casein proteins.[10,119]

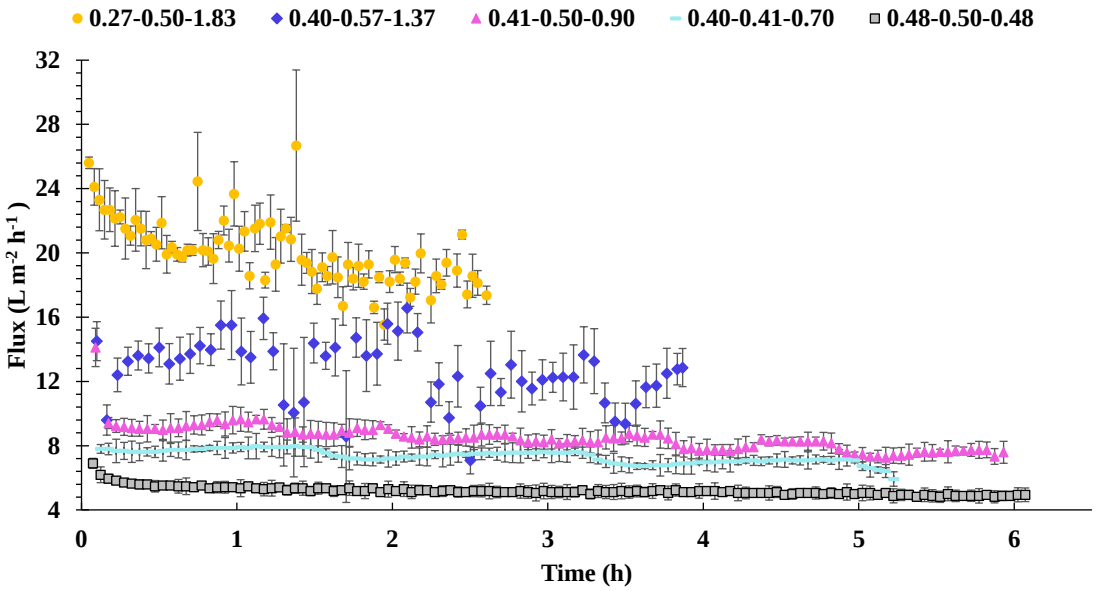

Figure 5-2: Flux decline curves of the permeate stream using the 0.1 µm membranes (Synder Filtration, V01). All samples were produced at 10 °C. Error bars correspond to the standard deviation of 2 repeats for each data point. Samples have been denoted as following: Outlet pressure-TMP-CFV.

The permeate curves can be used to indirectly estimate the magnitude of fouling that is growing on the membrane. As shown in equation 3-1 when TMP and viscosity are kept constant, the flux is the inverse of total resistance (R_t). The R_t depends on the combination of the membrane resistance (R_m, which is a constant value) and the fouling resistances (R_{cp}, R_c and R_i) that will change during the filtration process based on the feed and operational conditions. Therefore, in any filtration process when TMP and viscosity are kept constant and the permeate flux decreases, it can be assumed that fouling is present and is increasing if the permeate flux is decreasing.

From an industrial perspective, it is desired to process milk at the highest possible permeate flux and achieve high casein rejection and low whey rejection. These are the ideal conditions in order to achieve an energy efficient industrial milk filtration process.

The decline curves shown in Figure 5-2, coupled with the rejections shown in Table 5-1, indicate that higher fouling leads to lower permeate fluxes along with high casein and whey protein rejections, as observed when comparing sample 0.27-0.50-1.83 with the rest. The lower fouling content of sample 0.27-0.50-1.83 leads to the highest permeate flux values and lowest concentration time. However, this faster process also exhibits the lowest casein protein rejection, which goes against the industrial requirements of achieving high casein rejection values. When comparing all the other samples the reduction of flux does not correlate with neither an increase in casein rejection values nor a decrease in whey protein rejection values, since the difference amongst the samples fall within the analytical method error (see Table 5-1).

The results shown in Figure 5-2 and Table 5-1 indicate that a "sweet spot" of operational conditions can be found where the concentration step time can be minimised, while achieving the highest casein protein rejection values. The CFV modifications show that higher values prevent the fouling layer formation affecting both the protein rejection and the concentration step duration. The use of a CFV of 1.4 m s^{-1} shortened the concentration step duration around 2 hours (down from 6 to 4 hours) when compared to the lower CFV of 0.7 m s^{-1}, while keeping similar rejection values. This finding shows that operational conditions are key to define the fouling layer and interaction with the membrane that will condition the subsequent filtration step while minimising the preparation step reducing the time, energy and cost linked to the concentration.

Figure 5-2 shows that under certain operational conditions the fouling components are disrupted enough to allow a high permeate flux with low protein rejection values (see Table 5-1). On the other hand, after a threshold of operational conditions (mainly CFV below 1.37 m s^{-1}) there is a wide range of permeate flux values where the protein rejections are similar. This wide range implies a sweet spot of operational conditions that allow high permeate flux values and high casein protein rejection (and whey proteins as well), probably linked to an enhanced filtration layer formed by the fouling and concentration polarisation layers which had the effect of reducing the effective membrane cut-off and increasing the whey proteins rejection.

In summary, the chosen samples show that using the same feed and volume concentration factor of 2 different filtration behaviours can occur based on the operational conditions, and that similar filtration performances can be achieved through different concentration times that can oscillate between 3 and 6 hours.

Table 5-1: Protein rejections and processing conditions of Figure 5-2. All experiments were carried out at using the 0.1 µm PVDF membrane (Synder Filtration, V01) at 10 °C. Samples have been denoted as following: Outlet pressure-TMP-CFV.

Sample name	Inlet [bar]	Outlet [bar]	TMP [bar]	CFV [m s^{-1}]	Casein rejection [%]	Whey rejection [%]
0.27-0.50-1.83	0.73	0.27	0.50	1.83	76 ± 1	62 ± 1
0.40-0.57-1.37	0.75	0.40	0.57	1.37	96 ± 5	70 ± 1
0.41-0.50-0.90	0.60	0.41	0.50	0.90	96 ± 4	76 ± 7
0.40-0.41-0.70	0.41	0.41	0.41	0.70	94 ± 6	72 ± 5
0.48-0.50-0.48	0.52	0.48	0.50	0.48	91 ± 4	68 ± 3

Table 5-1 shows that sample 0.27-0.50-1.83 had the highest CFV of 1.83 m s^{-1} which led to the lowest concentration time and the lowest protein rejections, supporting the fact that the high CFV leads to lower protein rejection due to having a smaller fouling layer. On the other

hand, the CFV below 1.37 m s^{-1} show similar protein rejections values indicating that the fouling layers formed under these conditions have a similar effect on the separation even though the permeate flux data suggest that the lower CFV value led to much severe fouling layers.

The processing conditions can affect the fouling layer itself since the different components mainly reversible and irreversible fouling will vary depending on the pressure conditions, inlet/outlet pressure, TMP (as well as pressure drop) and CFV. This is an important factor to take into account since by varying the processing conditions the fouling layer can be modified and therefore the effect on the separation is mainly due to the modified fouling layer. The presence of fouling on membranes modifies its properties. In order to gain insight on this effect the resistance analysis was carried out and can be seen in Figure 5-3.

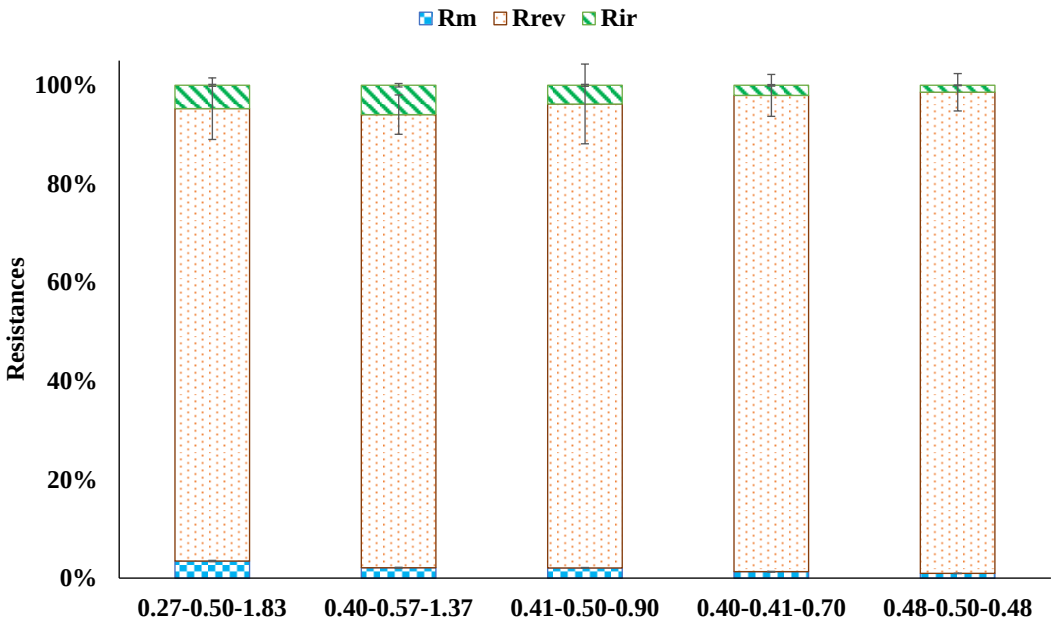

Figure 5-3: Membrane resistance values for filtration processes seen in Figure 5-2. Total ressistance values broken down into membrane resistance (Rm), reversible fouling resistance (Rrev) and Irreversible fouling resistance (Rir). All samples have been normalised for ease of comparison (calculated by dividing each resistance by the total resistance, see Equation 3-2), membrane resistance value was constant for all samples analysed. Error bars correspond to the standard deviation of 2 repeats for each data point. Samples have been denoted as following: Outlet pressure-TMP-CFV.

Figure 5-3 shows the resistances breakdown by the type of resistance (R_m, $R_{rev,}$ R_{ir}), as described in detail in Chapter 3. It is observed that reversible resistance accounts for most of the total resistance in any of the studied experimental conditions. The most surprising result is that high CFV and flux leads to having higher share of irreversible resistance than the samples with lower CFV and fluxes. The high CFV prevents the formation of higher amounts of reversible fouling phenomena leading to having a lower share of reversible fouling overall, which does not impact directly the irreversible fouling value.

Another highlight of Figure 5-3 is the high proportion of reversible fouling for all the studied conditions which indicates that both rinseable cake layer and concentration polarisation are dominant fouling mechanisms in the current study.

5.2 Full recirculation studies

The full recirculation studies encompass all the work carried out in full recirculation where the feed does not require any concentration step (see methodology section 0). The work had several aims towards understanding the combination of operational conditions that lead to protein rejections aiming to high casein rejection and low whey protein rejection.

The experiments span from the initial general tests of conditions, the DoE and the membrane concentration tests.

5.2.1 General tests

The first step to study the operational conditions and their effect on protein separation was to determine the broad effect of inlet/outlet pressure combinations and transmembrane pressure, as well as, crossflow velocity and temperature had on protein rejection values. The results shown in this section are used later on to define the experimental limits of the DoE.

5.2.1.1 Temperature effects

The analysis of the operational conditions started by comparing experiments carried out at the same processing temperature (samples at 50 °C) with different CFV as described in Table 5-2 and same pressures and CFV at different temperature. The two extreme processing temperatures (10 and 50 °C) were chosen to evaluate their effect on protein fractionation. It is known that at low temperatures around 8.9 °C (10 °C included) beta-casein transitions from the micellar form to the monomer form facilitating its permeation through the membrane and enhancing its separation from the rest of casein proteins.[10,119] The high temperature of 50 °C was chosen because of its contrast in terms of viscosity values and protein structure configuration since beta-casein does migrate back into the micelle and casein protein undergo protein configuration changes.[10]

Table 5-2: Operational conditions of flux decline curves 50°C-1.1 m s^{-1}, 50°C-1.6 m s^{-1} and 10°C-1.5 m s^{-1}. Samples have been denoted as following: Temperature-CFV.

Sample	Inlet [bar]	Outlet [bar]	TMP [bar]	CFV [m s^{-1}]	Temperature [°C]
50°C-1.1 m s^{-1}	1.08	0.98	1.03	1.10	50
50°C-1.6 m s^{-1}	1.24	0.90	1.07	1.60	50
10°C-1.5 m s^{-1}	1.19	0.91	1.05	1.50	10

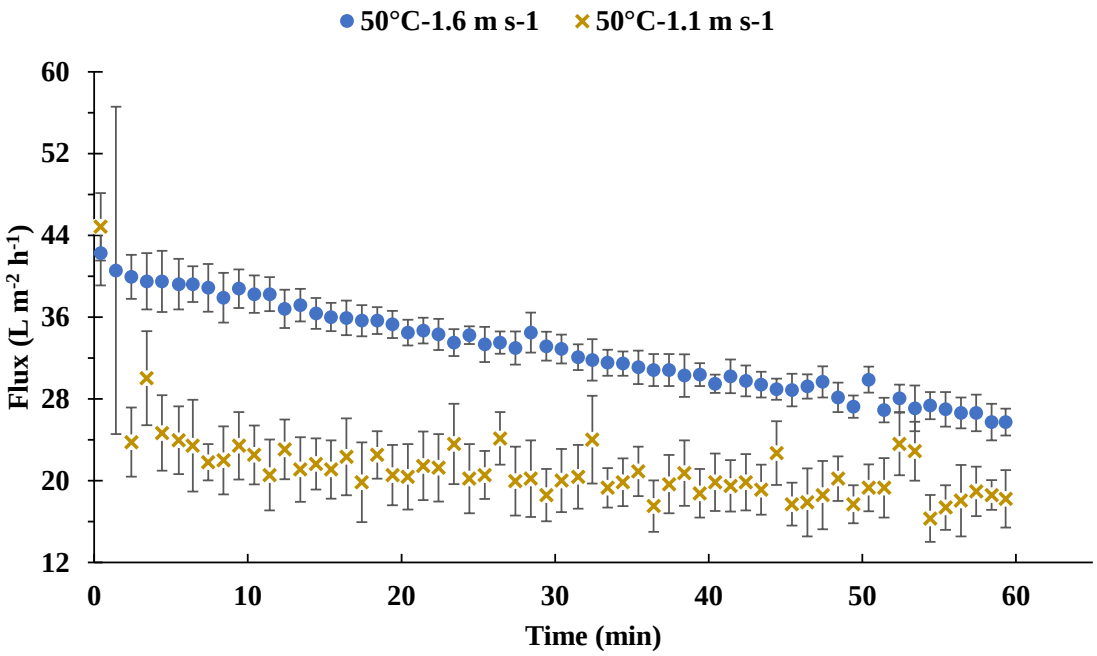

Figure 5-4: Flux decline curve of filtration at TMP of 1 bar and temperature of 50°C. 50°C-1.1 m s^{-1} and 50°C-1.6 m s^{-1} had CFV of 1.07 and 1.6 m s^{-1} respectively. Samples have been denoted as following: Temperature-CFV.

Figure 5-4 shows the effect that modifications of the CFV can have on the permeate flux when all the other parameters are kept constant. 50°C-1.1 m s^{-1} clearly had a much lower permeate flux than 50°C-1.6 m s^{-1}, mainly due to the significant difference in CFV from 1.07 to 1.6 m s^{-1}. The difference in CFV can then be attributed as a factor for the different protein rejections, with a higher overall rejection after the first hour of filtration for the 50°C-1.1 m s^{-1} (lower CFV) of 77% for casein proteins over the 66% for 50°C-1.6 m s^{-1} (see Table 5-3). The main effect observed here is the lower CFV conditions led to a higher degree of fouling that favoured an increased rejection of proteins as a side effect. The effect of the fouling layer as protein rejection driver can even surpass the effect of the membrane pore size as Lawrence *et al.* (2008) demonstrated, where they compare two pore sizes 0.3 and 0.5 µm and found that the fouling layer was the main component for protein rejection.[120]

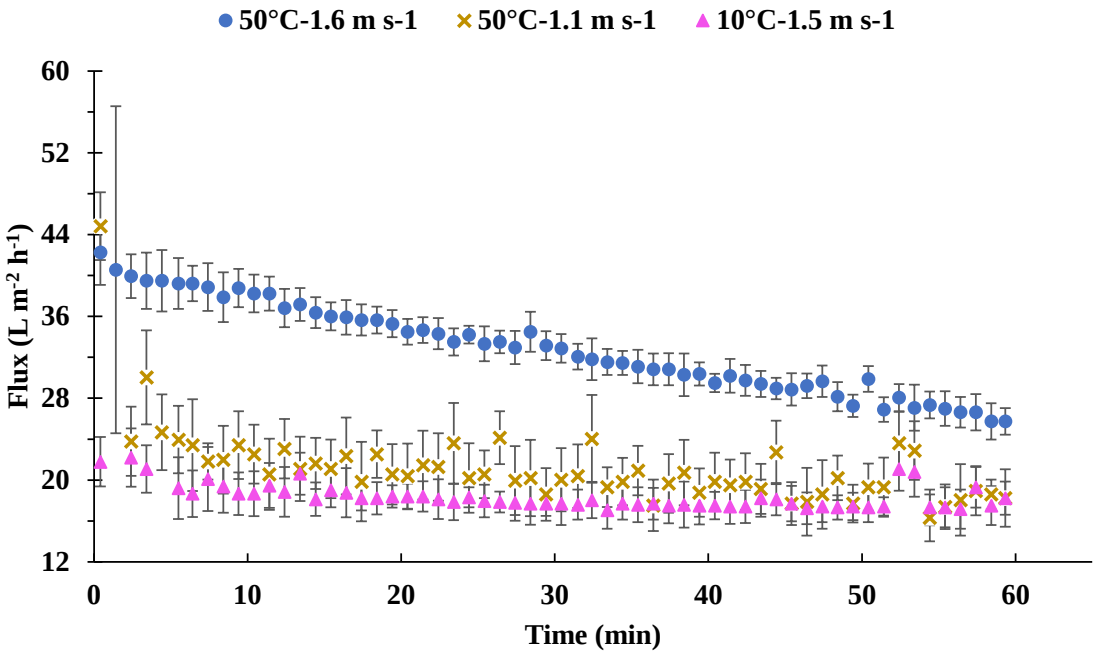

Figure 5-5: Flux decline curve for sample 50°C-1.1 m s^{-1}, 50°C-1.6 m s^{-1} and 10°C-1.5 m s^{-1}. Sample 10°C-1.5 m s^{-1} was processed at TMP 1 bar, temperature of 10°C and CFV of 1.53 m s^{-1}. Samples have been denoted as following: Temperature-CFV.

The first difference when comparing same processing conditions with the exception of the temperature as seen in Figure 5-5 (samples 50°C-1.6 m s^{-1} and 10°C-1.5 m s^{-1}) is that the permeate flux is strongly affected by the temperature, showing a stark decline from the initial 40 L m^{-2} h^{-1} at 50 °C to the initial 20 L m^{-2} h^{-1} at 10 °C. This difference in flux is associated to the viscosity of the milk that decreases with temperature and to the protein behaviour that is also affected with temperature (micelles contract)[48] and also promotes a fouling phenomenon that reduces the permeate flux even further.

Figure 5-6 contains the protein distribution for each experimental condition of Figure 5-5. The main highlight is that under the shown conditions the protein distribution of the final permeate does not vary enough to deem it statistically relevant, even though the permeate flux showed different behaviour. These first results are in line with the previous work shown with the volume reduction where different operational conditions and flux decline curves lead to similar protein rejections at the end, being the operational time the highest discrepancy.

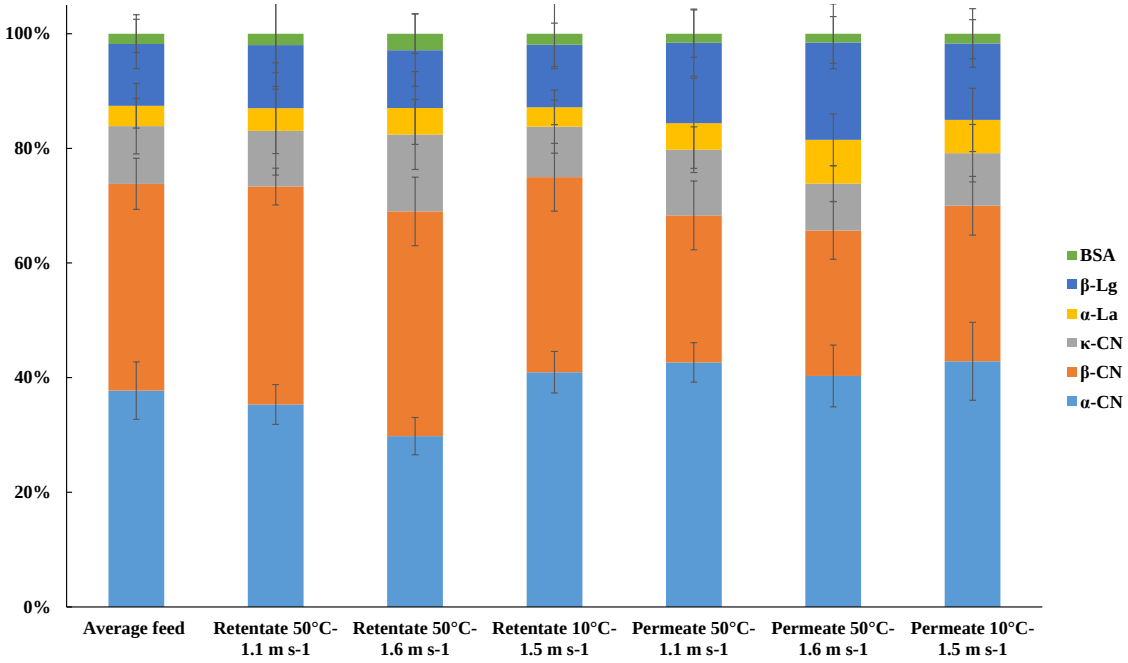

Figure 5-6: Protein fractions distribution by protein groups for 50°C-1.1 m s^{-1}, 50°C-1.6 m s^{-1} and 10°C-1.5 m s^{-1} experiments. Error bars correspond to the standard deviation of 3 repeats for each data point. Samples have been denoted as following: Temperature-CFV.

In summary, the use of these experimental conditions did not serve the purpose of modifying the permeate protein fractions in favour of whey proteins, however, these conditions may be useful to produce permeate lines with less overall protein concentration that can be further processed in order to obtain the desired protein fractionation.

Table 5-3 shows that even though the protein fractions did not vary much among the different processing conditions studied, the final rejections were different among these conditions. For example, the highest permeate flow of 50°C-1.6 m s^{-1} had also the worst overall fractionation, with almost the same values for both casein and whey (*ca.* 65%). On the other hand, the permeate fluxes of 50°C-1.1 m s^{-1} and 10°C-1.5 m s^{-1} were identical even though the conditions that lead to the same flux were different. Both sets of conditions (low temperature or low CFV) lead to having a lower final flux compared to 50°C-1.6 m s^{-1} which indicated a higher degree of resistance which also led to higher rejection values for both casein and whey proteins.

Table 5-3: Protein rejection values at the end of filtration time (3600s) for samples 50°C-1.1 m s^{-1}, 50°C-1.6 m s^{-1} and 10°C-1.5 m s^{-1}, with the casein to whey protein ratio at the final permeate. Samples have been denoted as following: Temperature-CFV.

Sample	Casein rejection [%]	Whey rejection [%]	CN/Wy permeate ratio
50°C-1.1 m s^{-1}	77 ± 2	69 ± 5	3.8
50°C-1.6 m s^{-1}	66 ± 7	65 ± 8	2.8
10°C-1.5 m s^{-1}	81 ± 3	76 ± 3	3.9

The higher rejection values of 10°C-1.5 m s^{-1} also coincide with higher differential rejection of casein and whey, where the casein fraction was rejected more than the whey fraction. However, all the experiments had at the end a similar protein fraction at the final permeate with no stride towards protein fractionation since for all conditions had protein ratios favouring casein proteins (see CN/Wy permeate ratio Table 5-3), as well as similar rejection values.

The permeate flux can be an indication of the overall protein rejections as was shown in the volume reduction experiments, where lower fluxes led to higher overall rejections. However, the permeate flux can also be misleading since it can be determined by parameters like temperature, pressure and CFV, which in turn each of them can have an effect on the protein separation.[120,126] As has been shown in this first set of examples, either temperature or CFV can determine the permeate flux, ending with a similar permeate flux for two sets of conditions which in turn affect the protein interactions with the membrane and final composition. The main limitation to the testing of the conditions were the inherent limitations of the rig itself that could not decouple CFV and TMP and did not allow the full study of the two factors limiting the scope of pressure and CFV combinations to the ones presented here.

The study then shifted towards analysing the effect that pressure and CFV changes had on protein behaviour at the stable temperature of 10 °C. Table 5-4 shows the four combination of pressure and CFV.

Table 5-4: Operational conditions of flux decline curves 10°C-1.5 m s^{-1}, 10°C-1.3 m s^{-1}, 10°C-0.8 m s^{-1} and 10°C-0.6 m s^{-1}. Samples have been denoted as following: Outlet pressure-TMP-CFV-Temperature.

Sample	Inlet [bar]	Outlet [bar]	TMP [bar]	CFV [m s^{-1}]	Temperature [°C]
10°C-1.5 m s^{-1}	1.19	0.91	1.05	1.50	10
10°C-1.3 m s^{-1}	1.11	0.95	1.03	1.35	10
10°C-0.8 m s^{-1}	0.60	0.39	0.50	0.85	10
10°C-0.6 m s^{-1}	0.32	0.19	0.25	0.65	10

In Figure 5-7 it can be seen that sample 10°C-1.5 m s^{-1} has a higher permeate flux than 10°C-1.3 m s^{-1}, linked to the higher CFV velocity 1.5 and 1.34 m s^{-1} respectively (since TMP and temperature were kept the same at 1 bar and 10 °C). As shown before, the lower permeate flux tended to give a higher overall protein rejection with 10°C-1.3 m s^{-1} having a casein rejection of 91% compared to the 81% of 10°C-1.5 m s^{-1} (see Table 5-5).

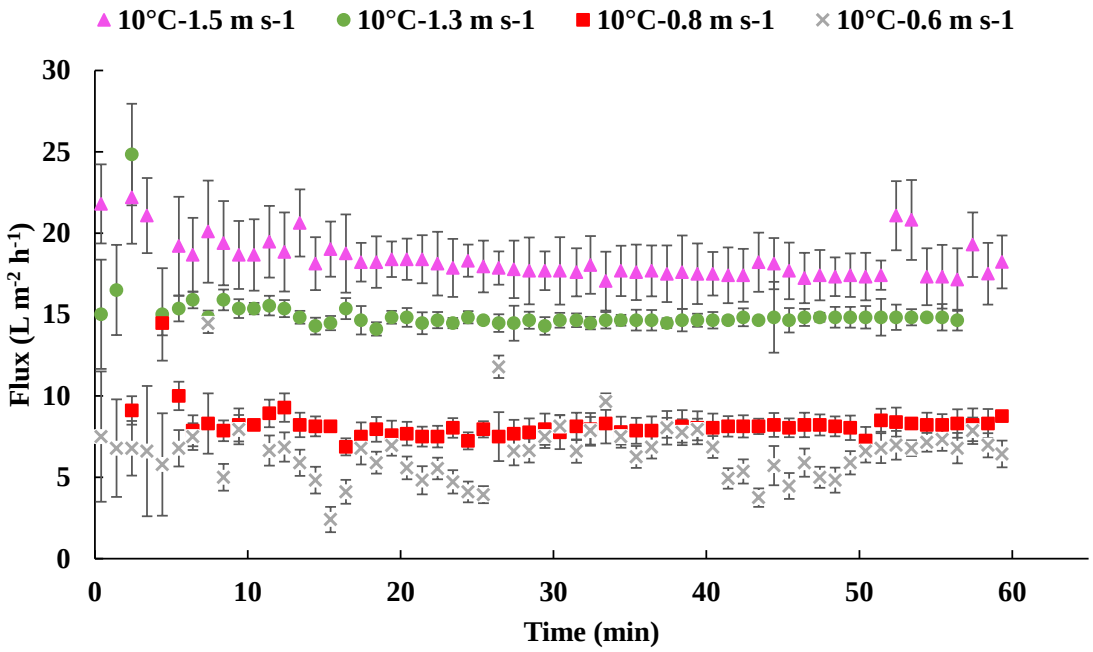

Figure 5-7: Flux decline curve for sample processed at 10°C (10°C-1.5 m s^{-1}, 10°C-1.3 m s^{-1}, 10°C-0.6 m s^{-1} and 10°C-0.8 m s^{-1}). Samples 10°C-1.5 m s^{-1} and 10°C-1.3 m s^{-1} were processed at TMP 1 bar, sample 10°C-0.6 m s^{-1} was processed at TMP of 0.25 bar and sample 10°C-0.8 m s^{-1} at TMP of 0.5 bar. Error bars correspond to the standard deviation of 3 repeats for each data point. Samples have been denoted as following: Temperature-CFV.

The permeate flux curves of 10°C-0.6 m s^{-1} and 10°C-0.8 m s^{-1} (Figure 5-7) have much lower values when compared to 10°C-1.5 m s^{-1} or 10°C-1.3 m s^{-1}. This might suggest that 10°C-0.6 m s^{-1} and 10°C-0.8 m s^{-1} should have higher protein rejections values, but the empirical results do not support this assumption, as shown in Table 5-5. For instance, 10°C-0.6 m s^{-1} and 10°C-1.5 m s^{-1} have similar casein protein rejection values (*ca.* 84%) with a major discrepancy in the whey protein rejection values of 51% and 76%, respectively. 10°C-0.8 m s^{-1} and 10°C-1.3 m s^{-1} also have similar casein rejection values (*ca.* 91%) with discrepancies in the whey protein rejections values 91% and 82%, respectively. These discrepancies are mainly due to the fact that similar permeate flux curves could arise from different operational conditions employed such as temperature and pressure. Therefore, the protein rejection linked to the fluxes would be radically different in each case. For example, Table 5-5 shows that different CFV (and the associated permeate fluxes Figure 5-7) result in similar casein rejection values but differ in whey rejection values.

Table 5-5: Protein rejection values at the end of filtration time (3600s) for samples 10°C-1.5 m s^{-1}, 10°C-1.3 m s^{-1}, 10°C-0.8 m s^{-1} and 10°C-0.6 m s^{-1}, with the casein to whey protein ratio at the final permeate. Samples have been denoted as following: Temperature-CFV.

Sample	Casein rejection [%]	Whey rejection [%]	CN/Wy permeate ratio
10°C-1.5 m s^{-1}	81 ± 2	76 ± 6	3.9
10°C-1.3 m s^{-1}	91 ± 3	82 ± 4	2.0
10°C-0.8 m s^{-1}	92 ± 5	91 ± 5	4.4
10°C-0.6 m s^{-1}	84 ± 3	51 ± 5	1.8

Surprisingly the low-pressure conditions of sample 10°C-0.6 m s^{-1} has the highest differential rejection of all samples at 10 °C, indicating that under low pressure conditions casein proteins are mostly rejected by the membrane (84 %) whereas whey proteins are only partially rejected (51%). This result indicates that there is a combination of optimal operational conditions (CFV of 0.64 m s^{-1} and temperature of 10 °C) that yields great rejection values, in which the separation of casein and whey proteins are maximised, however, the protein ratio at the permeate is still casein dominated with a value of 1.8 (see Table 5-5).

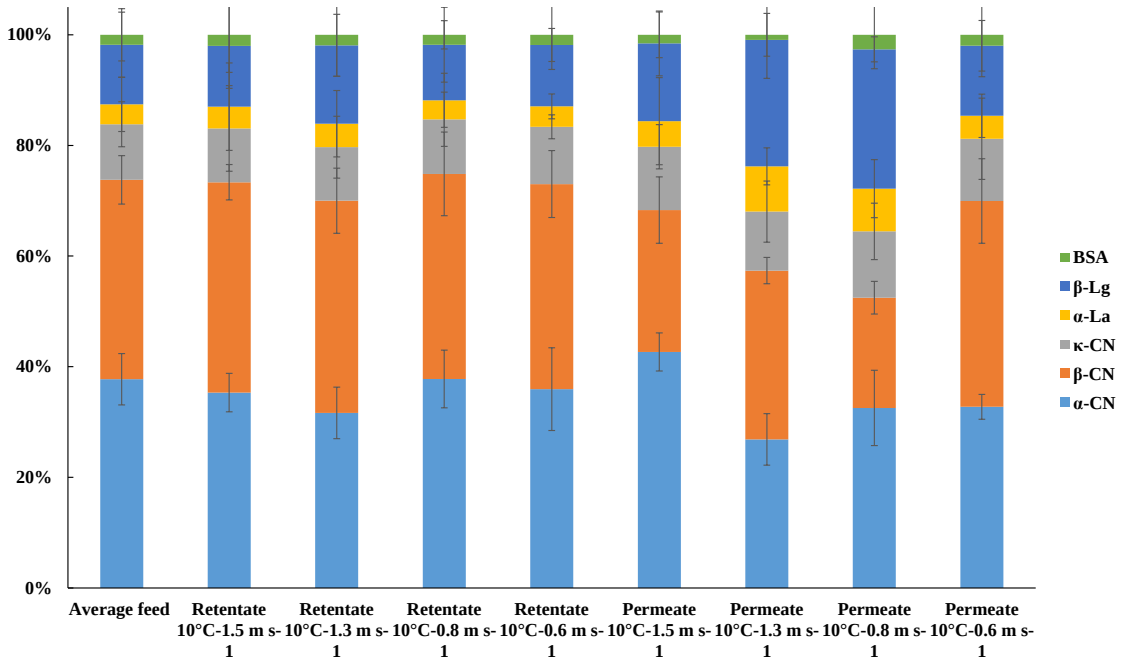

Figure 5-8: Protein fractions distribution by protein groups for 10°C-1.5 m s^{-1}, 10°C-1.3 m s^{-1}, 10°C-0.6 m s^{-1} and 10°C-0.8 m s^{-1} experiments at the initial feed, retentate and final permeate. Error bars correspond to the standard deviation of 3 repeats for each data point. Samples have been denoted as following: Temperature-CFV.

Figure 5-8 shows the protein distribution at the initial and final conditions of the abovementioned samples. The main highlight of these results is that 10°C-0.6 m s^{-1}, as shown above, achieved a casein protein reduction in favour of the whey proteins, mainly by the reduced presence of alpha and beta casein and the transmission of β-Lg. The 10°C-1.3 m s^{-1} operational conditions also managed to increase the ratio of whey proteins in the feed from the initial 84/16 (5.25) casein/whey proteins to the final 67/33 (2.0) with better beta-casein transmission and alpha casein rejection than 10°C-0.6 m s^{-1}, 10°C-1.3 m s^{-1} and 10°C-0.6 m s^{-1}. These results indicate that the current experimental conditions can be used to shift the final permeate concentration towards a more whey proteins rich fraction than the initial feed, however, the casein protein ratio is still too high.

5.2.1.2 Summary of volume reduction and full recirculation

The general tests have shown that high overall protein rejections can be obtained without the need of concentrating the feed by a factor of 2. All the samples at 10 °C with CFV below 1.5 m s^{-1} had casein rejection above 80%, and most of them above 90% in one cycle of 1 hour. This would corroborate the fact that the initial minutes of a filtration dictate the fouling layer that influences the overall protein rejection. This aligns with Lawrence *et al.* (2008)[120] results which claim that their filtration behaviour was entirely driven by the initial fouling layer independently of the membrane pore size.

The analogue conditions for both recirculation and concentration obtained at CFV 1.3 m s^{-1} for the permeate flow show that the concentration study behaviour does not differ from the recirculation. The concentration study did have a lower final permeate flux after 6 hours due to the build-up of foulants on the membrane. The volume reduction experiments highlighted the direction of aiming for CFV around 1.3 m s^{-1}, at higher values the casein rejection was too low (<80%), which was then corroborated with the 10°C-1.5 m s^{-1} sample of the recirculation tests. The combined results of the concentration and recirculation studies indicate that CFV must be below 1.3 m s^{-1} to have high casein rejections above 80% however, at 0.8 m s^{-1} the permeate flow will be halved compared to the 1.3 m s^{-1} (15 L m^{-2} h^{-1}).

From an industrial perspective, it is desired to process milk at the highest possible permeate flux and achieve high casein rejection and low whey rejection. These are the ideal conditions in order to achieve an energy efficient industrial milk filtration processes.

5.2.2 Membrane concentration study

The membrane concentration studies were carried out to quantify the build-up of solutes (proteins) on the membrane side (based on Evans and Bird, 2010)[140], which will be responsible for a diffusive backflow to the bulk feed (concentration polarisation effects as well). The concentration polarisation effect is defined by the steady-state conditions where the diffusive flow back from the membrane, the solute flux through the membrane and the convective solute flux are balanced. Equation 5-1 describes the simple concentration polarisation model, with no other fouling mechanisms considered.

$$\ln\left[\frac{C_m - C_p}{C_b - C_p}\right] = \frac{J_v\,\delta}{D} \qquad 5\text{-}1$$

The traditional film-layer theory states that working at high pressures leads to high degrees of concentration polarisation because of the increase of solutes at the surface of the membrane, C_m.

Assuming that the mass transfer coefficient k can be defined as:

$$k = \frac{D}{\delta} \qquad 5\text{-}2$$

And the maximum true rejection, R_{max} as:

$$R_{max} = 1 - \frac{C_p}{C_m} \qquad 5\text{-}3$$

The combination of equation 5-1 with equations 5-2 and 5-3 can be used to produce equation 5-4. Plotting the steady-state flux (J_v) vs ln([1 - Rcoeff]/Rcoeff) produces a straight line that has a slope of 1/k and the intercept corresponds to ln([1 – Rmax]/RMax).[141]

$$\ln\left[\frac{1 - R_{coeff}}{R_{coeff}}\right] = \ln\left[\frac{1 - R_{max}}{R_{max}}\right] + \frac{J_v}{k} \qquad 5\text{-}4$$

The tests were carried out at three different bulk concentrations that were produced by the dilution of milk using RO water, ensuring that the initial feed volume was kept constant (Table 5-6).

Table 5-6: Sample concentration used in the concentration tests feed, the volume was kept at 3.7 L.

Sample	Milk Volume [L]	RO Water volume [L]	Total volume [L]
Low concentration	1	2.7	3.7
Medium concentration	2	1.7	3.7
High concentration	3.7	0	3.7

Figure 5-9 can be used to calculate mass transfer data (k) and the protein concentration at the membrane (C_m) for the whole milk proteins. As will be shown later the data can be divided between casein and whey proteins which had a different behaviour.

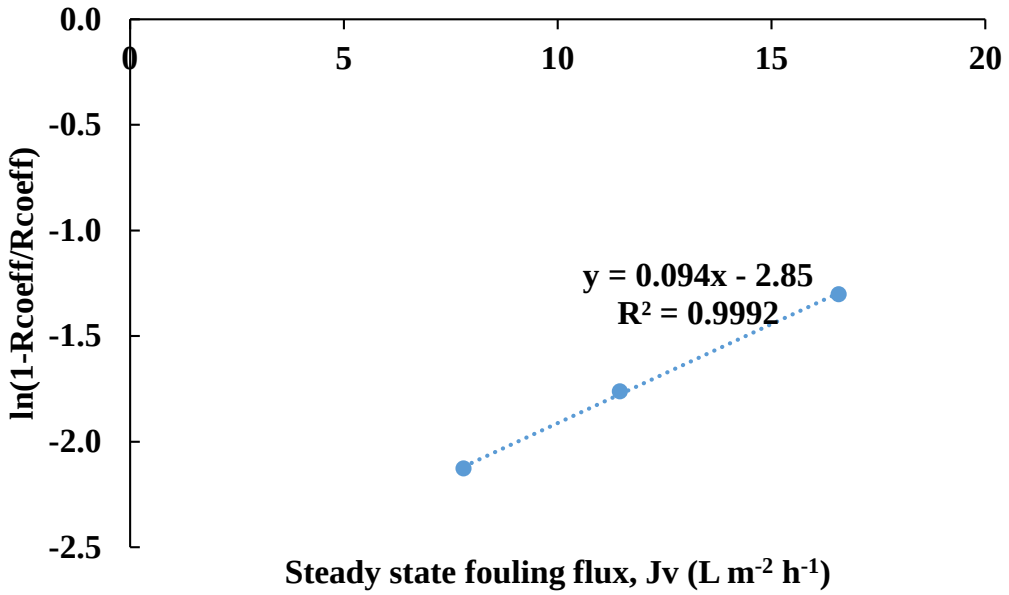

Figure 5-9: Steady-stat flux (Jv) vs ln[(1 - rcoeff)/rcoeff] were the bulk concentration of proteins was varied based on Table 5-7, operated at TMP of 0.5 bar, CFV 0.85 m s^{-1}, and temperature of 10 °C.

Table 5-7 highlights the increase of proteins at the membrane surface due to the proteins not getting through the membrane. The proteins' concentration increased at the membrane surface of the high concentration by a factor of 2, from the bulk concentration of 3.34 wt% to the membrane surface concentration of 6.5 wt%.

Table 5-7: Membrane concentration study data of all milk proteins, where low and medium concentrations were obtained by water dilution, always maintaining the same feed volume. The method error for protein concentration analysis was of ±5%.

Sample	C_B [wt %]	C_P [wt %]	R_{coeff}	R_{max}	K [m s^{-1}]	C_m [wt%]
Low concentration	0.26%	0.05%	0.81	0.95	2.96 x10^{-6}	0.9%
Medium concentration	0.97%	0.14%	0.85	0.95	2.96 x10^{-6}	2.6%
High concentration	3.34%	0.36%	0.89	0.95	2.96 x10^{-6}	6.5%

Table 5-8 shows the concentration study parameters and data obtained for the casein proteins group. Casein proteins membrane surface concentration was increased by a factor of 1.9 compared to the bulk concentration.

Table 5-8: Membrane concentration study data of casein proteins, where low and medium concentrations were obtained by water dilution, always maintaining the same feed volume. The method error for protein concentration was of ±5%.

Sample	C_B [wt %]	C_P [wt %]	R_{coeff}	R_{max}	K [m s^{-1}]	C_m [wt%]
Low concentration	0.22%	0.04%	0.80	0.95	3.1 $x10^{-6}$	0.8%
Medium concentration	0.81%	0.11%	0.86	0.95	3.1 $x10^{-6}$	2.1%
High concentration	2.78%	0.29%	0.90	0.95	3.1 $x10^{-6}$	5.3%

The membrane concentration study also allowed to test the effect of protein concentration on the total resistance values. Table 5-9 data shows that the reduction in milk content (compared to the undiluted milk or High concentration) did not lead to a linear reduction of total resistance, which highlights the impact that concentration polarisation can have on the milk filtration process.

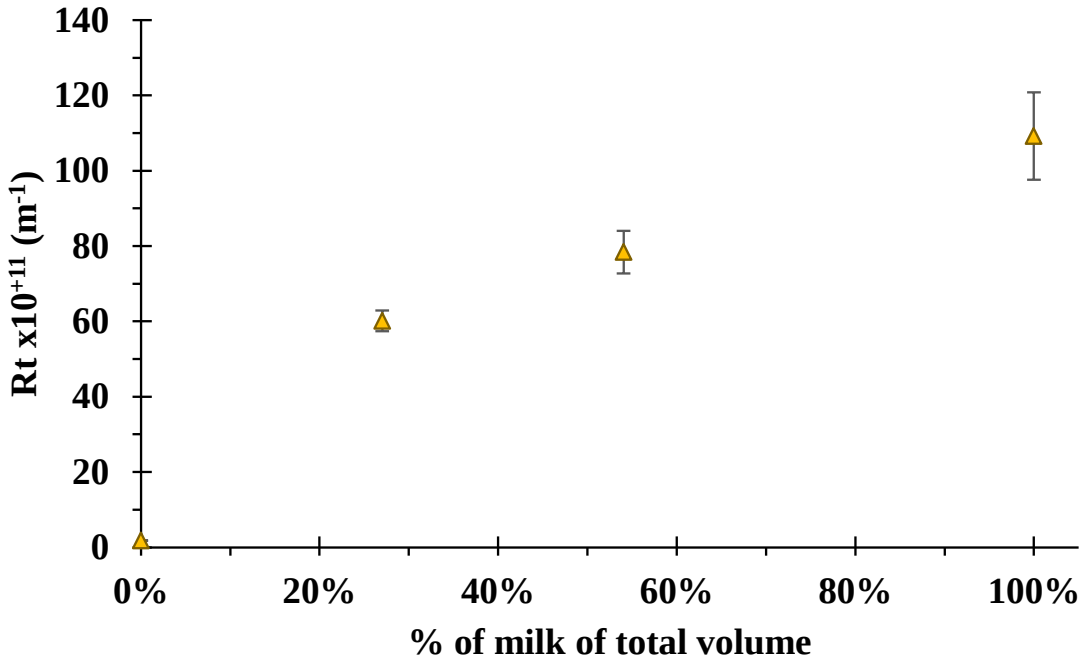

Figure 5-10: Total membrane resistance values based on milk concentration, from 100% milk to RO water. See Table 5-6 for exact dilutions. Error bars correspond to the standard deviation of 2 repeats for each data point.

The reduction of the milk volume of 46% (medium concentration) lead to a total resistance reduction of only 28% indicating that the effect of proteins in dictating the total resistance is significant and that increasing the milk concentration by a factor of 2 should increase the total resistance by a higher amount (Figure 5-10). The reduction of the milk volume by a factor of 73% lead to a total resistance reduction of only 45%, further increasing the difference between

volume reduction and resistance reduction. Figure 5-10 shows a liner decrease of total resistance with milk concentration as long as there is milk in the mix (0% data point is not included), which indicates that there must be a break point where the reduced milk content leads to a sharp decrease in total resistance towards the RO water conditions. However, due to operational reasons and the added environmental and economic costs of diluting milk this point would only have scientific interest for further studies.

The increase of resistance can be due to the high presence of soluble proteins, as the work of Jimenez-Lopez *et al.* (2008)[128] showed the presence of soluble proteins increased the irreversible fouling by 20%.

Table 5-9: Membrane resistance values breakdown for the concentration test, all test had feed volume of 3.7 L (Table 5-6). All resistances are $x10^{+11}$ (m^{-1}). Total resistance (Rt), membrane resistance (Rm), reversible fouling resistance (Rrev, obtained when subtracting Rir from Rt) and Irreversible fouling resistance (Rir, resistance measured after rinse step).

Sample	Milk content [L]	R_t [m^{-1}]	R_m [m^{-1}]	R_{rev} [m^{-1}]	R_{ir} [m^{-1}]
RO water	0	1.8	1.8	1.8	1.8
Low concentration	1	60.1	1.8	53.8	4.5
Medium concentration	2	78.4	1.8	70.9	5.7
High concentration	3.7	109.2	1.8	100.5	6.9

5.2.3 Design of Experiments

Results shown in previous sections clearly indicate the possibility of having a set of operational conditions that leads to the desired protein fractionation, meeting closely the industrial requirements and needs. To further understand the effect of outlet pressure and temperature on milk protein fractionation, as well as the possible synergies among them a design of experiments (DoE) approach was used and results are shown below.

The DoE consisted of studying the outlet pressure and temperature as the factors to modify while keeping the transmembrane pressure at 0.5 bar ± 0.01 bar and the crossflow velocity at 1.4 m s^{-1} ± 0.3 m s^{-1}. The chosen parameters were based on previous experiments (shown in section 5.2.1) where the use of low processing pressures demonstrated a higher degree of protein separation while allowing other operational parameters to influence the final rejection values. Conversely, the work carried out at a transmembrane pressure of 1.0 bar indicated that the pressure and temperature could be determining factors that heavily determine the final protein rejection values. The CFV selected was chosen to ensure high permeate fluxes, since

they have some effect on the final rejection values although it is not the most dominant factor. All the selected parameters for the study (temperature and outlet pressure) fall within the experimental limitations of the operational rig.

In particular, the outlet pressure values tested ranged from 0.2 to 0.4 bar with 0.3 bar as middle point and 0.16 and 0.44 bar as extreme conditions. The range of conditions for the temperature was 10-50 °C with 30 °C as middle point and 58.3 °C as extreme condition. The responses to analyse against the input factors were casein and whey protein rejection.

The experiments were then set by the DoE software MODDE (Sartorius Stedim Data Analytics AB) that determined the extreme conditions to test as well as the middle point conditions. The experiment order was randomised to reduce the experimental variations and to minimise operational error (Table 5-10).

Table 5-10: Experiments of DoE test with the experiment order and factors of each experiment.

Exp No	Run Order	Outlet pressure [bar]	Temperature [°C]
1	4	0.2	10
2	9	0.4	10
3	2	0.2	50
4	3	0.4	50
5	6	0.16	30
6	5	0.44	30
7	11	0.3	10
8	7	0.3	58.3
9	10	0.3	30
10	1	0.3	30
11	8	0.3	30

The DoE methodology used three repeats as a validation method of the reproducibility of the experiments to carry out and the capability of the analytical techniques to yield reproducible results. Experiments 9, 10 and 11 (Table 5-11) were the repeats and all were carried out under the same operational conditions (0.3 bar outlet pressure and 30 °C) at different moments of the test.

Table 5-11: Casein and whey proteins rejections values for the three repeats operated at the same conditions.

Exp No	Outlet pressure	Temperature	Casein rejection [%]	Whey rejection [%]
9	0.3	30	88	75
10	0.3	30	69	64
11	0.3	30	89	76

Table 5-11 shows the DoE protein rejection values for the three repeats (Exp 9-11) operated at the same conditions. Experiments 9 and 11 had almost identical protein rejection values of *ca*. 88.5 and 75.5 % for casein and whey, respectively and similar flux decline curves (Figure 5-11), validating the methodology employed to process the milk and analyse the samples. However, the third repeat (experiment number 10) did not yield a reproducible result due to an operational error (see Table 5-11) and was discarded for further analysis.

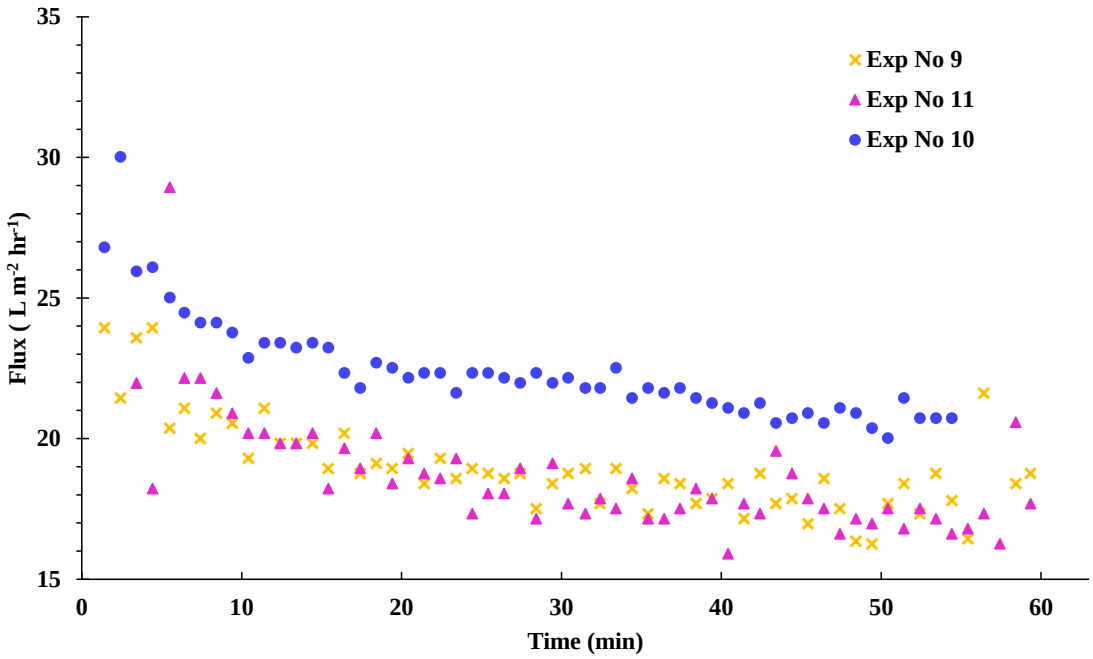

Figure 5-11: Flux decline curve for DoE repeats, all of them were processed at 30 °C and outlet pressure of 0.3 bar. TMP and CFV were kept constant at 0.5 bar ± 0.01 bar and 1.4 m s^{-1} ± 0.3 m s^{-1}, respectively.

The combined error of the control samples and the HPLC methodology defined the error of the DoE measurements, being of 3% for α and κ-CN and 4% for β-CN with a combined error of 3% for all casein proteins, and 5%, 2% and 6% for the α-La, β-Lg and BSA, respectively, and a combined error of 4% for whey proteins.

5.2.3.1 DoE aggregated results

Figure 5-12 analyses the response of casein rejection based on outlet pressure (a) and temperature (b). The casein rejection shows a positive trend with outlet pressure (Figure 5-12 a) indicating that at high outlet pressures the casein rejection tends to be at the higher spectrum. Similarly, samples processed at high outlet pressure values and at the three different temperatures studied show less variation in casein rejection values than the low outlet pressures, indicating that at high outlet pressure the effect that temperature has on casein rejection is reduced.

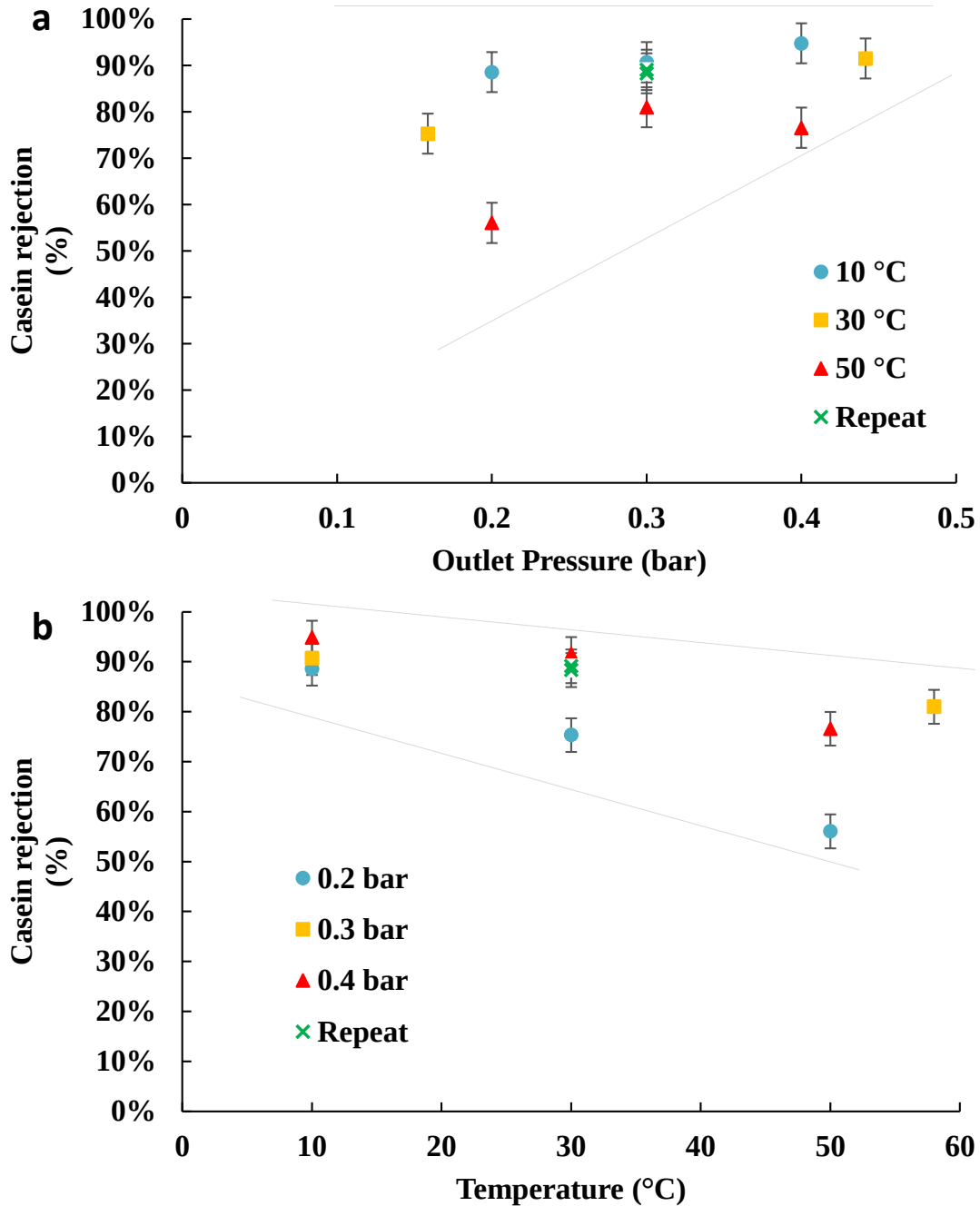

Figure 5-12: DoE summary of casein rejection. A) Casein rejection (%) based on outlet pressure (bar) sorted by temperatures. Circle 10°C, square 30°C, cross 50°C and triangle repeats. B) Casein rejection (%) based on temperature (°C). The lines indicate the tendencies observed during the DoE study, see Figure 5-15 for more information. Circle 0.2 bar, square 0.3 bar, triangle 0.4 bar and cross repeats.

The effect of temperature on casein rejection favours a concentration of the rejection values like the behaviour observed with the outlet pressure, however in this case it happens at the lowest values studied (Figure 5-12b). The increase of temperature tends to reduce the overall casein rejection and increases the effects that other parameters (*i.e* outlet pressure) can have on the final rejection. The reduction of temperature promotes casein rejection reaching some of the peak values studied in this DoE and reduces the influence of other operational factors like the outlet pressure. In summary, outlet pressure has a major impact on casein rejection at the high end (0.4 bar) of the analysed pressure range, whereas temperature has a major impact on the lowest range (10 °C) of temperatures analysed (Figure 5-12). The concentration value of casein rejection at low temperature is unexpected, since at low temperatures (10 °C or less) beta-casein does leave the casein micelle, easing the transmission through the membrane. The casein rejection values at low temperature should have been lower to the observed at the other temperatures because of the beta-casein. [10,110,119]

Figure 5-13 analyses the effect that outlet pressure (a) and temperature (b) have on whey proteins rejection. In contrast to the casein proteins, the whey protein rejection does not seem to have a direct correlation between any of the two aforementioned factors.

As a general trend an increase in outlet pressure seems to lead to an increase in whey rejection. However, this is not a definitive result since studies performed at 0.3 bar of outlet pressure showed a higher set of results with higher whey protein rejections than 0.4 bar. Figure 5-13 indicates that the minimum values for whey rejection correspond to the lowest outlet pressure plus the highest temperature of 50 °C for the 0.4 bar (Exp No 4). This assumption, however, was disproved due to the results of experiment number 8 at 0.3 bar of outlet pressure and 50 °C where the whey protein rejection reached 71%. Assuming the previous assumption that low outlet pressure and high temperature tend towards low whey rejection, the 0.3 bar outlet pressure should have a lower or similar rejection than 0.4 bar of outlet pressure at the same temperature. Several plausible reasons can be ascribed to this observation: At a first glance, one reason for this unexpected behaviour could be that the combined effect of outlet pressure and temperature at that range does promote high whey rejections. Similarly, another factor to consider, is the non-correlation of whey protein rejections with any of the factors analysed in Figure 5-13. Unlike casein proteins where clear trends were observed both for the outlet pressure and temperature, the non-correlation of whey proteins with outlet pressure and temperature could be due to the fact that the behaviour of whey proteins in the studied system

is strongly affected by the behaviour of casein proteins and the associated fouling and concentration polarisation phenomena.

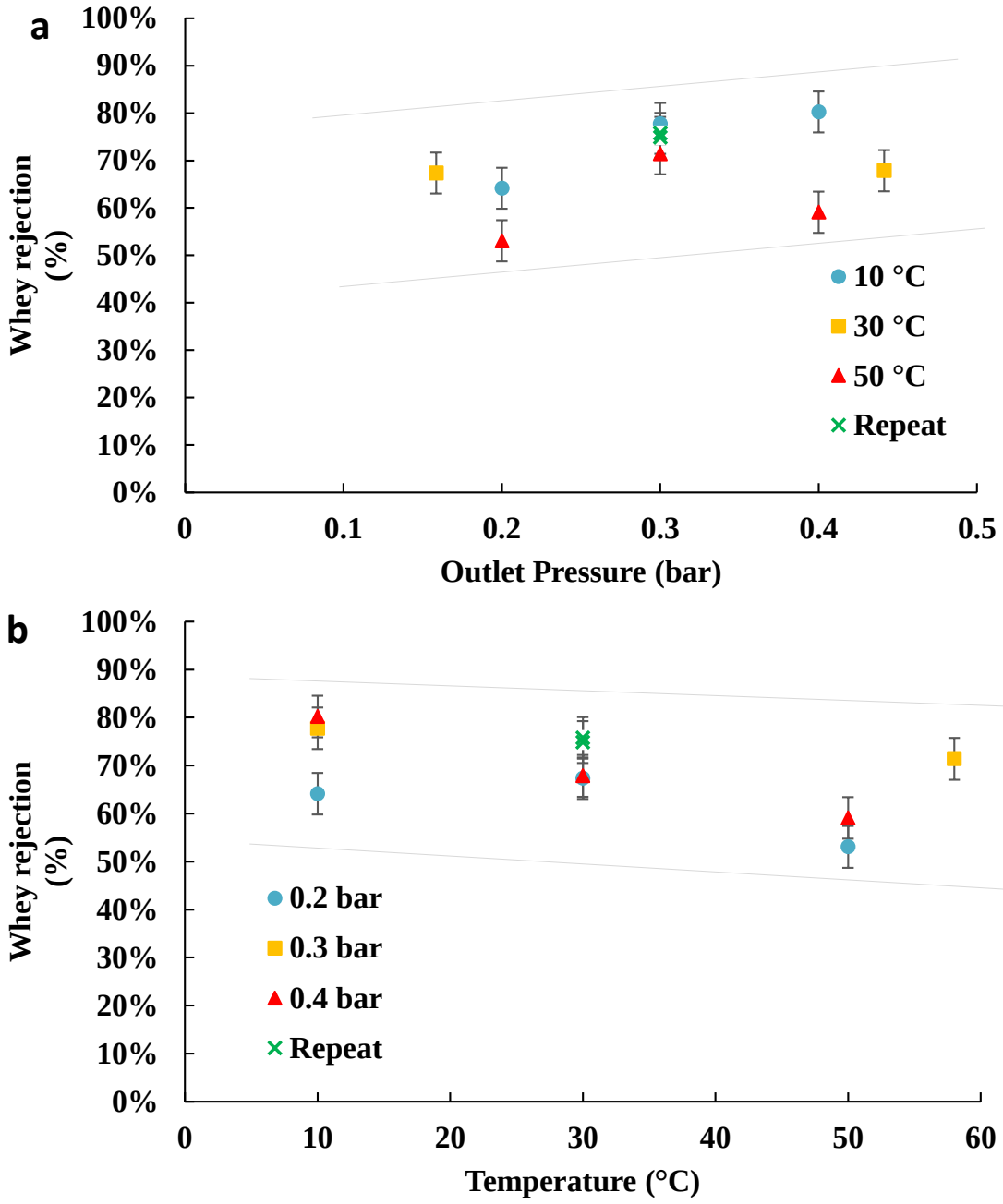

Figure 5-13: DoE summary of whey protein rejection. A) Whey proteins rejection (%) based on outlet pressure (bar) sorted by temperatures. Circle 10°C, square 30°C, cross 50°C and triangle repeats. B) Whey proteins rejection (%) based on temperature (°C). The lines indicate the tendencies observed during the DoE study, see Figure 5-15 for more information. Circle 0.2 bar, square 0.3 bar, triangle 0.4 bar and cross repeats.

Interestingly, for both casein and whey protein analyses all the repeats performed were almost identical, which indicates the reproducibility of these experiments and provides solid ground for the model employed for this study.

5.2.3.2 DoE conditions breakdown:

In order to further understand in detail, the effect that each operational factor had on protein rejection values, the whole set of experiments has been broken down into specific conditions in the following section.

Table 5-12 summarises the complete table of results including all the studied combinations of factors and the associated responses in protein rejections and fluxes ratios. The table has been broken down for better understanding of each operational factor in this section.

Table 5-12: DoE main results table, including input factors and analysed responses (casein and whey protein rejection and whey proteins ratio enhancement), as well as feed and permeate protein ratio based on responses data.

Exp No	Outlet pressure [bar]	Temperature [°C]	Casein rejection [%]	Whey rejection [%]	Feed ratio	Permeate ratio	Whey proteins enhancement [%]
1	0.2	10	89 ± 3	64 ± 4	84/16	63/37	129 ± 7
2	0.4	10	95 ± 3	80 ± 4	84/16	58/42	159 ± 7
3	0.2	50	56 ± 3	53 ± 4	83/17	82/18	10 ± 7
4	0.4	50	77 ± 3	59 ± 4	83/17	74/26	60 ± 7
5	0.16	30	75 ± 3	67 ± 4	84/16	80/20	22 ± 7
6	0.44	30	92 ± 3	68 ± 4	84/16	59/41	157 ± 7
7	0.3	10	91 ± 3	78 ± 4	84/16	68/32	98 ± 7
8	0.3	58	81 ± 3	71 ± 4	84/16	78/22	37 ± 7
9	0.3	30	88 ± 3	75 ± 4	83/17	70/30	85 ± 7
11	0.3	30	89 ± 3	76 ± 4	83/17	69/31	91 ± 7

Table 5-13 indicates that at an outlet pressure of 0.3 bar (medium analysed range) and at 10 and 30 °C the protein behaviour was similar with minor variations both at the casein and whey proteins and with quite similar permeate ratio. However, the addition of the extreme condition 58.3 °C modified the reaction of casein and whey proteins shifting it towards lower values and favouring a higher ratio of whey proteins at the final permeate. Figure 5-13 showed that whey proteins have a mix response to the studied factors so far, mainly due to the apparent dependency on the casein proteins behaviour and presence.

Table 5-13: DoE results based on outlet pressure 0.3 bar, showing the casein and whey proteins rejections and feed and permeate protein ratios (casein/whey) and the whey proteins ratio enhancement at the permeate line.

Exp No	Outlet pressure [bar]	Temperature [°C]	Casein rejection [%]	Whey rejection [%]	Feed ratio	Permeate ratio	Whey proteins enhancement [%]
7	0.3	10	91 ± 3	78 ± 4	84/16	68/32	98 ± 7
8	0.3	58	81 ± 3	71 ± 4	84/16	78/22	37 ± 7
9	0.3	30	88 ± 3	75 ± 4	83/17	70/30	85 ± 7
11	0.3	30	89 ± 3	76 ± 4	83/17	69/31	91 ± 7

Table 5-14 shows at the same time the effect of outlet pressure and temperature. The first set of experiments (3 and 4) have the same temperature (50 °C) and different outlet pressure, 0.2 and 0.4 bar, respectively. Experiment 3 showed almost identical values of casein and whey proteins rejection (56% and 53%) which lead to a permeate protein ratio of 82/18, being identical to the starting ratio. On the other hand, experiment 4 had a much higher casein rejection (77%) and most importantly it had a bigger difference between casein and whey with a differential rejection of 17% over the 3% of experiment 3. The final protein ratio for experiment 4 was more favourable to whey proteins than experiment 3 ending at a 74/26, which meant an increase in the whey proteins ratio of 60%. This first case shows the massive effect of outlet pressure on promoting casein rejection while keeping whey proteins transmission at a similar value for both 0.2 and 0.4 bar of outlet pressure. One reason for the benefits of using high outlet pressure could be that the compression of proteins led to the formation of an extra filtration layer that in this case favoured casein proteins rejection.[120]

Table 5-14: DoE results showing pairs of same temperature and different outlet pressures, showing the casein and whey proteins rejections and feed and permeate protein ratios (casein/whey) and the whey proteins ratio enhancement at the permeate line.

Exp No	Outlet pressure [bar]	Temperature [°C]	Casein rejection [%]	Whey rejection [%]	Feed ratio	Permeate ratio	Whey proteins enhancement [%]
3	0.2	50	56 ± 3	53 ± 4	83/17	82/18	10 ± 7
4	0.4	50	77 ± 3	59 ± 4	83/17	74/26	60 ± 7
5	0.16	30	75 ± 3	67 ± 4	84/16	80/20	22 ± 7
6	0.44	30	92 ± 3	68 ± 4	84/16	59/41	157 ± 7

The second set of data shown in Table 5-14, experiments 5 and 6, were carried out at the same operational temperature (30 °C). Interestingly, in this particular case the lower temperature led to having higher rejection values overall when compared with experiments performed at 50 °C (exp 3 and 4), although being “outlier” conditions. This set of experiments follows a similar trend as the above mentioned with the higher pressure leading to the higher rejections values overall with casein rejections values of 75% and 92%, respectively, for experiments 5 and 6. In this case the difference in rejection values between casein and whey proteins was mainly due to the high outlet pressure (0.44 bar) employed in experiment 6, which promoted an enhancement in casein rejection values (from 75 to 92 %), conversely to what is observed for whey proteins, where changes in the outlet pressure led to similar whey proteins rejection values of 67 and 68%, for experiment 5 and 6, respectively. The lower casein rejection of experiment 5 over experiment 6 lead to final ratio of casein over whey at the permeate stream of 80/20 and 59/41, respectively, which in turn also translates to whey proteins ratio

enhancements of 22% and 157%, respectively. Overall, the operational conditions employed for experiment 6 and the resultant protein rejection values are of great promise for achieving useful protein fractionations with industrial applications. For instance, the commercially available infant formula uses a ratio of 40/60,[142,143] which is very close to the permeate ratio obtained in the work carried out by Mccarthy *et al.* (2017) using ceramic membranes.[119] When using polymeric membranes the best protein ratio obtained for infant formula was of 49/51 by Crowley *et al*. (2015).[142] This is one example of the bridges that still need to be crossed in the transition between ceramic and polymeric membranes. However, our method offers alternatives to the current industrial methods of preparing infant formula (powder proteins mixing) with less contamination risk due to having far less processing steps and with much less energy and water consumption due to being single step.[143]

The final highlight from Table 5-14 is the comparison between experiments 3 and 5. Both of them have similar outlet pressure (0.2 and 0.16 bar, respectively) and were carried out at 50 and 30 °C respectively. The overall differential rejection has not increased much, from 3% to 8%, however, what has increased is the casein rejection value (mainly by the lower temperature). This tendency is also observed with experiments 4 and 6 that have similar outlet pressure and different temperature, where the lower temperature ended up with a higher casein rejection. The whole Table 5-14 dataset shows that higher outlet pressures favour whey transmission over casein, mainly because casein proteins rejection increases while keeping whey proteins rejections at relatively low values.

Table 5-15 shows the comparison of the temperature effect when the outlet pressure is fixed at 0.2 bar (plus the extreme condition of 0.16 bar). First, the effect of temperature is the same as seen in any of the other examples, that is when the temperature is increased the casein protein rejections decrease overall. For instance, experiment carried out at 10 °C (exp 1) shows a maximum rejection of 89%, whereas at 50 °C (exp 3) the maximum rejection is of 56%, with a middle point at 30 °C with 75% rejection, agreeing well with previous observations. The differential rejection (the difference between casein and whey rejection) is a key value on this project. As mentioned before, the highest the difference, the better the casein and whey separation. Table 5-15 shows that at 0.2 bar a 25% differential rejection can be achieved when coupled with a processing temperature of 10 °C. Interestingly, this is one of the best differential values obtained so far in this study. On the complete opposite picture, for 0.2 bar at 50 °C we have the lowest differential values obtained so far of only 3%. Therefore, these studies indicate that low temperatures, such as 10 °C, seem to be the optimal processing conditions that ensure a favourable casein and whey separation.

Table 5-15: DoE results showing the effect of temperature when outlet pressure is 0.2 bar, showing the casein and whey proteins rejections and feed and permeate protein ratios (casein/whey) and the whey proteins ratio enhancement at the permeate line.

Exp No	Outlet pressure [bar]	Temperature [°C]	Casein rejection [%]	Whey rejection [%]	Feed ratio	Permeate ratio	Whey proteins enhancement [%]
1	0.2	10	89 ± 3	64 ± 4	84/16	63/37	129 ± 7
3	0.2	50	56 ± 3	53 ± 4	83/17	82/18	10 ± 7
5	0.16	30	75 ± 3	67 ± 4	84/16	80/20	22 ± 7

Along the same lines, when glancing on the effect of temperature on whey protein transmission enhancement towards the permeate line, it can be seen in Table 5-15 that low temperatures favour higher whey proteins proportions in the permeate. This could mainly be due to the higher casein rejection linked to the low temperatures.

Table 5-16 highlights the temperature effect on the rejections when the pressure is fixed at 0.4 bar (with the extreme condition of 0.44 bar). Unlike results obtained at 0.2 bar (Table 5-16), at 0.4 bar of outlet pressure similar differential rejections can be achieved at 10 and 50 °C, being of 15 and 17% for experiments 2 and 4, respectively. However, at the highest temperature (50 °C) much higher whey protein content was present at the permeate (at 50 °C smaller rejection of whey proteins) than at lower temperatures, the use of this conditions should be considered in multistep processes in order to enhance the protein fractionation.

Table 5-16: DoE results showing the effect of temperature when outlet pressure is 0.4 bar, showing the casein and whey proteins rejections and feed and permeate protein ratios (casein/whey) and the whey proteins ratio enhancement at the permeate line.

Exp No	Outlet pressure [bar]	Temperature [°C]	Casein rejection [%]	Whey rejection [%]	Feed ratio	Permeate ratio	Whey proteins enhancement [%]
2	0.4	10	95 ± 3	80 ± 4	84/16	58/42	159 ± 7
4	0.4	50	77 ± 3	59 ± 4	83/17	74/26	60 ± 7
6	0.44	30	92 ± 3	68 ± 4	84/16	59/41	157 ± 7

On balance, Table 5-16 shows that higher outlet pressures (0.4 bar) promote whey proteins richer permeate, mainly by casein proteins rejection compared to the low-pressure studies of 0.2 bar (Table 5-15) at any of the studied temperature ranges.

Figure 5-14 shows the protein ratio at the permeate line at the end of each filtration cycle as a function of outlet pressure at three different operating temperatures (10, 30 and 50 °C). A clear tendency towards obtaining lower ratios of casein/whey at the high spectrum of outlet pressures at any temperature, with some of the highest permeate ratio at the lowest outlet pressures is observed. The lowest protein ratio values are obtained at processing temperatures

of 10 °C. At this temperature, the highest overall protein rejection values at a given outlet pressure are observed, favouring higher casein rejection values. Therefore, these data demonstrate that the combination of outlet pressure and temperature can achieve a protein ratio shift from the feed value of 4.6 to some of the final values around 1.4, obtained at higher outlet pressure and 10 or 30 °C.

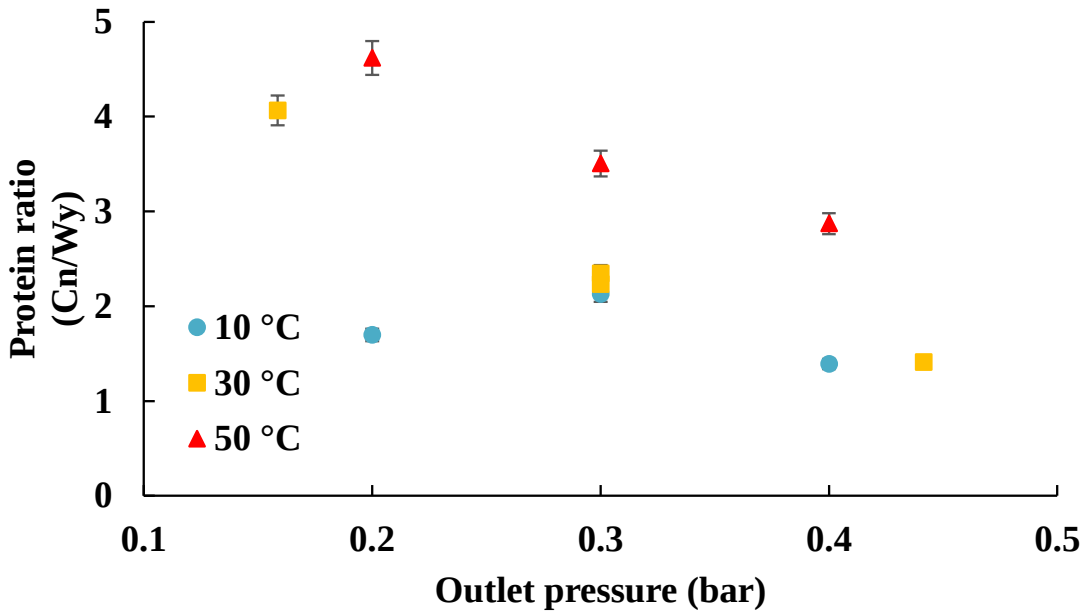

Figure 5-14: Permeate line protein ratio at the end of the filtration and outlet pressure of the processing sorted by processing temperature. Circle 10 °C, square 30 °C and triangle 50 °C.

The effect that each operational factor studied (outlet pressure and temperature) had on promoting casein and whey rejection was further evaluated by means of parameters coefficients and statistical reliance as shown in Figure 5-15. The graph on the left shows each factor influence over casein rejection and the graph on the right shows the effect on whey proteins rejection. The graph correlates the effect of each factor to the increase or decrease of protein rejection, meaning that a positive increase of casein rejection due to outlet pressure means that an increase of outlet pressure leads to an increase of protein rejection and vice versa.

It can be observed that an increase in outlet pressure leads to an increase of casein proteins rejection overall. Similarly, a reduction in the operating processing temperature has a positive impact on increasing the overall casein rejection and increasing the temperature reduces casein rejection, because casein micelles do contract with temperature increases, reducing the micelles diameter and facilitating their transmission through the membrane.[48] Overall, the effect of temperature seems to be slightly more relevant than the effect of outlet pressure for enhancing casein rejection. These results are in agreement with the observed tendencies of

casein proteins shown in Figure 5-12, where higher casein rejections at high outlet pressures and at low temperatures were obtained.

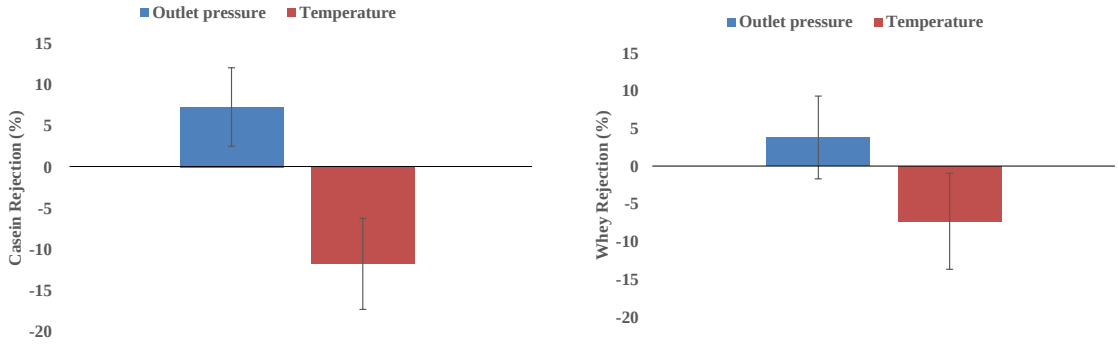

Figure 5-15: Parameters coefficients of the factors studied (Outlet pressure and temperature) and the statistical reliance on the responses obtained. Left graph is factor influence over casein rejection. Right graph is factor influence over whey proteins rejection.

Along the same lines, the right graph in Figure 5-15 shows the effect of outlet pressure and temperature to control whey proteins rejection. Similar to casein proteins the whey protein rejection is influenced by temperature and the increase of temperature is expected to reduce the overall whey proteins rejection. Unlike casein proteins, the results for outlet pressure applied to whey proteins is not conclusive enough to determine a correlation between modifications of outlet pressure and changes in whey proteins rejections since the confidence interval is too wide. This result links well with the observed behaviour of whey proteins in Figure 5-13, where no clear tendency was detected for the temperature and corroborates the initial impressions.

On balance, these results indicate that whey proteins are not fully expressed in the current experimental conditions, since their behaviour under the studied factors cannot be described based on the studied parameters. There are two main reasons for the lack of definition for the whey proteins; the first one is that the studied factors (outlet pressure and temperature) are not enough to define the behaviour of whey proteins. The second option is that whey proteins (less than 20% of all starting proteins and with a much smaller size) are “trapped” by the casein proteins and micelles and their behaviour depends on how the casein proteins are affected and the types of fouling and concentration polarisation that occur.

Resistance study

The changes in protein behaviour can in part be attributed to the changes in the membrane caused by the fouling layer and concentration polarisation phenomena. The fouling properties have been studied indirectly by means of a resistance breakdown, including total resistance and both reversible and irreversible fouling resistance.

Figure 5-16 shows the breakdown of membrane resistance values as a function of outlet pressure for samples processed at 30 °C, TMP 0.5 bar ± 0.01 bar and CFV 1.4 m s^{-1} ± 0.3 m s^{-1}. It can be seen that an increase in outlet pressure leads to an increase in total resistance, mainly due to the increase in reversible fouling, which includes rinseable fouling and concentration polarisation. Conversely, an increase in outlet pressure also results in a decrease in irreversible fouling from the 0.17 bar outlet pressure value of 25.7 $x10^{+11}$ m^{-1} to the 0.44 bar (outlet pressure) value of 16.9 $x10^{+11}$ m^{-1}.

This observed behaviour can be explained by assuming that at lower outlet pressure conditions, proteins are less compressed at the membrane side, leading to lower concentration polarisation phenomena and less total resistance. The reduction in irreversible fouling with the increase in outlet pressure could be linked to the increase of reversible fouling since the foulants trapped in the concentration polarisation layers do not form irreversible fouling.

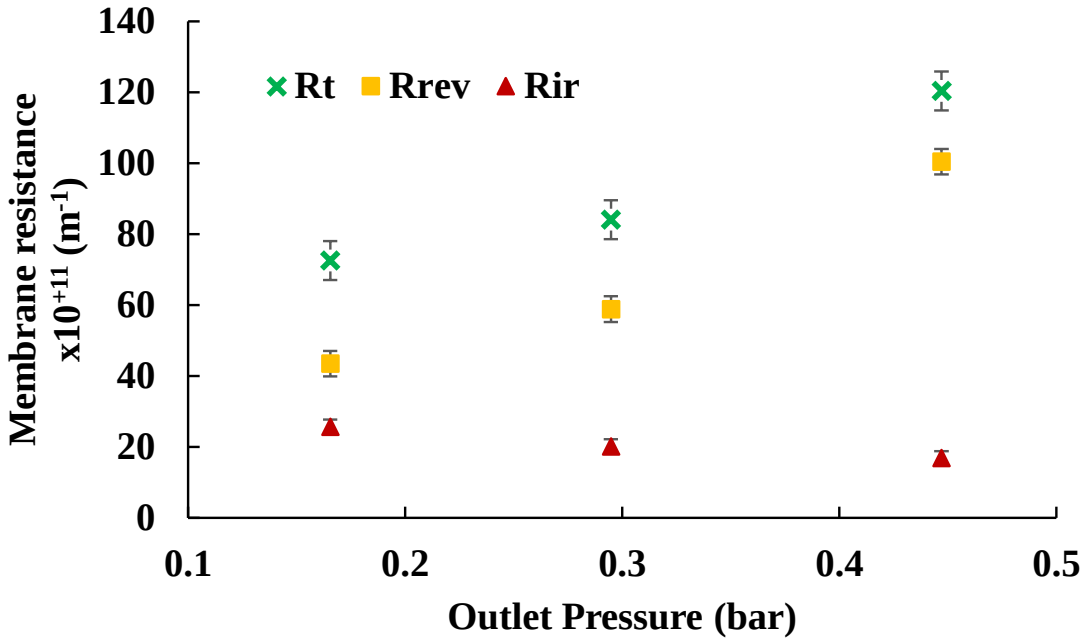

Figure 5-16: Resistance values for samples processed at 30 °C, TMP 0.5 bar ± 0.01 bar and CFV 1.4 m s^{-1} ± 0.3 m s^{-1}. Membrane resistance values of 3.3, 5.0 and 3.1 $x10^{+11}$ m^{-1} for the 0.17, 0.3 and 0.44 bar respectively. Total resistance (green cross), reversible fouling resistance (yellow square) and irreversible fouling resistance (red triangle).

5.2.3.3 Protein breakdown

In this section, a concise analysis of protein composition, such as alpha and beta casein, α-Lactalbumin and β-Lactoglobulin in the feed, retentate and permeate stream is presented and explained in detail. The aim of this study is to further understand the filtration process of casein and whey proteins and determine which subgroups have a major impact on the efficiency and rejection values of the milk filtration process.

In particular, the protein breakdown study has been evaluated at the three different processing temperatures studied in the DoE analysis (10, 30 and 50 °C) and at outlet pressures values ranging from 0.2 to 0.4 bar, approximately.

The protein breakdown analysis of samples processed at 10 °C is shown in Figure 5-17. This study indicates that irrespective of the outlet pressure values studied (0.2, 0.3 and 0.4 bar) the protein breakdown pattern tends to be the same at all the steps analysed, including initial feed, retentate and final permeate. In particular, at the three outlet pressures studied, the composition of the initial feed and retentate is very similar, with a majority of alpha and beta casein groups. However, a substantial decrease in alpha and beta casein groups is observed in the final permeate, indicating a higher rejection for these groups, as expected.

Beta-Lg is the whey protein group that increased the most in the permeate when operated at 10 °C at all of the studied outlet pressures, indicating that this type of filtration process works very well for this whey subgroup of proteins. On balance, the protein composition obtained in the three different streams indicate that this filtration approach can fractionate the casein and whey proteins favouring an increase of the whey proteins share in the permeate even though the casein fraction is still dominant in several cases. However, further work and knowledge is required to further understand the behaviour of other protein subgroups that show minimal variation in the three different streams studied, such as κ-CN and BSA. Nevertheless, the consistent changes in protein composition at the final permeate at the three different outlet pressures studied reinforce the results that indicate that temperature is a major factor to consider for both protein groups (whey and casein), and that under certain conditions slight changes in pressure might not affect the protein behaviour.

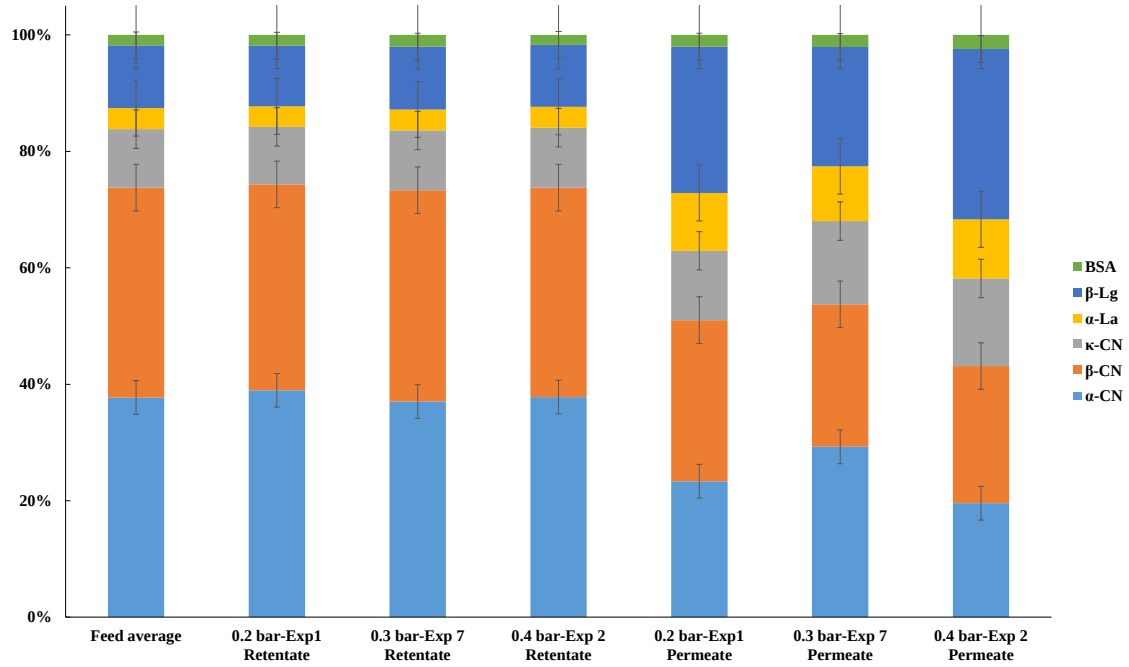

Figure 5-17: Protein breakdown of samples processed at an operating temperature of 10 °C. Processing outlet pressure of 0.2 bar for exp 1, 0.3 bar for exp 7, and 0.4 bar for exp 2.

Figure 5-18 shows the protein breakdown of samples processed at 30 °C and at three different outlet pressures (0.16, 0.3 and 0.44 bar). Unlike samples processed at 10 °C, the filtration at 30 °C yielded different protein breakdowns at the final permeate based on the outlet pressure applied. An increase in the outlet pressure led to an increase of the whey proteins fraction and a reduction of the casein proteins fraction. The whey protein fraction that benefits most of the increase of outlet pressure is the beta-Lg that increases from 13% to 31%, going from the low outlet pressure value to the high outlet pressure (Figure 5-18a, d).

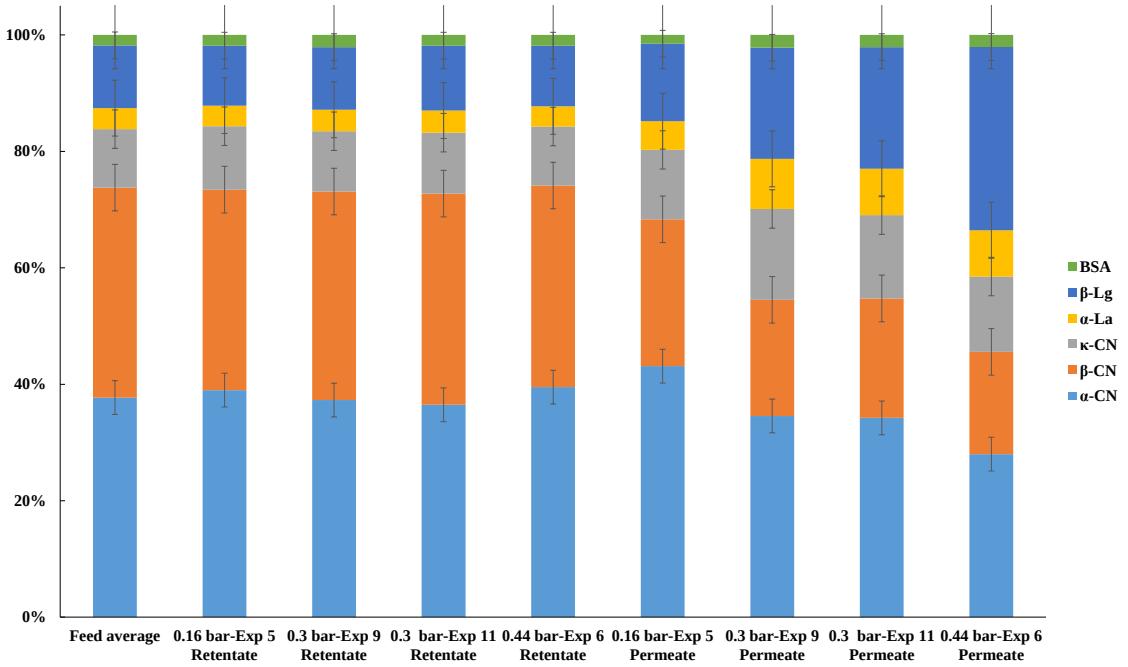

Figure 5-18: Protein breakdown of samples processed at an operating temperature of 30 °C. Processing outlet pressure of 0.16 bar for exp 5, 0.3 bar for exp 9, 0.3 bar for exp 11, and 0.44 bar for exp 6.

The casein protein groups that are reduced the most at 30 °C are alpha and beta casein, but unlike the 10 °C filtration in this case the beta-casein is the group that is reduced the most with the increase in outlet pressure.

Finally, Figure 5-19 shows the protein breakdown of samples processed at 50 °C and 58.3 °C (Figure 5-19c). Interestingly, this data shows that under certain conditions of temperature the protein transmission is strongly enhanced which then limits the effect of outlet pressure as control factor. For example, operating at 0.2 or 0.4 bar of outlet pressure (Figure 5-19a, b), leads to having quite identical proteins profiles. Exp 8 is hard to compare because it was one of the extreme conditions operated at 58 °C, however, the profile resembles the other two conditions explored at 50 °C and relevant shifts were not observed.

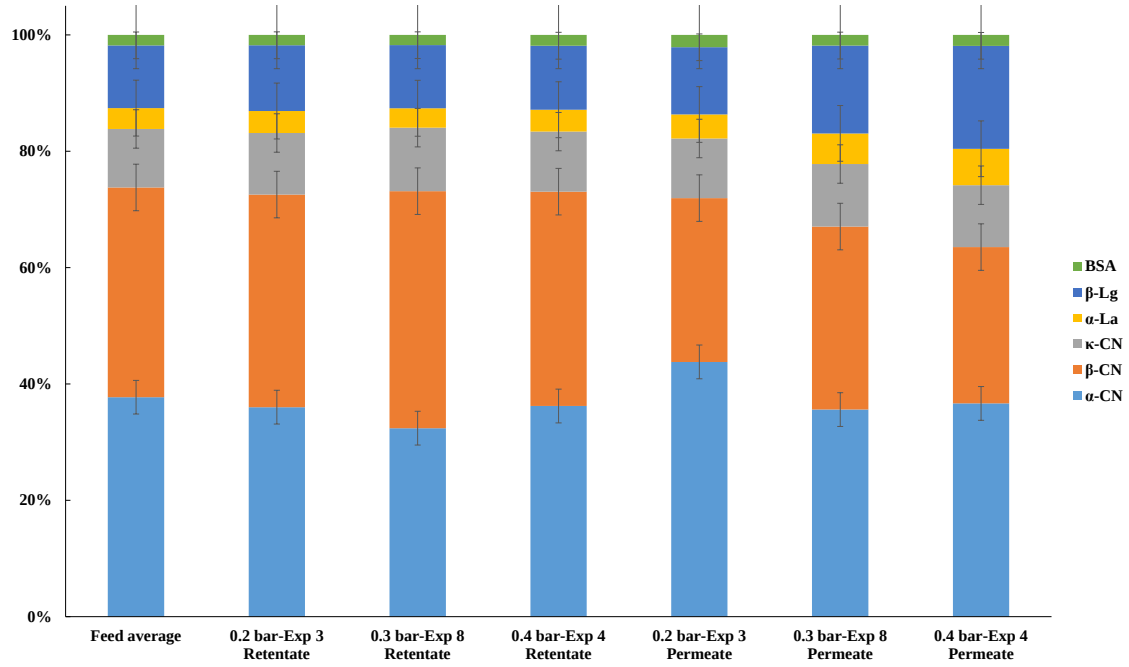

Figure 5-19: Protein breakdown of samples processed at an operating temperature of 50 °C, with the exception of exp no 8 that was at 58.3 °C. Processing outlet pressure of 0.2 bar for exp 3, 0.3 bar for exp 8, and 0.4 bar for exp 4.

One of the main challenges of the DoE has been defining the zones of maximum influence of each studied factor. For example, operating at low temperature did leave small margins of variability for the outlet pressure to influence the results as shown in Figure 5-17. To facilitate this comparison, Figure 5-20 shows the protein breakdown based on the three samples processed at high outlet pressure (0.4-0.44 bar) at all three temperatures tested.

The highlight of this figure is the fact that at 10 and 30 °C the protein separation were almost the same, but the results come from different interactions since the pressure alone does not explain them. For example, the temperature effect at 10 °C tends towards the protein breakdown of exp 2, as seen in Figure 5-17c, independently of the outlet pressure value. On the other hand, of the samples processed at 30 °C (Figure 5-18), the outlet pressure had a major impact on defining the protein breakdown, with a profile that tended towards the low temperature breakdowns with the increase of outlet pressure. These results align well with the parameter coefficients shown in Figure 5-15.

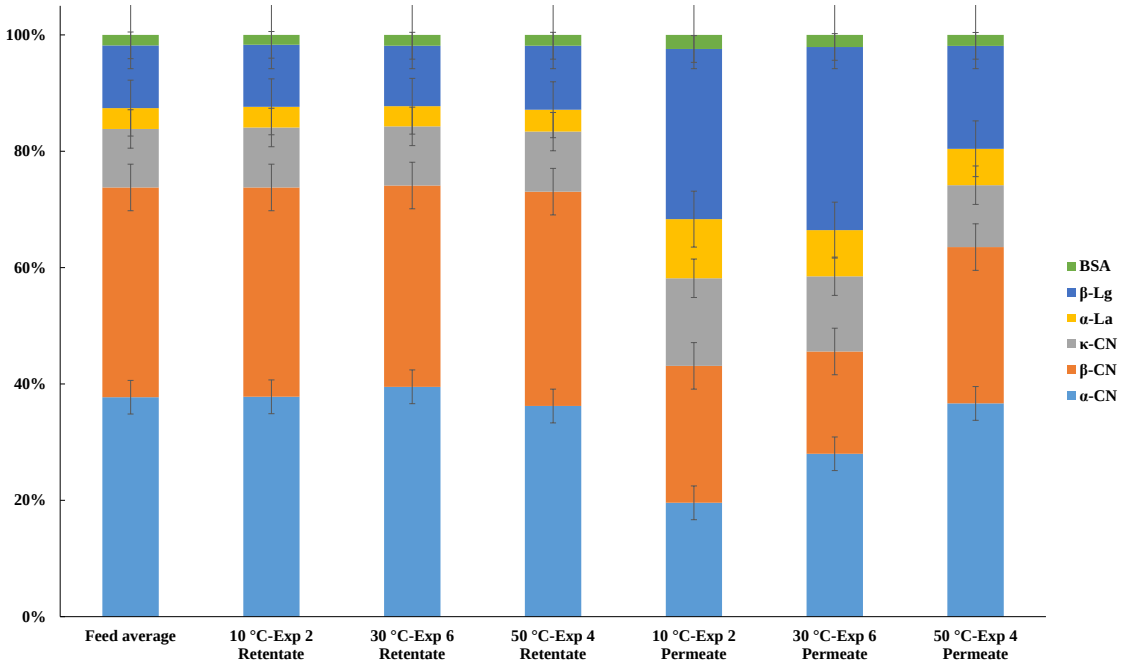

Figure 5-20: Protein breakdown of exp 2 and 4 processed at 0.4 bar and exp 6 operated at 0.44 bar of outlet pressure. Processing temperature 10 °C for exp 2, 30 °C for exp 6, and 50 °C for exp 4.

In summary, certain processing conditions favour the separation of certain protein groups within casein and whey proteins. For example, beta-Lactoglobulin is enhanced when filtering at 10 °C over the other whey proteins groups due to a better transmission, which in turn is an ideal situation for the production of infant formula since the human milk is mainly formed by beta-Cn and Beta-Lg.[144]

5.2.3.4 Summary of the DoE

The DoE study yielded two main conclusions based on the data analysed. First, the casein rejection is affected by both outlet pressure and temperature. Second the whey proteins rejection is also affected by temperature and not by the outlet pressure.

The casein rejection showed a positive effect due to outlet pressure, leading to higher casein rejections overall with the higher outlet pressure values when operated at a TMP of 0.5 bar. At 0.4 bar of outlet pressure the casein rejections ranged from 95% at 10 °C to 77% at 50 °C, unlike the 0.2 bar of outlet pressure that showed a higher span of results ranging from 89% to 56% for the 10 and 50 °C samples, respectively. The effect of temperature shows a negative effect on casein rejection, meaning that an increase in temperature does reduce the casein rejection final value. The DoE study highlighted the massive effect of temperature on casein rejection, at 10 °C the casein rejections range from 89% to 95% at 0.2 and 0.4 bar of outlet pressure, respectively. On the other hand, at 50 °C the casein rejection values range from 56% to 77% at 0.2 and 0.4 bar of outlet pressure, respectively. The reason for having lower rejection

at higher temperatures could be explained by the casein micelle contraction at high temperatures (50 °C) that would facilitate their transmission through the membrane.

The whey proteins rejection was only affected by temperature, and the effect of temperature was much lower compared to casein proteins interactions. The whey proteins suffer from being a minor fraction (around 18%) within a complex matrix, and for being smaller than casein micelles. The smaller presence of whey proteins could explain their behaviour as "captives" components observed in the DoE results.

5.3 Sequential filtration

In this section the results for a sequential filtration study are shown. The study consisted in initially filtering a feed and using the permeate and retentate of that initial filtration as feed for a subsequent filtration, accumulating filtration steps (see Figure 5-21 and Figure 5-22). These studies aimed to improve protein fractionation by taking advantage of the flexibility that sequentially filtering a feed and both the permeate and retentate obtained can provide.

The overall idea of this approach is to utilise the different permeate and retentate composition at each filtration step, in order to alter the fouling and concentration polarisation mechanisms, which in turn will define the protein fractionation.

These studies were performed using the 0.1 µm PVDF membrane (Synder Filtration, V01), and changing the operational conditions such as temperature, CFV and TMP. The two initial experiments shown in this section were carried out in the volume reduction mode (Section 0), in order to produce both permeate and retentate of similar volume without the need of adding the extra challenges of diafiltration.

The initial experiments were based on operational conditions that showed promise in preliminary studies, such as the ones obtained in the DoE. In particular, these studies were carried out at different CFV, temperature and transmembrane pressure, as shown in detail in Table 5-17 and denoted case study 1 and 2.

Table 5-17: Experimental conditions of the case study experiments that were used to define the initial conditions for the sequential filtration test.

	Inlet [bar]	Outlet [bar]	TMP [bar]	CFV [m s^{-1}]	Temperature [°C]
Case study 1	0.67	0.42	0.55	1.22	20
Case study 2	1.23	0.89	1.06	1.61	50

The obtained protein ratio (casein/whey) for each case of study is shown in Table 5-18.

Table 5-18: Protein ratios (Casein/Whey) for the case study experiments that were used to define the initial conditions for the sequential filtration test.

	Initial ratio feed	Final ratio retentate	Initial ratio permeate	Final ratio permeate
Case study 1	84/16	83/17	68/32	68/32
Case study 2	82/18	85/15	82/18	74/26

Case study 1 indicates a reduction in casein proteins and an increase in whey proteins when comparing the initial feed and the final permeate stream, shifting the protein ratio from 84/16 to 68/32, respectively. These are promising initial results that achieved a good casein and whey separation and are of interest for the sequential filtration studies in order to see if the separation can be further improved to achieve the desired industrial targets. It is to be noted that whey proteins do not entirely behave independently and that their behaviour depends on the amount of casein proteins present at the stream, as demonstrated in the DoE section. Therefore, the study aims to decouple casein and whey protein behaviour to gain further understanding of whey protein rejection in skimmed milk.

One of the mechanisms that could explain the "capture" of the whey proteins by the casein is the concentration polarisation effect that prevent most of the whey proteins from moving though the membrane.

The second set of experiments (based on case study 2) to test in the sequential filtration study aimed to use high temperatures to reduce the filtration time and to increase whey content in the permeate stream. The chosen operational conditions are radically different as the ones used in case study 1, with high pressures and processing temperatures. Although permeate stream protein composition has a similar casein to whey ratio for both cases of study after the initial filtration step (Table 5-18), the differences in the processing conditions should have affected the protein structures (morphology, aggregation of micelles, etc) yielding to different permeate properties. The aim of the sequential filtration will be to study if these different feeds with similar protein ratio behave differently upon sequential filtration.

Table 5-19 shows the operational conditions of all the sequential filtration tests carried out. SF1P and SF2P were both processed at the same operational conditions (see Table 5-19) in order to compare the response of the different compositions to the same processing conditions.

Table 5-19: Operational conditions of the sequential filtrations experiments.

Sample	Inlet [bar]	Outlet [bar]	TMP [bar]	CFV [m s^{-1}]	Temperature [°C]
SF1	0.66	0.40	0.53	1.23	20
SF1P	0.66	0.39	0.52	1.26	10
SF2	1.25	0.91	1.08	1.58	50
SF2P	0.64	0.37	0.51	1.26	10
SF2R	0.64	0.41	0.52	1.23	20

The sequential test carried out were SF1 and SF2, in both cases all the flows were analysed and the data can be found in Table 5-20 and Table 5-21.

Table 5-20: Sequential experiments data of experiment SF1 with the sequential permeate line (SF1P). The table shows the ratio of casein to whey proteins in each step of the respective filtration process with the final permeate whey protein ratio enhancement at each step. The permeate concentration corresponds to the initial feed for the permeate sequential filtration and the final whey protein enhancement corresponds to the process initial feed to final permeate.

Sample	Initial Feed	Retentate	End Permeate	Whey proteins enhancement [%]
SF1	84/16	83/17	60/40	146%
SF1P	60/40	61/39	58/42	5%
Start to end SF1P	84/16		58/42	159%

The first sequential filtration (SF1) was aimed to study the permeate route to analyse if the whey protein enhancement of 146% achieved in the first stage could be refined. The route to promote whey protein enhancement was by filtering at TMP of 0.5 bar, CFV of 1.25 m s^{-1} and at 10 °C, which had yielded encouraging results in previous work (Figure 5-2).

The added filtration step of SF1P did slightly improve the whey proteins presence in the retentate from 60/40 to 58/42. As shown in Figure 5-21 the selected conditions for the sequential filtration (SF1P) did not modify either the permeate or the retentate compositions ending at a ratio around 60/40, which was just an extra whey enhancement of 5%. In summary for SF1 both the ratio of the permeate line after the first filtration (SF1) and the whey enhancement point towards the fact that the first stage of the sequential filtration did achieve the main separation of whey proteins, with the second stage not adding any relevant improvement.

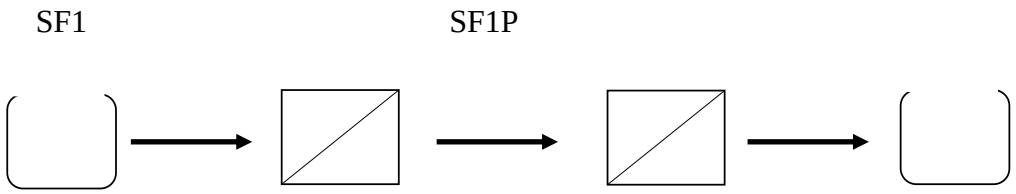

Ratio	Feed
Casein	84 ± 9%
Whey	16 ± 9%

Ratio	Permeate
Casein	60 ± 11%
Whey	40 ± 10%

Ratio	Permeate
Casein	58 ± 10%
Whey	42 ± 9%

Figure 5-21: Sequential filtration for the SF1 and SF1P experiment (values correspond to Table 5-20).

The protein ratios for SF2 can be found in Table 5-21 and a schematic representation of the sequential filtration process can be found in Figure 5-22.

Table 5-21: Sequential experiments data of experiment SF2 with respective permeate (SF2P) and retentate lines (SF2R). The table shows the ratio of casein to whey proteins in each step of the respective filtration process with the final permeate whey proteins enhancement at each step. The retentate and permeate concentrations correspond to the initial feed for the permeate and retentate sequential filtration and the final whey protein ratio enhancement corresponds to the process initial feed to final permeate.

Sample	Initial Feed ratio (CN/Wy)	Retentate ratio (CN/Wy)	End Permeate ratio (CN/Wy)	Whey proteins enhancement [%]
SF2	82/18	84/16	74/26	66%
SF2P	74/26	75/25	69/31	19%
Start to end SF2P	82/18		69/31	96%
SF2R	84/16	87/13	78/22	40%
Start to end SF2R	82/18		78/22	39%

SF2 first filtration stage did produce a permeate stream with a higher casein content compared to SF1, 74/26 and 60/40, respectively.

The initial set of conditions for SF2 (high pressure and temperature) did produce a permeate with a lower ratio of whey proteins compared to the one in SF1, with protein ratios of 74/26 and 60/40, respectively. The obtained results are in agreement with the selected case study 2.

Once the case of study results were achieved in the first step of SF2, both the permeate and retentate lines were further processed to study whey enhancement.

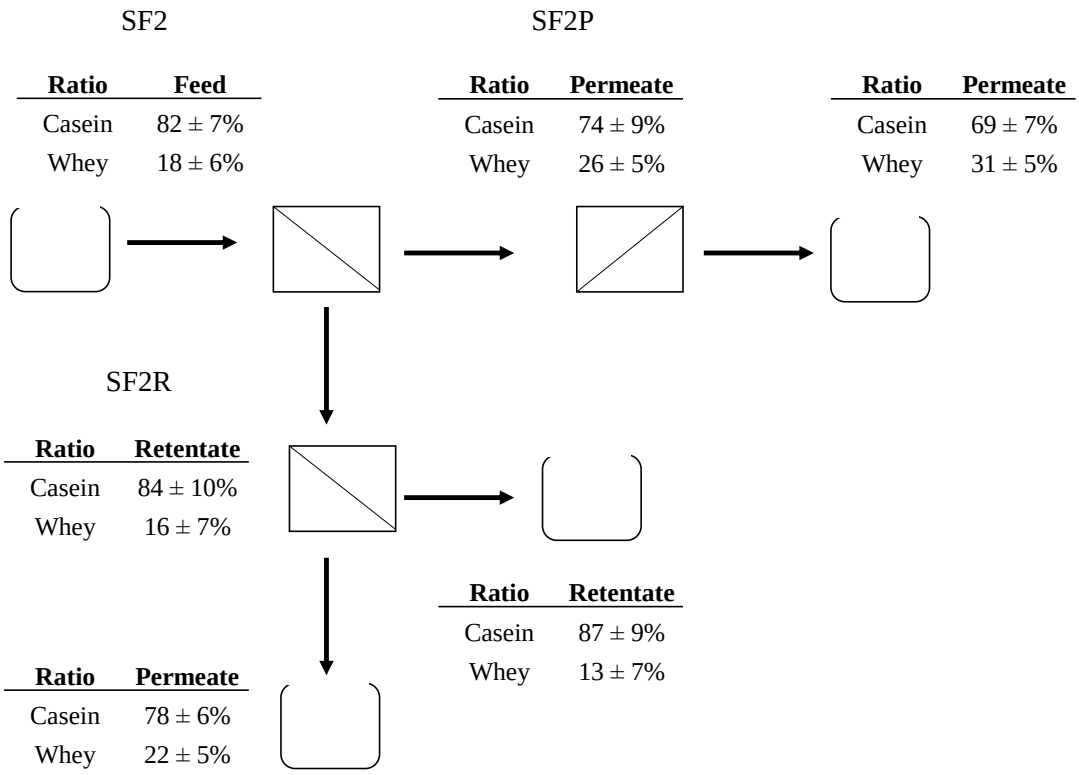

Figure 5-22: Sequential filtration for the SF2, SF2P (permeate line) and SF2R (retentate line) experiment (values correspond to Table 5-21.

The permeate line (SF2P) did achieve a constant increase of the whey presence in the overall protein content, from the initial 18% to the final 31%, which overall lead to an increase in whey proteins of 96%, with a final ratio of 69/31. However, the results of the SF1 are still better in regards the whey presence in the permeate line where they finished at a ratio of 58/42 (casein to whey proteins). From previous work, it was expected that the whey proteins presence would increase in the permeate line in SF2P, however, the 19% whey protein enhancement is well below the expected values, for example SF1 achieved 146% at 20 °C which as seen in the DoE section is worse for casein rejection than 10 °C. One of the reasons for the worse protein rejection could be that the lower concentration feed of SF2P lead to having lower fouling and concentration polarisation phenomena which in turn lead to worse casein rejection preventing the expected whey enhancement.

5.3.1 Analysis by protein groups

The study did not yield great protein ratios overall, however, the perfect separation of casein and whey proteins is not always needed, for example, the production of infant formula requires a whey favoured ratio of proteins, around 40/60 compared to the initial bovine 80/20, with a high content of beta-casein (of the casein proteins). The following section will cover the

analysis of the benefits of the sequential filtration for the separation or enrichment of certain casein or whey protein groups over the others.

SF1 experiments

The filtration of the experiment FS1P was carried out at 10 °C (Table 5-19) which is important to define the behaviour of beta-casein proteins, because they dissociate from the casein micelle around 8.9 °C and they transition to the monomer form which should get through the membrane more easily.[119]

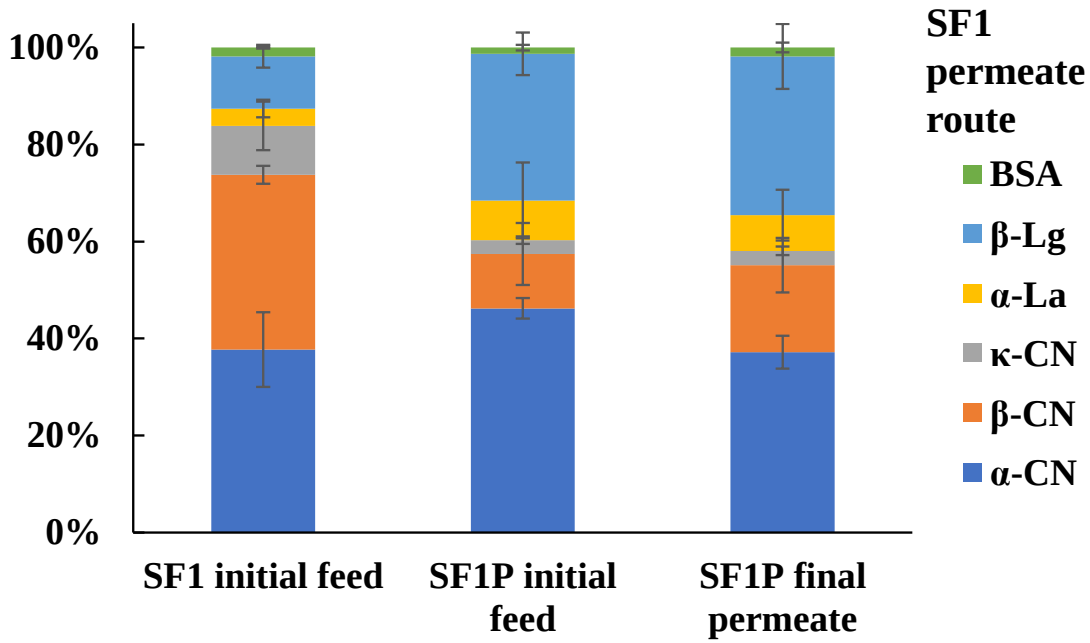

Figure 5-23: SF1 experiment protein breakdown distribution data. Error bars correspond to the standard deviation of 2 repeats for each data point.

Figure 5-23 shows that the fraction of beta casein increased when filtering at 10 °C from the FS1P feed to the FS1P permeate from 11% to 18% and the alpha-casein fraction was reduced from the 46% to 37%. Another relevant protein modification was the β-Lg that along the whole sequential filtration increased from the initial 11% to the final 33%.

The main drawback of this results is that the protein ratio is still favouring casein over whey and that from the casein fraction the alpha-casein ended up being the dominant fraction over the beta-casein. However, the use of this membrane and conditions indicated that the enrichment of beta-casein over alpha-casein was possible, even though further work is required to specify the right conditions.

SF2 experiments

The second set of experiments was operated at a higher pressure (1 bar) and at a higher temperature (50 °C) than the first set which led to having a permeate and retentate with different compositions and protein concentrations. For example, SF1P and SF2P had an initial concentrations of 3.4 and 7.0 mg ml^{-1}, respectevilly.

Figure 5-24 higlights that filtering at high temperature lead to a smaller protein fractionation in the permeate side compared to the SF1 experiments, ending up at a protein ratio of 74/26 (CN/Wy), where the beta-casein fraction was slighly reduced from the initial 36% to the 24% and the beta-Lg was increased in proportion from 11% to 18%.

The FS2P filtration (of the same conditions as FS1P) had a similar effect on the final permeate composition favouring beta-casein and beta-Lg transimission over alpha-casein that was reduced from 41% to 36%. However, the combined process of SF2 and SF2P can be deemed not applicable because at the end the only subtancial changes were at the beta-casein and whey fractions ending with a final protein ratio of 69/31. The final ratio of SF2 route was worse than the SF1 and SF1P of 58/42 with a high beta-Lg protein content of 33%.

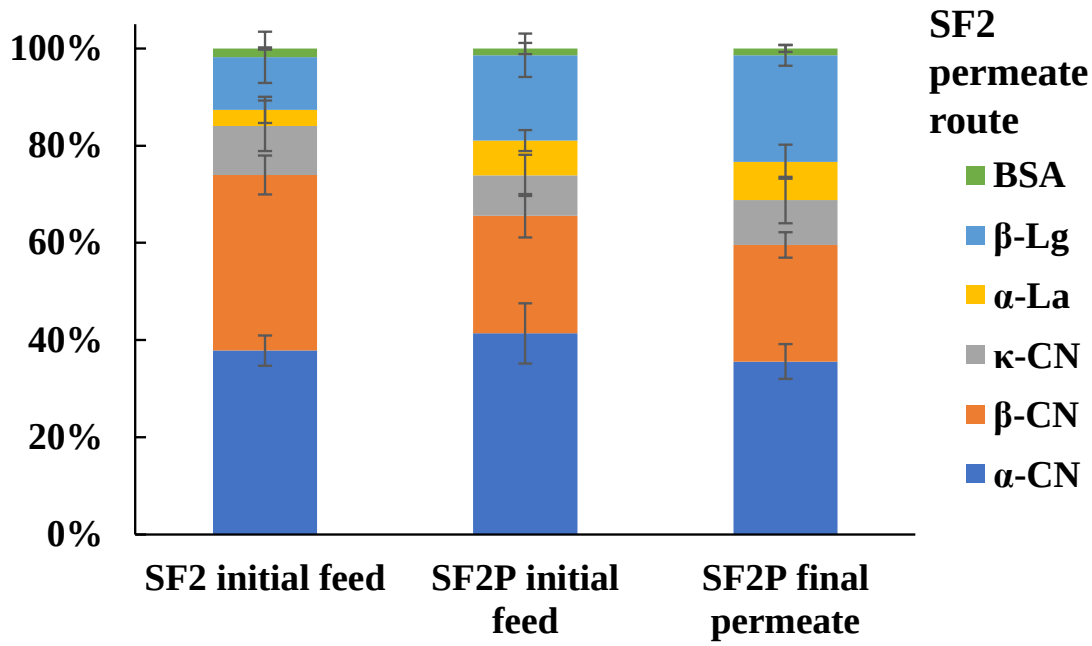

Figure 5-24: SF2 experiment protein distribution data for the permeate route. Error bars correspond to the standard deviation of 2 repeats for each data point.

The retentate route of SF2 lead to a retentate that technically had the same composition as the initial feed after FS2 processing. The main reason for this was that filtering at high temperature and CFV lead to having low protein fractionation, which in turn lead to a low concentration increase with a protein concentration change from the initial 34.4 mg ml^{-1} to the final retentate concentration of 35.9 mg ml^{-1}.

The processing of FS2R using the same operational conditions as the permeate line (FS2P), except for the temperature that was higher at 20 °C (Figure 5-25), implied a permeate with a smaller fraction of beta-casein (which is in the micellar form and should not get through the membrane easily), but it also yielded a high proportion of alpha-casein (which should not have happened because it is supposed to be in the micellar from as well).

The retentate fraction had a similar protein composition as the initial feed with a slight increase of the alpha-casein fraction mainly because of the reduction of the whey fractions. The beta-casein fraction did not appear either in the retentate or the feed and might be trapped in the membrane fouling in a higher proportion compared to the alpha-casein, which should be further studied.

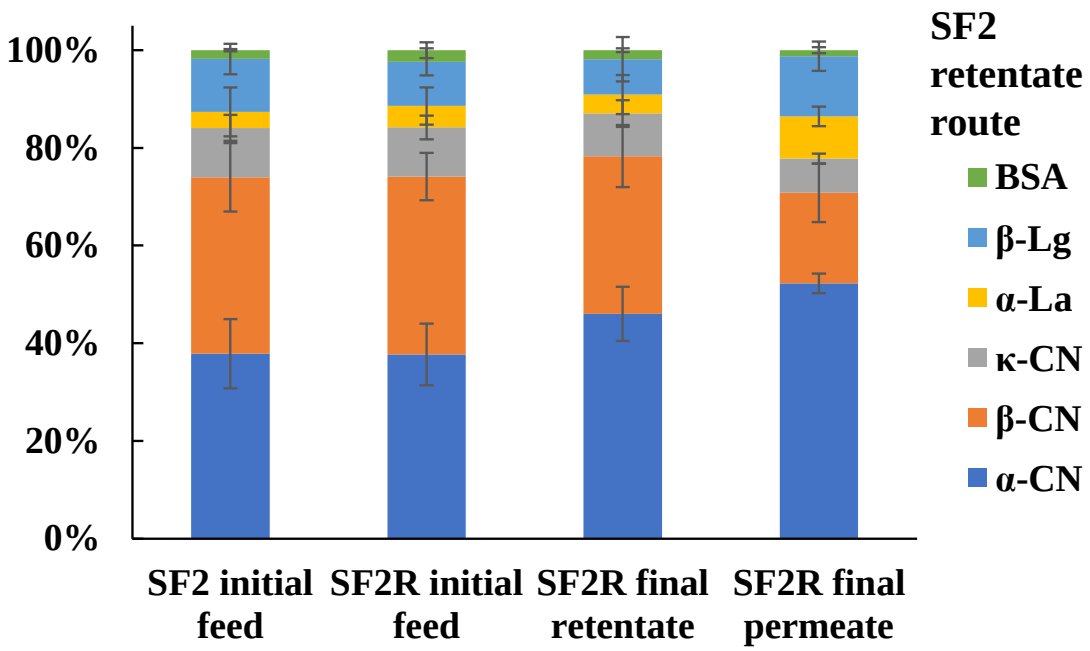

Figure 5-25: SF2 experiment protein distribution data for the retentate route. Error bars correspond to the standard deviation of 2 repeats for each data point.

5.3.2 Permeate flux

The permeate flux of samples was analysed to compare the benefits of processing permeate/retentate as feed compare to virgin "feed".

Figure 5-26 shows the final permeate protein ratio (CN/Wy) related to the final permeate flux for SF1 and SF1P. It can be seen that the use of the permeate as feed for the next filtration step did favour an increase in final permeate flow, mainly due to the reduced protein content in the permeate that did produce a reduced fouling phenomenon. However, it also shows that the

increase in permeate flux does not go in hand with an increase of whey content in the permeate, probably due to the reduction of fouling components.[120]

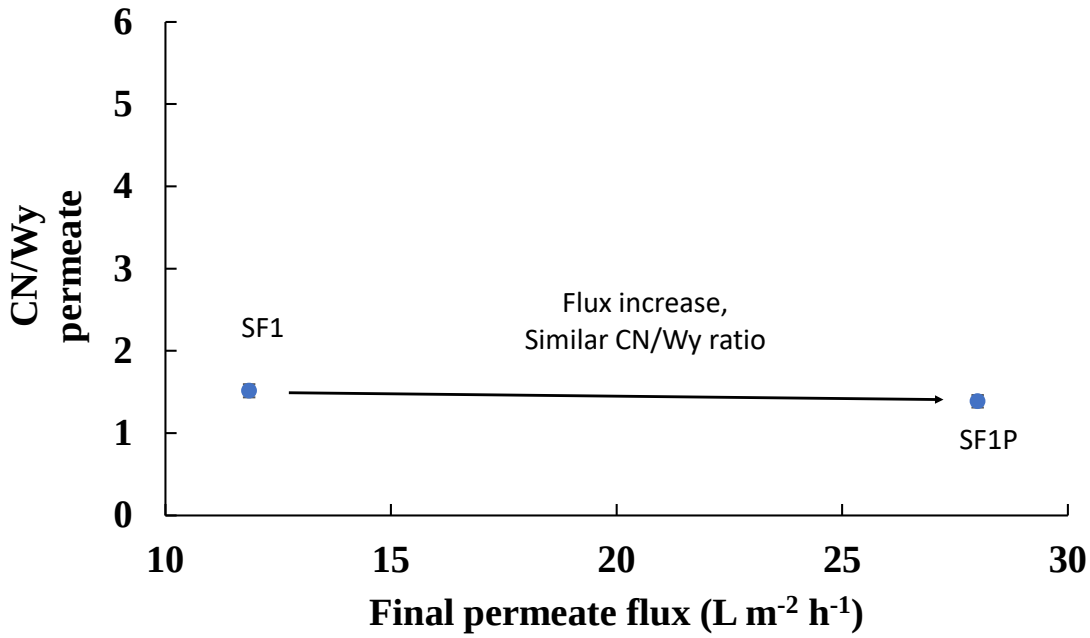

Figure 5-26: Final permeate flux and CN/Wy permeate ratio for sequential filtration 1, SF1 and SF1P final permeate data. Error bars correspond to the standard deviation of 2 repeats for each data point.

Figure 5-27 shows the final permeate protein ratio (CN/Wy) related to the final permeate flux for SF2, SF2R and SF2P. The SF2R flux behaviour was expected due to in one hand having a higher protein content than the "virgin" feed that promoted a lower permeate flux, as well as, having a lower temperature that also leads to having a lower permeate flux.

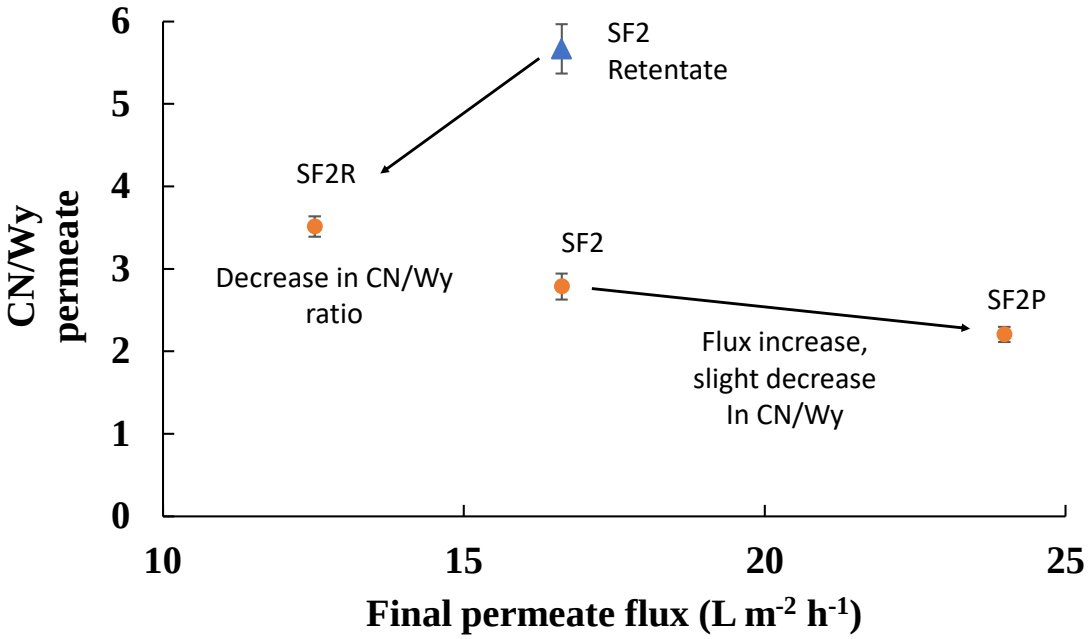

Figure 5-27: Final permeate flux and CN/Wy permeate ratio for sequential filtration 2, SF2, SF2R and SF2P final permeate data and SF2 retentate CN/Wy ratio (blue triangle). Error bars correspond to the standard deviation of 2 repeats for each data point.

The SF2P route showed that the combined protein fractionation of the two-step process ended up reducing the protein ratio (CN/Wy) from the initial feed value of 5.2 to the final SF2P value of 2.2 (a reduction of almost 60%), however the final protein ratio was still higher than the observed in the SF1 route. The SF2P final permeate flux also displayed an improvement compared to the SF2 even though the temperature was reduced from 50 to 10 °C, the same behaviour was observed in the SF1 route, when the feed protein concentration is reduced the permeate flux increases due to a lower fouling phenomenon (see section 5.2.2).

5.3.3 Summary of sequential filtration

The choice of two radical initial conditions was done to minimise similarity of results and as has been shown, the SF1 and SF2 routes obtained different results.

The SF1 filtration route proved that an initial first step can produce a permeate with a CN/Wy protein ratio of 60/40 which would be ideal for subsequent filtration steps, since the lower protein presence favours further processing, as has been shown, the permeate flux of SF1P increased from the SF1 12 to the SF1P 28 L m^{-2} h^{-1}. However, the chosen conditions did not improve any further the protein separation ending with a final protein composition identical between SF1 and SF1P.

The sequential filtration of SF1 lead to an increase of the whey fraction due to the removal of alpha-casein in the SF1P step with the added benefit that the beta-casein fraction was also

increased from 11% to 18% (but still falling short due to the massive alpha casein share of 32%), however, similar compositions have been achieved from fresh milk. In summary, the lower protein composition of SF1P does favour an increase in permeate flux, which favours further processing by reducing the operational time, but it did also add a layer of difficulty for the improvement of casein removal due to the lower fouling. Even though the casein protein had been reduced to the 60% of all proteins in the first step (SF1) the SF1P conditions did not manage to produce a whey rich permeate at the end.

The SF2 filtration route produced in the first filtration step a permeate fraction with a CN/Wy ratio of 2.8 which was higher than the obtained in the first step of the SF1 route (1.5). However, due to the higher protein content the second step did yield a much higher degree of removal reducing the SF2P permeate protein ratio to 2.2. The rate of removal of the second step was much better for SF2 route, it does indicate that the casein removal is improved by the presence of fouling.

The sequential study proved that for the extra time consumed to produce the initial samples the extra filtration steps did not provide any improvement compared to single step filtrations carried out in previous studies. Nevertheless, the sequential filtration studies should be further analysed since the results point towards the possibility of improvements like the improved processing time, but it would require an experimental setting designed for the sequential filtration and the accompanying laboratory facilities for the holding of the different streams which it was decided not to develop.

5.4 Membrane analysis

A membrane analysis was carried out to build up knowledge of the filtration process, the protein behaviour and to determine the presence and structure of the fouling layer. The studies were focused on confirming the membrane fouling layer using SEM analysis and FTIR spectroscopy, as well as determining in the detail the effects that the fouling had on the membrane physicochemical properties like hydrophobicity.

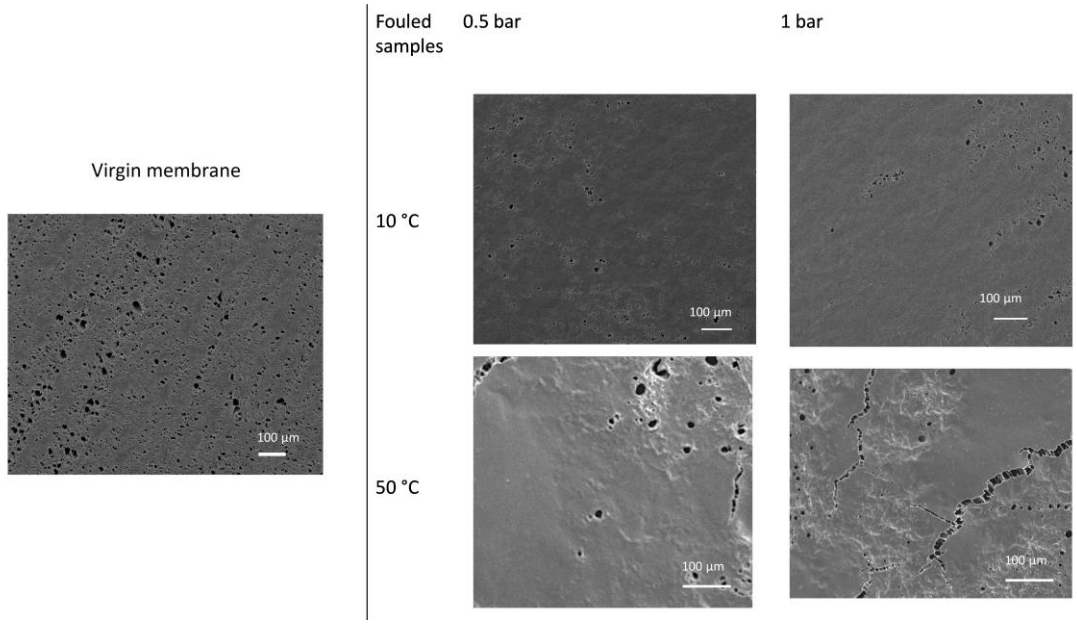

Figure 5-28: SEM pictures of virgin membrane vs fouled membranes at 0.5 or 1 bar of TMP and at 10 or 50 °C of temperature. CFV was maintained at 1.5 m s^{-1} for the 10 °C samples and 1.3 m s^{-1} for the 50 °C samples.

The SEM pictures taken show the presence of a fouling layer on the membrane at a wide range of processing conditions (Figure 5-28), low and high temperature and 0.5 and 1 bar of TMP. The fouling layer can be observed all over the range of operational conditions with minimal changes on its presence. However, the SEM images do not confirm the type of fouling present on the membrane, to do that the FTIR spectra was used to determine if the fouling present contained casein and whey proteins.

Figure 5-29 shows the FTIR spectra of a fouled membrane at TMP 0.5 bar and temperature 10 °C compared to a reference conditioned membrane. The red arrows point towards the reference peaks for casein and whey proteins at 3000 and 3200 cm^{-1}.[134] The peaks at 1500 and 1600 cm^{-1} can also be attributed to casein and whey proteins.[134] These FTIR spectra confirm that the fouling phenomenon observed on the SEM pictures contains protein components that correspond to the main protein groups in milk, even though it cannot differentiate among casein and whey proteins. K.S.Y. Ng *et al.* (2018)[125] studied the fouling phenomenon of milk filtration at different temperatures and found that for the range studied (10-50 °C) the main foulant components were proteins, with calcium representing less than 1% of the analysed fouling.

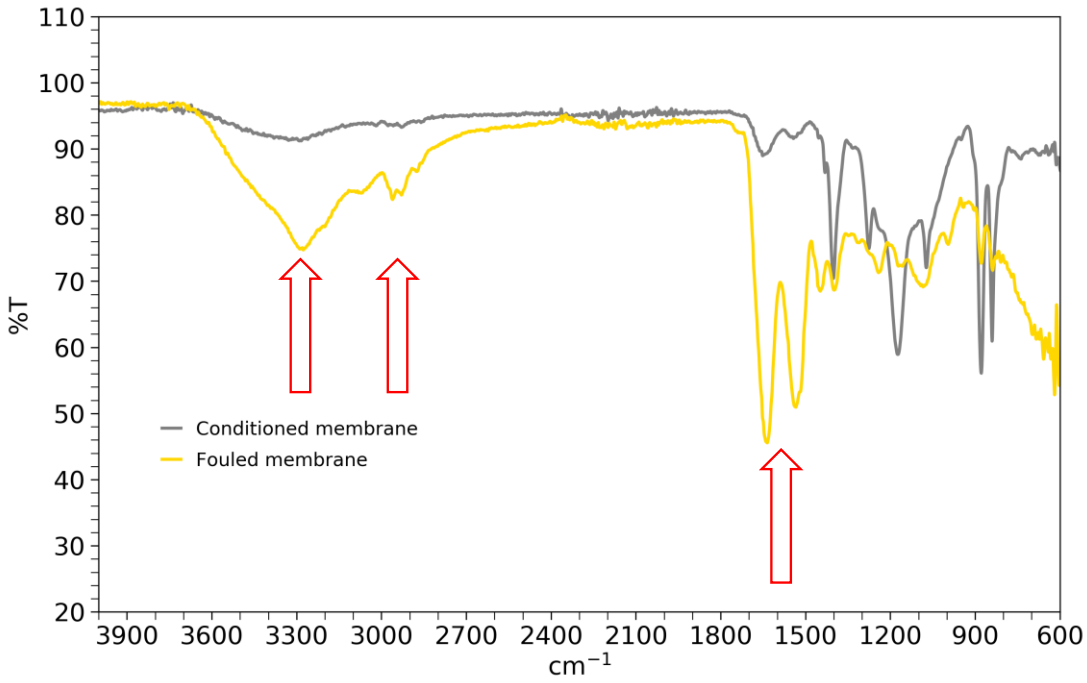

Figure 5-29: FTIR spectra of a conditioned membrane (grey) and a fouled membrane (yellow). Red arrows highlight casein and whey proteins reference peaks.

SEM and FTIR spectra were obtained for all the conditions studied and presented in this study most of them are not shown since they do not provide any extra knowledge beyond the confirmation of the fouling layer and the protein composition of it.

Figure 5-30 shows the changes on spectra intensity of the regions where casein and whey proteins can be detected (for example 3000 and 3200 cm^{-1}) due to the changes in CFV from the low value of 0.5 m s^{-1} to the high value of 1.7 m s^{-1}. Figure 5-30 highlights that in both CFV conditions the fouling detected is due to proteins from the casein and/or whey groups, since the peaks match the reference peaks showed in Figure 5-29 at the regions of at 3000 and 3200 cm^{-1} and 1500 and 1600 cm^{-1}.

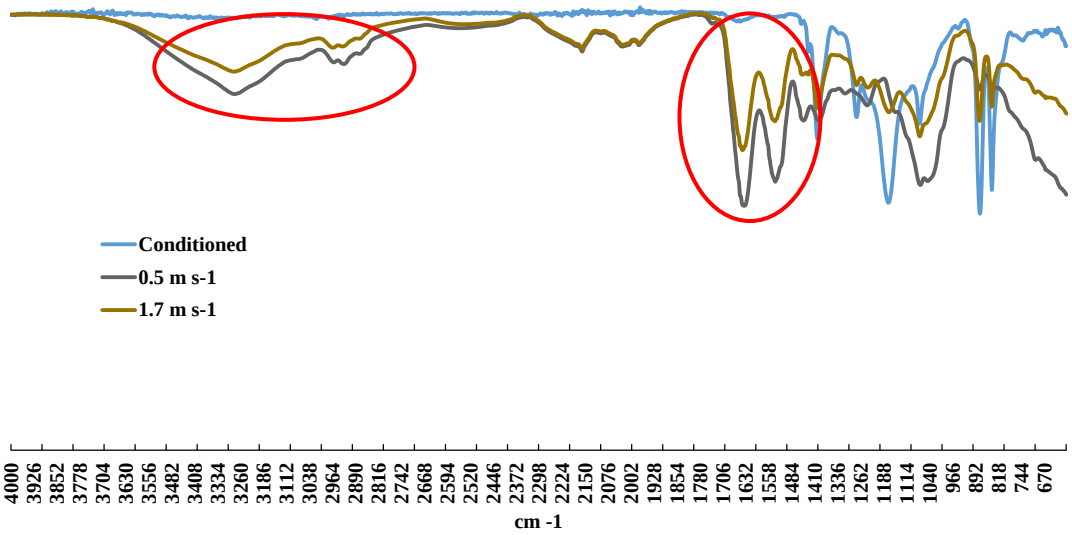

Figure 5-30: FTIR spectra of CFV changes on peak intensity. Fouled samples obtained at 10 °C and 0.5 bar of TMP. Red circles highlight casein and whey proteins reference peaks.

Chapter 6. Industrial conditions study

This chapter focuses on the results obtained using the Pilot scale filtration apparatus (see Figure 3-4). The use of this rig allowed to reach higher overall pressures, higher CFV and the pressurisation of the permeate line which was not possible with the Benchtop M10 filtration rig (Chapter 5). The unique properties of the big rig allowed the study of the effects of operational conditions on the fouling layer like protein composition. The main conditions studied were the inlet, outlet and permeate pressures and the effective transmembrane pressure. The use of the big rig allowed to keep the temperature, CFV and pressure constant at a wide range of conditions.

The results in Chapter 5 highlighted several limitations to the study performed, the main problem was the lack of certainty around the behaviour of whey proteins, that unlike casein proteins, did not behave linearly under the studied pressures and temperatures. The capabilities to add pressure to the permeate line, and to decouple TMP and CFV at any pressure should provide some insight into the whey proteins behaviour and a better understanding in casein interactions under the different operational factors.

One of the aims of the study was to deepen the understanding of the protein behaviour both in the liquid state (feed and permeate) and the fouling state, and to detect if there were any differences in composition between the fouled membranes and the fouled and rinsed membranes. The initial conditions were aligned with real industrial operational conditions to deepen the understanding, as well as some "extreme" conditions to detect if differences existed when operated with the present rig.

The set of initial industrial conditions to study can be seen in Figure 6-1. They are defined by real industrial operation conditions where the 1 bar-1 TMP and 0.5 bar-0.5 TMP pressure correspond to real inlet and outlet pressure of a spiral-wound membrane module. The 1 bar-0.5 TMP condition set is obtained by applying the 1 bar-1 TMP pressure (1 bar) with a permeate line pressure to end up with a TMP comparable with the 0.5 bar-0.5 TMP pressure (0.5 bar), allowing to compare same conditions of TMP at different initial pressures. The aim is to study if the difference in pressure does have an impact on the protein behaviour during the filtration or the fouling layer composition and properties. The initial conditions will also be compared to high temperature and pressure in order to gain perspective on the effect of the conditions, since 0.5 bar of difference may not be enough to detect significant changes.

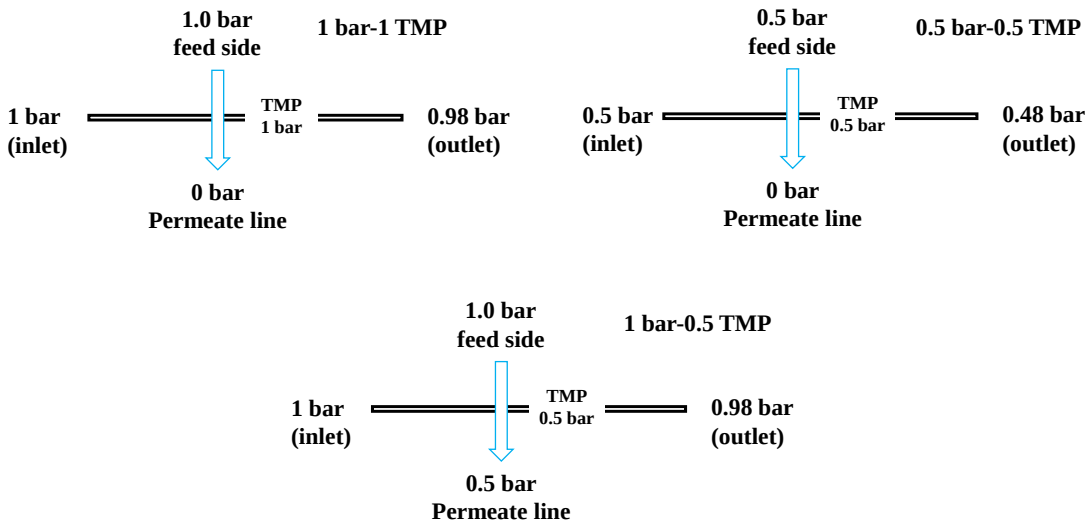

Figure 6-1: Set of initial industrial based conditions to study.

The initial conditions studied (shown in Figure 6-1) correspond to the inlet and outlet pressures 1 and 0.5 bar, respectively, of a membrane module. The aim of studying them within a flat sheet configuration was to focus on the protein behaviour in those sections of the membrane module and to observe the fouling changes under each pressure conditions.

6.1 Filtration results

The three industrial conditions studied aimed to understand the protein behaviour both for the interactions with the membrane and the fouling properties obtained under these conditions. In this first section, the results will focus on explaining the protein fractionation results.

6.1.1 Protein rejection

The filtration of milk proteins behaviour will be focused on the study of the protein interaction with the membrane, mainly rejection of the casein and whey proteins, and the analysis of the protein groups that get through the membrane, mainly based on CN/Wy ratio in the permeate line. The final protein ratio in the permeate line of CN/Wy (casein proteins/whey proteins) depends on the rejection of both casein and whey proteins. In order to produce whey-rich permeate streams (that can be pure whey proteins or not) the casein rejection has to be higher than the whey proteins rejection. When the casein proteins are rejected in a higher ratio than the whey proteins the CN/Wy ratio shifts from the initial value around 5 to lower values, and when the value gets below 1 it means that the whey fraction is the majority (ending with a casein-poor permeate).

The main difference among the three initial conditions will be the protein ratio found in the permeate line after any condition and how that will affect the possible uses for that permeate

composition, either for food applications or for further processing. The protein ratio will only define the relation among casein and whey proteins, it is also important to take into account the final concentration of proteins since removing water is a costly step, energetically and economically.

Figure 6-2 shows the protein rejections for the industrial based conditions. The first highlight is that both conditions that have high inlet pressure (1 bar) had casein rejections above 90%, independently of the TMP. The effect of TMP on protein fraction can be observed when comparing 1 bar-0.5 TMP and 0.5 bar-0.5 TMP, both obtained at TMP of 0.5 bar, but with a different outlet pressure value of 1 and 0.5 bar, respectively. The casein rejection for both cases is reduced from the 1 bar-0.5 TMP 90% to the 80% of the 0.5 bar-0.5 TMP, highlighting that having the same TMP did not lead directly to a similar filtration behaviour for the proteins.

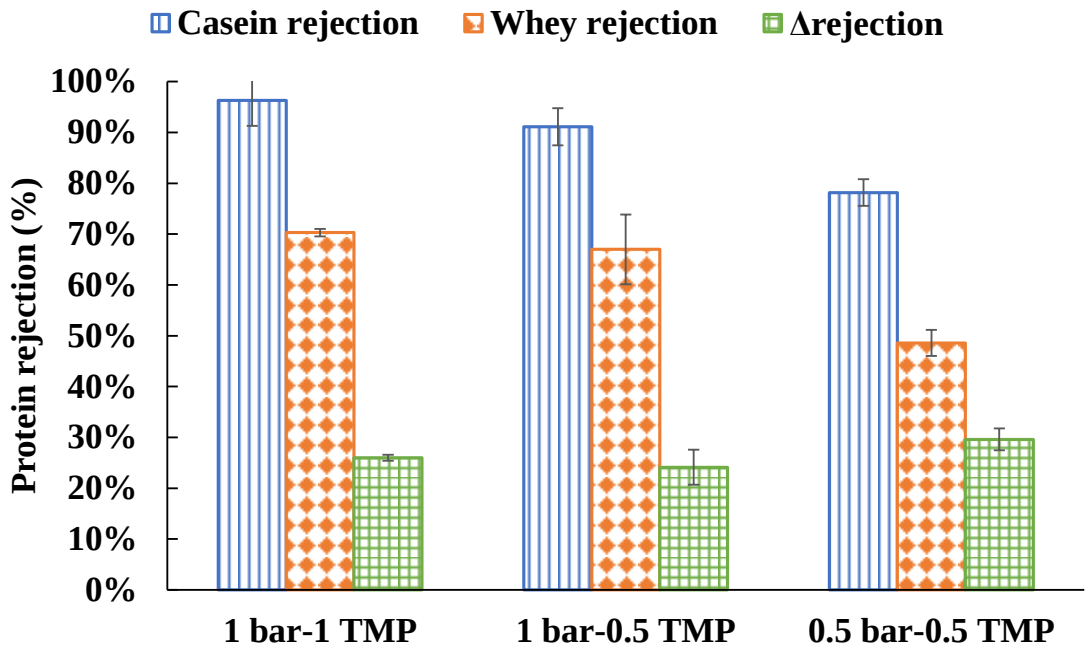

Figure 6-2: Casein (blue-straight lines), whey proteins (orange-diamonds) and differential rejection (casein rejection - whey rejection, green squares) values of the industrial conditions 1 bar-1 TMP, 1 bar-0.5 TMP and 0.5 bar-0.5 TMP as shown in Figure 6-1. Temperature and CFV for all samples were maintained at 10 °C and 1.3 m s^{-1}, respectively. Casein and whey rejection values are obtained compared to final feed composition. Samples have been denoted as shown in Figure 6-1. The error of the measurements was of 5%, 9% and 7% for the 1 bar-1 TMP, 1 bar-0.5 TMP and 0.5 bar-0.5 TMP, respectively.

On the other hand, if the differential rejection is compared among them it would appear that these filtration conditions yield similar permeate compositions since the values for their differential rejections (the difference between casein and whey proteins) are 29%, 26% and 30%, respectively for the 1 bar-1 TMP, 1 bar-0.5 TMP and 0.5 bar-0.5 TMP.

The CN/Wy ratio at the permeate line of the studied conditions, seen in Figure 6-3, shows that the set of conditions of 1 bar of inlet pressure and TMP favoured a high casein rejection that resulted in having a balanced permeate with a ratio of 1.0 ± 0.11. The 1 bar-0.5 TMP

conditions with inlet of 1 bar and 0.5 bar of TMP tended towards a CN/Wy ratio of 1.4 ± 0.25. The 0.5 bar-0.5 TMP pressure conditions with a lower inlet and TMP, both at 0.5 bar, led to a similar differential rejection of proteins (as seen above) but with less overall rejection of casein proteins which in turn lead to having a CN/Wy ratio at the permeate of 1.9 ± 0.15. The permeate line protein ratio also highlights that having the same TMP does not directly lead to having the same protein behaviour, on the other hand, from this initial set of conditions (pressure between 0.5 and 1 bar) it seems that the protein ratio at the permeate line can be determined by the inlet-Outlet pressure even more than the effective TMP applied to the membrane.

The conditions of the 1 bar-0.5 TMP were the ones to yield the permeate ratio of CN/Wy proteins with the highest variance in the results (Figure 6-3), flagging the challenges of using the permeate line backpressure to modify the transmembrane pressure of the system since slight changes on it can modify the early minutes of the filtration cycle. As has been discussed by several authors in the past,[80,145,146] the first minutes of a filtration cycle are key to determine the fouling layer composition and structure, which in turn affects the protein fractionation.

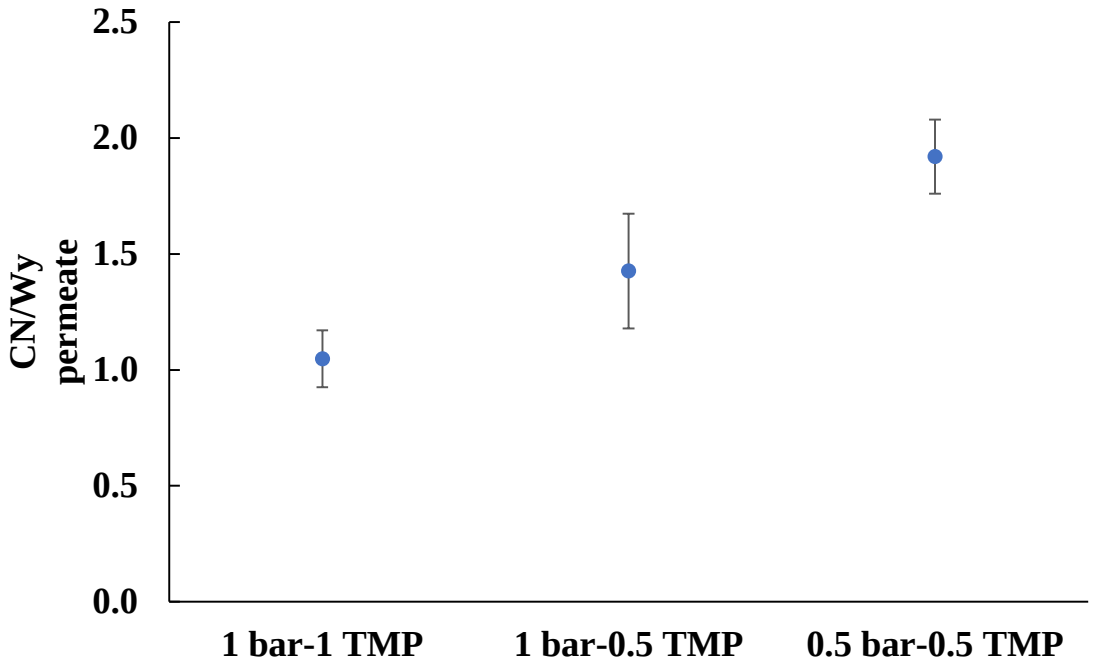

Figure 6-3: Comparison of Casein/whey proteins ratio at the permeate line of the industrial conditions shown in Figure 6-1. Temperature and CFV for all samples were maintained at 10 °C and 1.3 m s^{-1}, respectively. Error bar corresponds to the standard deviation of 3 repeats for each data point.

Another factor to analyse was the effect that changes in the temperature or the transmembrane pressure had on the protein rejections. Figure 6-4 focuses on samples obtained when inlet and

outlet pressure were maintained at 1 bar and the changes observed when either temperature or transmembrane pressure are modified. The protein behaviour when temperature is kept around 10 °C (samples 1 bar-1 TMP-11°C and 1 bar-0.5 TMP-11°C) due to changes in transmembrane pressure have been explained above (Figure 6-2). In summary they did not show any relevant change in protein rejection due to the effect of the modified transmembrane pressure.

The effect of temperature changes from 11 to 44 or 48 °C resulted in surprisingly different protein behaviour, at 44 °C the protein rejections were almost identical to the initial low temperature samples. Unlike at 48 °C where both protein groups slipped through the membrane reducing the rejection values when compared to the analogue low temperature conditions, where rejection values for casein proteins went from the 96% at 11 °C to 46% at 50 °C and from 70% to 41% for whey protein rejection. The increase of temperature, and the reduction in casein micelle diameter,[48] could explain the reduction of overall protein rejections observed with conditions 1 bar-1 TMP-48 °C, and it would partially explain the behaviour of conditions 1 bar-0.5 TMP-44 °C, that displays a lower reduction in protein transmission. As stated above the low temperature conditions did not show any difference in protein behaviour when permeate pressure was applied (see Figure 6-2). On the other hand, the high temperature conditions did show mild differences in protein rejection. This could indicate that the permeate pressure did promote a higher protein rejection overall, despite the high temperature. It could be that the forced permeate pressure induced a higher degree of fouling that induced higher rejection values at the end.

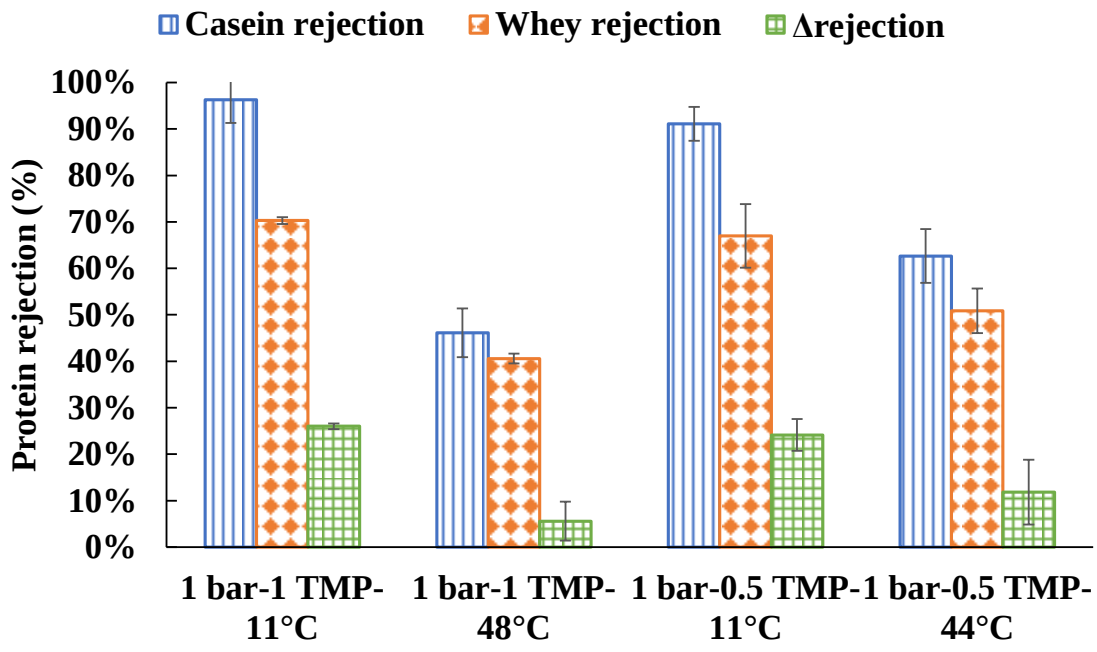

Figure 6-4: Casein (blue-straight lines), whey proteins (orange-diamonds) and differential rejection (casein rejection - whey rejection, green squares) values of the 1 bar-1 TMP-11°C (1 bar-1 TMP), the 1 bar-1 TMP-48°C,

the 1 bar-0.5 TMP-11°C (1 bar-0.5 TMP) and 1 bar-0.5 TMP-44°C. Outlet pressure and CFV for all samples were maintained at 1 bar and 1.3 m s^{-1}, respectively. Casein and whey rejection values are obtained compared to final feed composition. Samples have been denoted as Outlet pressure-TMP-Temperature. The error of the measurements was of 5%, 5%, 9% and 6% for the 1 bar-1 TMP-11°C (1 bar-1 TMP), the 1 bar-1 TMP-48°C, the 1 bar-0.5 TMP-11°C (1 bar-0.5 TMP) and 1 bar-0.5 TMP-44°C, respectively.

The changes in temperature have shown that rejections can vary depending on the effect of permeate line pressure, however, it does not reflect on the CN/Wy ratio in the permeate line. The high temperature (44-48 °C) samples did favour high transmission of casein proteins towards the permeate line which in turn lead to having a high CN/Wy ratio value (4.2-4.8), which basically corresponds to the initial ratio in the permeate (Figure 6-5).

The whey proteins removal does show similar results to the work carried out by Beckman *et al.* (2010)[94] where they achieved whey protein removals of 68% in a single stage PVDF MF.

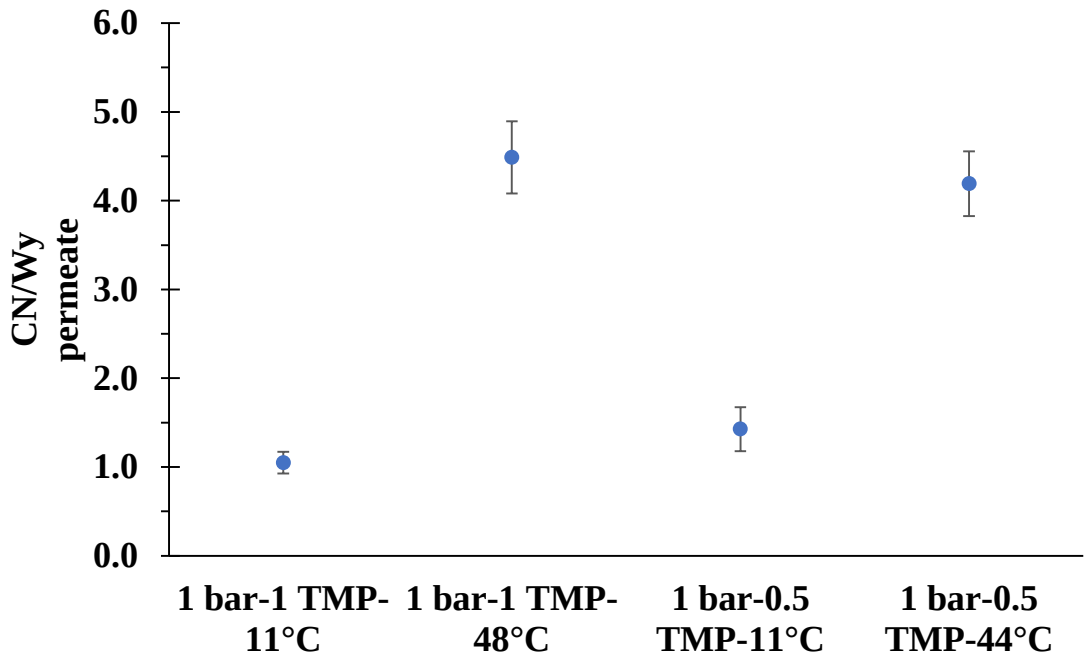

Figure 6-5: Comparison of Casein/whey proteins ratio at the permeate line of 1 bar-1 TMP-11°C (1 bar-1 TMP), the 1 bar-1 TMP-48°C, the 1 bar-0.5 TMP-11°C (1 bar-0.5 TMP) and 1 bar-0.5 TMP-44°C. Outlet pressure and CFV for all samples were maintained at 1 bar and 1.3 m s^{-1}, respectively. Error bar corresponds to the standard deviation of 3 repeats for each data point, with the exception of the 1 bar-1 TMP-48°C and the 1 bar-0.5 TMP-44°C that had 2 repeats each.

These results of casein rejections at high temperature contradict the work carried out by other researchers using higher pore 0.3-0.5 um PVDF membranes like Lawrence *et al.* (2008)[120] that obtained high casein rejections overall along with high whey proteins rejection. They claim that temperature had no effect on casein proteins behaviour, since the fouling layer rapidly blocked the membrane pores creating much tighter filtration conditions, which has been proven that it is not a universal truth of membrane filtration in this section. The main difference between Lawrence work and the present study would be the different pore sizes and the

membrane module. The work on this study only represents a section of an actual membrane module and results may differ from studies carried out on full SW modules since the fouling forming conditions will be different.

The effect of increasing the TMP was studied and the results are shown in Figure 6-6. The increase in TMP shows that the highest rejections observed for both casein and whey proteins were obtained at pressures around 1 bar, at the lower pressure of 0.5 bar the protein rejections were lower in total for both casein and whey proteins. At higher pressures the rejections were reduced below 70% favouring casein rich permeates (see Figure 6-7).

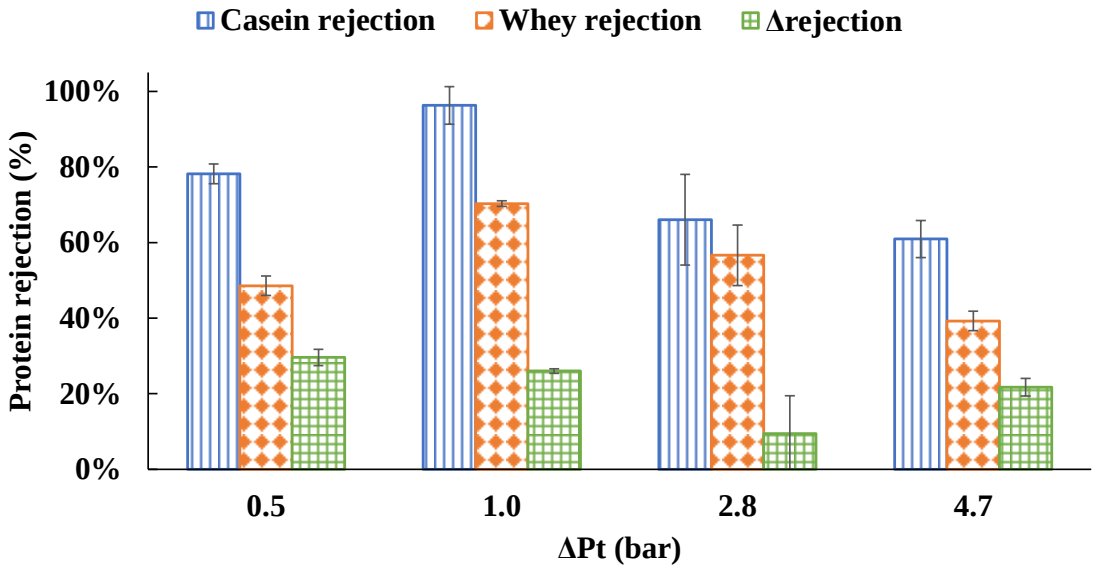

Figure 6-6: Casein (blue-straight lines), whey proteins (orange-diamonds) and differential rejection (casein rejection - whey rejection, green squares) values of samples obtained with increasing TMP: 0.5, 1, 1.4, 2.8 and 4.7 bar. CFV for all samples was at 1.3 m s^{-1} and temperature ranged between 10 and 20 °C. Casein and whey rejection values are obtained compared to final feed composition. Error bars correspond to the standard deviation of 3 repeats for each data point.

The main explanation for this behaviour would be the compaction of the casein micelles, reducing the average initial diameter from 100 nm to nanoclusters between 10-40 nm, small enough to transmit through the membrane.[45,147]. The work of Bouchoux *et al.* (2010)[45], studied casein micelle deformation and found that the compression of casein micelles at the surface of a membrane would induce a high osmotic pressure that would empty the micelles of water, inducing their collapse and reducing their size to the nanocluster structures (10-40 nm).

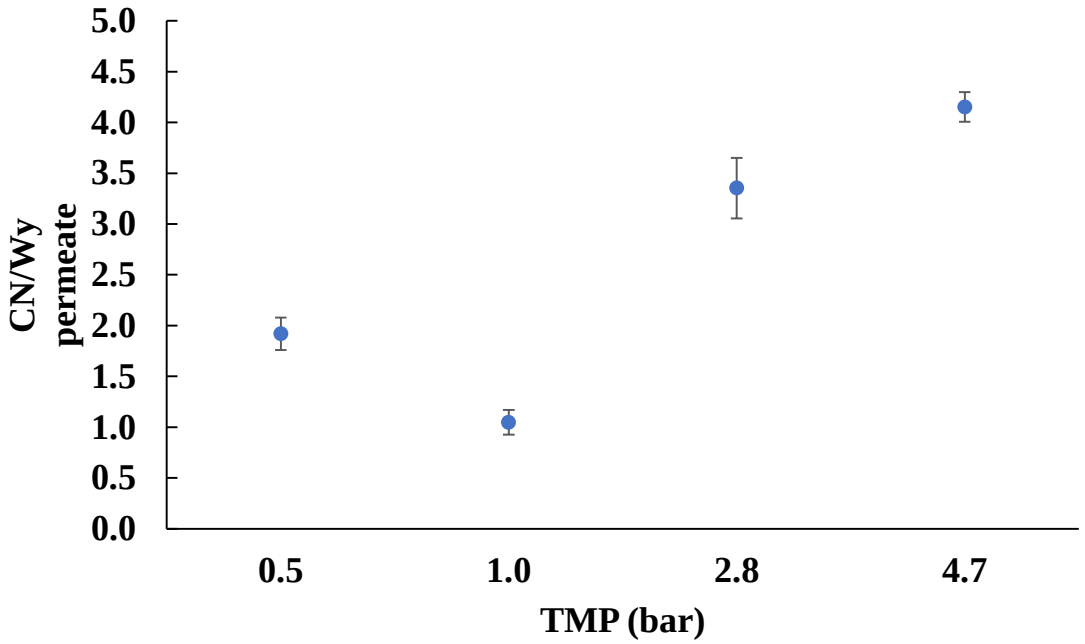

Figure 6-7: Comparison of Casein/whey proteins ratio at the permeate line of samples obtained with increasing TMP: 0.5, 1, 1.4, 2.8 and 4.7 bar. Outlet pressure and CFV for all samples were maintained at 1 bar and 1.3 m s^{-1}, respectively and temperature ranged between 10 and 20 °C. Error bars correspond to the standard deviation of 3 repeats for each data point.

The analysis of all the conditions studied and shown above lead Figure 6-8 where it can be clearly seen that to achieve a whey favoured or rich permeate line (CN/Wy ratio close to 1 or below 1) the temperature had to be close to 10 °C. At any other temperature studied the final protein composition was always casein rich with protein ratio (CN/Wy) ranging from around 2 to 4.5, close to the initial milk (around 5).

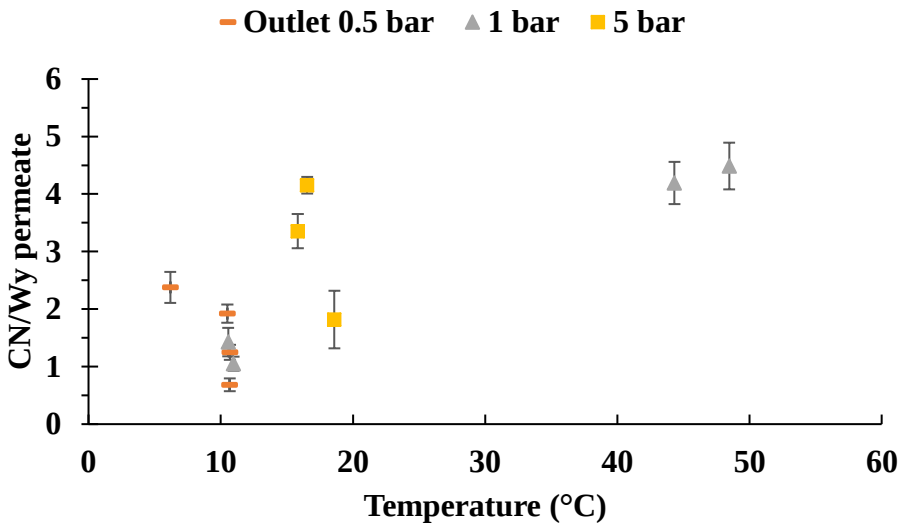

Figure 6-8: Comparison of Casein/whey proteins ratio at the permeate line of all samples analysed based on temperature changes. Outlet pressure of 0.5 bar (orange dash), 1 bar (grey triangles) and 5 bar (yellow squares). Error bars correspond to the standard deviation of 3 repeats for each data point.

6.1.2 Permeate flux

The filtration process can be defined by the selectivity of the membranes and the operational conditions that modify the selectivity itself, which in turn will affect the permeate flux. The permeate flux is a critical aspect of membrane filtration since it can be where the target proteins can be found and therefore the amount of the flow determines the cost in resources (energy, water and cleaning agents) and amount of the desired product to obtain. The permeate flux can also be an indication of the fouling process happening.

The analysis of the permeate flux (Figure 6-9) of the initial conditions revealed that the 1 bar-0.5 TMP condition show the highest dispersion of results when compared to the initial and 0.5 bar-0.5 TMP conditions. In this case the main assumption that could explain this behaviour is that the first minutes of operation are critical to determine the fouling layer and therefore the whole process, the slight adjustments in the early minutes of operation lead to high error, compared to the other conditions. Once adjusted, after the first 5 minutes the flux did settle into slightly lower values (around 13 L m^{-2} h^{-1} ± 2.6) compared to the 1 bar-1 TMP and 0.5 bar-0.5 TMP conditions that settled around 20 L m^{-2} h^{-1} ± 1. Despite of the permeate flux similarities the 1 bar-1 TMP and 0.5 bar-0.5 TMP conditions had quite different protein composition at the end, as has been shown before in Figure 6-2.

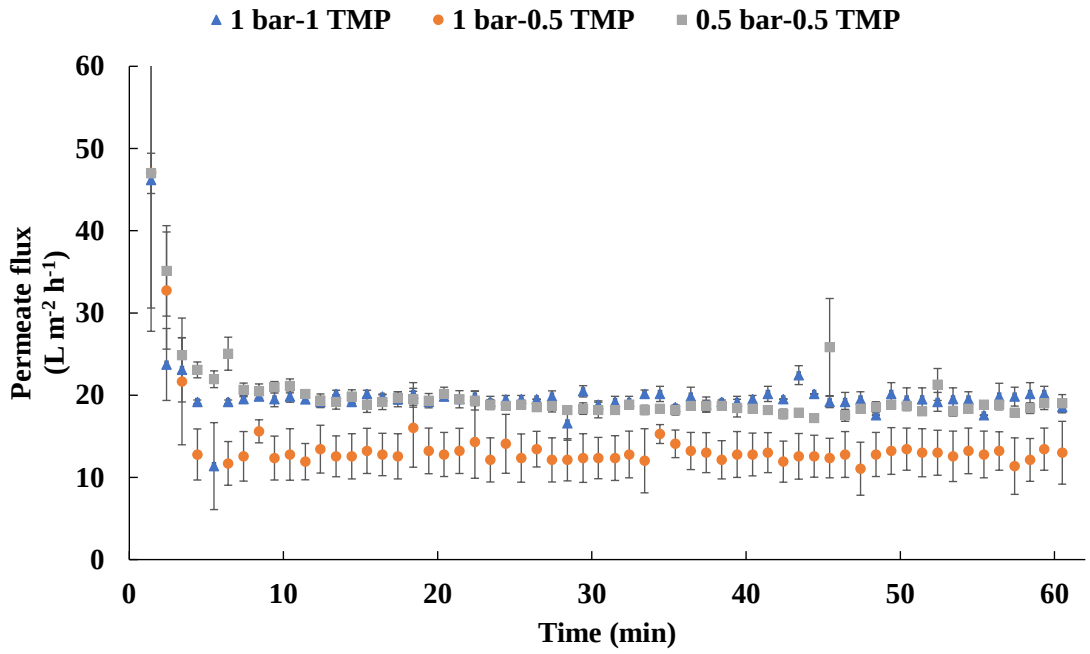

Figure 6-9: Flux decline curves of the 1 bar-1 TMP (Inlet and TMP at 1 bar), 1 bar-0.5 TMP (Inlet at 1 bar and TMP at 0.5 bar) and 0.5 bar-0.5 TMP (Inlet and TMP at 0.5 bar) conditions, processed at 10 °C and CFV of 1.3 m s^{-1}. 1 bar-1 TMP (blue triangles), 1 bar-0.5 TMP (orange dots) and 0.5 bar-0.5 TMP (grey squares). Error bars correspond to the standard deviation of 3 repeats for each data point.

On the other hand, the 1 bar-1 TMP and 0.5 bar-0.5 TMP conditions had a quite identical permeate flux behaviour from the initial decline (first 5 minutes) to the rest of the filtration, stabilising around 20 L m^{-2} h^{-1} ± 1 for the rest of the filtration run. The surprising fact was the stabilisation of both 1 bar-1 TMP and 0.5 bar-0.5 TMP at the same value since both of them had different pressure conditions (TMP of 1 and 0.5 bar, respectively). It could be that both conditions are already above the pressure dependent region where pressure and flux are connected and when one increases the other does as well.

In this data set, it can be seen that using the 0.1 µm PVDF membrane (Synder Filtration) in flat sheet mode, at the conditions of 1 bar-1 TMP (1 bar of Inlet and TMP) and 0.5 bar-0.5 TMP (0.5 bar of Inlet and TMP) there is no permeate flux increase to accommodate for the pressure increase. These results are in contradiction with the work carried out by Hartinger *et al.* (2019)[146] where they found that increasing the pressure from 0.5 bar to 1 bar lead to a doubling of the permeate flux. However, the work of Hartinger *et al.* (2019)[146] was carried out using spiral-wound membranes (a different membrane configuration) compared to the present flat sheet membrane configuration. This is an indication that membrane configuration strongly affects permeate flux results and therefore this will be needed to take into account when comparing protein rejections and membrane selectivity.

Figure 6-10 shows the effect of high temperature and the comparison of the modification of TMP at the high temperature (for a clear picture of TMP changes at low temperature see Figure 6-9). Both sets of conditions at low temperature display minor changes in permeate flux compared to the effect of increasing the temperature, that initially shows a massive increase in permeate flux (both starting above 100 L m^{-2} h^{-1}) that displayed a high reduction in flux ending at 39 and 58 L m^{-2} h^{-1} for the 1 bar-0.5 TMP-44°C and 1 bar-1 TMP-48°C, respectively. The overall flux reduction was of 70% and 40% for the 1 bar-0.5 TMP-44°C and 1 bar-1 TMP-48°C processing conditions, respectively. The behaviour of the 1 bar-0.5 TMP-44°C data shows a high degree of variance for the first 20 minutes that could explain the apparent higher flux (unlike the 11 °C conditions where the lower TMP had a lower flux overall) that due to a constant reduction of flux ended up at a much lower final flux.

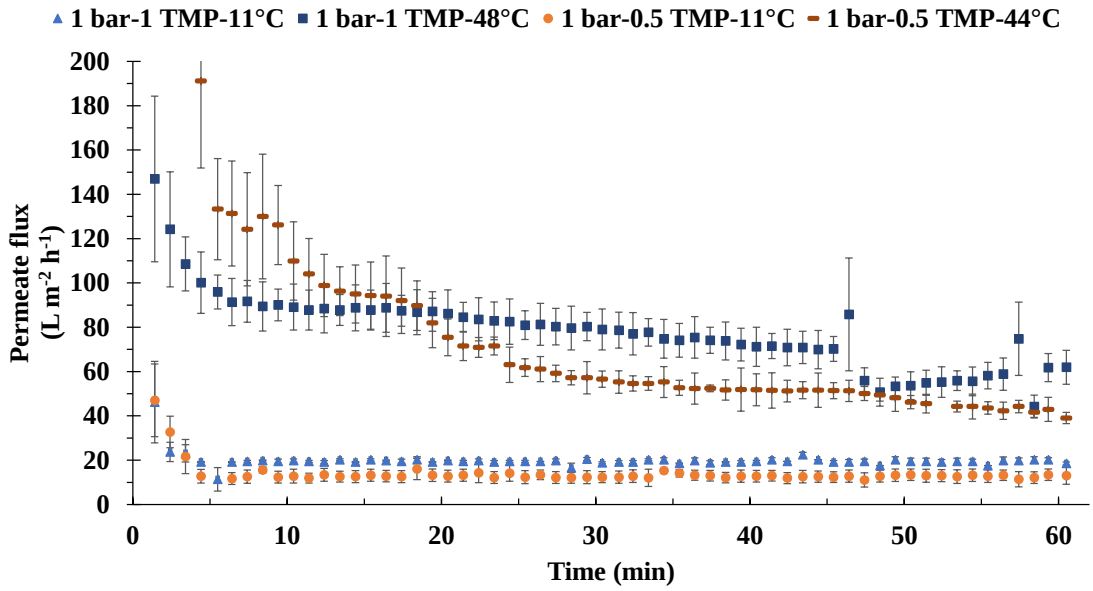

Figure 6-10: Flux decline curves of the temperature modified Initial and 1 bar-0.5 TMP conditions: 1 bar-1 TMP-11°C (1 bar-1 TMP, blue triangle), the 1 bar-1 TMP-48°C (dark blue square), the 1 bar-0.5 TMP-11°C (1 bar-0.5 TMP, orange dot) and 1 bar-0.5 TMP-44°C (brown dash). Outlet pressure and CFV for all samples were maintained at 1 bar and 1.3 m s^{-1}, respectively. Samples have been denoted as Outlet pressure-TMP-Temperature. Error bars correspond to the standard deviation of 3 repeats for each data point, with the exception of the 1 bar-1 TMP-48°C and the 1 bar-0.5 TMP-44°C that had 2 repeats each.

The high degree of flux reduction could be attributed to fouling components reducing the overall flux. The 1 bar-1 TMP-48°C filtration run yielded a permeate protein composition identical to the initial feed, with casein and whey proteins in an almost identical distribution, similar to the 1 bar-0.5 TMP-44°C protein distribution that had less casein but it was still casein dominated. The protein composition for the 1 bar-0.5 TMP-44°C and the high flux reduction could be linked to a more severe level of fouling, and to be precise, to a fouling phenomenon combination that favours blocking of the membrane while adding an extra layer of filtration that removes some of the casein proteins.

Figure 6-11 shows the permeate flux of samples processed at increasing TMP, it does show that the higher TMP values do also translate to higher permeate fluxes which in turn also coincides with lower protein rejections (see Figure 6-6), for example casein rejection at 1 and 4.7 bar were of 96% and 61%, respectively. The higher fluxes at high TMP would also be compatible with the casein deformation theory of Bouchoux *et al.* (2010)[45,147], since they assumed that high concentration favoured casein micelles deformation. The high pressure then favour accumulation of casein micelles that in tandem with the pressure would favour a higher permeate flux, overriding the concentration polarisation flux loses.

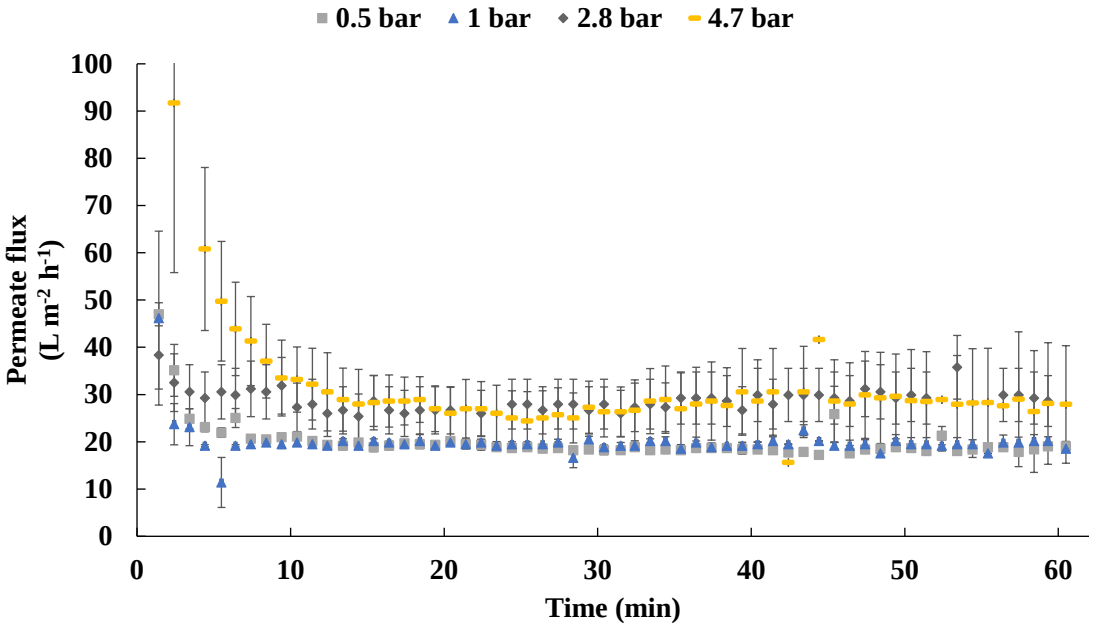

Figure 6-11: Flux decline curves of the samples obtained with increasing TMP: 0.5 (grey squares), 1 (blue triangles), 2.8 (dark-grey diamond) and 4.7 bar (yellow dash). CFV for all samples was at 1.3 m s^{-1} and temperature ranged between 10 and 20 °C. Casein and whey rejection values are obtained compared to final feed composition. Error bars correspond to the standard deviation of 3 repeats for each data point.

6.1.3 Summary of permeate flux and protein ratio

The comparison of CN/Wy ratio at the permeate line with the final permeate flow (as shown in Figure 6-12 shows an increase in final permeate flow is directly correlated to an increase in the presence of casein proteins in the permeate.

One of the factors to keep in mind to explain the protein behaviour at high temperature is that they imply modifications of the proteins, with an important focus on the casein properties like shape and configuration (as it was demonstrated during the HPLC method development at chapter 5 and by the work of Guillarme *et al.*[137] and the work of Beliciu and Moraru[48]). The changes in protein and micelle shape led to having a different effective particle size and therefore reducing the proteins interactions with the membrane easing the transmission towards the permeate line. This was the assumption based on past experiences in which high temperatures had led to having lower protein rejection and high casein content in the permeate.

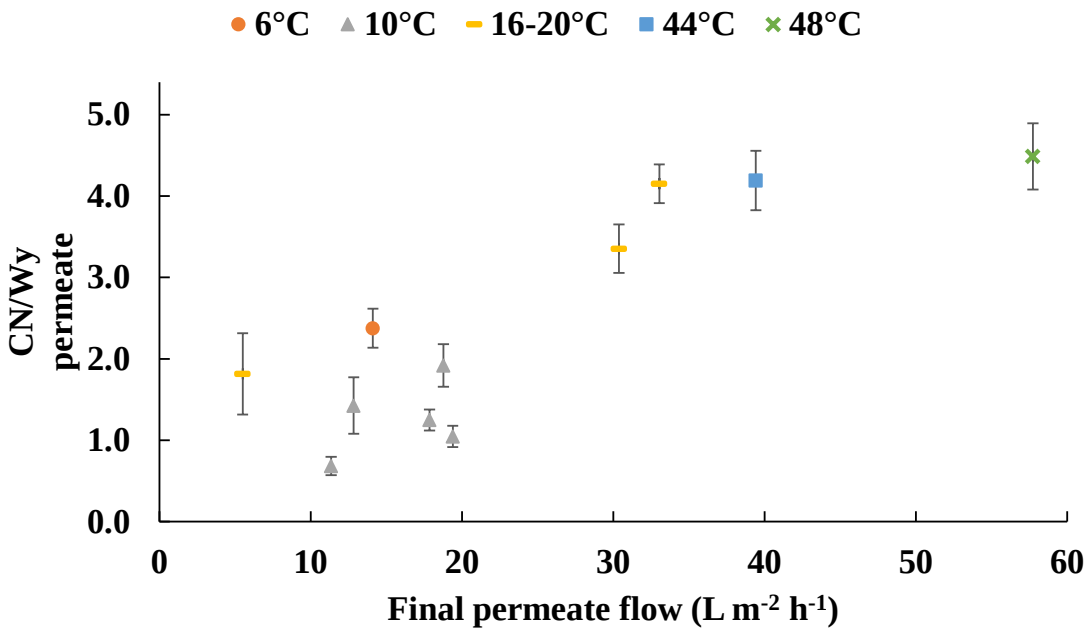

Figure 6-12: Comparison of final permeate flux to the CN/Wy ratio, based on processing temperature: at 6 °C (orange dots), 10 °C (grey triangles), 16-20 °C (yellow dash), 44 °C (blue square) and 48 °C (green cross). Error bars correspond to the standard deviation of 3 repeats for each data point, with the exception of the 44 and 48 °C conditions that have 2 repeats each.

Figure 6-12 also highlights samples processed at the same temperature displayed significatively different permeate fluxes and slight changes in permeate protein ratio (ranging from around 1 to 2). The main assumption is that the higher flux, obtained at the same temperature, is due to less fouling or concentration polarisation effect, which in turn should lead to different final rejections. However, several results at the range of 20 L m^{-2} h^{-1} show that same flux can lead to highly differentiated protein ratio at the permeate overall. The advantage of having a decoupling of flux and permeate protein ratio (and application for the permeate product) is that "ideal" protein ratios can be obtained at high fluxes of operation which in turn would reduce the amount of time that equipment runs, and probably reduced the amount of cleaning required. The downside is that the highest flux at a low protein ratio was due to a combination of temperature and permeate line pressure, both of which would require energy to create and maintain, and at the end it would come down to a balance between the extra flow gained and the extra energy required.

The correlations of protein behaviour and final permeate flow can clearly be seen when comparing the flow to casein rejection. Figure 6-13 shows the final casein rejections compared to the final flux of the filtration cycles divided by temperature of operation. As explained above a wide range of permeate flow, from 5 to 20 L m^{-2} h^{-1}, can lead to having high casein rejection values above 90%, however, above 30 L m^{-2} h^{-1} the casein rejection drops below 70% by the combined effect of high pressures and temperatures.

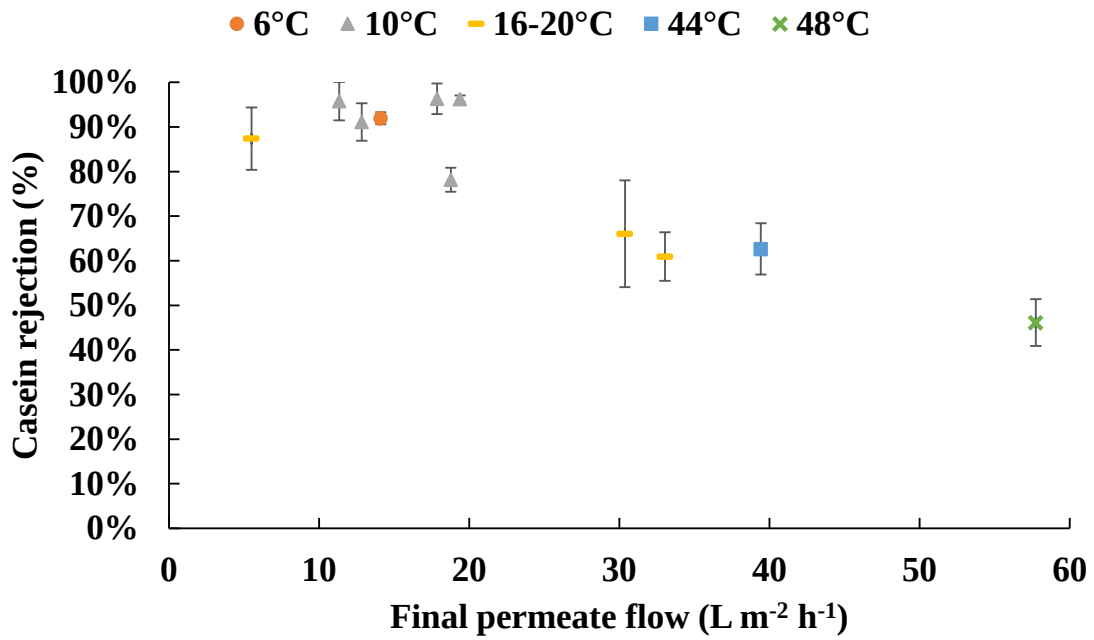

Figure 6-13: Casein rejection in the permeate line compared to final permeate flux. Labels based on processing temperature: 6 °C (orange dots), 10 °C (grey triangles), 16-20 °C (yellow dash), 44 °C (blue square) and 48 °C (green cross). Error bars correspond to the standard deviation of 3 repeats for each data point, with the exception of the 44 and 48 °C conditions that have 2 repeats each.

The wide disparity in permeate flux could indicate that there is a lack of relation between casein rejection and flux, although the caveat is that at low fluxes there is little to no dispersion of rejections and at higher permeate flux the casein rejection values tend to be more dispersed, for example, around 20 L m^{-2} h^{-1} the casein rejections range from 70-96%. The dispersion of results indicates that a high casein rejection can be obtained while keeping permeate flux high, which would be the most desirable for industrial applications.

6.2 Membrane fouling composition

The proteins found on the fouled membranes were analysed using the HPLC method for milk analysis explained in the methodology section (section 4.7). The method uses a regent mixture designed to suspend each main protein group individually, and it was tested for stability and protein extraction. The summary is that the method can detect all the protein groups found on a membrane and make a partial quantification.

The analysis of membrane samples was carried out for fouled and fouled and rinsed samples, in order to compare if there were any particular protein group that attached to different types of fouling (reversible or irreversible) and to determine the changes in protein presence.

The comparison of fouled and rinsed samples showed that all the studied fouled samples had a higher amount of proteins than the rinsed counterparts (Figure 6-14), clearly indicating that the rising step removed protein fouling (as observed in the resistances analysis, section 6.3).

It can also be observed that the high-pressure conditions (inlet and outlet in this case) favoured having higher protein content.

Figure 6-14 shows the effect that rinsing the membrane with RO water has on the protein presence on it. All fouled samples under the studied conditions showed a higher presence of proteins that the rinsed counterparts with reductions between 50-80%, showcasing the effect of the rising step in removing protein fouling, as was expected.

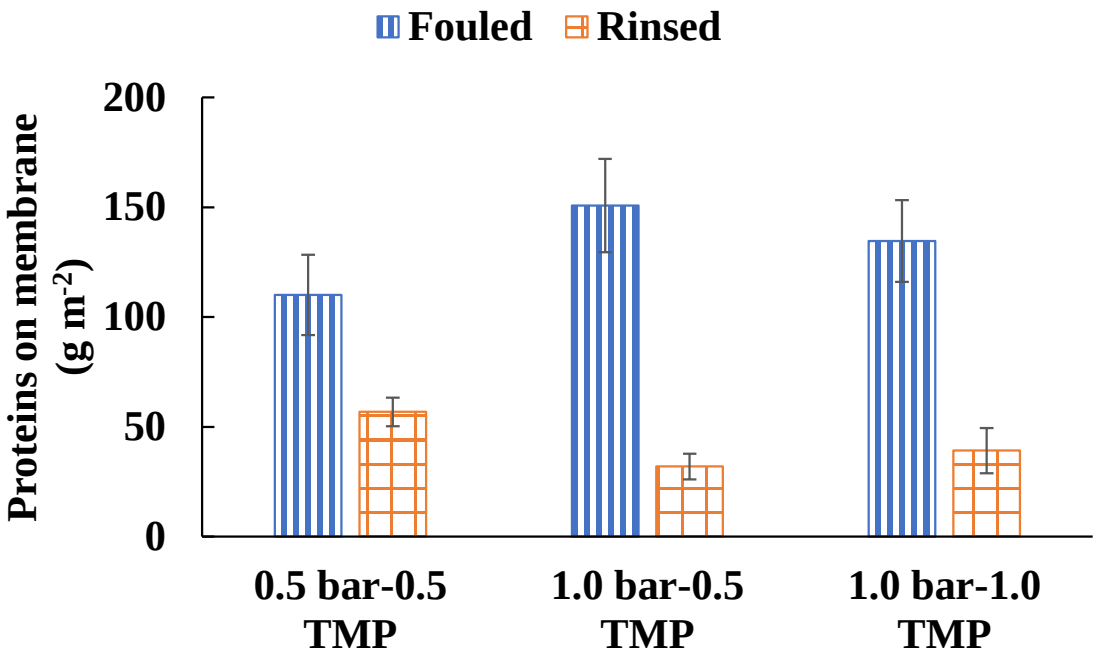

Figure 6-14: Protein concentration on measured membranes, comparing fouled and rinsed membranes under the same conditions. Error bars correspond to the standard deviation of 2 repeats for each data point. Sample names are as follow: Outlet Pressure-TMP.

The Figure 6-14 also shows that the current method of analysis, at least partially, measures the rinseable fouling (fouling layer removed by the rinse step) along with the irreversible fouling. However, from the figure it cannot be precisely determined if the irreversible fouling is just in-pore, cake fouling or both. Figure 6-15 shows the chromatogram of fouled and fouled and rinsed samples, which highlights the effectiveness of the rinse step in order to remove fouling components.

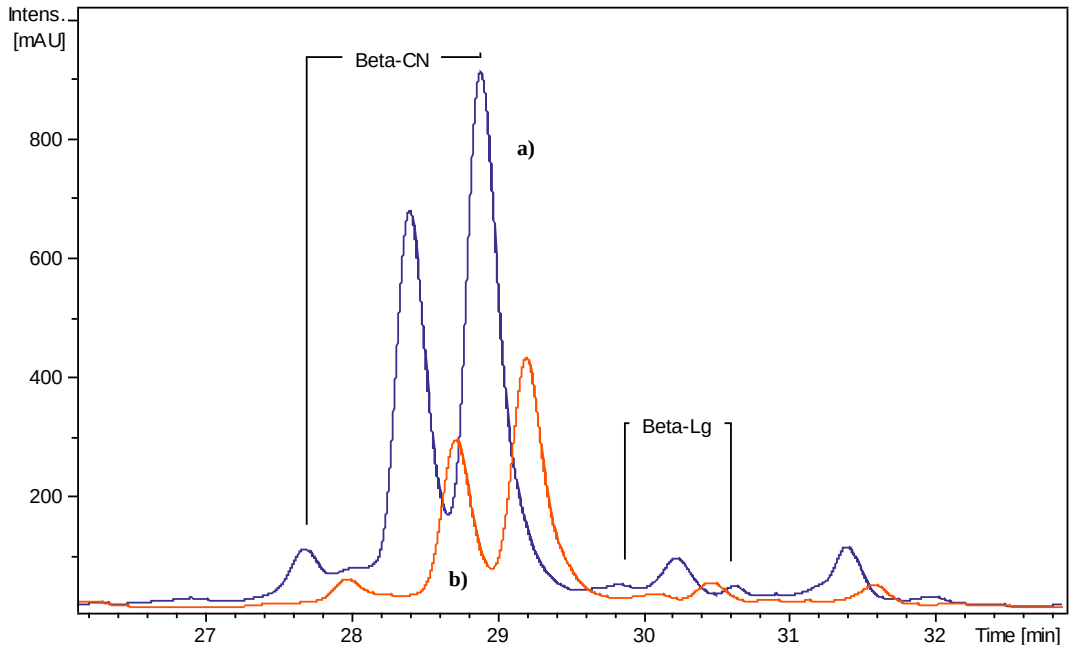

Figure 6-15: Chromatogram comparing fouled (a) and rinsed (b) samples obtained at 0.5 bar outlet pressure and 0.5 bar of TMP. The chromatogram is a representative example of all conditions shown in Figure 6-14. RP-HPLC system with UV-Vis detection at 214 nm, centred into the beta casein and whey peaks.

The analysis of membrane samples was carried out for fouled and fouled and rinsed samples, to compare if there was any particular protein group that attached to different types of fouling. The results indicate that fouled and rinsed samples obtained during the exact same processing conditions have an almost identical distribution of proteins groups on them (see Figure 6-16) that consists of mainly casein proteins (>90% in all cases). The casein dominated fouling layer has been observed in the past using other processing conditions as well.[122,126,145]

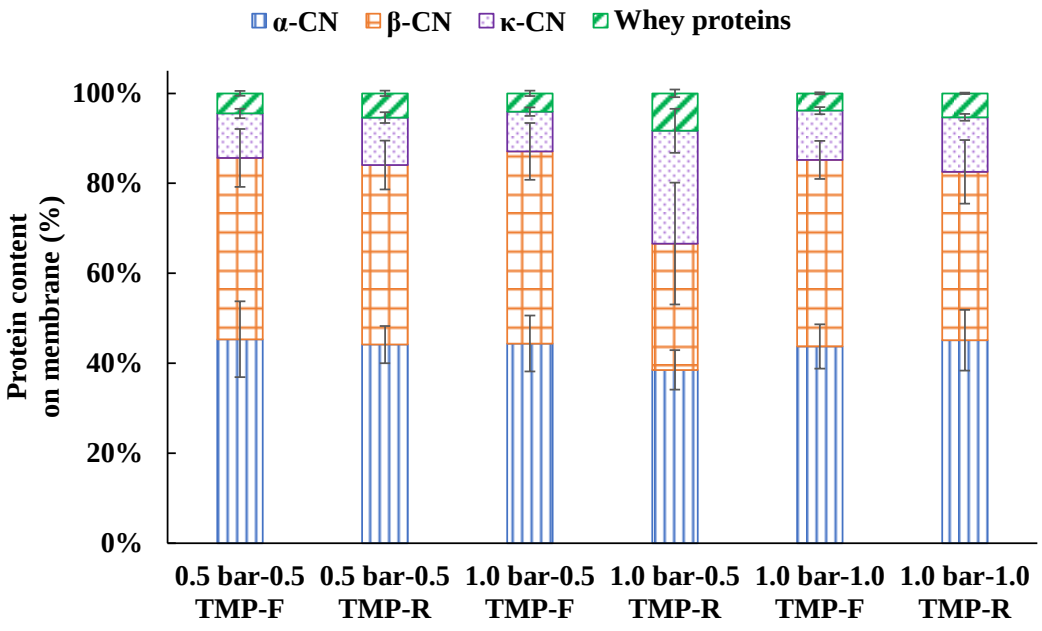

Figure 6-16: Protein distribution of fouled and rinsed samples obtained under the same conditions (Figure 6-14). Error bars correspond to the standard deviation of 2 repeats for each data point. Sample names are as follow: Outlet Pressure-TMP.

The almost identical protein distributions for fouled and rinsed conditions indicates that the reversible and irreversible fouling components of the studied conditions have the same protein composition.

The analysis of the fouled and rinsed samples of the same conditions was used to compare the effect of the rinsing step, to analyse if there were changes in composition before and after and to determine which source of proteins was being detected, since the main limitation of the above-mentioned HPLC method (chapter 5 section 4.7) was the lack of precision on detecting different types of fouling sources (in-pore, cake layer, other).

Membrane fouling vs Milk composition

The analysis of the membrane layer fouling showed that the protein composition of the fouled membranes is stable (Figure 6-16), mainly composed of casein proteins with a tiny proportion of whey proteins (<6%) when the fouling layer is produced at low TMP and temperature. Milk composition on the other hand has a much higher content of whey proteins, representing around 20% of milk composition that amounts to a CN/Wy ratio of 5.

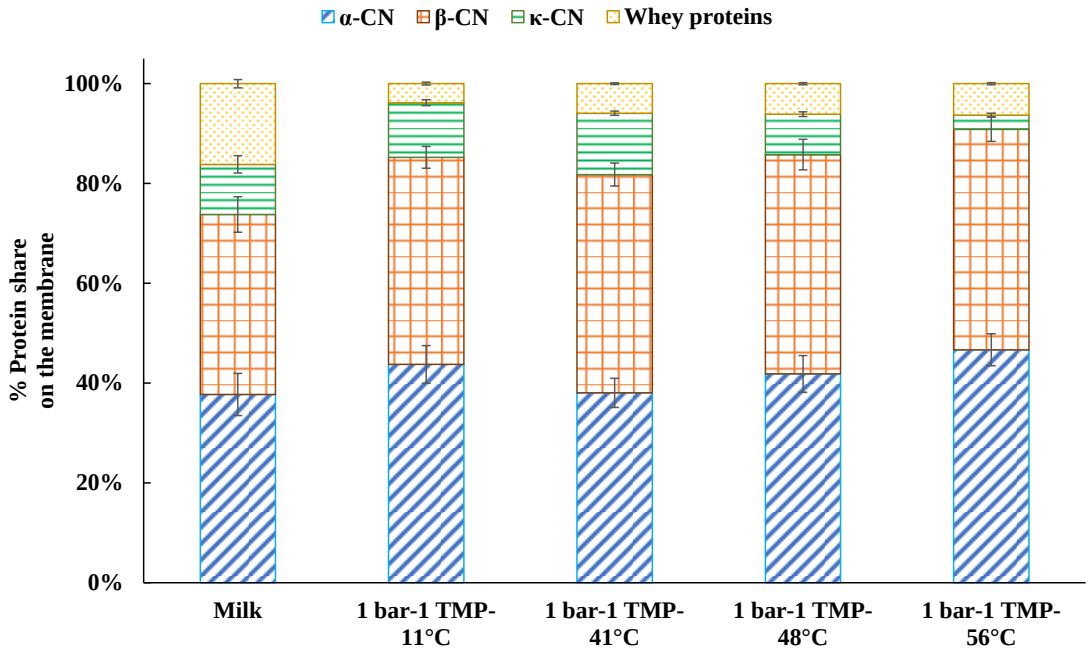

Figure 6-17: Protein distribution of milk compared to fouled samples obtained at increasing temperature. Error bars correspond to the standard deviation of 2 repeats for each data point. Sample names are as follow: Outlet Pressure-TMP-Temperature.

Figure 6-17 demonstrates that an increase in processing temperature does no modify substantially the protein composition of the fouling layer, whey proteins still represent less

than 6% of all proteins in the fouling layer. Even though, the amount of foulants trapped on the fouling layer does increase with temperature the composition does not change.

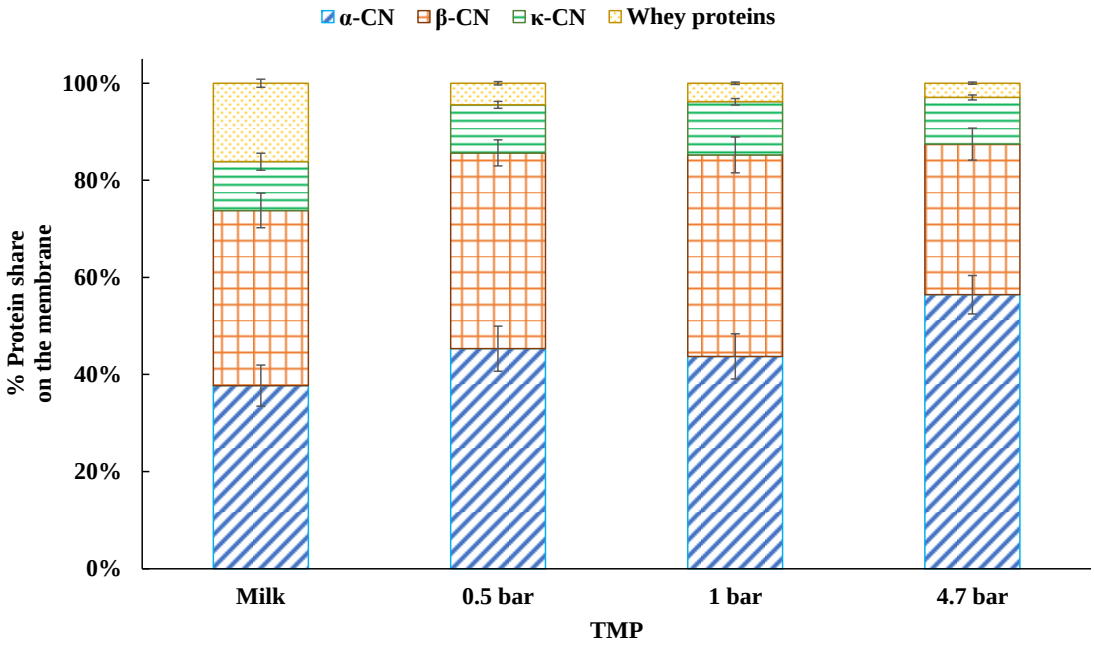

Figure 6-18: Protein distribution of milk compared to fouled samples obtained at increasing TMP. Error bars correspond to the standard deviation of 2 repeats for each data point.

Figure 6-18 follows a similar pattern to the temperature results, the protein distribution is maintained with whey proteins representing less than 6% of all fouling proteins at any of the TMP studied, unlike the milk used for the experiments which had around 20% of whey proteins.

The fouled membranes analysed showed casein to whey protein ratios at least triple the initial milk protein ratio (Figure 6-19), signalling an increase in the casein fraction.

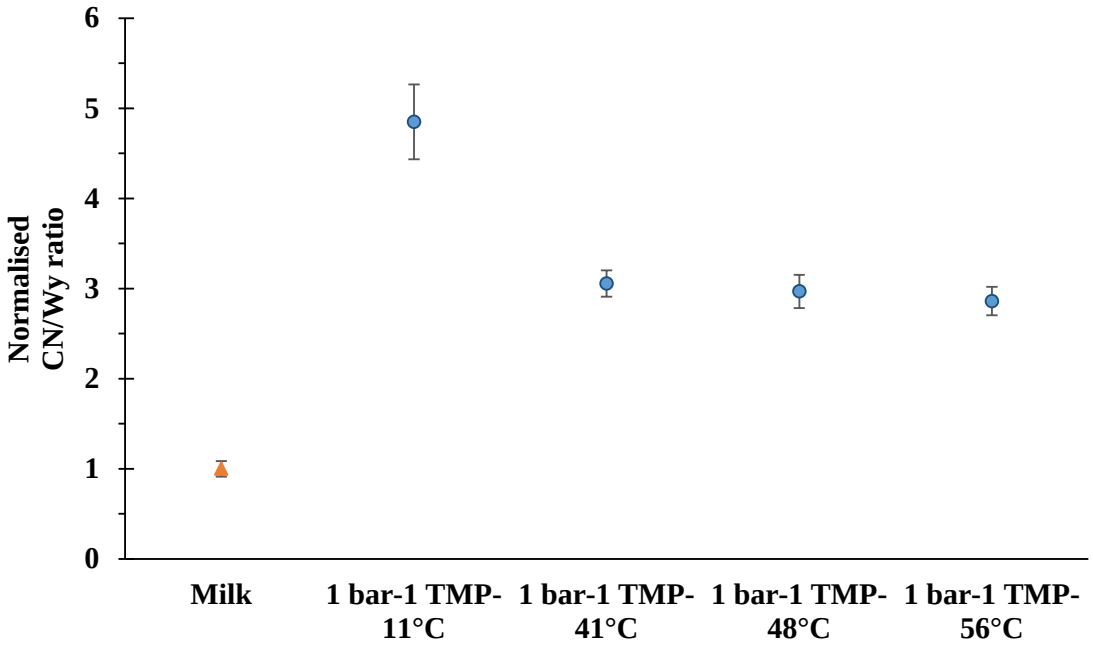

Figure 6-19: Comparison of Normalised Casein/whey proteins ratio of milk and fouled samples shown in Figure 6-17. Error bar corresponds to the standard deviation of 2 repeats for each data point. Sample names are as follow: Outlet Pressure-TMP-Temperature.

The results shown in this section highlight the stark difference in composition between the milk used in the filtration and the fouling layers generated at any temperature or TMP. The composition changes for all the studied conditions show that the kappa-CN proteins share is maintained (around 10%) both for the milk and fouling layer, unlike the alpha and beta casein than slightly increase up to 45% and 41%, respectively. Due to the role that is attributed to kappa-casein as the micelle stabiliser preventing aggregation of micelles,[33,34] the change in ratio between the casein proteins could indicate that some of the foulants come from the soluble fraction of milk. Since removing kappa-casein from the micelles would force the aggregation of the micelles and that should maintain the protein ratios among the three casein groups stable.

Fouling thickness measurements

The fouling layer data was then used to estimate the fouling layer thickness by assuming that the fouling was mainly on the membrane and that the density estimated by Mahdi *et al.* (2009)[148] and Pan *et al.* (2019)[149] of 1030 kg m^{-3} was representative of my sample.

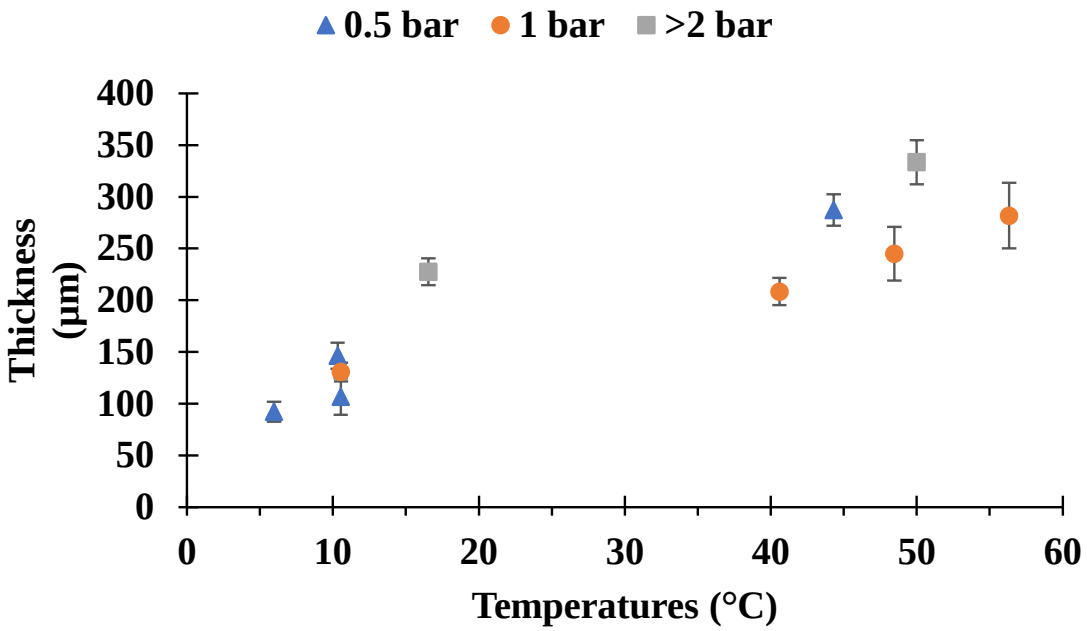

Figure 6-20: Estimated fouling layer thickness based on protein amount on membranes. Blue triangles (TMP of 1 bar), orange dots (TMP 1 bar) and grey squares (TMP >1 bar). Error bars correspond to the standard deviation of 2 repeats for each data point.

Figure 6-20 shows the estimated membrane thickness based on processing temperature. It can be seen that higher temperatures favour higher thicknesses. The observed results approximate well with the measured fouling layer thicknesses of Schopf *et al.* (2020)[126], which reported thicknesses at similar pressure ranges of 150 µm for 15 °C and 200 µm at 45 °C.

6.2.1 Temperature effect on membrane fouling

Figure 6-14 showed that the total protein content can be affected by the operational factors (TMP, inlet/outlet pressure, temperature). Figure 6-21 focuses on the comparison of samples produced at different temperatures and same TMP and outlet pressure, both at 1 bar. The results show that increasing the temperature leads to an increase of total proteins on the membrane. A similar trend of increased protein content at the membrane fouling with temperature was observed by Schopf *et al.* (2020).[126]

The mechanism that explains the high protein concentration at high temperatures could be related to protein conformation shifts at high temperatures. A modification on the protein structure and interactions points could trigger a higher degree of aggregation or cross-linking, for example, the β-Lg favours the monomer form at high temperatures which facilitates the aggregation of proteins and favours higher fouling content,[125] as well as, some confirmation changes that increase the hydrophobicity (and affinity for certain membranes) of the proteins known as Tanford Transition.[150]

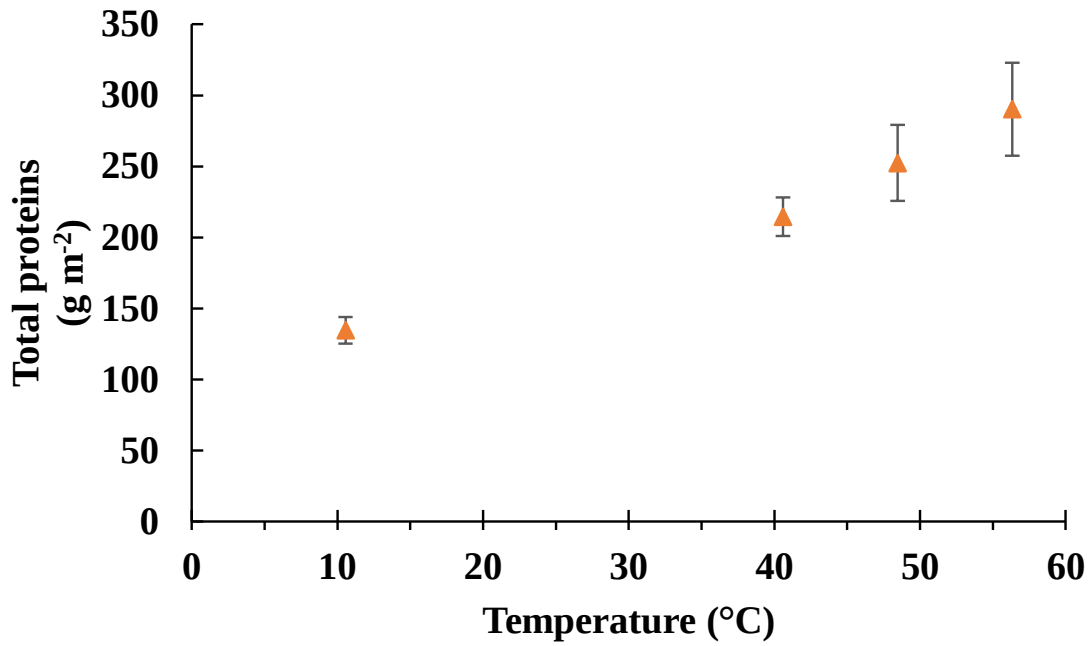

Figure 6-21: Protein concentration on samples produced at increasing temperature while maintaining TMP and inlet/outlet pressures constant at 1 bar. Error bars correspond to the standard deviation of 2 repeats for each data point.

However, the analysis can be deepened if the amount of milk that was processed and passed through the membrane is taken into account to normalise the results. Figure 6-22 shows the fouling content on the membrane normalise for the milk that went through the membrane, and therefore the amount of milk that could have induced extra fouling. Comparing both figures at the highest temperature the results shift, since the higher fouling was partially due to the higher amount of foulants that interacted with the membrane rather just an effect of protein confirmation.

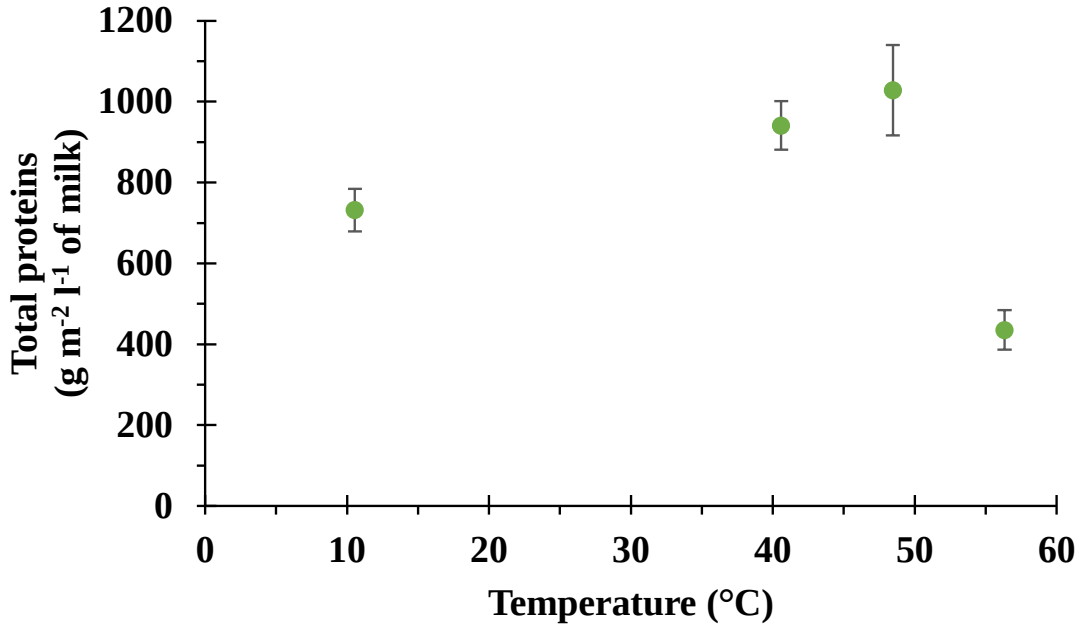

Figure 6-22: Protein concentration on samples produced normalised by the amount of milk processed through the membrane, obtained at increasing temperature while maintaining TMP and inlet/outlet pressures constant at 1 bar. Error bars correspond to the standard deviation of 2 repeats for each data point. Sample names are as follow: Temperature.

Considering the effect of milk processed the gap reduced the protein ratio comparing the 11 °C to the rest (Table 6-1). The 56 °C high protein concentration on the membrane gets reduced to the lowest value after correcting by the amount of milk filtered. This effect can be explained by the high flux observed at 56 °C that would have facilitated an enhanced fouling by the mechanisms explained above combining the protein shift configurations and aggregation to the higher amount of interactions between membrane and proteins. It is noteworthy that the sample at 41 and 48 °C maintain the higher content of foulants once corrected since it does provide validity to the observation that higher fouling can be associated to higher temperatures.

Table 6-1: Ratio of fouling components on the membrane, comparing all temperatures to 11 °C. Corresponding to Figure 6-21 and Figure 6-22 the total proteins and corrected total proteins, respectively.

Temperature [°C]	Total proteins	Corrected total proteins
11	1 ± 0.1	1 ± 0.1
41	1.6 ± 0.1	1.3 ± 0.1
48	1.9 ± 0.2	1.4 ± 0.2
56	2.2 ± 0.3	0.6 ± 0.1

6.2.2 Summary of membrane fouling composition

The fouling layer studies showed the composition of the fouling layer by protein groups, the comparison between fouling layer and the filtered milk and the fouling amount changes due to temperature.

The fouling layer protein groups composition was casein dominated for all conditions studied, which was expected since the milk proteins are mainly casein (80%). However, what it was not expected was the share of casein proteins that rose from the 80% of the milk to the 94% of the fouling layer, which meant that whey proteins share was reduced from the milk 20% to the fouling layer 6%. The higher content of casein proteins was constant all over the range of temperatures from 10-50 °C and TMP from 0.5 to 4.7 bar.

The higher share of casein proteins in the fouling indicates that they are the protein group to analyse to better understand the behaviour of fouling. A key aspect for milk processing with membranes would be the selection of anti-casein fouling membranes that seek to reduce the interactions with the casein groups, reducing the overall fouling of the membrane, that in turn, would reduce cleaning requirements and increase permeate flux.

The temperature analysis also revealed that the total amount of fouling layer does increase with the processing temperature within the studied range 10-56 °C. The increase in fouling on the membrane went up from 135 to 290 g m^{-2} (Figure 6-21) for the 10 and 56 °C, respectively. The normalisation of the protein fouling by the total milk filtered revealed that the increasing tendency was maintained within the range 10-48 °C, with values of 730 and 1030 g m^{-2} L^{-1}. The normalisation of the total fouling on the membrane was important to deepen the understanding of the different factors that influence the fouling layer formation. However, the main finding for (industrial) membrane applications is that higher temperatures will induce a higher degree of accumulated fouling on the membrane which will require more frequent cleaning to prevent membrane blocking and more importantly for health-and-safety.

6.3 Rinsing study

The analysis of the fouling layers was carried out to determine the conditions that lead to reversible and irreversible fouling and the importance of each in milk membrane fouling.

For this study reversible fouling has been defined as the fouling components that can be removed after a rinsing step using RO water, and irreversible fouling has been defined as the remaining fouling after the rising step. However, by this definition a standardised and repeatable method for rinsing is required to define both types of fouling. In this section, the process used to define a rinsing method is shown.

6.3.1 Rinsing time vs CFV

The first step was to determine the effect of both time of rinsing and speed/intensity of rinsing (CFV), to do so, a combination for the rinse step were chosen where the time or CFV were modified. Table 6-2 shows the conditions that were analysed for both time and CFV.

The membranes were fouled beforehand under the same conditions for each rinsing test. The temperature was kept at 20.8 ± 1.1 °C, the TMP was 0.27 ± 0.01 bar and the CFV was 1.3 ± 0.02 m s^{-1}. The membrane resistance values (1.8 $x10^{+11}$ ± 1.9x^{+10} m^{-1}) have been removed from all the data shown in this section.

Table 6-2: Processing conditions of time (left) and CFV (right) tests. The order of the tests was randomised for either factor, first condition for both tables is the same.

Name	CFV [m s^{-1}]	Time [min]
Sample 1	0.53	10
Sample 2	0.54	1
Sample 3	0.51	5
Sample 4	0.52	15

Name	CFV [m s^{-1}]	Time [min]
Sample 1	0.53	10
Sample 5	0.2	10
Sample 6	0.36	10
Sample 7	0.74	10

The increase of time allotted to the rinse step does show a stark improvement during the first 5 min of rinsing (Figure 6-23), reducing the total resistance from 90 to 27 $x10^{+11}$ m^{-1}, for the 1 min and 5 min rinse time samples, respectively. Further increases in rinse time did lead to greater reductions of total resistance but with diminishing returns for every extra minute.

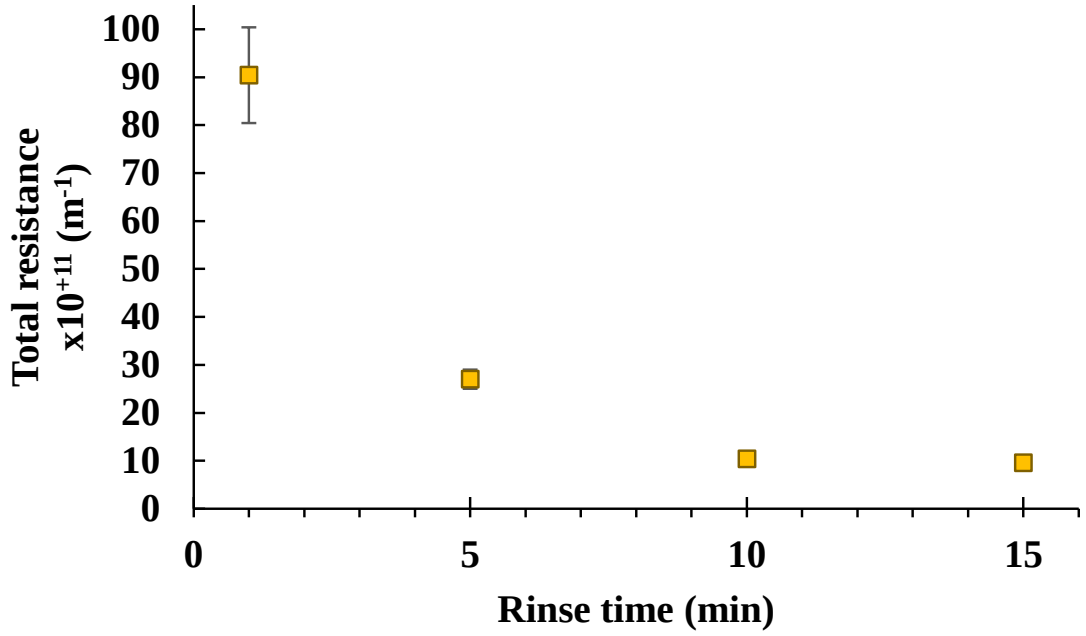

Figure 6-23: Effect of rinse step time duration modification while CFV was kept constant at 0.53 m s^{-1}. Error bars correspond to the standard deviation of 2 repeats for each data point.

The final increase in rinse time from 10 to 15 min does not provide any remarkable benefit, as can be seen in Table 6-3, the increase in rinse time (and water use) does not lead to a statistical reduction of total resistance.

Another aspect that was analysed was the colour of the retentate line, in order to visually assume the state of the retentate water. For example, the rinse step of 1 min did not have enough time to remove all the milk from the system leading to having a milk-like retentate (almost as white as milk). However, as with the total resistance, after the first five minutes the differences in retentate were much smaller, going from visible turbid water to almost clear water (for the 15 min rinse step).

Table 6-3: Total resistance values shown in Figure 6-23, along with, description of retentate features. Error values correspond to the standard deviation of 2 repeats for each data point.

Sample name	CFV [m s^{-1}]	Time [min]	R_t x10^{+11} [m^{-1}]	Retentate
Sample 2	0.54 ± 0.04	1 ± 0.08	90.4 ± 10	Milk-like
Sample 3	0.51 ± 0.03	5 ± 0.03	27.0 ± 2	turbid water
Sample 1	0.53 ± 0.02	10 ± 0.02	10.4 ± 0.7	turbid water
Sample 4	0.52 ± 0.02	15 ± 0.01	9.6 ± 0.4	low turbidity (clear)

The CFV is a determinant factor for the total resistance, as can be seen in Figure 6-24 the increase from 0.2 m s^{-1} to 0.36 m s^{-1} reduced the total resistance (and the associated fouling)

from 329 to 16 $x10^{+11}$ m^{-1}. Further increases in CFV speed led to higher reduction in total resistance but with diminishing returns for the extra energy cost.

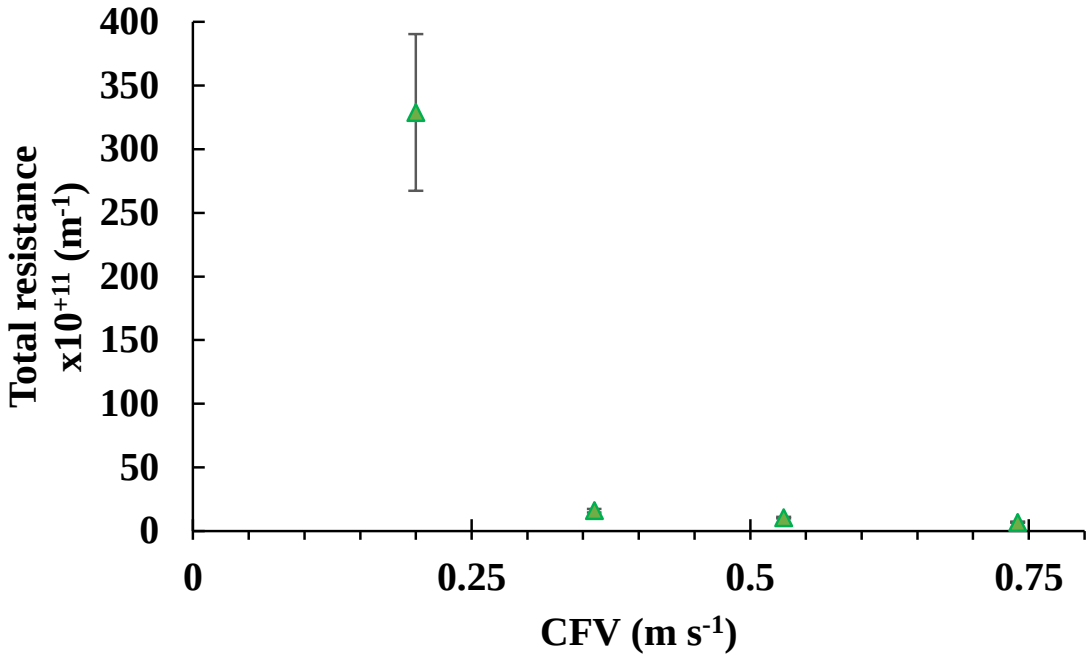

Figure 6-24: Effect of rinse step CFV modification while time was kept constant at 10 min. Error bars correspond to the standard deviation of 2 repeats for each data point.

The colour of the retentate line showed a similar trend for increase of CFV as for increase of time (see Table 6-4). Unlike the 1 min of rinse step, the 0.2 m s^{-1} did have time to remove the milk from the system, however, even though the water was turbid the final resistance was much higher.

Table 6-4: Total resistance values shown in Figure 6-24, along with, description of retentate features. Error values correspond to the standard deviation of 2 repeats for each data point.

Sample name	Time [min]	CFV [m s^{-1}]	R_t $x10^{+11}$ [m^{-1}]	Retentate
Sample 5	10 ± 0.03	0.2 ± 0.02	329 ± 61.6	turbid water
Sample 6	10 ± 0.01	0.36 ± 0.02	16.0 ± 1.5	turbid water
Sample 1	10 ± 0.02	0.53 ± 0.02	10.4 ± 0.7	turbid water
Sample 7	10 ± 0.03	0.74 ± 0.06	6.8 ± 0.5	low turbidity (clear)

In summary, the CFV must be higher than 0.2 m s^{-1} in order to start the removal of foulants from the membrane, from the tested velocities the minimum acceptable was 0.36 m s^{-1} (Table 6-5). In order to achieve a proper removal it is also important to perform a rinse step of more than 1 min, in the tested conditions 5 min is enough to achieve high removal of foulants.

Sample 3, 5 min at 0.51 m s^{-1}, are the bare minimum conditions to obtain a high degree of fouling removal during the rinse step.

Table 6-5: Summary of all conditions studied in descending order of total resistance. Error values correspond to the standard deviation of 2 repeats for each data point.

Sample name	Time [min]	CFV [m s^{-1}]	R_t x10^{+11} [m^{-1}]
Sample 5	10 ± 0.03	0.2 ± 0.02	329 ± 61.6
Sample 2	1 ± 0.08	0.54 ± 0.04	90.4 ± 10
Sample 3	5 ± 0.03	0.51 ± 0.03	27.0 ± 2
Sample 6	10 ± 0.01	0.36 ± 0.02	16.0 ± 1.5
Sample 1	10 ± 0.02	0.53 ± 0.02	10.4 ± 0.7
Sample 4	15 ± 0.01	0.52 ± 0.02	9.6 ± 0.4
Sample 7	10 ± 0.03	0.74 ± 0.06	6.8 ± 0.5

After analysing all the results in this section, the speed and time of all the rinse step performed in this chapter were 5 min and 0.53 m s^{-1} of CFV using RO water, unless stated otherwise. The main reason for choosing these conditions was that they maximised fouling removal that facilitated complete removal of the remaining fouling after the chemical cleaning step and it reduced the water consumption when compared to the higher CFV speeds and higher time conditions. As has been shown, extra rinse time leads to increasingly reduced fouling resistance, however, each extra minute of operation carries with it a high consumption of water that cannot be justified for the reduced gains of going over 5 minutes, unless there is a specific test or condition to analyse. The same applies to CFV increases that carry extra water use and energy consumption. The reason for choosing 0.53 over 0.36 m s^{-1} is that even though 0.36 m s^{-1} has been shown to achieve a low resistance values at lower CFV (and energy) is mainly due the fact that it was operated for 10 min, increasing the water consumption compared to the 0.53 m s^{-1} for 5 min.

6.3.2 Rinse study: effect on reversible and irreversible fouling

The results of the first study were the used to perform a subsequent fouling and cleaning study to observe the ratio between reversible and irreversible fouling at two different TMP and the changes in fouling resistances over three cycles. The chosen conditions to perform the next step of the trial were the 10 min of rinse step at 0.53 m s^{-1} of CFV. The main reason for these conditions was that they removed a significant portion of fouling compared to the same CFV at 5 min, even though there was a water consumption increase.

The study consisted in comparing if different fouling conditions, in this case different TMP, 0.28 and 1.47 bar, would lead to different values of reversible, and more importantly, irreversible fouling. The study also aimed to observe if there were any changes in the ratio of reversible/irreversible fouling when using the same membrane for several cycles.

The fouling step was carried out at different TMP while keeping the other variable constant, temperature at 11.7 ± 0.9 °C and CFV at 1.3 ± 0.08 m s^{-1}. After each rinse step the membrane was cleaned using the cleaning cycle explained in the methodology (Chapter 4, section 4.1.4) using NaOH and a final rinse step.

The first result is that reversible fouling is way bigger than irreversible fouling, as can be seen in Figure 6-25, for almost all cycles, and it is more constant for the high TMP conditions than for the low TMP. For example, cycle 3 for 0.28 bar of TMP the irreversible fouling had grown due to accumulation of repeated cycles and had matched the reversible fouling.

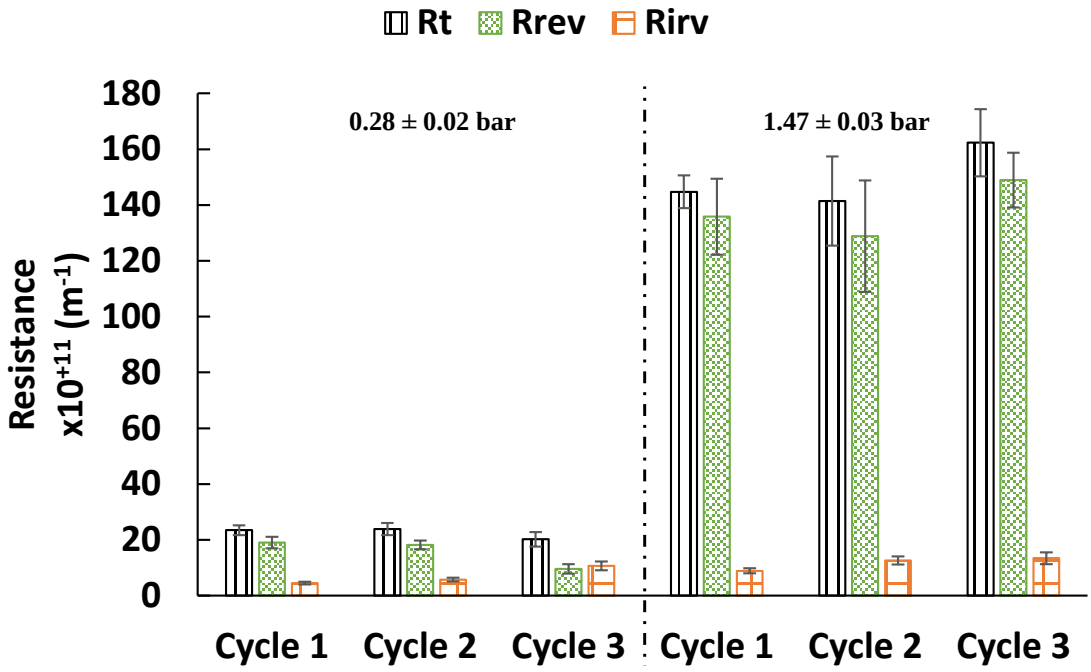

Figure 6-25: Total (resistance due to all fouling phenomenon), reversible (resistance due to fouling removed after the rinse step), and irreversible (resistance due to fouling that is not removed after the rinse step) resistances for fouling conditions at TMP 0.28 bar and 1.47 bar. Error bars correspond to the standard deviation of 2 repeats for each data point.

The study showed that repeated cycles with the same membrane led to a slight accumulation of irreversible fouling that was not removable using the chemical cleaning. However, the accumulation of irreversible did not have the same effect for both TMP conditions. At low TMP the final total resistance seemed constant balancing reversible and irreversible fouling, probably due to the low pressure not pushing enough proteins towards the membrane to form multiple layers of fouling, since the CFV was "high" at 1.3 m s^{-1} during the fouling step. On the other hand, the high-pressure conditions did have a final total resistance higher than the

first cycle due to the combined increase in irreversible and reversible fouling, being the reversible fouling the main component.

The high-pressure conditions (1.47 bar) did have a dominant share of reversible fouling, representing between 91-94% of the total resistance, unlike the low-pressure conditions (0.28 bar) where the reversible fouling descended from the initial share of 81% to the final 47% (Table 6-6). In both cases, high and low-pressure conditions, the final value for the irreversible fouling was similar in magnitude 13 and 11 $x10^{+11}$ m^{-1}, respectively, despite the significant differences (one order of magnitude) in total resistance (and reversible fouling). The increased share of irreversible fouling observed aligns with the results of Jimenez-Lopez *et al.* (2008)[128] that observed increases of 20% of irreversible fouling when the soluble proteins fraction was promoted. These findings align with the conditions of the rinsing study operated at low temperature and promoting beta-casein out of the micelles into soluble form.

Table 6-6: Total, reversible and irreversible resistance of fouling conditions TMP 0.28 bar and 1.47 bar. Error values correspond to the standard deviation of 2 repeats for each data point.

Sample name	R_t $x10^{+11}$ [m^{-1}]	R_{rev} $x10^{+11}$ [m^{-1}]	R_{irv} $x10^{+11}$ [m^{-1}]	% Rev	% Irv
Cycle 1 - 0.28bar	23 ± 1.8	19 ± 2	4 ± 0.5	81%	19%
Cycle 2 - 0.28bar	24 ± 2.2	18 ± 1.6	6 ± 0.7	76%	24%
Cycle 3 - 0.28bar	20 ± 2.6	10 ± 1.7	11 ± 1.6	47%	53%
Cycle 1 - 1.47bar	145 ± 5.9	136 ± 13.6	9 ± 0.9	94%	6%
Cycle 2 - 1.47bar	141 ± 16	129 ± 20	13 ± 1.5	91%	9%
Cycle 3 - 1.47bar	162 ± 12	149 ± 9.9	13 ± 2.1	92%	8%

6.3.3 Summary of rinse study

The rinse step efficacy is clearly a combination of CFV and time, of which the CFV is the main limiting factor, since as long as the CFV is below 0.2 m s^{-1} there is no effective removal of fouling. Once the CFV is above 0.2 m s^{-1} time pays a major role in reducing the fouling layer achieving maximum reductions for all CFV (above 0.2 m s^{-1}) at 10 min. A rinse step of just 5 min has been shown to be enough for the reduction of the total resistance to a value comparable with the best conditions studied (10 min, 0.74 m s^{-1}), while reducing the amount of water consumed in the process.

The 1.47 bar (high) TMP conditions had a much higher total resistance mainly due to the high reversible fouling that formed on the membrane, that represented up 94% of the total fouling resistance. On the other hand, 0.28 bar (low) TMP conditions had reversible and irreversible fouling of comparable magnitude that shifted from the initial reversible dominated (81% of

all fouling resistance) to irreversible favoured at cycle 3 (53% of all fouling resistance). At cycle 3 both low and high TMP conditions had irreversible fouling of comparable magnitude, 11 and 13 $x10^{+11}$ m^{-1}, respectively. Unlike the reversible fouling that was of 10 and 149 $x10^{+11}$ m^{-1} for the low and high TMP, respectively. The full cleaning cycle did not achieve full removal of foulants as can be seen by the stepwise increase in irreversible fouling for both TMP conditions.

However, it is important to highlight that increasing the rinse time and/or the CFV to achieve higher removal of reversible fouling is directly linked to an increase in energy and mainly water consumption. Therefore, the marginal gains in fouling components removal obtained by the increase of either component (and the reduction in chemical cleaning step requirement) will not balance the high increase in water demand. The present study did not focus on the environmental costs or benefits of each situation presented.

6.4 Membrane compaction

The changes in flux could be due to fouling, temperature effects and/or pressure compaction, either alone or by a combination of the above mentioned. In order to gain insight on the effects of compaction a TMP incremental study was carried out. The study consisted in a set of incremental variations of TMP, using the same membrane, within the range of pressure 0.25 to 4 bar, while maintaining temperature constant at 30 ± 1.5 °C and CFV at 1.3 ± 0.12 m s^{-1}. The aim was to observe if after increasing and decreasing the TMP applied to the membrane the water permeate flux would return to each original value.

Figure 6-26 shows the flux data of incremental increases and decreases of TMP at a rate of 0.5 bar each, with the exception of the first change from 0.25 to 0.5 bar, ranging from the 0.25 bar increasing up to 4 bars.

The Figure 6-26 shows that the membrane tested (0.1 µm PVDF, Synder Filtration, code: V01) does suffer significative pore compaction due to pressure increase resulting in a severe flux reduction for all TMP analysed. The degree of flux reduction increased after reaching the 4 bar value, as can be observed in Figure 6-26, which seems to indicate that a hysteresis point was triggered, it could be due to the irreversible blocking of pores.

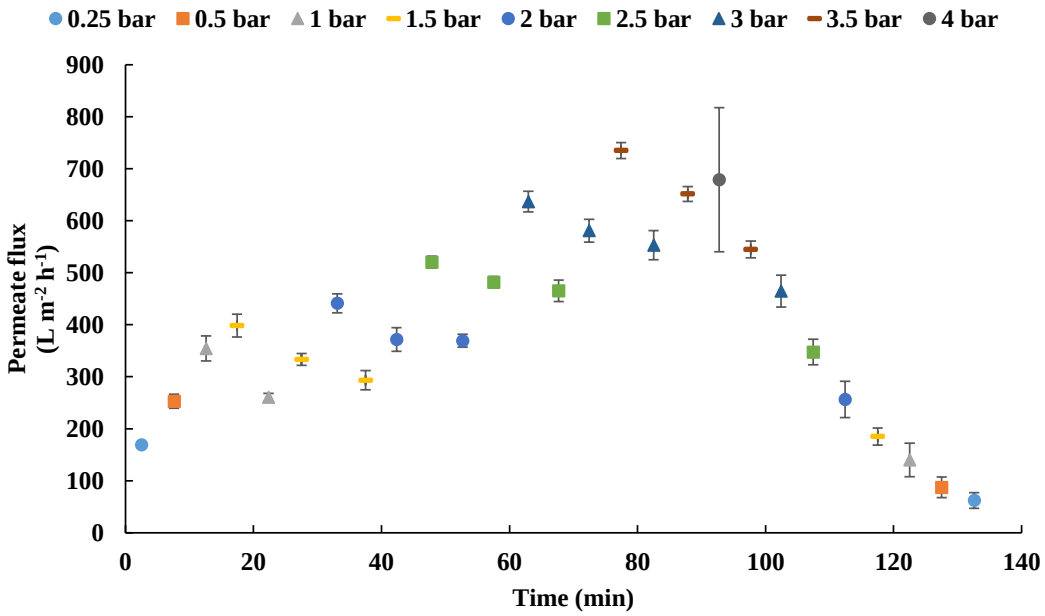

Figure 6-26: Flux data over time for incremental pressure modifications of 0.5 bar/step, using RO water at 30 ± 1.5 °C.

Figure 6-27 shows permeate flux vs TMP highlighting the flux reduction after each modification in TMP. As it can be seen the initial measurement (1st) is always higher than the returned measurements after the TMP is increased and reduced (2nd, 3rd and 4th). For example, the 0.25 bar initial flux was 170 ± 4 L m^{-2} h^{-1} and after increasing the TMP gradually up to 4 bar the recovered flux at TMP 0.25 bar was of 60 ± 15 L m^{-2} h^{-1}, a reduction of 63%.

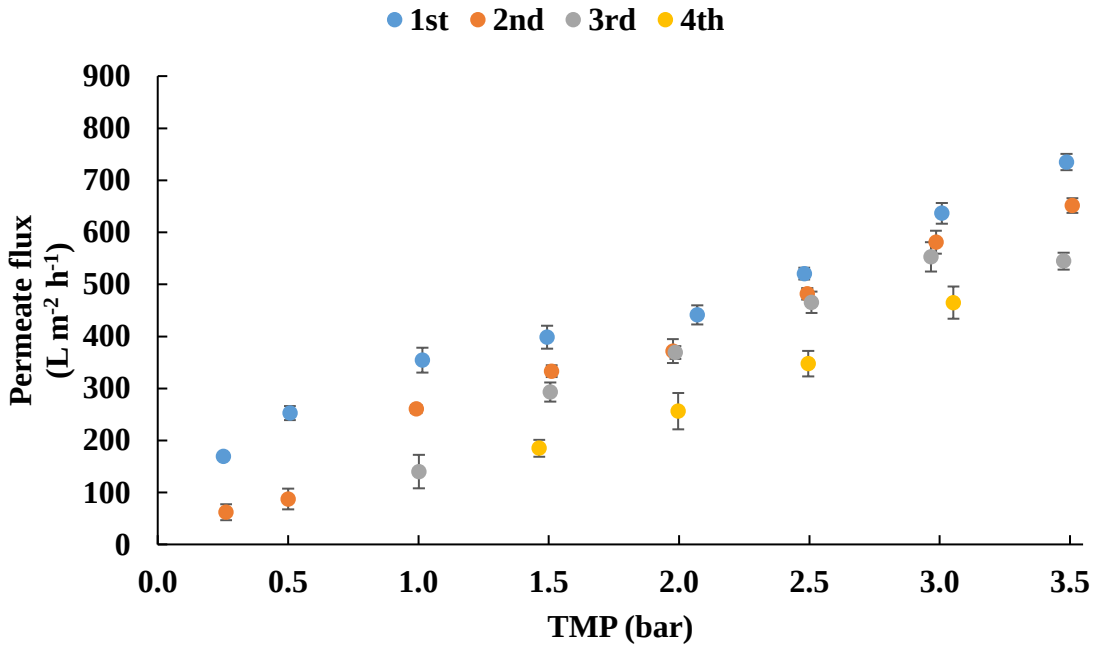

Figure 6-27: Flux data over TMP comparing the flux reduction at each step of pressure change, complementary to Figure 6-26, using RO water at 30 ± 1.5 °C. 1st, 2nd, 3rd and 4th make reference to the measurements order, after the 1st measurement all the other measurements were taken after the TMP had been increased and decreased.

The overall flux decrease observed for the different TMP can be seen in Table 6-7. Overall the decrease of flux is magnified at low pressure conditions with values around 60%, the effect of pressure to reduce flux goes down as the TMP is increased.

The main reason is assumed to be that the increase in TMP lead to a compression of the membrane due to the stress that the pressure which can increase the density of the microporous support layer, the membrane top layer and even the support layer, as has been shown in a wide range of studies like Aerts *et al.* (2001) and Davenport *et al.* (2020).[151,152]

The work carried out by Ebert *et al.* (2004) showed that the addition of TiO2 as inorganic fillers to PVDF membranes lead to better compaction resistance under pressure conditions up to 30 bar.[153] They claimed that the compaction of the membranes depended to the material characteristics like the elastic modulus and the bulk porosities of the membranes. Their results showed that the compaction usually focused on the layers of the membrane that host the larger pores and spaces ("macrovoids"). The compaction of the "macrovoids" explains why reaching high TMP conditions has a major effect on the flux for the low TMP conditions, since high TMP conditions already block these voids by themselves.

The study of Remanan and Chandra Das (2019)[154] produced EMA/PVDF membranes of different ratios that showed that compaction was less severe for the high EMA membranes (90/10) even though the flux of those was always lower. For example, the 60/40 membrane showed a high initial flux of around 1600 L m^{-2} h^{-1} that dropped by almost half in 1 hour to around 850 L m^{-2} h^{-1}, flux decline that are in line with the observed in Table 6-7.

Table 6-7: Flux decrease after incremental pressure reached the 4.0 bar max value and it was returned to the original pressures, as shown above.

TMP [bar]	Flux decrease [%]
0.25	63 ± 9
0.5	65 ± 10
1.0	60 ± 12
1.5	54 ± 7
2.0	42 ± 9
2.5	33 ± 5
3.0	27 ± 6
3.5	26 ± 3

In order to remove coating components, the membranes were conditioned (protocol can be found in methodology section 3.1.1) for 90 minutes at the pressure that the membrane was expected to be used, which in turn should prevent any effects of compaction since any

compaction effect should already be applied after 90 minutes. Membrane compaction is mainly defined at the initial stage of the pressure process and therefore once a TMP condition is set the compaction should not change, preventing further compaction as long as pressure is not modified. The membrane compaction and the changes in flux (reduction) and thickness can per temporary or permanent, but since most of the membranes in this study were never removed from the system to be re-used the was no option for changes in compaction among cycles.[151]

Chapter 7. General conclusions

The work carried out in this project has focused on deepening the understanding of milk processing using polymeric membranes to fractionate casein and whey proteins and the effect of the operational factors. This study has focused on the processing of milk, operational conditions and proteins detection. The main conclusions of this thesis are listed below according to the defined objectives set in Chapter 1.

Analytical method

One of the main objectives of this thesis was to develop an analytical method able to detect and quantify the main protein groups in bovine milk. The challenge resided in detecting and quantifying the α-CN, β-CN and κ-CN for the casein proteins and, α-La, β-Lg and BSA for the whey proteins in a single injection to simplify milk samples analysis. The novelty of the work carried out in this thesis is twofold:

On one hand it was found that the detection and quantification of all target protein groups were accomplished when using the Agilent ZORBAX StableBond C8 300Å, 3.5 µm, 4.6 x 150 mm column, using gradient 6 and at a temperature of 45 °C. This revealed that both gradient and temperature had major impact on ensuring protein detection. There is a clear operational advantage in time saved for analysis and sample preparation with a single injection that aligns well with industry requirements where time optimisation is a must.

On the other hand, the expertise gained throughout the thesis lead to adapting the HPLC method for the analysis of fouling layers protein composition. The method adaptation process found that protein extraction defined the reproducibility of the analysis. In particular, of the three tested extraction method the samples soaking in HPLC solvents proved to yield the most reliable results, with a soaking time of 1 hour providing the highest reliability.

Interactions between skimmed milk and PVDF membrane

Another key point of this thesis was to understand the interactions between milk proteins and PVDF membrane and how the operational conditions may affect them. The interactions between membranes and milk proteins are defined by the operational conditions since temperature and pressure modify the feed and therefore how it does interact with the membrane.

Temperature changes are a major factor to take into account since they affect both the feed viscosity and the proteins configuration as well as the composition of the casein micelles. This

thesis performed a DoE study to analyse both temperature and pressure effect on the protein fractionation. The temperature results indicated that increasing the temperature from 10 to 50 °C had a negative effect on casein proteins rejection, meaning that higher temperatures favoured casein proteins transmission reducing the fractionation of casein and whey proteins. It was observed that in spite of the outlet pressure, at 10 °C the casein rejections were all around 91 ± 5.9%. This can be attributed to the fact that casein micelles at high temperatures (50 °C) contract reducing their diameter as was shown by Beliciu and Moraru (2009),[48] which does facilitate the transmission through the membrane. The temperature effect was also observed for the whey proteins, following the same pattern. An increase of temperature at a fixed outlet pressure of 0.4 bar from 10 to 50 °C led to whey protein rejections reduction from 80% to 59%, respectively.

Pressure changes were studied by comparing changes at the outlet pressure. They showed that at constant TMP of 0.5 bar an increase in outlet pressure (reducing the pressure drop of the system), from 0.2 to 0.4 bar favours an increase of casein rejections. On the other hand, whey proteins did not show the same behaviour indicating that they were less affected by pressure changes than temperature changes.

Industrial conditions study

Understanding how industrial conditions for milk processing filtration affect protein separation and membrane fouling was needed to bridge the gap between lab scale experiments and industrial conditions.

The study focused on the effect that changes in TMP (including permeate line pressure), temperature and CFV had on protein fractionation when comparing to the initially defined industrial conditions.

The TMP study revealed that in order to produce whey rich permeates the TMP should not exceed 1 bar. For instance, it was found that at TMP of 0.5 and 1.0 bar the CN/Wy ratio at the permeate was of 1.9 and 1.0, respectively. However, above 1 bar, at TMP of 2.8 and 4.7 bar the CN/Wy ratio were of 3.4 and 4.2, respectively. This increase in CN/Wy ratio at high TMP is due to the high transmission of casein proteins through the membrane. This can be explained by the sponge model described by Bouchoux *et al.* (2010)[45], which assumes that high concentration of casein micelles produce osmotic pressure that empties the micelles of their water. The water removal induces a collapse of the micelles structure that ends up reducing their diameter to 10-40 nm, facilitating their transmission through the membrane.

The effect of temperature followed the same pattern observed in the previous studies independently of CFV and TMP changes.

Even though these conditions were studied (industrial and modified versions) the original industrial conditions outperformed any modification tested, highlighting that at low TMP and Temperature the filtration behaviour was the best to produce casein rich retentate and whey-richer permeates.

The other key study performed was the analysis of the fouling layer composition at different temperatures and pressures. The main findings were that temperature had a capital role in defining the amount of foulants that attached to the membrane, increasing with temperature, and that at any of the studied pressure and temperature ranges casein proteins were dominant in the fouling layer (>94% of all detected proteins).

The fouling layer study revealed that an increase in temperature from 10 to 56 °C always led to higher total proteins on the fouling layer from 135 g m^{-2} to 290 g m^{-2}, respectively. The higher protein content could be explained by the protein conformation shifts at high temperatures, that favour cross-linking of the protein groups.[125]

The fouling layer study also showed that the fouling layer protein composition was casein dominated (>94% of all proteins) with a minor fraction of whey proteins (<6%). The casein-rich fouling layer was constant all over the temperature and pressure range studied, from 10 to 50 °C and from 0.5 to 4.7 bar of TMP. The high casein content contrasted with the milk protein ratio of 80/20 for casein and whey proteins. This result showed that the main fouling contributors are the casein proteins with a minor contribution of the whey proteins. The CN/Wy ratio of the fouled membranes was between 3 to 6 times larger than the milk protein ratio, which aligns well with the results obtained by Schopf *et al.* (2020).[126]

Finally, the cleanability of the fouling layer using a rinse step and the compaction of the membrane itself due to pressure were studied. These conditions were studied because both of them influence the lifespan of the membrane, providing insights in how to operate a membrane. The rinse study also provides indications in how to best utilise water as part of the cleaning cycle of the membranes to optimise its use.

The rinse study analysed the effect of rinse speed and time on fouling layer removal. The study of the rinse speed revealed that CFV below 0.36 m s^{-1} did not remove the generated fouling layer, independently of the rinsing time. The CFV study was carried out with a rinsing time of 10 min for all CFV studied, at 0.2 and 0.36 m s^{-1} the final total resistances were of 329 and 16 $x10^{+11}$ m^{-1}, respectively. The analysis of the rinsing time showed it is a factor with diminishing returns. It revealed that the first 5 minutes of rinsing provided the greatest

reduction in total resistance, with diminishing returns for every extra minute beyond that. The initial 5 minutes of cleaning reduced the fouling resistance from 90 to 27 $x10^{+11}$ (m^{-1}), with lower reductions for the following 10 and 15 min of 10.4 and 9.6 $x10^{+11}$ (m^{-1}), respectively. The added extra water consumption for the 10 and 15 minutes conditions did not balance with the minimal resistance reductions observed.

Finally, membrane compaction was studied since it can have an effect on the permeate flow and composition. The experiments showed that membrane compaction for the 0.1 um PVDF was severe with flux reductions for RO water of 63, 65 and 60% at TMP of 0.25, 0.5 and 1 bar. The membrane compaction observed when increasing the pressure up to 4 bar showed flux reduction of more than 50% at the commonly used pressures of 0.25, 0.5 and 1 bar. These results showed the need to pre-conditioning the membrane at a TMP closer to the forecasted for filtration, otherwise the permeate results could be misleading.

Future work

This thesis has primarily focused on the milk processing side, however, the environmental impacts of the milk production and processing should also be addressed in future studies of dairy products processing. Just focusing on the environmental impacts of milk processing the use of membranes has a proven track record of minimising energy consumption per unit of product, as well as, a minimal impact on the food quality itself, since it does not apply any thermal treatment beyond safety standards or chemical product to it, which is great to prevent food loses, minimising the need of milk production. One of the key challenges for improving the sustainability of the milk processing would be water consumption at the cleaning steps, since water is a scarce resource becoming scarer with each passing year. As has been proven in the rinse analysis tests, the same level of fouling removal can be achieved with varied levels of time, energy and water usage. Those experiments demonstrated that there is a wide range of cleaning conditions that can obtain the same result, minimising resources like water while keeping the cleaning step above the safety thresholds.

Another level of impacts can be found at the milk production and those should also be looked at to ensure that scare water resources are not overexploited since they will probably have competing interest with other types of food production, mainly crops.

In spite of the environmental challenges described above, this thesis has also presented some processing challenges that still require further work in order to understand in detail the complex protein interactions with membranes and fouling.

The work of this thesis has laid the foundations for new paths of research both in the analytical and processing sides. The continuous development of the HPLC equipment could open the opportunity to reduce operation time of the method, which would allow to reduce solvent consumption, as well. The developments also allow improvements in the detection and quantification of proteins, allowing the targeting of smaller fractions of proteins that have demonstrated interest like immunoglobulins.[69] The work of Heidebrecht *et al.*[15–18] demonstrated health benefits by using enhanced immunoglobulins of milk.

The fouling layer protein detection application does require further testing to ensure full protein quantification and the study of the limits of application like the effect of fouling layer thickness as a threshold of detection. These improvements would be key for industrial applications since they would provide a tool to study any milk fouling deposit (membranes, heat exchangers or piping) and the dominant groups at the processed conditions. The current method already allows the study of the fouling layer formation and the main components of the fouling layer which has demonstrated that low temperature filtration is the path forward to keep a lower degree of fouling which allows longer filtration runs (from the food safety side).

The temperature studies revealed that operating at lower temperatures has many operational benefits, from having high casein rejections to having lower fouling that will probably establish it as the operational temperature for milk filtration. Future milk filtration should focus on operating at low temperature (10 °C) to obtain high casein rejections in detriment of having lower fluxes than 50 °C filtration. The lower temperature filtration has the added benefit of longer operational time due to having less bacterial growth and due to having less fouling growth, as has been demonstrated. The lower fouling will also impact on the cleaning step since less water, chemicals and energy will be required.

The compaction study showed the effect that increasing TMP had on the overall permeate of the membrane in short spans of time. A future study should focus on studying the stability of the membrane over long time, up to 8-10 hours, at a low pressure to compare the accumulated effect.

Finally, the rinse study showed a clear cut of CFV that allowed fouling removal (0.36 m s^{-1}). A future study should zoom in the range between 0.2-0.36 m s^{-1} in order to determine the minimal CFV that ensures proper cleaning of the membrane. The determination of the minimal CFV and rinsing time would be crucial to reduce water consumption during the cleaning step.

Bibliography

(1) Us, T.; Database, E. V. Technology Trends in Membrane Filtration Use. *Filtration+Separation*. 2018, pp 30–33. https://doi.org/10.1016/S0015-1882(18)30174-5.

(2) Pouliot, Y. Membrane Processes in Dairy Technology-From a Simple Idea to Worldwide Panacea. *Int. Dairy J.* **2008**, *18* (7), 735–740. https://doi.org/10.1016/j.idairyj.2008.03.005.

(3) Mulder, M. *Basic Principles of Membrane Technology*, 1st Editio.; Kluwer Academic Publishers, 1991.

(4) Pouliot, Y. Membrane Processes in Dairy Technology—From a Simple Idea to Worldwide Panacea. *Int. Dairy J.* **2008**, *18* (7), 735–740. https://doi.org/10.1016/j.idairyj.2008.03.005.

(5) Lipnizki, F. Cross-Flow Membrane Applications in the Food Industry. In *Membrane Technology,Volume 3: Membranes for Food Applications*; Klaus-Viktor Peinemann, Suzana Pereira Nunes, and L. G., Ed.; WILEY-VCH Verlag GmbH & Co. KGaA, 2010; pp 1–24.

(6) Kotsanopoulos, K. V. K. V.; Arvanitoyannis, I. S. I. S. Membrane Processing Technology in the Food Industry: Food Processing, Wastewater Treatment, and Effects on Physical, Microbiological, Organoleptic, and Nutritional Properties of Foods. *Crit. Rev. Food Sci. Nutr.* **2015**, *55* (9), 1147–1175. https://doi.org/10.1080/10408398.2012.685992.

(7) FAO. *Food Outlook*; 2021.

(8) Data, O. W. in. Meat and Dairy Production - Our World in Data https://ourworldindata.org/meat-production?country= (accessed Aug 11, 2021).

(9) Gaspard, S. J.; Auty, M. A. E.; Kelly, A. L.; Mahony, J. A. O. Isolation and Characterisation of k -Casein / Whey Protein Particles from Heated Milk Protein Concentrate and Role of k -Casein in Whey Protein Aggregation. *Int. Dairy J.* **2017**, *73*, 98–108. https://doi.org/10.1016/j.idairyj.2017.05.012.

(10) Fox, P. F.; Uniacke-Lowe, T.; McSweeney, P. L. H.; O'Mahony, J. A. *Dairy Chemistry and Biochemistry*, Second Edi.; Springer, Ed.; Springer, 2015. https://doi.org/10.1007/978-3-319-14892-2.

(11) Guo, M. *Human Milk Chemical Composition of Human Milk*; Elsevier, 2014.

https://doi.org/10.1016/C2013-0-17349-7.

(12) Lamiot, E.; Ca, D.; Juneau, C.; Asbill, S.; Llp, B. METHOD FOR SELECTIVE FRACTIONATION OF GROWTH FACTORS FROM DAIRY PRODUCTS. US 2010/0121037 A1, 2010.

(13) Singh, H. Milk Protein Products | Functional Properties of Milk Proteins. In *Encyclopedia of Dairy Sciences*; 2011; pp 887–893. https://doi.org/10.1016/B978-0-12-374407-4.00352-6.

(14) Agarwal, S.; Beausire, R. L. W.; Patel, S.; Patel, H. Innovative Uses of Milk Protein Concentrates in Product Development. *J. Food Sci.* **2015**, *80* (S1), A23–A29. https://doi.org/10.1111/1750-3841.12807.

(15) Hartinger, M.; Heidebrecht, H.-J.; Schiffer, S.; Dumpler, J.; Kulozik, U. Milk Protein Fractionation by Means of Spiral-Wound Microfiltration Membranes: Effect of the Pressure Adjustment Mode and Temperature on Flux and Protein Permeation. *Foods* **2019**, *8* (6), 180. https://doi.org/10.3390/foods8060180.

(16) Heidebrecht, H. J.; Weiss, W. J.; Pulse, M.; Lange, A.; Gisch, K.; Kliem, H.; Mann, S.; Pfaffl, M. W.; Kulozik, U.; von Eichel-Streiber, C. Treatment and Prevention of Recurrent Clostridium Difficile Infection with Functionalized Bovine Antibody-Enriched Whey in a Hamster Primary Infection Model. *Toxins (Basel).* **2019**, *11 (2)* (98). https://doi.org/10.3390/toxins11020098.

(17) Heidebrecht, H. J.; Kulozik, U. Fractionation of Casein Micelles and Minor Proteins by Microfiltration in Diafiltration Mode. Study of the Transmission and Yield of the Immunoglobulins IgG, IgA and IgM. *Int. Dairy J.* **2019**, *93*, 1–10. https://doi.org/10.1016/j.idairyj.2019.01.009.

(18) Heidebrecht, H. J.; Toro-Sierra, J.; Kulozik, U. Concentration of Immunoglobulins in Microfiltration Permeates of Skim Milk: Impact of Transmembrane Pressure and Temperature on the IgG Transmission Using Different Ceramic Membrane Types and Pore Sizes. *Foods* **2018**, *7* (7), 101. https://doi.org/10.3390/foods7070101.

(19) OECD-FAO. *OECD-FAO Agricultural Outlook 2019-2028*; 2019.

(20) Lagrange, V.; Whitsett, D.; Burris, C. Global Market for Dairy Proteins. *J. Food Sci.* **2015**, *80* (S1), A16–A22. https://doi.org/10.1111/1750-3841.12801.

(21) Bonizzi, I.; Buffoni, J. N.; Feligini, M. *Quantification of Bovine Casein Fractions by Direct Chromatographic Analysis of Milk. Approaching the Application to a Real*

Production Context; 2009; Vol. 1216. https://doi.org/10.1016/j.chroma.2008.11.045.

(22) Akbache, A.; Lamiot, É.; Moroni, O.; Turgeon, S.; Gauthier, S. F.; Pouliot, Y. Use of Membrane Processing to Concentrate TGF-B2 and IGF-I from Bovine Milk and Whey. *J. Memb. Sci.* **2009**, *326* (2), 435–440. https://doi.org/10.1016/j.memsci.2008.10.026.

(23) Bakshi, A. S.; Smith, D. E. Effect of Fat Content and Temperature on Viscosity in Relation to Pumping Requirements of Fluid Milk Products. *J. Dairy Sci.* **1984**, *67* (6), 1157–1160. https://doi.org/10.3168/jds.s0022-0302(84)81417-4.

(24) Moon, T. W.; Peng, I. C.; Lonergan, D. A. Chemical Properties of Cryocasein. *J. Food Sci.* **1988**, *53* (6), 1687–1693. https://doi.org/10.1111/j.1365-2621.1988.tb07816.x.

(25) Bordin, G.; Cordeiro Raposo, F.; de la Calle, B.; Rodriguez, A. R. Identification and Quantification of Major Bovine Milk Proteins by Liquid Chromatography. *J. Chromatogr. A* **2001**, *928* (1), 63–76. https://doi.org/10.1016/S0021-9673(01)01097-4.

(26) Bonfatti, V.; Grigoletto, L.; Cecchinato, A.; Gallo, L.; Carnier, P. Validation of a New Reversed-Phase High-Performance Liquid Chromatography Method for Separation and Quantification of Bovine Milk Protein Genetic Variants. *J. Chromatogr. A* **2008**, *1195* (1), 101–106. https://doi.org/10.1016/j.chroma.2008.04.075.

(27) Lucey, J. A.; Horne, D. S. Perspectives on Casein Interactions. *Int. Dairy J.* **2018**, *85*, 56–65. https://doi.org/10.1016/j.idairyj.2018.04.010.

(28) Horne, D. S. Casein Interactions: Casting Light on the Black Boxes, the Structure in Dairy Products. *Int. Dairy J.* **1998**, *8* (3), 171–177.

(29) McMahon, D. J.; McManus, W. R. Rethinking Casein Micelle Structure Using Electron Microscopy. *J. Dairy Sci.* **1998**, *81* (11), 2985–2993. https://doi.org/10.3168/jds.S0022-0302(98)75862-X.

(30) Schmidt, D. G. Colloidal Aspects of Casein. *Netherlands Milk Dairy J.* **1980**, *34* (1), 42–64.

(31) HOLT, C. Structure and Stability of Bovine Casein Micelles. *Adv. Protein Chem.* **1992**, *43*, 63–151. https://doi.org/10.1016/S0065-3233(08)60554-9.

(32) Horne, D. S. Casein Micelles as Hard Spheres: Limitations of the Model in Acidified Gel Formation. *Colloids Surfaces A Physicochem. Eng. Asp.* **2003**, *213* (2–3), 255–263.

(33) Thompson, A.; Boland, M.; Singh, H. *Milk Proteins from Expression to Food*; 2009.

(34) HOLT, C.; Horne, D. S. The Hairy Casein Micelle : Evolution of the Concept and Its Implications for Dairy Technology. *Ned. melk en Zuiveltijdschr.* **1996**, *50* (2), 85–111.

(35) De Kruif, C. G.; Holt, C. Casein Micelle Structure, Functions and Interactions. In *Advanced Dairy Chemistry---1 Proteins: Part A / Part B*; Fox, P. F., McSweeney, P. L. H., Eds.; Springer US: Boston, MA, 2003; pp 233–276. https://doi.org/10.1007/978-1-4419-8602-3_5.

(36) Mcgann, T. C. A.; Donnelly, W. J.; Kearney, R. D.; Buchheim, W. Composition and Size Distribution of Bovine Casein Micelles. *Biochim. Biophys. Acta* **1980**, *630* (2), 261–270.

(37) Alexander, M.; Rojas-Ochoa, L. F.; Leser, M.; Schurtenberger, P. Structure, Dynamics, and Optical Properties of Concentrated Milk Suspensions: An Analogy to Hard-Sphere Liquids. *J. Colloid Interface Sci.* **2002**, *253* (1), 35–46. https://doi.org/10.1006/jcis.2002.8452.

(38) Slaltery, C. W.; Evard, R. A Model for the Formation and Structure of Casein Micelles from Subunits of Variable Composition. *Biochim. Biophys. Acta* **1973**, *317*, 529–538.

(39) Slaltery, C. W. Model Calculations of Casein Micelle Size Distribution. *Biophys. Chem.* **1977**, *6*, 59–64.

(40) Horne, D. S. Casein Micelle Structure: Models and Muddles. *Curr. Opin. Colloid Interface Sci.* **2006**, *11* (2–3), 148–153. https://doi.org/10.1016/j.cocis.2005.11.004.

(41) Fox, P. F. Milk Proteins: General and Historical Aspects. In *Advanced Dairy Chemistry---1 Proteins: Part A / Part B*; Fox, P. F., McSweeney, P. L. H., Eds.; Springer US: Boston, MA, 2003; pp 1–48. https://doi.org/10.1007/978-1-4419-8602-3_1.

(42) De Kruif, C. G.; Huppertz, T.; Urban, V. S.; Petukhov, A. V. Casein Micelles and Their Internal Structure. *Adv. Colloid Interface Sci.* **2012**, *171–172*, 36–52. https://doi.org/10.1016/j.cis.2012.01.002.

(43) Horne, D. S. A Balanced View of Casein Interactions. *Curr. Opin. Colloid Interface Sci.* **2017**, *28*, 74–86. https://doi.org/10.1016/j.cocis.2017.03.009.

(44) Slattery, C. W. Casein Micelle Structure; An Examination of Models. *J. Dairy Sci.* **1976**, *59* (9), 1547–1556. https://doi.org/10.3168/jds.s0022-0302(76)84403-7.

(45) Pe, J.; Cabane, B.; Bouchoux, A. How to Squeeze a Sponge : Casein Micelles under Osmotic Stress , a SAXS Study. **2010**, *99* (December), 3754–3762.

https://doi.org/10.1016/j.bpj.2010.10.019.

(46) Bouchoux, A.; Debbou, B.; Gésan-Guiziou, G.; Famelart, M. H.; Doublier, J. L.; Cabane, B. Rheology and Phase Behavior of Dense Casein Micelle Dispersions. *J. Chem. Phys.* **2009**, *131* (16), 165106. https://doi.org/10.1063/1.3245956.

(47) Fox, P. F.; Brodkorb, A. The Casein Micelle: Historical Aspects, Current Concepts and Significance. *Int. Dairy J.* **2008**, *18* (7), 677–684. https://doi.org/10.1016/j.idairyj.2008.03.002.

(48) Beliciu, C. M.; Moraru, C. I. Effect of Solvent and Temperature on the Size Distribution of Casein Micelles Measured by Dynamic Light Scattering. *J. Dairy Sci.* **2009**, *92* (5), 1829–1839. https://doi.org/10.3168/jds.2008-1467.

(49) Leonil, J.; Molle, D.; Fauquant, J.; Maubois, J. L.; Pearce, R. J.; Bouhallab, S. Characterization by Ionization Mass Spectrometry of Lactosyl β-Lactoglobulin Conjugates Formed During Heat Treatment of Milk and Whey and Identification of One Lactose-Binding Site. *J. Dairy Sci.* **1997**, *80* (10), 2270–2281. https://doi.org/10.3168/jds.S0022-0302(97)76176-9.

(50) Kamizake, N. K. .; Gonçalves, M. M.; Zaia, C. T. B. .; Zaia, D. A. . Determination of Total Proteins in Cow Milk Powder Samples: A Comparative Study between the Kjeldahl Method and Spectrophotometric Methods. *J. Food Compos. Anal.* **2003**, *16* (4), 507–516. https://doi.org/10.1016/S0889-1575(03)00004-8.

(51) Gao, P.; Li, Z.; Zan, L.; Yue, T.; Shi, B. A Non-Protein Nitrogen Index for Discriminating Raw Milk Protein Adulteration via the Kjeldahl Method. *Anal. Methods* **2015**, *7* (21), 9166–9170. https://doi.org/10.1039/C5AY01422K.

(52) Aguilar, M.-I. *HPLC of Peptides and Proteins*; Humana Press: New Jersey, 2004; Vol. 251. https://doi.org/10.1385/1592597424.

(53) Veloso, A. C. .; Teixeira, N.; Ferreira, I. M. P. L. V. . P. L. V. O. Separation and Quantification of the Major Casein Fractions by Reverse-Phase High-Performance Liquid Chromatography and Urea–Polyacrylamide Gel Electrophoresis Detection of Milk Adulterations. *J. Chromatogr. A* **2002**, *967* (2), 209–218. https://doi.org/10.1016/S0021-9673(02)00787-2.

(54) WANG, J.; ZHANG, Q.-H.; WANG, Z.-H.; LI, H.-M. Determination of Major Bovine Milk Proteins by Reversed Phase High Performance Liquid Chromatography. *Chinese J. Anal. Chem.* **2009**, *37* (11), 1667–1670. https://doi.org/10.1016/S1872-2040(08)60146-2.

(55) Boitz, L. I.; Fiechter, G.; Seifried, R. K.; Mayer, H. K. A Novel Ultra-High Performance Liquid Chromatography Method for the Rapid Determination of b-Lactoglobulin as Heat Load Indicator in Commercial Milk Samples. *J. Chromatogr. A* **2015**, *1386*, 98–102. https://doi.org/10.1016/j.chroma.2015.01.081.

(56) Holland, B.; Rahimi Yazdi, S.; Ion Titapiccolo, G.; Corredig, M. Short Communication: Separation and Quantification of Caseins and Casein Macropeptide Using Ion-Exchange Chromatography. *J. Dairy Sci.* **2010**, *93* (3), 893–900. https://doi.org/10.3168/jds.2009-2820.

(57) Lecoeur, M.; Gareil, P.; Varenne, A. Separation and Quantitation of Milk Whey Proteins of Close Isoelectric Points by On-Line Capillary Isoelectric Focusing—Electrospray Ionization Mass Spectrometry in Glycerol–Water Media. *J. Chromatogr. A* **2010**, *1217* (46), 7293–7301. https://doi.org/10.1016/j.chroma.2010.09.043.

(58) Pierri, G.; Kotoni, D.; Simone, P.; Villani, C.; Pepe, G.; Campiglia, P.; Dugo, P.; Gasparrini, F. Analysis of Bovine Milk Caseins on Organic Monolithic Columns: An Integrated Capillary Liquid Chromatography–High Resolution Mass Spectrometry Approach for the Study of Time-Dependent Casein Degradation. *J. Chromatogr. A* **2013**, *1313*, 259–269. https://doi.org/10.1016/j.chroma.2013.08.083.

(59) Ye, X.; Yoshida, S.; Ng, T. B. Isolation of Lactoperoxidase, Lactoferrin, α-Lactalbumin, β-Lactoglobulin B and β-Lactoglobulin A from Bovine Rennet Whey Using Ion Exchange Chromatography. *Int. J. Biochem. Cell Biol.* **2000**, *32* (11), 1143–1150. https://doi.org/10.1016/S1357-2725(00)00063-7.

(60) Santos, M. J.; Teixeira, J. A.; Rodrigues, L. R. Fractionation of the Major Whey Proteins and Isolation of β-Lactoglobulin Variants by Anion Exchange Chromatography. *Sep. Purif. Technol.* **2012**, *90*, 133–139. https://doi.org/10.1016/j.seppur.2012.02.030.

(61) Snyder, L. R.; Kirkland, J. J.; Dolan, J. W. *Introduction to Modern Liquid Chromatography*, Third.; John Wiley & Sons, Inc.: Hoboken, NJ, USA, 2009. https://doi.org/10.1002/9780470508183.

(62) Jandera, P.; Henze, G. Liquid Chromatography, 1. Fundamentals, History, Instrumentation, Materials. In *Ullmann's Encyclopedia of Industrial Chemistry*; Wiley-VCH Verlag GmbH & Co. KGaA: Weinheim, Germany, 2011. https://doi.org/10.1002/14356007.b05_237.pub2.

(63) Yates, J. R. *Mass Spectrometry*; 2000; Vol. 16. https://doi.org/10.1016/S0168-

9525(99)01879-X.

(64) Gerd Bobe; Donald C. Beitz; Albert E. Freeman, A.; Lindberg*, G. L. Separation and Quantification of Bovine Milk Proteins by Reversed-Phase High-Performance Liquid Chromatography. *J. Agric. Food Chem.* **1998**, *46* (2), 458–463. https://doi.org/10.1021/JF970499P.

(65) CHROMacademy. The Theory Of HPLC - Reverse phase chromatography - Mechanism of Reversed Phase HPLC http://www.chromacademy.com/lms/sco5/02-Mechanism-of-Reversed-Phase-HPLC.html?fChannel=0&fCourse=0&fSco=5&fPath=sco5/02-Mechanism-of-Reversed-Phase-HPLC.html (accessed Sep 6, 2017).

(66) Gilar, M.; Olivova, P.; Daly, A. E.; Gebler, J. C. Two-Dimensional Separation of Peptides Using RP-RP-HPLC System with Different PH in First and Second Separation Dimensions. *J. Sep. Sci.* **2005**, *28* (14), 1694–1703. https://doi.org/10.1002/jssc.200500116.

(67) Healthcare, G. *Ion Exchange Chromatography & Chromatofocusing: Principles and Methods*; 2016.

(68) Gasilova, N.; Gassner, A.-L.; Girault, H. H. Analysis of Major Milk Whey Proteins by Immunoaffinity Capillary Electrophoresis Coupled with MALDI-MS. *Electrophoresis* **2012**, *33* (15), 2390–2398. https://doi.org/10.1002/elps.201200079.

(69) Léonil, J.; Mollé, D.; Gaucheron, F.; Arpino, P.; Guénot, P.; Maubois, J. L. Analysis of Major Bovine Milk Proteins by On-Line High-Performance Liquid Chromatography and Electrospray Ionization-Mass Spectrometry. *Lait* **1995**, *75* (3), 193–210. https://doi.org/10.1051/lait:1995314.

(70) de la Fuente, M. A.; Juárez, M. Authenticity Assessment of Dairy Products. *Crit. Rev. Food Sci. Nutr.* **2005**, *45* (7–8), 563–585. https://doi.org/10.1080/10408690490478127.

(71) Bradford, M. M. A Rapid and Sensitive Method for the Quantitation of Microgram Quantities of Protein Utilizing the Principle of Protein-Dye Binding. *Anal. Biochem.* **1976**, *72*, 248–254.

(72) Standardization, I. O. for. BSI Standards Publication Milk and Milk Products — Determination of Nitrogen Content Part 1 : Kjeldahl Principle and Crude Protein Calculation. *ISO* **2014**.

(73) Standardization, I. O. for. BSI Standards Publication Milk and Milk Products — Determination of Nitrogen Content Part 4: Determination of Protein and Non- Protein Nitrogen Content and True Protein Content Calculation (Reference. *ISO* **2014**, No. February.

(74) Jørgensen, C. E.; Abrahamsen, R. K.; Rukke, E.-O.; Johansen, A.-G.; Schüller, R. B.; Skeie, S. B. Optimization of Protein Fractionation by Skim Milk Microfiltration: Choice of Ceramic Membrane Pore Size and Filtration Temperature. *J. Dairy Sci.* **2016**, *99* (8), 6164–6179. https://doi.org/10.3168/jds.2016-11090.

(75) DeVries, J. W.; Greene, G. W.; Payne, A.; Zbylut, S.; Scholl, P. F.; Wehling, P.; Evers, J. M.; Moore, J. C. *Non-Protein Nitrogen Determination: A Screening Tool for Nitrogenous Compound Adulteration of Milk Powder*; 2017; Vol. 68. https://doi.org/10.1016/j.idairyj.2016.12.003.

(76) Pierri, G.; Kotoni, D.; Simone, P.; Villani, C.; Pepe, G.; Campiglia, P.; Dugo, P.; Gasparrini, F. Analysis of Bovine Milk Caseins on Organic Monolithic Columns: An Integrated Capillary Liquid Chromatography-High Resolution Mass Spectrometry Approach for the Study of Time-Dependent Casein Degradation. *J. Chromatogr. A* **2013**, *1313*, 259–269. https://doi.org/10.1016/j.chroma.2013.08.083.

(77) Strathmann, H. *Introduction to Membrane Science and Technology*; Wiley-VCH, 2011.

(78) Steinhauer, T.; Marx, M.; Bogendörfer, K.; Kulozik, U. Membrane Fouling during Ultra- and Microfiltration of Whey and Whey Proteins at Different Environmental Conditions: The Role of Aggregated Whey Proteins as Fouling Initiators. *J. Memb. Sci.* **2015**, *489*, 20–27. https://doi.org/10.1016/j.memsci.2015.04.002.

(79) Espina, V. S.; Jaffrin, M. Y.; Ding, L. H. Comparison of Rotating Ceramic Membranes and Polymeric Membranes in Fractionation of Milk Proteins by Microfiltration. *Desalination* **2009**, *245* (1), 714–722. https://doi.org/10.1016/j.desal.2009.02.042.

(80) Saxena, A.; Tripathi, B. P.; Kumar, M.; Shahi, V. K. Membrane-Based Techniques for the Separation and Purification of Proteins: An Overview. *Adv. Colloid Interface Sci.* **2009**, *145* (1), 1–22. https://doi.org/10.1016/j.cis.2008.07.004.

(81) Neocleous, M.; Barbano, D. M.; Rudan, M. A. Impact of Low Concentration Factor Microfiltration on Milk Component Recovery and Cheddar Cheese Yield. *J. Dairy Sci.* **2002**, *85* (10), 2425–2437.

(82) Hurt, E.; Barbano, D. M. Processing Factors That Influence Casein and Serum Protein

Separation by Microfiltration. *J. Dairy Sci.* **2010**, *93* (10), 4928–4941. https://doi.org/10.3168/jds.2010-3121.

(83) Dong, J.-Y.; Chen, L.-J.; Maubois, J.-L.; Ma, Y. Influence of Medium-Concentration Factor Microfiltration Treatment on the Characteristics of Low-Moisture Mozzarella Cheese. *Dairy Sci. Technol* **2009**, *89*, 139–154. https://doi.org/10.1051/dst/2009002.

(84) Heino, A.; Outinen, M.; Uusi-Rauva, J. Removal of Whey Proteins from Skimmed Milk with Polymeric Microfiltration Membranes. *MILCAD* **2010**, *65* (1).

(85) Beckman, S. L.; Barbano, D. M. Effect of Microfiltration Concentration Factor on Serum Protein Removal from Skim Milk Using Spiral-Wound Polymeric Membranes. *J. Dairy Sci.* **2013**, *96* (10), 6199–6212. https://doi.org/10.3168/jds.2013-6655.

(86) Argyle, I. Synthetic Membrane Performance Modification by Selective Species Adsorption, University of Bath, 2015.

(87) van Reis, R.; Zydney, A. Bioprocess Membrane Technology. *J. Memb. Sci.* **2007**, *297* (1–2), 16–50. https://doi.org/10.1016/j.memsci.2007.02.045.

(88) Jönsson, A. S.; Lindau, J.; Wimmerstedt, R.; Brinck, J.; Jönsson, B. Influence of the Concentration of a Low-Molecular Organic Solute on the Flux Reduction of a Polyethersulphone Ultrafiltration Membrane. *J. Memb. Sci.* **1997**, *135* (1), 117–128. https://doi.org/10.1016/S0376-7388(97)00135-X.

(89) Lindau, J.; Förvaltningsavd:s repro, S. *Fouling of Ultrafiltration Membranes Due to Adsorption of a Fatty Acid*; Chemical Engineering, Lund University, 1998.

(90) Bowen, W. R.; Calvo, J. I.; Hernández, A. Steps of Membrane Blocking in Flux Decline during Protein Microfiltration. *J. Memb. Sci.* **1995**, *101* (1–2), 153–165. https://doi.org/10.1016/0376-7388(94)00295-A.

(91) Field, R. W.; Wu, D.; Howell, J. A.; Gupta, B. B. Critical Flux Concept for Microfiltration Fouling. *J. Memb. Sci.* **1995**, *100* (3), 259–272. https://doi.org/10.1016/0376-7388(94)00265-Z.

(92) Hayward, E. R. Investigating Fouling and Cleaning during the Filtration of Gum Arabic to Save Water and Reduce Energy, 2015.

(93) Lindau, J.; Jönsson, A. S.; Wimmerstedt, R. The Influence of a Low-Molecular Hydrophobic Solute on the Flux of Polysulphone Ultrafiltration Membranes with Different Cut-Off. *J. Memb. Sci.* **1995**, *106* (1–2), 9–16. https://doi.org/10.1016/0376-7388(95)00072-K.

(94) Beckman, S. L.; Zulewska, J.; Newbold, M.; Barbano, D. M. Production Efficiency of Micellar Casein Concentrate Using Polymeric Spiral-Wound Microfiltration Membranes. *J. Dairy Sci.* **2010**, *93* (10), 4506–4517. https://doi.org/10.3168/jds.2010-3261.

(95) WU, D.; BIRD, M. R. The Fouling and Cleaning of Ultrafiltration Membranes During the Filtration of Model Tea Component Solutions. *J. Food Process Eng.* **2007**, *30* (3), 293–323. https://doi.org/10.1111/j.1745-4530.2007.00115.x.

(96) Bird, M. R.; BARTLETT, M. CIP Optimisation for the Food Industry: Relationships between Detergent Concentration, Temperature and Cleaning Time. *Inst. Chem. Eng.* **1995**, *73* (2), 63–70. https://doi.org/10.119/J.0960-3085.

(97) Jones, S. A.; Chew, Y. M. J.; Wilson, D. I.; Bird, M. R. Fluid Dynamic Gauging of Microfiltration Membranes Fouled with Sugar Beet Molasses. *J. Food Eng.* **2012**, *108* (1), 22–29. https://doi.org/10.1016/j.jfoodeng.2011.08.001.

(98) Weis, A.; Bird, M. R.; Nyström, M.; Wright, C. The Influence of Morphology, Hydrophobicity and Charge upon the Long-Term Performance of Ultrafiltration Membranes Fouled with Spent Sulphite Liquor. *Desalination* **2005**, *175* (1), 73–85. https://doi.org/10.1016/j.desal.2004.09.024.

(99) Bird, M. R.; Bartlett, M. Measuring and Modelling Flux Recovery during the Chemical Cleaning of MF Membranes for the Processing of Whey Protein Concentrate. *J. Food Eng.* **2002**, *53* (2), 143–152. https://doi.org/https://doi.org/10.1016/S0260-8774(01)00151-0.

(100) Kazemimoghadam, M.; Mohammadi, T. Chemical Cleaning of Ultrafiltration Membranes in the Milk Industry. *Desalination* **2007**, *204* (1–3), 213–218. https://doi.org/10.1016/j.desal.2006.04.030.

(101) Bartlett, M.; Bird, M. R.; Howell, J. A. An Experimental Study for the Development of a Qualitative Membrane Cleaning Model. *J. Memb. Sci.* **1995**, *105* (1), 147–157. https://doi.org/10.1016/0376-7388(95)00052-E.

(102) Liu, D. Z.; Weeks, M. G.; Dunstan, D. E.; Martin, G. J. O. O. Alterations to the Composition of Casein Micelles and Retentate Serum during Ultrafiltration of Skim Milk at 10 and 40 C. *Int. Dairy J.* **2014**, *35* (1), 63–69. https://doi.org/10.1016/j.idairyj.2013.10.017.

(103) Evans, P. J.; Bird, M. R. Solute-Membrane Fouling Interactions During the Ultrafiltration of Black Tea Liquor. *Food Bioprod. Process.* **2006**, *84* (4), 292–301.

https://doi.org/10.1205/fbp06030.

(104) Argyle, I. S.; Bird, M. R. Microfiltration of High Concentration Black Tea Streams for Haze Removal Using Polymeric Membranes. *Desalin. Water Treat.* **2015**, *53* (6), 1516–1531. https://doi.org/10.1080/19443994.2014.953401.

(105) Shorrock, C. J.; Bird, M. R. Membrane Cleaning: Chemically Enhanced Removal of Deposits Formed During Yeast Cell Harvesting. *Food Bioprod. Process.* **1998**, *76* (March), 30–38. https://doi.org/10.1205/096030898531729.

(106) Brans, G.; Schroën, C. G. P. H.; Van Der Sman, R. G. M.; Boom, R. M. Membrane Fractionation of Milk: State of the Art and Challenges. *J. Memb. Sci.* **2004**, *243* (1–2), 263–272. https://doi.org/10.1016/j.memsci.2004.06.029.

(107) Mercier-Bouchard, D.; Benoit, S.; Doyen, A.; Britten, M.; Pouliot, Y. Process Efficiency of Casein Separation from Milk Using Polymeric Spiral-Wound Microfiltration Membranes. *J. Dairy Sci.* **2017**, *100* (11), 8838–8848. https://doi.org/10.3168/jds.2017-13015.

(108) Tian, M.; Qu, L.; Zhang, X.; Zhang, K.; Zhu, S.; Guo, X.; Han, G.; Tang, X.; Sun, Y. Enhanced Mechanical and Thermal Properties of Regenerated Cellulose/Graphene Composite Fibers. *Carbohydr. Polym.* **2014**, *111*, 456–462. https://doi.org/10.1016/j.carbpol.2014.05.016.

(109) Liu, S.; Zeng, J.; Tao, D.; Zhang, L. Microfiltration Performance of Regenerated Cellulose Membrane Prepared at Low Temperature for Wastewater Treatment. *Cellulose* **2010**, *17* (6), 1159–1169. https://doi.org/10.1007/s10570-010-9450-6.

(110) Crowley, S. V; Caldeo, V.; Mccarthy, N. A.; Fenelon, M. A.; Kelly, A. L.; Mahony, J. A. O. Processing and Protein-Fractionation Characteristics of Different Polymeric Membranes during Filtration of Skim Milk at Refrigeration Temperatures. *Int. Dairy J.* **2015**, *48*, 23–30. https://doi.org/10.1016/j.idairyj.2015.01.005.

(111) Arkhangelsky, E.; Kuzmenko, D.; Gitis, V. Impact of Chemical Cleaning on Properties and Functioning of Polyethersulfone Membranes. *J. Memb. Sci.* **2007**, *305* (1–2), 176–184. https://doi.org/10.1016/j.memsci.2007.08.007.

(112) Sman, R. G. M. Van Der; Boom, R. M. M.; Brans, G.; Schroën, C. G. P. H.; van der Sman, R. G. M.; Boom, R. M. M. Membrane Fractionation of Milk: State of the Art and Challenges. *J. Memb. Sci.* **2004**, *243* (1), 263–272. https://doi.org/10.1016/j.memsci.2004.06.029.

(113) Pouliot, M.; Pouliot, Y.; Britten, M. On the Conventional Cross-Flow Microfiltration of Skim Milk for the Production of Native Phosphocaseinate. *Int. Dairy J.* **1996**, *6* (1), 105–111.

(114) Punidadas, P.; Rizvi, S. S. H. Separation of Milk Proteins into Fractions Rich in Casein or Whey Proteins by Cross Flow Filtration. *Food Res. Int.* **1998**, *31* (4), 265–272. https://doi.org/10.1016/S0963-9969(98)00088-X.

(115) Pearce, G. K. Quantifying the Benefit of Membrane Improvement on the Total Water Cost of Drinking Water Production. *Procedia Eng.* **2012**, *44*, 204–205. https://doi.org/10.1016/j.proeng.2012.08.359.

(116) Vadi, P. .; Rizvi, S. S. . Experimental Evaluation of a Uniform Transmembrane Pressure Crossflow Microfiltration Unit for the Concentration of Micellar Casein from Skim Milk. *J. Memb. Sci.* **2001**, *189* (1), 69–82. https://doi.org/10.1016/S0376-7388(01)00396-9.

(117) Hurt, E.; Zulewska, J.; Newbold, M.; Barbano, D. M. Micellar Casein Concentrate Production with a 3X, 3-Stage, Uniform Transmembrane Pressure Ceramic Membrane Process at 50°C. *J. Dairy Sci.* **2010**, *93* (12), 5588–5600. https://doi.org/10.3168/jds.2010-3169.

(118) Tremblay-Marchand, D.; Doyen, A.; Britten, M.; Pouliot, Y. A Process Efficiency Assessment of Serum Protein Removal from Milk Using Ceramic Graded Permeability Microfiltration Membrane. *J. Dairy Sci.* **2016**, *99* (7), 5230–5243. https://doi.org/10.3168/jds.2016-10914.

(119) Mccarthy, N. A.; Wijayanti, H. B.; Crowley, S. V; Mahony, J. A. O.; Fenelon, M. A. Pilot-Scale Ceramic Membrane Filtration of Skim Milk for the Production of a Protein Base Ingredient for Use in Infant Milk Formula. *Int. Dairy J.* **2017**, *73*, 57–62. https://doi.org/10.1016/j.idairyj.2017.04.010.

(120) Lawrence, N. D.; Kentish, S. E.; O 'connor, A. J.; Barber, A. R.; Stevens, G. W. Microfiltration of Skim Milk Using Polymeric Membranes for Casein Concentrate Manufacture. *Sep. Purif. Technol.* **2008**, *60*, 237–244. https://doi.org/10.1016/j.seppur.2007.08.016.

(121) Hurt, E. E.; Adams, M. C.; Barbano, D. M. Microfiltration of Skim Milk and Modified Skim Milk Using a 0.1-Mm Ceramic Uniform Transmembrane Pressure System at Temperatures of 50, 55, 60, and 65°C. *J. Dairy Sci.* **2015**, *98* (2), 765–780. https://doi.org/10.3168/jds.2014-8775.

(122) Doudies, F.; Loginov, M.; Hengl, N.; Karrouch, M.; Leconte, N.; Garnier-lambrouin, F.; Javier, P. Build-up and Relaxation of Membrane Fouling Deposits Produced during Crossflow Ultrafiltration of Casein Micelle Dispersions at 12 ◦ C and 42 ◦ C Probed by in Situ SAXS. *J. Memb. Sci.* **2021**, *618*, 118700 Contents. https://doi.org/10.1016/j.memsci.2020.118700.

(123) Nöbel, S.; Weidendorfer, K.; Hinrichs, J. Journal of Colloid and Interface Science Apparent Voluminosity of Casein Micelles Determined by Rheometry. *J. Colloid Interface Sci.* **2012**, *386*, 174–180. https://doi.org/10.1016/j.jcis.2012.07.075.

(124) Kern, C.; Sonne, A.; Balz, B. Apparent Voluminosity of Casein Micelles in the Temperature Range 35-70 °C. *Int. Dairy J.* **2016**, *59*, 80–84. https://doi.org/10.1016/j.idairyj.2016.03.010.

(125) Ng, K. S. Y.; Dunstan, D. E.; Martin, G. J. O. Influence of Processing Temperature on Flux Decline during Skim Milk Ultrafiltration. *Sep. Purif. Technol.* **2018**, *195* (December 2017), 322–331. https://doi.org/10.1016/j.seppur.2017.12.029.

(126) Schopf, R.; Schork, N.; Amling, E.; Nirschl, H.; Guthausen, G.; Kulozik, U. Structural Characterisation of Deposit Layer during Milk Protein Microfiltration by Means of In-Situ MRI and Compositional Analysis. *Membranes (Basel).* **2020**, *10* (4), 59.

(127) France, T. C.; Bot, F.; Kelly, A. L.; Crowley, S. V.; O'Mahony, J. A. The Influence of Temperature on Filtration Performance and Fouling during Cold Microfiltration of Skim Milk. *Sep. Purif. Technol.* **2021**, *262* (July 2020), 118256. https://doi.org/10.1016/j.seppur.2020.118256.

(128) Jimenez-Lopez, A. J. E.; Leconte, N.; Dehainault, O.; Geneste, C.; Fromont, L.; Gésan-Guiziou, G. Role of Milk Constituents on Critical Conditions and Deposit Structure in Skim Milk Microfiltration (0.1 Mm). *Sep. Purif. Technol.* **2008**, *61* (1), 33–43. https://doi.org/10.1016/j.seppur.2007.09.023.

(129) Argyle, I. S.; Pihlajamaki, A.; Bird, M. R. Ultrafiltration of Black Tea Using Diafiltration to Recover Valuable Components. *Desalin. Water Treat.* **2015**, *53* (6), 1532–1546. https://doi.org/10.1080/19443994.2014.953400.

(130) Argyle, I. S.; Pihlajamaki, A.; Bird, M. R. Desalination and Water Treatment Ultrafiltration of Black Tea Using Diafiltration to Recover Valuable Components. **2016**. https://doi.org/10.1080/19443994.2014.953400.

(131) Argyle, I. S.; Pihlajamaki, A.; Bird, M. R. Desalination and Water Treatment Ultrafiltration of Black Tea Using Diafiltration to Recover Valuable Components.

Desalin. Water Treat. **2016**, *53* (6), 1532–1546. https://doi.org/10.1080/19443994.2014.953400.

(132) Head, L. E.; Bird, M. R. The Removal of Psychrotropic Spores from Milk Protein Isolate Feeds Using Tubular Ceramic Microfilters. *J. Food Process Eng.* **2013**, *36* (1), 113–124. https://doi.org/10.1111/j.1745-4530.2011.00661.x.

(133) Harvard University. A Summary of Error Propagation. Harvard University 2007, pp 3–7.

(134) Casein–Database of ATR-FTIR spectra of various materials http://lisa.chem.ut.ee/IR_spectra/paint/binders/casein/ (accessed Sep 10, 2018).

(135) Klinkenberg, A.; Zuiderweg, F. J. Longitudinal Diffusion and Resistance to Mass Transfer as Causes of Nonideality in Chromatography. *Chem. Eng. Sci.* **1956**, *5* (6), 271–289. https://doi.org/10.1016/0009-2509(56)80003-1.

(136) Gritti, F.; Guiochon, G. The van Deemter Equation: Assumptions, Limits, and Adjustment to Modern High Performance Liquid Chromatography. *J. Chromatogr. A* **2013**, *1302*, 1–13. https://doi.org/10.1016/j.chroma.2013.06.032.

(137) Guillarme, D.; Heinisch, S.; Rocca, J. L. Effect of Temperature in Reversed Phase Liquid Chromatography. *J. Chromatogr. A* **2004**, *1052* (1–2), 39–51. https://doi.org/10.1016/j.chroma.2004.08.052.

(138) Tran, J. V; Molander, P.; Greibrokk, T.; Lundanes, E. Temperature Effects on Retention in Reversed Phase Liquid Chromatography Original Paper. *J. Seperation Sci.* **2001**, *24* (1), 930–940.

(139) McCalley, D. V. Effect of Temperature and Flow-Rate on Analysis of Basic Compounds in High-Performance Liquid Chromatography Using a Reversed-Phase Column. *J. Chromatogr. A* **2000**, *902* (2), 311–321. https://doi.org/10.1016/S0021-9673(00)00924-9.

(140) Evans, P. J.; Bird, M. R. THE ROLE OF BLACK TEA FEED CONDITIONS UPON ULTRAFILTRATION PERFORMANCE DURING MEMBRANE FOULING AND CLEANING. *J. Food Process Eng.* **2010**, *33* (2), 309–332. https://doi.org/10.1111/j.1745-4530.2008.00276.x.

(141) Mulder, M. *Basic Principles of Membrane Technology, 2nd Edition*, 2nd editio.; 2000.

(142) Crowley, S. V.; O'Callaghan, T. F.; Kelly, A. L.; Fenelon, M. A.; O'Mahony, J. A. Use of Ultrafiltration to Prepare a Novel Permeate for Application in the Functionality

Testing of Infant Formula Ingredients. *Sep. Purif. Technol.* **2015**, *141*, 294–300. https://doi.org/10.1016/j.seppur.2014.11.047.

(143) Happe, R. P.; Gambelli, L. Specialty Oils and Fats in Food and Nutrition - Properties, Processing and Applications: 12-Infant Formula; 2015.

(144) Lönnerdal, B. Nutritional and Physiologic Significance of Human Milk Proteins. *Am. J. Clin. Nutr.* **2003**, *77* (6), 1537S-1543S. https://doi.org/10.1093/ajcn/77.6.1537s.

(145) Zulewska, J.; Barbano, D. M. Influence of Casein on Flux and Passage of Serum Proteins during Microfiltration Using Polymeric Spiral-Wound Membranes at 50°C. *J. Dairy Sci.* **2013**, *96* (4), 2048–2060. https://doi.org/10.3168/jds.2012-6032.

(146) Hartinger, M.; Heidebrecht, H. J.; Schiffer, S.; Dumpler, J.; Kulozik, U. Milk Protein Fractionation by Means of Spiral-Wound Microfiltration Membranes: Effect of the Pressure Adjustment Mode and Temperature on Flux and Protein Permeation. *Foods* **2019**, *8* (6), 1–17. https://doi.org/10.3390/foods8060180.

(147) Haribabu, M. Simulating the Behaviour of Skim-Milk during Ultrafiltration, University of Melbourne, 2018.

(148) Mahdi, Y.; Mouheb, A.; Oufer, L. A Dynamic Model for Milk Fouling in a Plate Heat Exchanger. *Appl. Math. Model.* **2009**, *33* (2), 648–662. https://doi.org/10.1016/j.apm.2007.11.030.

(149) Pan, F.; Dong, X.; Mercadé-prieto, R.; Xiao, J. Numerical Simulation of Milk Fouling : Taking Fouling Layer Domain and Localized Surface Reaction Kinetics into Account. *Chem. Eng. Sci.* **2019**, *197*, 306–316. https://doi.org/10.1016/j.ces.2018.12.021.

(150) Qin, B. Y.; Bewley, M. C.; Creamer, L. K.; Baker, H. M.; Baker, E. N.; Jameson, G. B. Structural Basis of the Tanford Transition of Bovine -Lactoglobulin. *Am. Chem. Soc.* **1998**, *2960* (98), 14014–14023. https://doi.org/10.1021/bi981016t.

(151) Aerts, P.; Greenberg, A. R.; Leysen, R.; Krantz, W. B.; Reinsch, V. E.; Jacobs, P. A. The Influence of Filler Concentration on the Compaction and Filtration Properties of Zirfon®-Composite Ultrafiltration Membranes. *Sep. Purif. Technol.* **2001**, *22–23*, 663–669. https://doi.org/10.1016/S1383-5866(00)00165-9.

(152) Davenport, D. M.; Ritt, C. L.; Verbeke, R.; Dickmann, M.; Egger, W.; Vankelecom, I. F. J.; Elimelech, M. Thin Film Composite Membrane Compaction in High-Pressure Reverse Osmosis. *J. Memb. Sci.* **2020**, *610* (March), 118268. https://doi.org/10.1016/j.memsci.2020.118268.

(153) Ebert, K.; Fritsch, D.; Koll, J.; Tjahjawiguna, C. Influence of Inorganic Fillers on the Compaction Behaviour of Porous Polymer Based Membranes. *J. Memb. Sci.* **2004**, *233* (1–2), 71–78. https://doi.org/10.1016/j.memsci.2003.12.012.

(154) Remanan, S.; Chandra Das, N. A Unique Micofiltration Membrane Derived from the Poly(Ethylene-Co-Methyl Acrylate)/Poly(Vinylidene Fluoride) (EMA/PVDF) Biphasic Blends and Surface Modification for Antifouling Application. *Polym. Test.* **2019**, *79* (April), 106031. https://doi.org/10.1016/j.polymertesting.2019.106031.